Towards the Development of Alternative Platinum-Based Anticancer Drugs: A Kinetic and Mechanistic Study of Mono and Dinuclear *Trans*-Platinum(II) Complexes

By

Moses Ariyo OLUSEGUN

B.Sc. Ed. (Hons), MSc. (Lagos, Nigeria)

Submitted in partial fulfilment of the academic requirements for the degree of

Doctor of Philosophy

in the College of Agriculture, Engineering and Science

School of Chemistry and Physics

University of KwaZulu-Natal

Pietermaritzburg

February 2019

UNIVERSITY OF
KWAZULU-NATAL

INYUVESI
YAKWAZULU-NATALI

Abstract

The kinetic and mechanistic study of the ligand substitution reactions of a series of *trans*-platinum(II) complexes was performed. To this end, three sets of mononuclear *trans*-platinum(II) complexes and one set of flexible alkyl-α,ω-diamine linkers dinuclear *trans*-platinum(II) complexes were synthesised and characterised by different spectroscopic methods and elemental analysis. Substitution of either the coordinated chloride or aqua moeities were investigated under pseudo first-order conditions as a function of concentration and temperature. Experimental data were corroborated with DFT calculations.

In the first instance, a comparative study of the kinetic and mechanistic behaviour of ligand substitution reactions of some bifunctional analogous *cis*- and *trans*-platinum(II) complexes with dialkylamine ligands was performed. The reaction of the *cis*-complexes proceeded in two concerted steps whereas those of the *trans*-complexes followed a single step. The *trans*-complexes were found to be approximately 10^3 more reactive than their corresponding *cis*-analogues. The decrease in the rate of ligand substitution in the *cis*-platinum(II) complexes was attributed largely to the steric hindrance due to their structural arrangement. The *cis*- and the *trans*-complexes were found to form different kinetic products. The *cis*-complexes were observed to undergo complete substitution (dechelation) due to the presence of the strong labilising effects of the thiourea-based nucleophiles, unlike the *trans*-complexes which were partially substituted by these nucleophiles. ^{195}Pt NMR spectroscopy was employed to confirm the final kinetic products and to demonstrate the stepwise substitution of the respective series of complexes with thiourea.

Ligand substitution reactions of the second set of *trans*-platinum(II) complexes with mixed amine ligands were found to proceed by first-order kinetics in a single step. The reactivity of the complexes was largely dependent on the length of the alkyl chain of the alkylamine moiety of the complexes. Density functional theory (DFT) calculations showed that an increase in chain length by a methylene unit has no direct electronic significance on the metal centre. The increase in chain length, however, posed significant steric hindrance on the substitution sites due to the flexibility of the alkyl chains and thus governed the overall reaction pattern. The ^{195}Pt NMR spectroscopic results established that the mixed amine ligands remain coordinated to the metal centre in the final kinetic product. In the third scheme, aqua ligand substitution reactions were performed to investigate the comparative substitution behaviour of some mononuclear *trans*-platinum(II) complexes with symmetric and asymmetric amine ligands respectively. The

substitution reactions of each of the *trans*-platinum(II) complexes proceed by first-order kinetics in a single step. The reactivity of the complexes was mainly governed by both steric and electronic factors. Unlike the *trans*-platinum(II) complexes with asymmetric amine ligands, the ligand system around the complexes with symmetrical amine groups has significant electronic effect on the electrophilicity of the metal centre depending on the number of carbon atoms around the dialkylamine moieties. The nature of the alkylamine ligand, whether long or a branched chain, also play a role on the rate of substitution. The flexible long chain of the alkylamine ligand in the asymmetric complexes posed more steric hindrance on the reactive centre than the branched chain of the dialkylamine ligand in the symmetric complexes.

Lastly, we investigated the role of flexible alkyl-α,ω-diamine linkers on the substitution behaviour of dinuclear *trans*-platinum(II) complexes. The ligand substitution reaction of the complexes proceeded in three consecutive steps. Each step follows first-order kinetics with the respective complex and nucleophile. Both electronic and steric effects drive the overall substitution pattern. However, our findings revealed that upon the substitution of the chloro moieties by the thiourea-based nucleophiles at the platinum centres, the σ-donor capacity via inductive effect of these electron-rich nucleophiles override the steric strain imposed by the nucleophiles as well as by the alkanediamine linker on the substitution sites. Consequently, electronic factors governed the overall reaction pattern of these complexes. ^{195}Pt NMR results confirmed the simultaneous substitution of all the chloride leaving groups by thiourea-based nucleophiles, followed by the subsequent but successive displacement of the ammine groups and the flexible alkanediamine linker from the metal centres. In general, the small positive enthalpy and the large but negative entropy confirm an associative mode of activation for all the studied complexes.
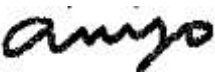
Dedication

To the Glory of Almighty God

and

to the loving Memory of my Late Mum,

Mrs. Abeo Alade (1945-2017)

Declaration - Plagiarism

I, Moses Ariyo Olusegun declare that

1. The research reported in this thesis, except where otherwise indicated, is my original research.
2. This thesis has not been submitted for any degree or examination at any other university.
3. This thesis does not contain other persons' data, pictures, graphs or other information, unless specifically acknowledged as being sourced from other persons.
4. This thesis does not contain other persons' writing, unless specifically acknowledged as being sourced from other researchers. Where other written sources have been quoted, then:
   a. Their words have been re-written, but the general information attributed to them has been referenced

   b. Where their exact words have been used, then their writing has been placed in italics and inside quotation marks and referenced

5. This thesis does not contain text, graphics or tables copied and pasted from the Internet, unless specifically acknowledged, and the source being detailed in the thesis and in the references sections.

Signed: … *ariyo* …

I hereby certify that the statement is true.

Signed: ………………………………   Signed…………………….

Dr. D. Reddy   **Prof. D. Jaganyi**

Supervisor   Co-supervisor

Table of Contents

Acknowledgements

I would like to appreciate the following people and institutions whose immense support and encouragement helped to bring this research efforts to fruition:

Conference Contributions

Publications

All the work presented in **Chapters Three** to **Six** are already compiled in manuscript formats for publication in peer-reviewed journals.

Conference Contributions

Oral Presentation

South African Chemical Institute KwaZulu-Natal Region Postgraduate Colloquium 2018, Durban University of Technology, Durban , on 2 February 2018. *A Kinetic and Mechanistic Study of Analogous Bifunctional Dialkylamine Platinum(II) Complexes*.

Poster Presentation

Postgraduate Research and Innovation Symposium 2018, College of Agriculture, Engineering and Science, University of KwaZulu-Natal, Westville Campus, on 25 October 2018. *A Kinetic Investigation of Mononuclear Trans-Platinum(II) Complexes with Mixed Amine Ligands.*

List of Abbreviations and Symbols

A2780cis   Cisplatin-sensitive human ovarian carcinoma cell line

A2780R   Cisplatin-resistant human ovarian carcinoma cell line

A549   Human lung tumour cells (lung carcinoma, epithelial cells)

Å   Angstrom (10^{-10} m)

A   Associative mechanism

B3LYP   Functional hybrid exchange of Becke with the functional correlation
                  gradient of Lee and Yang

BBR3464 $[\{trans\text{-}PtCl(NH_3)_2\}_2\{\mu\text{-}trans\text{-}Pt(NH_3)_2\text{-}(HN_2(CH_2)_6NH_2)_2\}]^{4+}$

C-PCM   Conductor Polarizable Continuum Model

Cisplatin   *cis*-Diaminedichloroplatinum(II)

CTR1   Constructive triple response 1

Cys   Cysteine

D   Dissociative

δ/ppm   Chemical shift in parts per million

DFT   Density functional theory

DMSO   Dimethyl sulfoxide

DMF   Dimethylformamide

DMTU   1,3-Dimethylthourea

DNA   Deoxyribonucleic acid

Ea   Activation energy

ε	Molar absorptivity coefficient
e	Exponential
en	Ethylene diamine
eqm	Equilibrium
eqv	Equivalence
G	Guanine
$\Delta G^{\#}$	Gibbs free energy of activation
5´-GMP	Guanisine-5´-monophosphate
GSH	Glutathione
h	Planck constant (6.626×10^{-34} J/s)
$\Delta H^{\#}$	Activation enthalpy
HCC827	Human lung tumour cells
HMG	High-mobility group proteins
HOMO	Highest occupied molecular orbital
I	Ionic strength
I	Interchange
I_a	Associatively interchange
IC_{50}	Concentration of a compound that induces 50 % of growth inhibition of cells compared to untreated cells
I_d	Dissociatively interchange
5´IMP	Inosine-5´-monophosphate
INO	Inosine

K	Kelvin
k_1, k_{-1}, k_2, k_{-2}	Rate constants
k_b	Boltzmann constant (1.3807×10^{-23} J/K)
k_{obs}	Observed pseudo first-order constant
k_{cal}	Kilocalorie
kJ	Kilojoules
λ	Wavelength
L	Ligand
LANL2DZ	Los Alamos National Laboratory 2 Double ζ
L1210	Murine leukemia cell-line
LFER	Linear free energy relationship
$LiCF_3SO_3$	Lithium triflate
LUMO	Lowest unoccupied molecular orbital
M	Molarity (mol dm^{-3}) or metal
MeOH	Methanol
mL	Millilitre
MLCT	Metal to ligand charge transition
MO	Molecular orbital
MTU	Methyl thiourea
NBO	Natural bond orbital
NER	Nucleotide excision repair
nm	Nanometer
NMR	Nuclear magnetic resonance
NU	Nucleophile
OH•	Hydroxide radical
Pa	Pascal
PDT	Photodynamic therapy
pK_a	Acid dissociation constant
ppm	Parts per million
py	Pyridine/pyridyl
R	Universal gas constant (8.315 JK^{-1} mol^{-1})
RF	Resistance factor
RNA	Ribonucleic acid
s	Mucleophilic discrimination factor

s	Singlet or strong
$\Delta S^{\#}$	Activation entropy
SAR	Structure-activity relationship
$Si(CH_3)_4$	tetramethyl silane
T	Temperature
TOF MS-ES+	A time-of-flight mass spectrometer with an electron spray source operated in the positive ion mode
TMTU	1,1,3,3-Tetramethyl-2-thiourea
TU	Thiourea
UV/vis	Ultraviolet/Visible
$\Delta V^{\#}$	Activation volume
X	Leaving group (unless otherwise mentioned)
Y	Incoming group (unless otherwise mentioned)
υ	Frequency
n_{pt}	Nucleophilicity
μ	Electronic chemical potential
ω	Electrophilicity index
η	Chemical hardness

List of Figures

List of Schemes

List of Tables

Chapter One

From Obscurity to Prominence: The Prospect of *Trans*-Platinum Compounds in Anticancer Chemotherapy

1.1 Introduction

Cancer is an enormous global health burden, touching every region and socioeconomic level. Today, cancer accounts for about 15% of deaths worldwide – more than HIV/AIDS, tuberculosis and malaria combined [1]. Cancer is caused by mutational changes in genes that are responsible for cell growth and repair. These changes are mostly because of internal factors such as hormones, inherited genetic mutations and immune conditions; and external factors such as tobacco, harmful radiation and infectious organisms. Several approaches are employed to treat cancer, such as surgery, chemotherapy, radiation therapy, immunotherapy or a combined therapy approach [2]. The choice of treatment depends on the nature of the tumour, the stage of the disease and the general state of the patient. However, intrinsic resistance of certain cancer cell-lines have limited the effectiveness of the available anticancer treatment options [3]. As a result, the number one priority of medicinal inorganic chemists is to develop new anticancer agents with improved cytotoxicity [4]. Subsequently, metal-based anticancer agents have continued to show some promise.

Despite the vital role some essential metals play in many biological processes, the intrinsic toxic nature of most metals make them to be widely reckoned as uncongenial, beyond a certain threshold, in the human body [5]. Their importance in anticancer chemotherapy is hinged on the fact that the electrophilic metal sites interact with the nucleophilic groups such as, proteins, DNA etc., in the cancer cells. In spite of their relevance, the statistics of clinically approved metal-based anticancer agents are veritably low compared to the amount of metal compounds which are reported annually. Moreover, the majority of these drugs are platinum compounds. Cisplatin, since its serendipitous discovery by Barnet Rosenberg in 1969, is still increasingly used worldwide in the treatment of different types of cancers such as testicular, ovarian, head, neck, cervical and other cancers [6, 7]. It is generally accepted that the distortion of DNA generated upon binding of cisplatin is largely responsible for its antitumor properties [8]. Following the example of cisplatin, thousands of platinum-containing compounds have been synthesised and evaluated as potential antitumour drugs but only a few compounds reached

worldwide clinical applications viz. Carboplatin and Oxaliplatin; while Nedaplatin, Heptaplatin and Lobaplatin have been regionally approved in Japan, South Korea and China respectively [9].
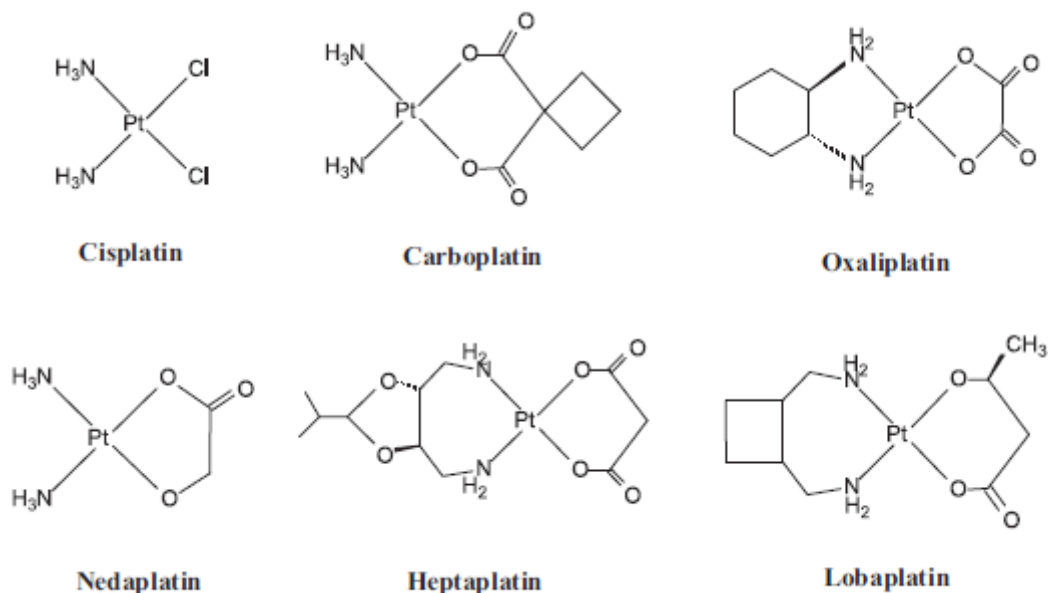
Figure 1.1: Cisplatin and its derivatives clinically approved for use globally and regionally respectively [10].

However, despite the success of cisplatin and carboplatin, side-effects and resistance are their main drawbacks [11, 12]. The search for novel platinum compounds that can suppress the side-effects, overcome the intrinsic and acquired resistance and achieve a broader spectrum of cytostatic applications, has been a constant factor among medical inorganic researchers [1]. *Trans*-platinum compounds, which are initially thought to be redundant, have in the recent times started to gain some prominence in cancer treatment. This chapter examines the historical development of platinum-based anticancer agents and the promising prospect *trans*-platinum complexes have in both the proximate and the remote future.

1.2 Historical Development of Platinum-Based Anticancer Agents: The Accidental Discovery of Cisplatin

The fortuitous revelation of the cytotoxic properties of cisplatin did not only mark a watershed in anticancer studies but also was the genesis of the use of coordination compounds in anticancer chemotherapy. The synthesis of *cis*-diamminedichloroplatinum(II), also known as

cisplatin, was first reported by Michel Peyrone in 1844 [13]. As it was commonly done at that time, it was called Peyrone's chloride, named after the man who synthesised it, even though, its structure was not yet known. It took nearly five decades for its chemical structure to be eventually figured out by Alfred Werner [14-17]. Werner was the first to distinguish, through structural elucidation, between cisplatin and its *trans*-isomer transplatin. However, nothing was known about the biological importance of cisplatin until Barnett Rosenberg and his colleagues in the late 1960s observed, during an electrolytic procedure, that the cell division of *Escherichia coli* was inhibited and filamentous growth took place when an electric current was applied to bacteria growth cultured in ammonium chloride solution using platinum electrode [6, 14, 15, 18]. The inhibition was established to have been caused by the formation of cisplatin and some platinum(IV) complexes. Following this discovery, cisplatin, for the first time, was administered to a cancer patient in 1971 and by 1978, the drug was finally approved for clinical use in the United States of America [15, 19]. Despite the drug activity against several types of tumour cells, its severe side effects, intrinsic and acquired resistance, among others, are its major limitations. Consequently, extensive research efforts amongst medicinal inorganic chemists are targeted at designing and synthesising compounds, whether platinum-based or otherwise, that can afford superior cytostatic activity against cancer cells, minimise toxic side effects, and overcome cross resistance relative to cisplatin. However, before all these could be achieved, the mechanism of action of cisplatin must be well understood and established.

1.3   Mode of Action of Cisplatin

Research efforts aimed to understand the mode of action of cisplatin have not only helped to reveal the mechanism of most platinum-based compounds but also unveiled how they terminate tumour cells in the humans. It is predominantly accepted that the central binding target of cisplatin is the DNA of the tumour cells [10, 15, 20-23]. The drug could reach its target because the chloride ion concentration in the blood plasma, which has been estimated to be approximately ~100 mM, helps to suppress the hydrolysis of the complex; consequently the structure of the complex is largely unaltered [23, 24]. The chloride coordinated complex gains access into the cell either through passive diffusion or active uptake, a process involving copper transporter proteins, which is known as the constitutive triple response 1 (CTR1) sites, as an integral part [25-27]. Once the neutral cisplatin molecule enters into the cell, it undergoes

hydrolysis, because of the low concentration of chloride ions (~4 mM) inside the cell, resulting in the loss of one or both chloride ligands to produce a charged complex [28, 29] **(Figure 1.2)**.
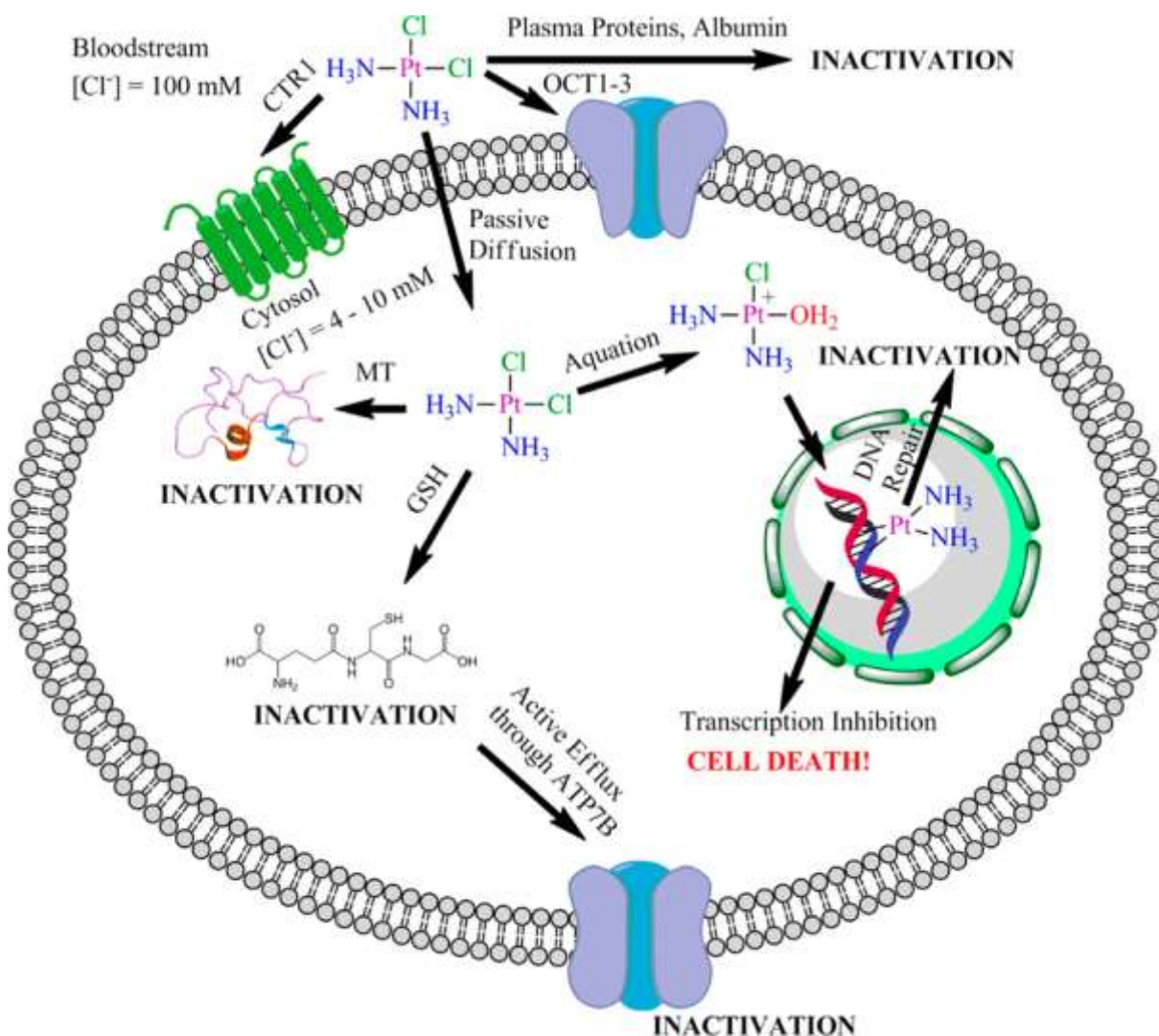
Figure 1.2:   Extracellular and intracellular events that influence cisplatin's activity. Attention is drawn to instances where deactivation/sequestration can occur [30].

The rate at which cisplatin binds to DNA depends upon this aquation process [29], the charged complex produced from this process is more reactive towards biomolecules because aqua moieties are substituted faster than chlorides [31]. The cytostatic activity of cisplatin is interfered with through the recognition of platinated DNA adducts [32] by the proteins such as high-mobility group proteins (HMG)) which proscribed cisplatin from obstructing with DNA transcription. Moreover, there are many biomolecules and ions such as chloride ions, hydroxyl ions, aqua molecules and other sulfur containing species, such as proteins, peptides and

enzymes, inside the cell competing for direct interaction with cisplatin. Some of the drug may interact with sulfur donor molecules which are quite abundant in the blood because of the strong affinity for the platinum centre has for such molecules [22, 33], to yield kinetically stable or inert platinum-sulfur bonded adducts. The agglomeration of bonded sulfur containing proteins and amino acids [34] to the platinum centre usually result in the potential deactivation of the drug and this has been established to be essentially responsible for some of the toxic side effects [22, 31, 35]. This phenomenon limits the bio-distribution and pharmacokinetics of the drug, consequently lowering the formation of the expected platinum-DNA adducts and the accumulation of the drug in the cell [15, 36]. Likewise, the strong *trans* influence of certain thio-based compounds, such as thioethers [34] or methionine derivatives [37], to the platinum(II) centre elicit the displacement of the amine ligand *trans* to the chloride or aqua nucleofuge by the entering groups before the DNA could bind to the metal site [22, 37]. Subsequently, the anticipated mechanism of action of the metal complex is impeded and hence, its cytostatic effect.

1.4   Binding of Cisplatin to DNA

Since the preponderance of evidence has established the fact that DNA bases, such as adenine, cytosine, guanine and thymine, are the major targets of cisplatin in cells [38], it is pertinent to examine in detail the interaction of cisplatin with DNA. The platinum(II) ion preferentially coordinates with nitrogen atoms of the DNA [39]. This is expected since platinum is a soft centre [40]. The process of interaction of cisplatin with DNA has been adduced to proceed through six stages viz. aquation of the complex; pre-association with the DNA; monofunctional adduct formation; closure to a bifunctional adduct; distortion of the DNA and; recognition of this distortion [41]. Essentially, the binding of cisplatin to DNA of the cancer cell will normally cause programmed cell death (apoptosis) [42-47]. Although, the N1 of adenine and the N3 atom of cytosine are suitable positions for platinum binding, the preferred binding site in DNA is the N7 atom of guanine [48-55]. It is believed that at physiological pH, the N3 atom of thymine is protonated, hence, it is sterically hindered. Besides, the non-planar nitrogen lacks a lone pair electron requisite for sigma bond formation to the platinum centre. Nonetheless, the N3 atom of thymine becomes a potential binding site with the loss of the hydrogen atom. In **Figure 1.3** a scheme with all the potential binding positions is represented. The strong kinetic preference for the N7 atom of guanine, the most favoured position for platinum binding [48, 49, 51], has

been attributed to three factors which include: the strong basicity of that position; the hydrogen bond interactions between ammine protons of cisplatin with O6 in guanine and; the accessibility of the N7 atom of guanine for the platinum complexes [20].
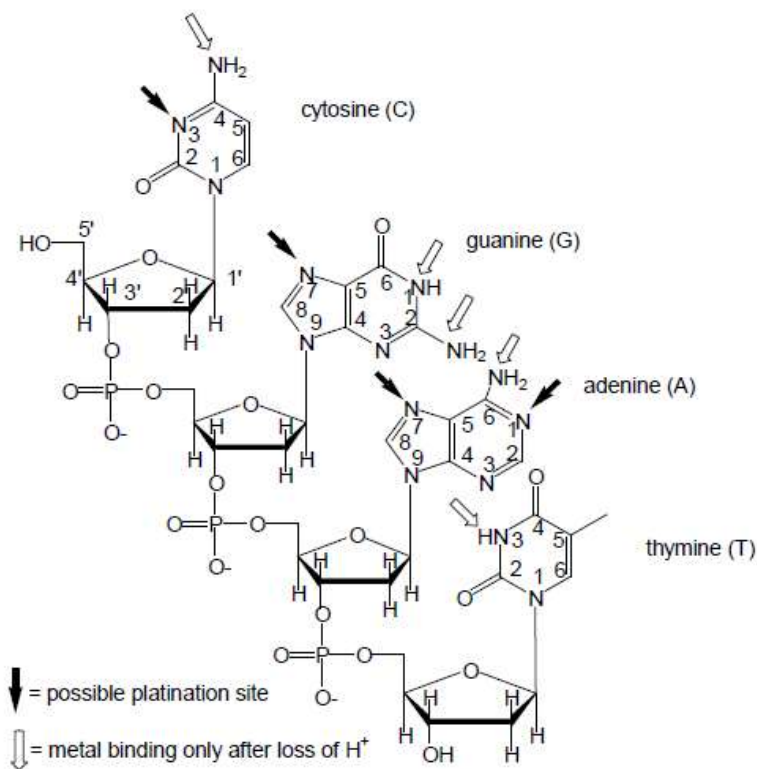
Figure 1.3: Possible cisplatin binding sites on DNA. N3 are sterically hindered for possible binding [56].

The interaction of cisplatin with DNA leads to the formation of six different types of platinum-DNA adducts. The most prominent among them in order of their decreasing priorities include the following: 1,2-intrastrand d(GpG) cross-links on adjacent guanines; 1,2-intrastrand d(ApG) cross-links between an adjacent adenine and guanine, 1,3-intrastrand d(GXG) cross-links between alternate guanines separated by one DNA base and 1,4-intrastrand d(GXXG) cross-links between guanines separated by two DNA bases. In addition to this, a small fraction of cisplatin was posited to interact with DNA bases either via interstrand cross-links, involving two strands of the DNA double helix, or in monofunctional adducts bonded to a single purine and protein DNA cross-link [41, 57, 58]. In the latter, cisplatin is coordinated to a protein molecule and a DNA base (**Figure 1.4**).
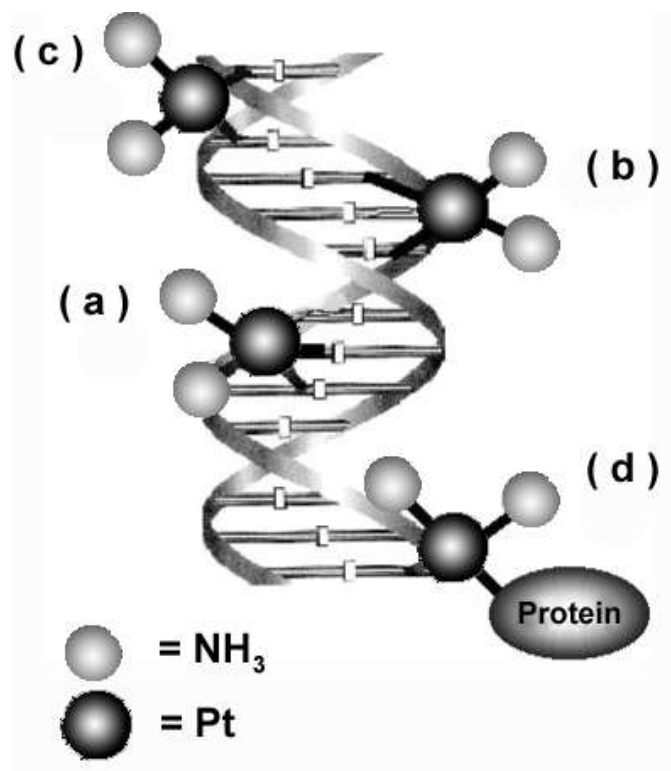
Figure 1.4:   Main adducts formed in the interaction of cisplatin with DNA. (a) 1,2-Intrastrand cross-link; (b) 1,3-Intrastrand cross-link; (c) Interstrand cross-link; (d) Protein-DNA cross-link [59].

In essence, these cross-links to the cancer cell and how they lead to cell death are still just vaguely understood. However, it is generally accepted that the binding of cisplatin to DNA transmutes the DNA conformation resulting in the distortion of its structure. This subsequently causes unwinding, bending and flattening of the minor grooves in the DNA helix [60, 61]. The alteration results in the suppression of DNA transcription, a step which is very crucial for protein synthesis and cell division. Cisplatin will normally attack the telomere, which is a regions of recurrent nucleotide sequences at each end of a chromosome inside the DNA, that protect the ends of chromosomes from degradation during cell division [62, 63]. The deterioration of the telomeric regions of the chromosomes by cisplatin suppresses cell division leading to fatal damages in the DNA and subsequently, prohibits replication of the DNA resulting in apoptosis. Nevertheless, this process is sometimes circumvented which will usually result in the inactivation and resistance to the drug [60].

1.5   Mechanism of Inactivation and Resistance of Cisplatin

One of the major drawbacks of cisplatin in anticancer chemotherapy is the inherent and acquired resistance of the drug [30, 64, 65]. This has limited its success despite its general application to different cancer types. Several factors have been posited for cisplatin inactivation and resistance. Effectively, a combination of these factors may, to a large extent, be probably responsible for the resistance; some of which are briefly highlighted. Firstly, the transformation in the properties of the membrane [56], upon which the drug transported and/or effluxed could result in low intracellular accumulation of the drug and hence, its resistance. Previous studies have suggested that a P-glycoprotein, found in multidrug-resistant cell lines, acts as a pump, which limits the accumulation of the drug in the cell [66-69]. Secondly, the presence of thiol-donor groups in the cell, such as the intracellular peptide glutathione and metallothionine, is another cause of cisplatin resistance [70-72]. Since platinum, being a soft centre, has a strong affinity for sulfur, the amount of platinum binding to the DNA target will subsequently decrease. An increase in the level of glutathione have been observed in some cisplatin-resistant cancer cells [73, 74]. Similarly, metallothionien, which is a protein from amino acids [75-78], containing twenty cysteines residues involved in metabolizing heavy metals, such as zinc, cadmium, and copper, is also believed to be involved in the mechanism of resistance. Elevated levels of metallothionien have been reported in some cisplatin-resistant cells [75-78]. Thirdly, increased tolerance to platinum-DNA adducts has also been proposed to be culpable for the resistance of the drug [79-82] and finally, an increase in DNA repair resulting from nucleotide excision repair (NER) may also be instrumental to cisplatin resistance [83-86]. Enhanced DNA repair was observed in some cisplatin-resistant cell lines. However, there have been continued research efforts with hope to overcome the inactivation and resistance of the drug.

1.6   Other Platinum-Based Complexes of *Cis*-Configuration

Following the major limitations to therapeutic efficacy of cisplatin as a result of its severe side effects and resistance in certain tumour cells, hundreds of thousands of platinum complexes have been synthesised with the aim of improving the clinical limitations of cisplatin [87]. At present, most newly developed platinum compounds could not make it to clinical approval, even though, many of them are screened for biological activity. In fact, as of 2016, only about twenty-two platinum-based cytostatic agents have reached clinical trials [9]. Moreover, the preponderance of the synthesised platinum-based compounds is of *cis*-geometry such as, *cis-*

diamine(1,1cyclobutanedicarboxylato)platinum(II) (carboplatin) [32], *trans*-L-1,2-diaminocyclohexaneoxalato platinum(II) (oxaliplatin), *cis* diammineglycolatoplatinum(II), (nedaplatin), [*cis*-diammineglycolatoplatinum(II)] (heptaplatin) and lobaplatin [10, 30, 70]. Carboplatin and Oxaliplatin are often referred to as the second and third generations of cisplatin derivatives [30, 48]. The former has been reported to be less toxic [48, 88-90] and hence, the drug is usually dispensed at higher doses (2000 mg/dose) [56] than standard course of therapy (900 mg/ml) [91]. This is due to its very slow aquation process, relative to other drugs currently in use [92, 93]. The cyclobutanedicarboxylato ligand is far less labile compared to the chloride ligands in cisplatin [94-96]. Carboplatin is reportedly being used as a first-line drug for the treatment of ovarian cancer. One advantage of this drug is its remarkably less toxicity towards the kidneys and the nervous system [97-100]. The drug is, however, less potent and not as versatile in the treatment diverse kinds of cancer as compared to cisplatin [101, 102]. Consequently, 1,2-diaminocyclohexaneplatinum(II) (oxaliplatin) which has a bidentate leaving group, enhanced water solubility and slower hydrolysis process aiding its cellular uptake level [103-105], was developed. The drug was effective for the treatment of colorectal cancer, a type of cancer which is resistant to cisplatin and carboplatin [106]. Essentially, despite a large of number platinum drugs that are being screened yearly for cytotoxic properties, only cisplatin, carboplatin and oxaliplatin have gained worldwide approval. Others such as nedaplatin, the carboplatin analogue, has been approved in Japan for the treatment of head, neck, lung and oesophageal cancer while lobaplatin has been clinically registered in China [9, 30].

However, because most of these cytotoxic complexes are mainly of *cis*-stereochemistry akin to cisplatin, they are generally still encumbered with many of the flaws that are associated with cisplatin. In fact, some *cis*-configured platinum(II) compounds were recently discontinued from clinical trials because of these limitations that have been highlighted before [9]. Hence, the need to design and develop alternative platinum-based anticancer agents that will exhibit superior cytotoxicity and less toxicity. The structure and pharmacodynamics of these compounds may, however, be much more complex and radically different from those already established for cisplatin and its *cis*-configured derivatives. To achieve the foregoing, there is obviously the demand for a paradigm shift in our thinking.

1.7 Structure-Activity Relationship (SAR): The Paradigm Shift

The thinking among medicinal inorganic researchers that informed the earlier structure-activity relationship with respect to designing and synthesising alternative platinum-based compounds to cisplatin was based on the following:

Firstly, a *cis* configuration, with the general formula *cis*-[PtX$_2$(amine)$_2$] where the X stands for the nucleofuge which are normally in a *cis*-position to each other, is a prerequisite for cytotoxic properties of all platinum(II) compounds. All monofunctional binding cationic complexes were considered inactive. It is generally believed that the nature of the non-leaving groups influences the reactivity of platinum compounds. Since complexes with general formula *cis*-[PtCl$_2$(amine)$_2$] of different ligand systems, such as monodentate ligand (ammine, NH$_3$), bidentate ligands (diethylenediamine, en) or diaminocyclohexane (dach), as non-leaving species, have shown antitumour activity. The activity of these platinum complexes has been found to decrease in the following order NH$_3$>RNH$_2$>R$_2$NH>R$_3$N, where R is an alkyl substituent [107]. In other words, as the steric demands via the alkyl group substitution of the hydrogen atoms on the ammine ligand increases, the cytotoxic properties of the resulting platinum complexes decrease.

Secondly, the nucleofuge, X ligands, such as Cl$^-$, SO$_4^{2-}$ or carboxylate ligands, must be of intermediate strength. This is largely because the ligand exchange kinetics of platinum compounds are mainly determined by the nature of the leaving groups. This follows the rationale that complexes with strong coordinating leaving groups do not have antitumor activity. This is due to the fact that the *trans* effect of the strongly coordinating group will cause prompt substitution of the spectator amine ligand. Similarly, it is believed that weakly coordinating leaving groups, such as water, do not lead to high cytostatic activity [30, 56]. This is because platinum complexes with weakly coordinating ligands react rapidly which makes them to be susceptible to forming by-products with other intracellular components.

Thirdly, the spectator amine ligands are designed to consist of at least one NHR moiety, which is necessary for hydrogen-bonding interactions with DNA via the O6 of guanine and to the 5' phosphate group. It is predominantly accepted that the hydrogen-bonding ability of the ligands, which will normally elicit steric hindrance around the metal centre, is a crucial factor in determining the reactivity of these complexes [20]. The amines can act as hydrogen donors to the O6 atom of a guanine and to a 5' phosphate group in DNA, thus stabilizing platinum-guanine binding [70]. These interactions are critical for the thermodynamic stability of the

resultant platinum-d(pGpG) adduct formed and for the kinetics of the reaction by driving the platinum complex to the target, the N7 of guanine.

Consequently, these factors, especially the first one, became the all-important requirements for the structure of platinum complexes expected to exhibit cytostatic activity according to the initial structure-activity relationships (SARs). However, Farrell and his co-workers were the first to extend the frontier of development of novel anticancer agents which incorporated non-classical platinum complexes such as *trans*-platinum and polynuclear platinum complexes which have shown remarkable cytostatic potentials even against cisplatin resistant cell lines[108, 109]. He suggested that the cytotoxic potential of *trans*-platinum complexes could be greatly enhanced by bulky spectator monodentate amine ligands. Recent reports indicating some *trans*-platinum(II) compounds with superior cytostatic activity relative to most *cis*-configured complexes [18] have made synthetic inorganic chemists, nowadays, to jettison the earlier held notion that only *cis*-configured complexes, in which the leaving groups are at *cis*-position to each other, can show anticancer activity.

1.8 Unconventional Platinum-Based Anticancer Agents

The classical structure-activity relationship which has led to the production of the analogues of cisplatin, some of which are either now in clinical trials or currently being administered in anticancer chemotherapy, is presently being reckoned obsolete. This idea is fundamentally flawed because the greater number of the drugs produced from this notion have not transcend most of the defects of cisplatin, let alone achieve superior cytotoxicity and wide applicability against different cancer types. Hence, the expansive interest among medicinal inorganic chemists to explore, in tandem, other unconventional metal-based complexes and alternative platinum-based compounds of non-classical structures, in the anticancer research. Most importantly, this research effort is focused on those alternative platinum-based anticancer agents, particularly the development of *trans*-platinum(II) complexes in anticancer chemotherapy. These complexes can display a distinct mechanism of action in their interaction with DNA and possibly could be active against different spectrums of anticancer cells as compared to cisplatin and its derivatives. Besides the *trans*-platinum(II) complexes, other non-classical platinum-based complexes, such as platinum(IV) complexes, monofunctional platinum(II) complexes and multinuclear platinum compounds shall be briefly discussed.

1.8.1 Platinum(IV) Complexes

The cytotoxic potentials of platinum(IV) complexes are not really new as far as anticancer research is concerned. When Rosenberg and his co-workers serendipitously discovered the biological activity of cisplatin, some platinum(IV) complexes were actually present in the mixture of platinum complexes that inhibited the growth of *E. coli* during the electrolytic process using platinum electrodes. However, it is only until recently that interest in their deployment as anticancer drugs is becoming more attractive among medicinal inorganic researchers. Platinum(IV) complexes have low-spin d^6 metal centres which usually assume octahedral geometry with six coordinating ligands, unlike platinum(II) complexes that normally adopt square-planar geometry because of their low-spin d^8 metal centres. The ligand system around the platinum(IV) centre mostly consists of two spectator or non-leaving group ligands, two leaving groups and two axial ligands.

The axial ligands are only peculiar to platinum(IV) complexes and normally possess some biological importance because some of these ligands can interact with DNA via an intercalative mode of binding. The addition of one or two biologically active ligands within the platinum(IV) scaffold can generate what is now referred to as "dual-threat" platinum(IV) compounds [30]. Examples of some dual-threat platinum(IV) complexes include: ethacraplatin, chalcoplatin, mitaplatin, endothall platinum(IV) complex, etc. The biologically active axial ligands in these complexes are particularly incorporated in their structures to have the non-DNA targets so as to limit cross-resistance with the DNA-targeting platinum(II) species released. In addition to this, the inclusion of the axial ligands with the platinum(IV) scaffold enhances the lipophilicity, redox stability, solubility and cancer-cell targeting of the drugs. Formation of by-products, other than the expected platinum-DNA adducts, are mostly minimised in the platinum(IV) complexes because of the kinetically inert nature of its coordination sphere which make them resistant to ligand substitution reactions by the biomolecules. It is widely accepted that the extra two axial ligands in platinum(IV) complexes enhance their ability to attach to nanoparticles or other carrier agents.

Furthermore, the two non-leaving group and the two leaving group ligands at the platinum(IV) centre are mostly similar to those of platinum(II) complexes. The non-leaving groups are designed to enhance, inter alia, the resistance profile, the solubility and the lipophilicity of the compound. One key aspect of the function of the non-leaving group ligands is that they help to determine the nature of the platinum-DNA adduct form from the interaction of the drug with

the target biomolecule, the DNA. The leaving group ligands, on the other hand, assist to determine the following viz. the toxicity profile, lipophilicity and the solubility of the drug. More importantly, the leaving group ligands govern the reaction kinetics of the platinum(IV) complexes, just like in other platinum compounds.

Initially, each of the two non-leaving group and the leaving group ligands in the platinum(IV) complexes are patterned like those of cisplatin i.e. they are of *cis*-geometry. Currently, some platinum(IV) compounds are designed to include other conformations, such as those in which the leaving and the non-leaving groups are of *trans* configurations, those in which the non-leaving group ligand is bidentate and those with mono functional centre i.e. having only one leaving group. Moreover, the reactivity of the platinum(IV) complexes with DNA and other biomolecules depend on their reduction and substitution rates. The inert nature of the platinum(IV) centre makes the chances of direct platination of DNA and other biomolecules in that oxidation state nearly impossible because the adducts that are formed through ligand substitution will normally occur in weeks. This would have, consequently, made the drug of no clinical value given that the platinum drug has a very low retention time in the body.

However, the simultaneous reduction of platinum(IV) to platinum(II) coupled with the substitution of the leaving group ligands, has been considered to be crucial for the cytotoxic activity of platinum(IV) compounds. It is widely accepted that the reduction of platinum(IV) to platinum(II) through the removal of the two axial ligands, facilitates the binding of the resultant divalent complex to bind to DNA which impede transcription and replication and subsequently initiate apoptotic processes in the cancer cell. The nature of the axial ligands was initially thought to influence the reduction process. Nonetheless, more recent studies have disabused researchers of that notion. By and large, platinum(IV) complexes are essentially seen as pro-drug because they are useful as anticancer agents after the reduction of the platinum centre from the oxidation state of IV to give a more active divalent form of the drugs.

Some remarkable platinum(IV) complexes, such as ormaplatin, iproplatin, LA-12 and satraplatin, have recently undergone clinical trials. Tetraplatin, tetrachloro(trans-1,2-diaminocyclohexane)platinum(IV), commonly referred to as ormaplatin was among the first platinum(IV) drugs to enter into clinical screening. The reduction of tetraplatin to a more active divalent specie, dichloro(*trans*-1,2-diaminocyclohexane)platinum(II) which is related to Oxaliplatin but for the display of isomerism, is quite fast and instantaneous. The platinum(IV) drug has half-lives of 5-15 minutes and 3 seconds In vitro and In vivo respectively. It has been

found to be active against some cisplatin-resistant cell lines. However, the drug is still encumbered with some toxic behaviour, such as neurotoxicity, which is believed to have risen from its rapid reduction to the divalent form resulting from the loss of the two axial chloride ligands.

Figure 1.5:   Chemical structures of platinum(IV) agents that have undergone clinical trials [30].

Iproplatin, *cis,trans,cis*-dichlorodihydroxobis(isopropylamine)platinum(IV), is a slight modified form of ormaplatin where the two axial chloride ligands have been changed to hydroxide ligands and the *trans*-1,2-diaminocyclohexane was modified to diisopropylamine. The two hydroxide axial ligands make the reduction in the platinum(IV) complex to be less rapid and subsequent deactivation by reducing biomolecules, compared to ormaplatin. The drug is well circulated throughout the body as a result of its slower deactivation. The hydroxide ligands also enhance the solubility of the drug in the body. Despite these advantages, the general conclusion at the final stage of its clinical trials is that the drug lacks the overall effectiveness that transcend those already established for cisplatin and carboplatin.

Satraplatin and LA-12 are quite synonymous except that in the latter the cyclohexylamine is substituted with adamantylamine. LA-12, *trans,cis,cis*-bis(acetato)ammineadamantylamine platinum(IV), is currently in the first phase of its clinical trials. Satraplatin, *trans,cis,cis*-bis(acetato)amminecyclohexylamineplatinum(IV), on the other hand, was the first platinum-based drug whose intrinsic lipophilicity and stability makes it appropriate for oral administration. Satraplatin undergo reduction by some biological reducing agents, such as ascorbate, with a half-life of 50 minutes which is suitable for the platinum(IV) drug to be absorbed into the bloodstream. Once the drug enters the bloodstream, it is reduced to six different divalent platinum forms. The one equipped with the most cytotoxic properties of the

six divalent platinum species is the ammine(cyclohexylamine)dichloroplatinum(II) arising from the removal of the two axial acetate ligands. Satraplatin was found to exhibit superior cytostatic activity against some human cisplatin-resistant cancer cell lines and less toxic than cisplatin at both *In vitro* and *In vivo* studies respectively. Its mechanism of action was, however, found to be similar to that of cisplatin involving DNA cross-links, DNA distortion leading to the obstruction of transcription and replication of the DNA. It is widely accepted that satraplatin is able to overcome cisplatin resistance because of the asymmetrical nature of the DNA adducts formed from its interaction with DNA which can circumvent recognition by DNA repair proteins such as high-mobility group proteins. Despite a few successes experienced from the clinical phase trials by satraplatin, the overall effectiveness and side effects are still in doubt. Attempts to combine it with other cytostatic drugs, such as prednisone, has not yielded much success either because rather than the expected synergistic effect between the drugs, the overall effectiveness of the combined therapy was less than the use of the individual drug alone.

1.8.2   Monofunctional Platinum(II) Complexes

Monofunctional platinum(II) complexes are a recent category of prospective antineoplastic compounds which incorporate only one leaving group ligand in their structures. They consist of only one platinum centre. Owing to the one leaving group ligand, they are anticipated to interact with the DNA via only one covalent bond. Generally, most other categories of platinum-based cytostatic agents can form both monofunctional and bifunctional adducts with the DNA. However, the monofunctional platinum(II) complexes via their motif can only form monofunctional platinum-DNA adducts. According to the early SARs, all monofunctional platinum complexes were reckoned to be lacking cytotoxic properties because certain monofunctional platinum(II) complexes, such as $[Pt(NH_3)_3Cl]^+$ and $[Pt(dien)Cl]^+$ were found to be inactive both In vitro and In vivo [30]. However, research conducted by Engelhard Industries, revealed that monofunctional platinum(II) complexes with general formula cis-$[Pt(NH_3)_2(Am)Cl]^+$, where Am is an aromatic N-heterocyclic amine, inhibited tumour cell growth In vitro and in certain leukemia cancer cell lines in mouse [30]. Consequently, cis-[Pt-$(NH_3)_2$(9-aminoacridine)Cl] $^+$ and cis-[Pt-$(NH_3)_2$(chloroquine)Cl]$^+$, were synthesised and observed to interact with DNA via both monofunctional covalent bond formation and intercalative mode. However, other studies [110, 111] suggested that there was the possibility of the formation of bifunctional adducts via the loss of one of the ammine ligands after the

initial covalent bond interaction with the DNA. This suggestion was quickly quashed through the NMR analysis of some adducts formed by monofunctional platinum(II) complexes with DNA. The NMR spectra clearly showed no evidence of the release of either of the ammine ligands for the possibility of bifunctional adduct formation. More recently [112], monofunctional platinum(II) complexes, such as pyriplatin, phenanthriplatin, Pt-ACRAMTU and derivatives etc. are currently being studied for their anticancer potentials (**Figure 1.6**).
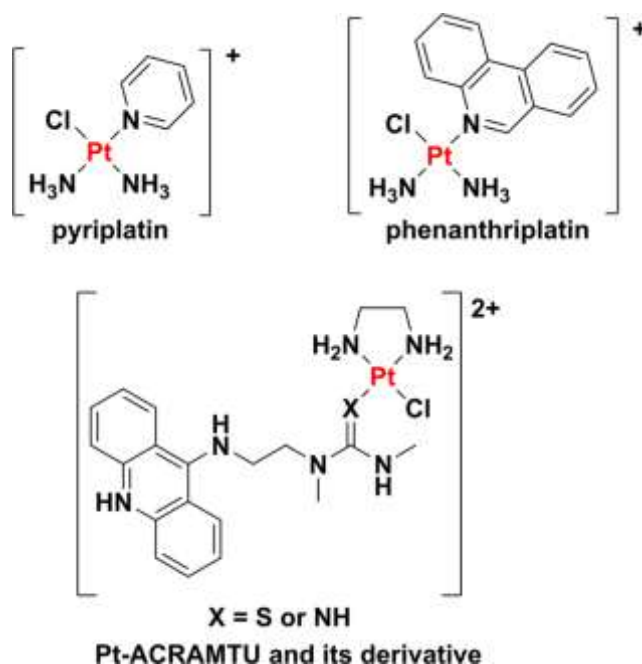
Figure 1.6:   Chemical structures of some monofunctional platinum(II) complexes [30].

1.8.3   Non-functional Mononuclear Platinum(II) Compounds

The non-functional mononuclear platinum(II) complexes, commonly referred to as metallointercalators, another class of alternative platinum-based cytostatic agents, are beginning to attract significant attention amongst medicinal inorganic chemists. They are essentially of the general formula $[Pt(I_L)(A_L)]^{2+}$, where I_L is referred to as the intercalating ligand and A_L is known as the ancillary ligand. These complexes have only one platinum centre and do not incorporate any known leaving group ligands in the structural motif. They mainly interact with the DNA via a noncovalent intercalative mode of binding. Metallointercalators with π-conjugated heterocyclic ligands, such as bipyridine, terpyridine, and phenanthroline, employ $\pi-\pi$ stacking and dipole−dipole interactions to intercalate between base pairs in double-

stranded DNA. The π-conjugated heterocyclic ligands allow these platinum(II) compounds to unwind, bend, and distort the arrangement within the DNA structure, and it is their structural effect on DNA that is believed to mediate their antineoplastic properties. Examples of some metallointercator complexes include: $[Pt(BDI^{QQ})]^+$, PHENRR and the PHENSS series etc.(**Figure 1.7**).
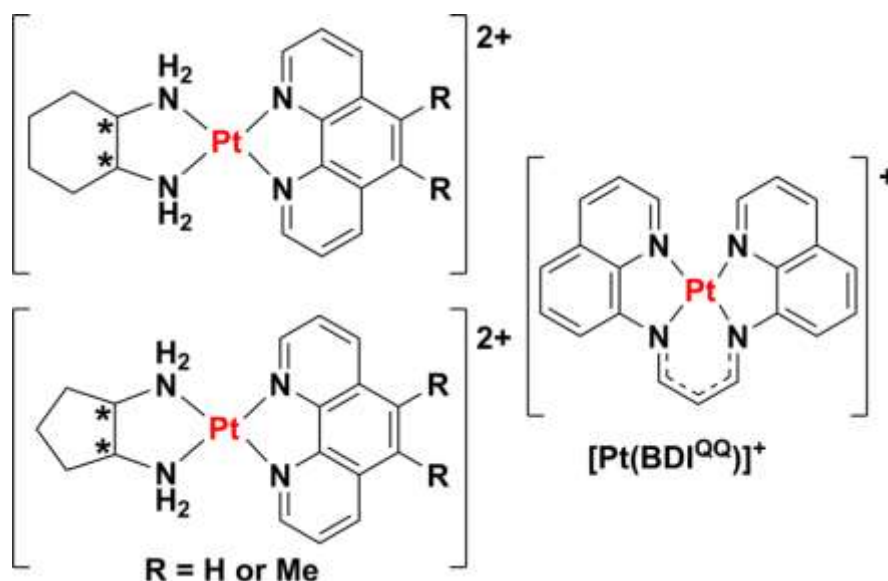
Figure 1.7:   Chemical structures of non-functional platinum(II) complexes that bind to DNA through noncovalent interactions [30].

1.8.4   Multinuclear Platinum Compounds

Farrell and his co-workers were the first to extend the frontier of development of novel anticancer agents which incorporated non-classical platinum complexes, such as *trans*-platinum and polynuclear platinum complexes. Some of these complexes have showed remarkable cytostatic potentials even against cisplatin resistant cell lines. Ever since Farrell *et al.* developed the trinuclear BBR3464 and its dinuclear analogues namely: BBR3571 and BBR3610 (**Figure 1.8**), research activities are now being centred around developing more multinuclear platinum(II) complexes which can show tremendous potential in cancer chemotherapy [87]. The multinuclear platinum complexes are more water soluble and exhibit better DNA interactions because of certain features, such as high charge, hydrophilicity and/or flexibility, in comparison to cisplatin [30, 87, 113]. The earlier multinuclear compounds that were synthesised by Farrell *et al.* contain *trans*-[Pt(NH$_3$)$_2$Cl] units with bridging alkanediamine

linkers of variable length, designed to facilitate long-distance, flexible intrastrand and interstrand cross-links. Such adducts cannot be formed by classical mononuclear platinum(II) compounds, such as cisplatin and transplatin. The dinuclear platinum(II) complexes, such as BBR3535, *trans*-[(PtCl(NH$_3$)$_2$)$_2$μ-(H$_2$N(CH$_2$)$_4$NH$_2$)]Cl$_2$ can form 1,2-, 1,3-, and 1,4-interstand cross-links between guanines on opposite strands [30, 114, 115]. The 1,3- and 1,4-cross-links with guanines are separated by one and two nucleobase pairs, respectively, whereas the 1,2-cross-link is formed between guanines of neighbouring nucleobase pairs [30]. These unconventional DNA adducts facilitate the dinuclear platinum(II) complex to circumvent cisplatin resistance in certain cancer cells, such as ovarian cancer [30, 116]. To improve the DNA binding ability of the dinuclear platinum(II) complexes, the trinuclear platinum(II) series, such as BBR3464, were synthesised by incorporating a third platinum centre within the alkanediamine linker scaffold. Both the *di-* and *tri*-nuclear platinum(II) complexes were quite successful in their preclinical trials and have, subsequently, undergone different stages of clinical developments. However, none of them, including the BBR3464 despite its initial success at the phase I and II clinical trials, have not been advanced for full human use.
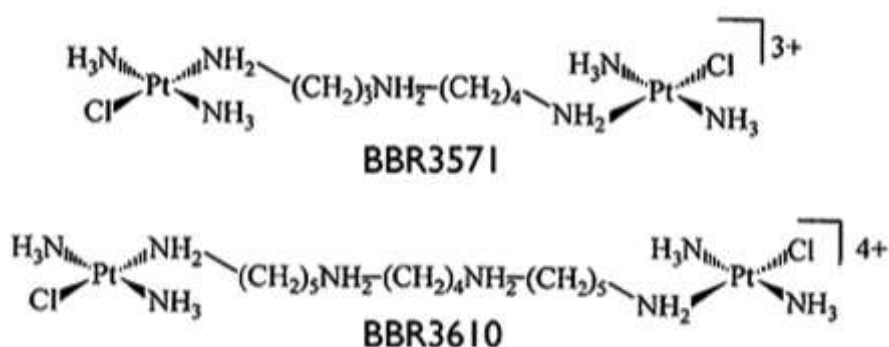
Figure 1.8:   Structure of dinuclear complexes: BBR3571 and BBR3610 [117].

Following the success of these multinuclear complexes with at least one leaving group ligand on at least two of the platinum(II) centres, some multinuclear platinum(II) complexes, that are based on BBR3464 (**Figure 1.9**), in which each of the labile chloride ligands on the platinum(II) complexes have been replaced by ammine ligands were synthesised. These complexes, such as TriplatinNC and TriplatinNC-A (**Figure 1.9**), react with the DNA noncovalently via electrostatic and hydrogen-bonding interactions. The terminal platinum units are believed to form distinct amine-phosphate-ammine binding patterns called "phosphate clamps" within the

minor groove, which induce B-to-A and B-to-Z conformational changes in canonical DNA sequences. These trinuclear complexes can also condense DNA and induce aggregation of small transfer RNA molecules because of their high cationic nature. These highly charged complexes exhibit micromolar toxicity against cisplatin-sensitive and cisplatin-resistant ovarian cancer cells [30, 118]. Their ability to overcome cisplatin resistance was attributed to their high cellular accumulation, presumably because of their cationic nature and their unique mode of binding to DNA.
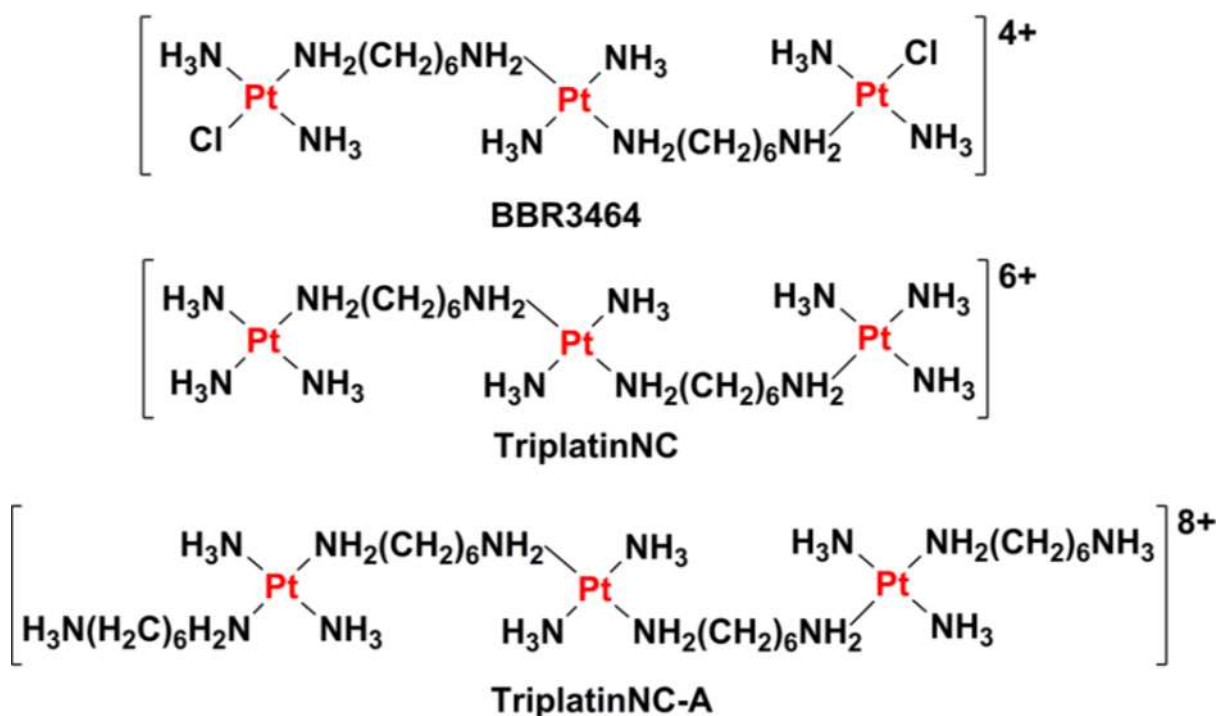
Figure 1.9:   Chemical structures of trinuclear platinum agents. The pendant aliphatic groups of TriplatinNC-A are shown in the protonated state, raising the overall charge of the complex to 8+ [30].

1.9 *Trans*-Platinum Complexes: The Veritable Alternative to *Cis*-Configured Platinum Complexes

For well over two decades after the accidental realisation of the antineoplastic properties of cisplatin, all platinum(II) complexes of *trans* stereochemistry were presumably considered inconsequential as far as development of new cytostatic agents were concerned [18, 119]. This was justifiably so because transplatin, which is the *trans* isomer of cisplatin, was observed to

be biologically inactive [120-127]. Therefore, research efforts to understand its lack of activity led to the following widely accepted findings [108, 119, 121, 126, 128-130]: One, the kinetic instability of the transplatin makes it susceptible to prompt deactivation by other biomolecules before it could reach its target- the DNA; Two, the formation of platinum-DNA adducts with a distinct regioselectivity and stereochemistry that is different from those already established for cisplatin; and three, transplatin was typically non-toxic. However, the limitations of cisplatin and derivatives, such as severe side effects, lack of selectivity, inherent and acquired resistance etc., spurred the need amongst medicinal inorganic chemists to seek an alternative platinum-based drugs with improved selectivity and display a distinct mechanism of action from that of cisplatin. Based on these criteria, the anticancer potential of t*rans* platinum complexes was revisited since the non-toxic behaviour of transplatin coupled with its regioselectivity and distinct binding mode to DNA makes this class of platinum compounds appear promising. Farrell and his group were the first to report the anticancer activity of some *trans* platinum(II) complexes of general formula [PtCl$_2$L$_2$] that showed significant cytotoxic properties, where L is a planar heterocyclic ligand such as pyridine, thiazole, quinoline etc. [108, 131-136]. They believed that incorporating bulky monodentate amine ligands into the structure of transplatin, can reduce its kinetic instability and once this is achieved, the distinct DNA binding mode of these complexes can then be an additional advantage. He also pioneered some dinuclear platinum(II) compounds in which the two chloride leaving group ligands have *trans* orientation [109]. The latter marked the beginning of polynuclear platinum-based complexes in anticancer research. Much later, Navarro-Ranninger and his co-workers reported a new class of biologically active *trans*-platinum(II) complexes with asymmetric aliphatic amines, *trans*-[PtCl$_2$(L)(L') [137]. The reports of these active *trans* platinum complexes made the earlier SARs pioneered by Cleare and Hoescheles [138, 139] to be altogether discarded and consequently, many prospective *trans* platinum compounds are being developed including those of the platinum(IV) prodrug which on reduction furnishes divalent platinum species with *trans*-geometry.

This subsection presents an overview of biologically active platinum(II) compounds of *trans*-geometry in anticancer research. The historical development of these active *trans*-platinum(II) complexes, some of which were designed and prepared as platinum(IV) prodrugs and/or multinuclear platinum(II) complexes, will be examined sequentially in the following subunits.

1.9.1 *Trans*-Platinum(II) Complexes with General Formula *trans*-[PtCl$_2$(L)(L')] where L = N-Donor Aromatic Heterocycle and L' = Ammine, Sulphoxide or a Second Molecule of L Ligand)

Farrell and his group [108, 116, 131, 132, 134-136, 138, 139] were the first to be designed and synthesised *trans*-platinum(II) complexes consisting of three different series of compounds which include: Firstly, L = L' = pyridine (**1**), N-methylimidazole (**2**), or thiazole (**3**); Secondly, L = quinoline and L' = RR'SO (R= Me, R' = Me, Bz, or Ph) (**4**) and; Thirdly, L = quinoline (**5**) or thiazole (**6**) and L' = NH$_3$ (**Figure 1.10**). The design of these complexes follows a simple replacement of one and/or both ammine ligands in transplatin with bulky planar nitrogen donor ligands and/or with aliphatic/aromatic sulphur containing ligands.
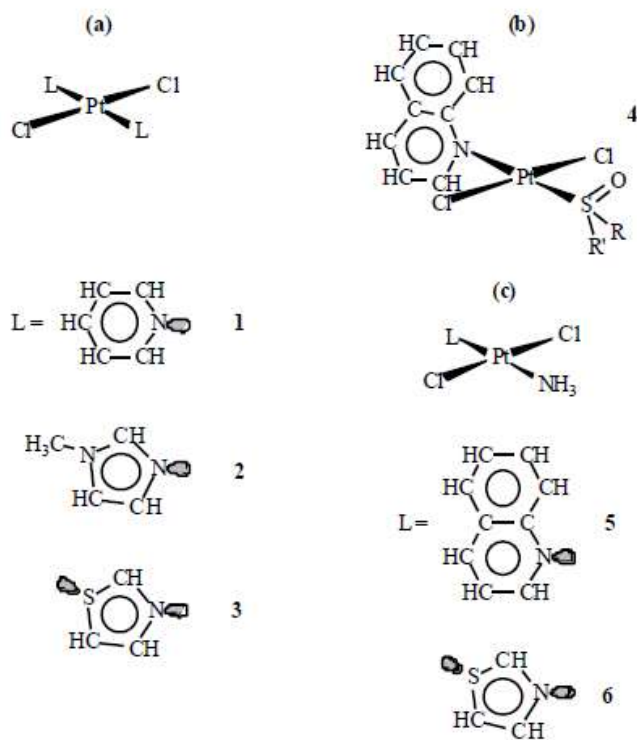
Figure 1.10:   Structures of *trans*-platinum(II) complexes with symmetric and asymmetric N- and S-donor aromatic heterocycles [140].

Table 1.1: IC$_{50}$ values for compounds 1, 3. 4, 5 as compared to transplatin and cisplatin

1	HX/62	SKOV-3	PXN94	41M	41McisR	CH1	CH1cisR	L1210	L1210cisR
1	4.5	5.9	7.7	2.2	2.0(0.91)	1.6	1.7(1.1)		
3	4.1	6.2	9.6	2.2	1.6(0.73)	1.3	1.4(1.1)		
4	5.1	4.4	8.2	1.32	1.9(1.4)	0.89	1.0(1.1)		
5								0.51	1.35(2.65)
transplatin	245	255	222	57	69(1.2)	30	68.5(2.3)	15.7	22.0(1.40)
cisplatin	12.6	4.4	3.0	0.23	1.4(6.1)	0.1	0.67(6.7)	0.33	9.22(28)

Values are IC50 (at least three independent experiments) in mM (96 h drug exposure for all cell lines except for L1210 and L1210cisR for which the exposure time was 72 h). Values in parentheses are resistance factors (RF = IC50 resistant/IC50 sensitive parent line). [140]

The resulting *trans*-platinum(II) complexes produced were of remarkable cytotoxicity similar to those of their corresponding *cis*-analogues and cisplatin. In fact, some derivatives, such as *trans*-[PtCl$_2$(NH$_3$)L] and *trans*-[PtCl$_2$L$_2$], where L = pyridine, quinoline, isoquinoline, thiazole, or benzothiazole exhibited remarkable cytotoxic behaviour in cisplatin- and oxaliplatin-resistant cell lines. From the results shown in **Table 1.1**, these *trans*-platinum(II) complexes were found to be nearly hundred times more active than transplatin, and of comparable activity to cisplatin, in certain murine and human tumour cell lines. Reports from the National Cancer Institute (NCI) panel on human tumour cell line testing studies revealed that these *trans*-platinum(II) compounds demonstrated a wide range of antineoplastic activity that is entirely different from that of any other anticancer agents. The distinctive cytotoxicity profiles of these complexes are not only attributed to their structure but to the way to it binds to DNA in cancer cells.

Furthermore, it is quite interesting to realise that the substitution of one of the ammine ligands by quinolone and thiazole is enough to bring about such a phenomenal improvement in the cytotoxicity of *trans*-platinum compounds. Also remarkable is the display of activity, *In vivo*, against the leukaemia cell line by the complex formed from the thiazole substitution. This has quashed the presumption that *trans* complexes cannot show any In vivo anticancer activity. Similarly, *In vitro* studies in cultured breast cancer cells revealed that these *trans* complexes with bulky N-donor heterocyclic amine ligands formed DNA-topoisomerase I cross-links that are capable of causing a DNA strand to break and induce apoptosis. These ternary DNA−protein

cross-links are not observed following cisplatin treatment and thus, characterise the uniqueness of these *trans*-platinum(II) complexes.

1.9.2 Some Platinum(IV) Complexes with *Trans*-Geometry

A bid to achieve orally active platinum drugs has led to the design of some platinum(IV) complexes with *trans* geometry of leaving group ligands. A series of platinum-based compounds consisting of platinum(IV) complexes and their corresponding *trans*-platinum(II) analogues were synthesised and investigated for their cytostatic activity *In vitro* and *In vivo* respectively (**Figure 1.11** and **Table 1.2** for selected compounds) [32]. Several of the platinum(IV) complexes were observed to exhibit a potency comparable to that of cisplatin when they were tested against a group of human ovarian carcinoma cell lines (SKOV-3, A2780, HX/62, CH1, and 41M) [140]. However, most of their corresponding *trans*-platinum(II) analogues did not show any activity. The antineoplastic efficacy of the platinum complexes towards pairs of cisplatin sensitive/resistant human ovarian cancer cell lines (41M/41McisR, CH1/CH1cisR, and A2780/A2780cisR) was also investigated to determine the Resistance Factor (RF).
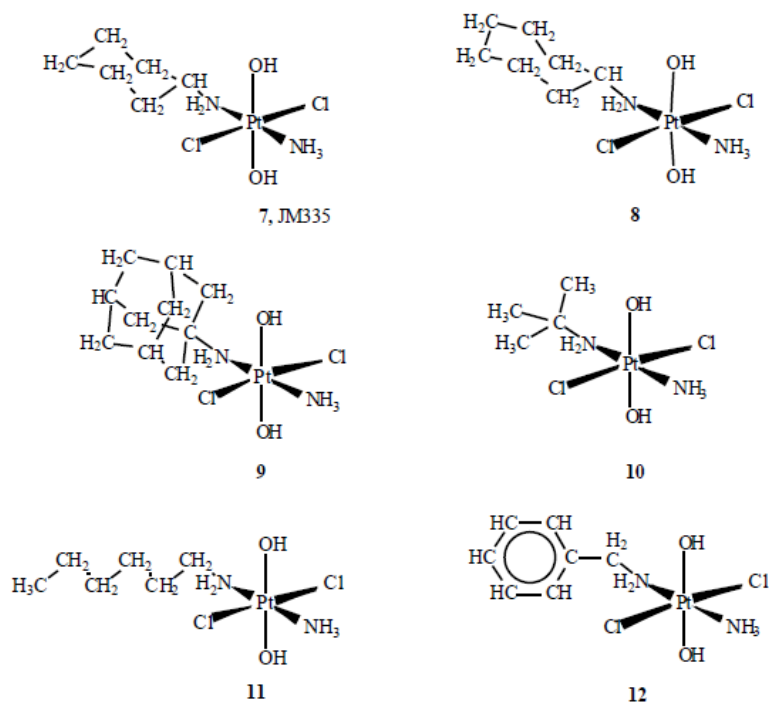
Figure 1.11: Structures of *trans*-platinum(II) complexes with symmetric and asymmetric N- and S-donor aromatic heterocycles [140].

23

Table 1.2: IC$_{50}$ mean values (±SD) for compounds 7-12 as compared to transplatin and cisplatin

	HX/62	SKOV-3	4IM	4IMcisR	CH1	CH1cisR	A2780	A2780cisR
7	4.4±0.5	6±0.9	1.3±0.13	1.4±0.12 (1.1)	1.1±0.33	2.1±0.2 (1.9)	0.42±0.07	3.0±0.26 (7.1)
8	3.4	3.9	1.3	1.4 (1.1)	1.1	1.7 (1.5)	0.61	2.5 (4.2)
9	1.2	2.5	0.84	1.3 (1.5)	0.44	0.62 (1.4)	0.49	1.6 (3.3)
10	1.8	4.7	1.1	0.9 (0.8)	0.74	1.62 (2.2)	0.21	4.2 (20)
11	14.2	10.3	4.6	4.4 (1)	3.7	5.4 (1.4)	1.9	6.4 (3.3)
12	10.2	8.2	1.3	1.3 (1)	1.1	1.9 (1.7)	1.1	4.2 (4)
transplatin	245±45	255±77	57±18	70±13 (1.2)	30±38	68.5±11 (2.3)	32±8	260±46 (8.1)
cisplatin	12.6±2.9	4.4±3.1	0.26±0.078	1.2±0.4 (4.7)	0.11±0.02	0.71±0.2 (0.4)	0.33±0.1	5.2±1.3 (15.7)

Values are IC$_{50}$ values (at least two experiments) in mM (96 h drug exposure). The numbers in parentheses are the resistance factors (RF = IC$_{50}$ resistant line/IC50 sensitive parent line) [140, 141].

The cancer cell lines selected were typical of the major mechanisms of resistance to cisplatin. 41McisR cells have been known to show resistance against cisplatin mainly because of reduced drug accumulation. Still in the same vein, CH1cisR cells display resistance to cisplatin through enhanced DNA repair/tolerance while A2780cisR cells, on the other hand, show resistant to cisplatin via a combination of decreased accumulation, enhanced DNA repair/tolerance, and elevated glutathione levels [142, 143]. Most of the *trans*-platinum(IV) complexes exhibited potency that completely overcome the cisplatin resistance of 41McisR and CH1cisR (RF of *ca*. 1.5), but were able to overcome that of A2780cisR, only to a certain extent (**Table 1.2**). Fourteen *trans*-platinum(IV) complexes, possessing axial hydroxide ligands, displayed remarkable *In vivo* antitumour activity against the subcutaneous murine ADJ/PC6 plasmacytoma model. Nevertheless, the *trans*-platinum(IV) complex, having axial ethylcarbamate ligands, did not show any activity against murine cell line.

Surprisingly, all the *trans*-platinum(II) and *trans*-platinum(IV) complexes possessing dichloro and tetrachloro ligands were found to be inactive. Three of the *trans*-platinum(IV) complexes **7-9,** (see **Figure 1.11**) maintain some potency against a cisplatin resistant variant of the ADJ/PC6 plasmacytoma and several others exhibited antitumour activity against subcutaneously grown advanced-stage human ovarian carcinoma xenografts. Interestingly, complex **7** which is known as JM335, has been reported to be the first *trans*-platinum complex

showing significant *In vivo* antitumour activity towards models of acquired cisplatin resistance [144].

1.9.3 *Trans*-Platinum(II) Complexes with Asymmetric Aliphatic Amine Ligands of the General Formula *trans*-[PtCl₂(L)(L')]

Transplatin derivatives with aliphatic amines, such as *trans*-[PtCl₂(isopropylamine)(L')] (L'=dimethylamine, isopropylamine, or propylamine) denote another category of *trans*-platinum(II) complexes that have shown remarkable cytotoxic properties [137, 145, 146]. These complexes (**Figure 1.12**) were found to have comparable activity in cisplatin sensitive cells to that of cisplatin and significantly higher than that of cisplatin in several cisplatin resistant cancer cells (**Table 1.3**). Compound **13** was observed to circumvent cisplatin resistance in cell lines, such as HL60 human leukemic cells and Pam 212-*ras* murine keratinocytes, which are *ras*-related resistance through its ability to form interstrand cross-links within a short time as compared to cisplatin [137]. Similarly, the complex was found to exhibit superior cytotoxicity against the multifactorial cisplatin resistance and other *ras*-related resistance. However, detailed *In vivo* studies have not been done on these promising *trans*-platinum(II) cytostatic agents.
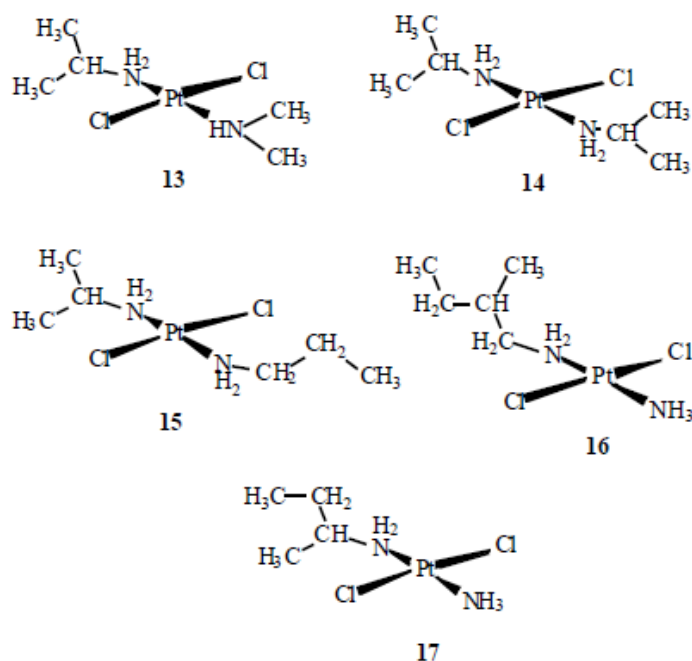
Figure 1.12: Structures of *trans*-platinum(II) complexes with asymmetric aliphatic amine ligands [140].

Table 1.3: IC$_{50}$ Mean Values (±SD) for Compounds 18-23 (**Figure 1.12**)

	HL-60	JURKAT	HeLa	VERO	PAM212	PAM212-ras	A2780	A2780cisR	CH1	CH1cisR
13	17±2	5±0.3	32±3 (1.9)	47±4	56±2	6±0.5				
15	20±2	5±0.4	43±3	52±4	50±3	32±1				
16							1.7	9.3(5.5)	4.2	15.1(3.6)
17							2.1	15.5(7.4)	5.5	18.0(3.3)
Transplatin	50±3	22±0.7	89±4	148±6	123±5	164±8	>200	>200	>200	>200
cisplatin	25±1	7±0.3	38±1	50±3	114±3	156±6	2.2	38(17.3)	6.0	23.0(3.8)

Values are IC$_{50}$ Values in mM (24 h incubation time). The numbers in parentheses are resistance factors (RF = IC$_{50}$ resistant line/IC$_{50}$ sensitive parent line [137,147].

1.9.4 *Trans*-Platinum(II) Complexes with Mixed Amine Ligands of the General Formula *trans*-[PtCl$_2$(L)(L')] Containing Non-planar and Planar N-donor Amine Ligands

T*rans*-Platinum(II) complexes with asymmetric amine ligands were observed to have problems, especially in aqueous medium despite their effective antineoplastic activities [140]. Hence, water soluble platinum complexes which are able to interact rapidly with DNA and form DNA adducts different from those formed by cisplatin and transplatin, were designed and synthesised. These cationic *trans*-platinum(II) complexes consist of non-planar and planar amine ligands [148] (**Figure 1.13**). The ligand systems, L and L', around the platinum centre consist of piperazine, L and a variation of the L' ligands from non-planar, cyclic and non-cyclic, to planar N-donor amine ligands. The choice of piperazine as a fixed ligand in this class of *trans*-platinum(II) complexes was informed by the following: Firstly, the positive charge on the non-coordinating nitrogen would enhance solubility in aqueous medium and facilitate rapid interaction with the polyanionic DNA; Secondly, piperazine is a nonplanar cyclic amine ligand that is flexible and has a hydrogen bond donor that can react with the DNA to possibly form new types of lesions and; Thirdly, it is bulky enough to influence the substitution of the chloride ligands [149].

Table 1.4: IC$_{50}$ Mean Values ($\pm$SD) for Compounds 18-23

	A2780	A2780cisR	CH1	CH1cisR	41M	41McisR
18	5 ± 1	44 ± 4 (8.8)	12 ± 3	34 ± 4 (2.8)	52 ± 5	155 ± 12 (3.0)
19	16 ± 2	28 ± 2 (1.8)	17 ± 2	19 ± 3 (1.1)	32 ± 5	48 ± 3 (1.5)
20	14 ± 1	30 ± 2 (2.1)	10 ± 1	50 ± 3 (5.0)	38 ± 3	122 ± 8 (3.2)
21	18 ± 2	64 ± 5 (3.6)	22 ± 3	85 ± 7 (3.9)	37 ± 4	118 ± 9 (3.2)
22	10 ± 3	24 ± 3 (2.4)	16 ± 2	43 ± 3 (2.6)	45 ± 3	147 ± 10 (3.3)
23	17 ± 3	43 ± 3 (2.5)	26 ± 2	53 ± 3 (2.0)	43 ± 3	153 ± 10 (3.6)
24	5 ± 0.7	20 ± 2 (4.0)	15 ± 2	94 ± 6 (6.0)	27 ± 2	150 ± 8 (5.5)
26	7 ± 1	80 ± 5 (11)	22 ± 3	154 ± 8 (7.0)	37 ± 4	118 ± 9 (3.2)
Transplatin	>200	>200	>200	>200	>200	>200
cisplatin	2.2 ± 0.6	38 ± 3 (17.3)	6 ± 1	23 ± 3 (3.8)	26 ± 2	107 ± 8 (4.1)

IC$_{50}$ values in mM (24 h incubation time). The numbers in parentheses are the resistance factor (RF = IC$_{50}$ resistant/IC$_{50}$ sensitive parent line) [150, 151].

One of the most active complexes among this category of *trans*-platinum(II) compounds is Compound **19,** illustrated in Figure 1.13. The complex has the ability to overcome cisplatin-resistance resulting from reduced accumulation of the drug and enhanced DNA repair/damage tolerance (**Table 1.4**). Besides *trans*-platinum compounds having piperazine ligand, other compounds containing a piperidine and/or a 4-Me-pyridine were also synthesised viz. *trans*-[PtCl$_2$(piperidine)(L')] (L' = ammine or 4-Me-pyridine) and *trans*-[PtCl$_2$(NH$_3$)(4-Me-pyridine)] compounds **24**, **25**, and **26** (**Figure 1.13**). These compounds were observed to show potential for superior cytotoxic activities against human ovarian carcinoma (OV-1063) and colon carcinoma (C-26) cancer cells [148]. Moreover, compounds **24** and **26** circumvent, to some extent, cisplatin resistance of A2780cisR cells but are highly cross-resistant to cisplatin in the case of CH1cisR and 41McisR cells respectively (**Table 1.4**) [150].
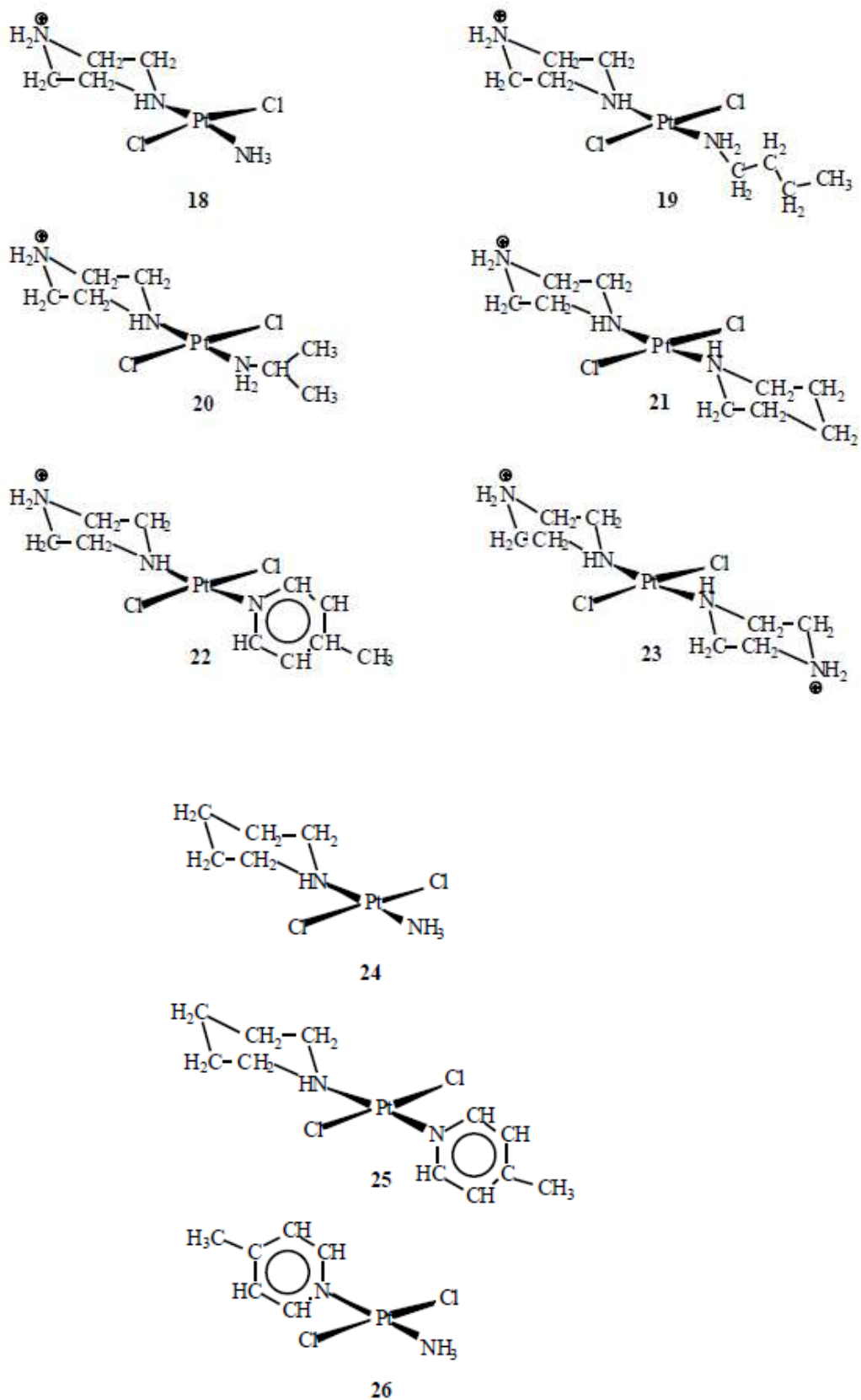
Figure 1.13: Structures of *trans*-platinum(II) complexes with mixed planar and non-planar amine ligands [140, 148-150].

1.9.5 *Trans*-Platinum(II) Complexes with Iminoether Ligands General Formula *trans*-[PtCl$_2$\{HN=C(OR)R'\}$_2$] or *trans*-[PtCl$_2$(NH$_3$)\{HN=C(OR)R'\}]

In order to improve on the solubility of the foregoing *trans*-platinum(II) compounds, the acetate ligands were introduced into the structure as the leaving group instead of the chloride ligands. Surprisingly, these complexes are similar to carboplatin except for the fact that they are of *trans* geometry. The *trans*-platinum(II) complexes with iminoether ligands maintained the cytotoxicity profile of the parent chloro complexes despite the slight modification of their structures to overcome solubility problems. Some of these complexes have one or two iminoether ligands and are of the general formula *trans*-[PtCl$_2$\{HN=C(OR)R'\}$_2$] or *trans*-[PtCl$_2$(NH$_3$)\{HN=C(OR)R'\}] (compounds **27**-**29** in **Figure 1.14**). The iminoether ligand can exist in two different conformations- E and Z, because of the non-symmetrical nature of the groups around the imine (C=N) bond. Consequently, the platinum(II) complexes with iminoether ligands do not just exist in their traditional *cis* and *trans* isomers but also exhibit extended isomerism at the coordinated ligand sites. Iminoethers exhibit some of the characteristics of both the aromatic N-donor heterocycles, such as pyridine, and the aliphatic amines. In other words, they exist as the intermediate between the N-donor aliphatic and aromatic amines because like the aromatic N-donor heterocycles, iminoether ligands are planar resulting from the *sp*2 hybridization of the nitrogen atom and like aliphatic amines, they have one hydrogen atom linked to the nitrogen, which in most cases, is susceptible to hydrogen-bond formation. Detailed mechanistic studies showed that, similar to transplatin, the *trans*-[PtCl$_2$(HN=C(OMe)Me)(NH$_3$)] series formed monofunctional adducts that developed into interstrand cross-links between adjacent guanine and cytosine nucleobases [152, 153]. The *trans*-platinum(II) complexes with iminoether ligands formed lesions which are thought to be flexible as a result of the imine bond, thereby inducing structural effects on DNA different from the more rigid lesion formed by transplatin [152].

Table 1.5: IC$_{50}$ Mean Values (±SD) for Compounds **27, 28** and **29** (**Figure 1.14**)

	A2780	A2780cisR	4IM	4IMcisR	SKOV-3	HCT-116	KM12	A549	MDA	MCF7
27	1.5±0.2	10.8±1.8 (7.2)	3.3±1.2 (1.9)	6.2±1.9	19±4	4.5±1.8	6±2.4	2.1±1.0	11.5±3.1	3.5±1.4
28	1.3±0.3	7.0±1.3 (5.4)	3.4±1	8.5±1.1 (2.5)	120±24	20±4.5	55±8	14±2	61±1	1.5±0.2
29	2.8±0.7	10.6±2 (3.8)	5.6±1.2	7.8±0.5 (1.4)	43±12	12.6±3	18.9±5	4.9±1	36±5	12.3±3
Transplatin	14±4	118.2±11 (8.4)	36±5	61.2±8 (1.7)	170±25	35±5	355±36	360±24	140±21	45±7
cisplatin	0.2±0.05	3.2±0.8 (16)	0.6±0.01	2.7±0.3 (4.5)	4±0.9	1.9±0.3	8±1.5	1.3±0.2	2.5±0.3	1.2±0.2

IC$_{50}$ values in μM (96 h incubation time). The numbers in parentheses are the resistance factor (RF = IC$_{50}$ resistant/IC$_{50}$ sensitive parent line) [140, 152].

One of the first *trans*-platinum(II) complexes with iminoether ligands that was investigated in full for its cytotoxicity profile is *trans*-EE-[PtCl$_2$(HN=C(OMe)Me)$_2$] complex, compound **27**. The complex demonstrated a growth inhibitory effectiveness similar to those of cisplatin when it was tested against colon, lung, ovary and breast cancer cell lines (**Table 1.5**).

Furthermore, the complex displayed no cross-resistance with cisplatin in ovarian cancer cells and substantial In vivo activity in P388 murine leukemia cancer cells [154, 155]. The cellular uptake and extent of platinum-DNA binding were found to be remarkably better for *trans*-platinum(II) complexes with iminoether ligands than that of cisplatin, which indicates that DNA was the central intracellular target [155]. Consequently, compound **27** was to overcome the cisplatin-resistance of A2780/cp8 cells, a resistance that is due to the low accumulation of cisplatin and a greater amount of glutathione in the cell line. The *trans*-Pt(II) complexes with iminoether ligands form stable monofunctional adducts with double helix DNA [154, 156], which direct the DNA toward the minor groove [157]. The monofunctional platinum-DNA adducts formed were not recognised by repair proteins, such as HMGB proteins, and thus were readily removed by nucleotide excision repair (NER). However, conversion of the monofunctional adducts into DNA−protein cross-links generated lesions that were able to circumvent NER, impede DNA polymerases, or lead to apoptosis. SAR investigations established that *trans*-platinum(II) derivatives with only one iminoether ligand were less toxic than those with two of these ligands [152]. Regarding the additional isomerism that occurs within the *trans*-[PtCl$_2$(HN=C(OCH$_3$)CH$_3$)(NH$_3$)] series, the E conformation, compound **29** showed greater inhibitory potency against cancer cells than the Z conformation, compound **28**. These analogues contain only iminoether ligands compared to compound **27**. However, the complexes, are less cytotoxic than compound **27**. This suggests that the iminoether ligand configuration is a major determinant of cytotoxic activity. Additionally, the inhibitory potency is reduced for compound **28** in relation to compound **29**. Essentially, compounds **28** and **29** partially bypass the cisplatin resistance dependent upon multifactorial mechanisms, such as A2780cisR cells, RF of 5.4 and 3.8, respectively.
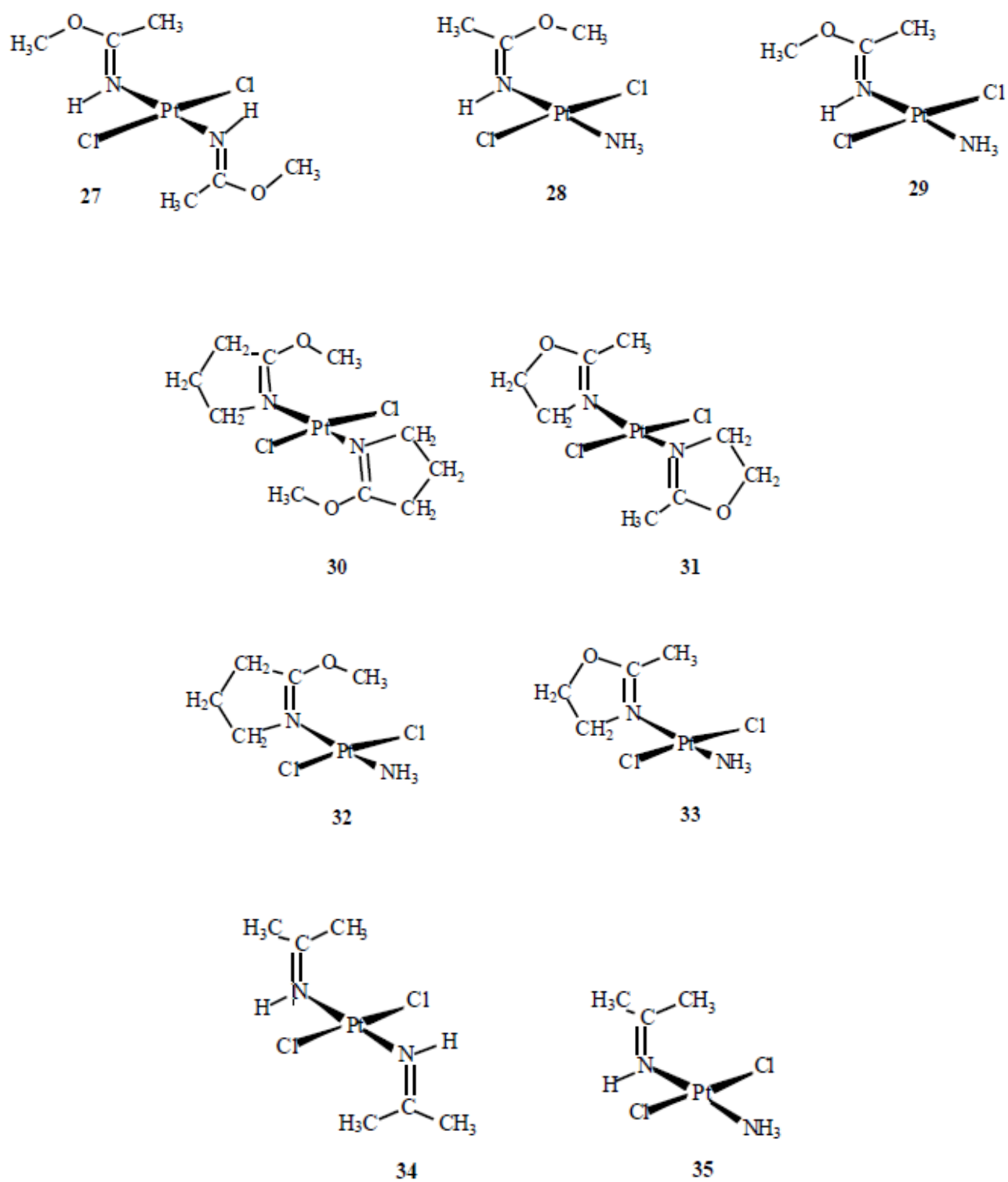
Figure 1.14: Structures of *trans*-platinum(II) complexes with iminoether-ligands [140, 152-153].

The complexes also overcome resistance due to low accumulation, such as in 41McisR cells, RF of 2.5 and 1.4, respectively. Their activity profiles are different from that already established for cisplatin. Compounds **27**, **28** and **29** all exhibit an *In vivo* antitumor activity comparable to that of cisplatin towards murine leukemic and solid metastasising tumours, as well as towards human xenografts [153, 158, 159].

Furthermore, in order to efficiently investigate the effect of different conformations of the iminoether ligand on the *trans*-platinum(II) activity, *trans*-platinum(II) complexes bearing cyclic iminoether ligands mimicking the E and Z configuration were synthesised, compounds **30-33** [160]. Complexes **30** and **32** with cyclic ligands mimicked the *Z* conformation while **31** and **33** mimicked the *E* conformation. With the cyclic ligands the complexities that are associated with the E/Z isomerization encountered in acyclic iminoether compounds were readily bypassed. Moreover, compounds **32** and **33** showed better cytotoxic profiles than their corresponding isomers, compounds **28** and **29**. Nonetheless, they all displayed similar activity profiles, effect of ligand configuration, and activity towards cisplatin resistant cells [152].

In a bid to extend the structure-activity relationship of the *trans*-platinum(II) complexes with iminoether ligands, two compounds, *trans*-[PtCl$_2${HN=C(CH$_3$)$_2$}], **34** which has two acetonimines and (*trans*-[PtCl$_2$(NH$_3$){HN=C(CH$_3$)$_2$}], **35** which has one acetonimine and one ammine were synthesised and studied (**Figure 1.14**) [161]. Acetonimines are like iminoethers because they have sp^2-hybridization of the nitrogen atom, akin to pyridine, with a proton still bound to nitrogen like in secondary aliphatic amines, and a planar shape with the steric bulk localised only on one side of the donor atom. Compounds **34** and **35**, in a panel of human tumour cell lines of different sources, both demonstrated remarkable cytotoxic activity, mean IC$_{50}$ = 10.6, and 26 μM, respectively and bypassed the cisplatin resistance of ovarian cell sublines, A2780cisR and 41McisR, RF of approximately 1.8, hence, showing that the imino- group can also determine the activity of the *trans* geometry.

.

1.10   Aim of this Study

Platinum-based anticancer agents are among the most widely accepted metal-based [162-168] chemotherapeutics with cisplatin, despite its profound drawbacks [169-176], such as severe toxicity, lack of selectivity, inherent and acquired resistance, and transient retention in the bloodstream, still the most clinically, universally used agent [169, 170, 177-188]. Several

research efforts have been targeted towards developing alternative platinum-based cytostatic agents that will not only eliminate some of the challenges that are associated with cisplatin but also improve on its cytotoxicity. Most of the synthesised *cis*-configured complexes, which comprised of mainly the second-generation platinum-based drugs, such as carboplatin, oxaliplatin etc., are yet to be globally accepted and moreover, many of them are still encumbered with some of the limitations that are plaguing the continued use of cisplatin [48, 93, 178, 189-193]. Burgeoning interests among medicinal inorganic chemists, in recent years, have been to develop platinum-based anticancer agents with pharmacodynamics that are relatively complex and radically different from those already established for *cis*-configured platinum(II) based complexes. Among compounds that are currently being considered, platinum(II) complexes with *trans*-stereochemistry are starting to gain a lot of research attentions [194, 195].

The initial thought amongst many medicinal inorganic researchers that *cis*-configuration is a prerequisite for cytotoxicity because of the dearth of activity of the non-toxic transplatin, the *trans*-isomer of cisplatin, has been discarded with recent developments. This non-toxic nature of transplatin motivated research efforts to understand the dearth of activity of transplatin and these efforts brought about two major findings [18, 119, 125, 194]. First, kinetic instability which bring about prompt deactivation of the complex and second, the formation of DNA adducts characterised by a regioselectivity and a stereochemistry that are radically different from those of cisplatin and its derivatives. The second finding was reckoned to be a remarkable breakthrough since it offers an alternative mode of action to those already established for cisplatin. However, for this to be achieved, the first problem on kinetic instability must be resolved. Farrell *et al.* [135] and much later Ranninger *et al.*[196], were able to overcome this challenge when they incorporated bulky amine ligands into the structure of transplatin which elicit some symmetrical and asymmetrical *trans*-configured platinum(II) complexes with significantly high cytotoxicity, better than cisplatin both *in vitro* and *in vivo* and with relatively less toxicity. Following this success, many other *trans*-platinum(II) complexes have been synthesised including the polynuclear *trans*-platinum(II) complexes which were introduced by Farrell.

Furthermore, most of these platinum compounds with *trans* stereochemistry have showed promising prospect as alternative anticancer drugs. However, the mechanism of action of these compounds are still not quite understood. Moreover, the literature is inundated annually with

kinetic and mechanistic studies of *cis*-configured platinum(II) complexes, all in an effort to better understand their mechanism of action as well as facilitate the design and synthesis of complexes with superior cytotoxic properties. Since *trans*-platinum compounds offer an alternative prospect in metal-based anticancer research, efforts to provide detailed kinetic and mechanistic studies of this class of alternative platinum-based compounds will be important not only to enhance a better understanding of their mechanism of action but also in the design and synthesis of *trans*-compounds with superior cytotoxicity and comparably low toxicity. To our knowledge, no such detailed kinetic and mechanistic study of *trans*-platinum-based compounds are currently available in literature.

Hence, the central aim of this research is to provide a detailed kinetic and mechanistic study of some mononuclear and dinuclear *trans*-platinum(II) complexes. In this study, mononuclear and dinuclear *trans*-platinum(II) complexes were investigated with neutral thiourea-based nucleophiles, such as thiourea (TU), 1-methyl-2-thiourea (MTU), 1,3-dimethyl-2-thiourea (DMTU), 1,1,3,3-tetramethyl-2-thiourea (TMTU). The choice of thiourea-based nucleophiles varies according to their steric demands. Sulfur donor thiourea-based nucleophiles represent a typical example of the interaction of the sulfur containing biomolecules, such as proteins, peptides and enzymes, in the body with platinum-based drugs [197-199]. Platinum being a soft centre [200] has a very strong affinity for sulfur [201-203] containing molecules which are quite abundant in the human body. More so, the interaction of platinum-based anticancer drugs with biomolecules has been established to be responsible for the high toxic behaviour of these drugs [204-207]. Furthermore, computational modelling through density functional theory at the level B3LYP with LANL2DZ basis set using the Gaussian 09 programme suite [208] is incorporated in this study to a facilitate theoretical interpretation of the kinetic and mechanistic behaviour of the investigated *trans*-platinum(II) complexes.

To this end, the specific objectives of this study include:

1. To investigate the kinetic and mechanistic behaviour of analogous *cis* and *trans*-dialkylamine diaquaplatinum(II) complexes of the general form, $[PtX_2L_2]$. This is aimed to ascertain how bifunctional *trans*-platinum(II) complexes will substitute kinetically in comparison to their corresponding *cis* isomers. This is presented in **Chapter Three**.

2. To extend the understanding of ligand substitution kinetics of mononuclear *trans*-platinum(II) complexes further mixed amine ligands with varying the chain lengths of

the alkylamine ligand with be used. The studied *trans*-platinum compounds are of the general form, $[Pt(NH_3)LX_2]$. This is covered in **Chapter Four**.

3. To carry out a comparative study of the substitution behaviour of some bifunctional mononuclear *trans*-platinum(II) complexes with symmetric and asymmetric dialkylamine and alkylamine ligands respectively. This work is reported in **Chapter Five**.

4. To gain an in-depth understanding through a kinetic and mechanistic investigation of the role of flexible alkyl-α,ω-diamine linkers on the substitution behaviour of some dinuclear *trans*-platinum(II) complexes. The chloride leaving groups are *trans* to each other on the platinum centre. Mechanistic behaviour of these dinuclear *trans*-platinum(II) compounds were compared to those of their corresponding mononuclear counterparts. This work is presented in **Chapter Six**.

.

References

[1] R. Siegel, A. Jemal, American Cancer Society. Cancer Facts & Figures, (2015) 25-55.

[2] S.J. McPhee, M.A. Papadakis, M.W. Rabow, Current Medical Diagnosis & Treatment, McGraw-Hill Medical New York:, (2010) 1-100.

[3] V. Panda, P. Khambat, S. Patil, International Journal of Clinical Medicine, 2 (2011) 512-517.

[4] I. Kostova, Current Medicinal Chemistry, 13 (2006) 1085-1107.

[5] I. Kostova, Recent Patents on Anti-Cancer Drug Discovery, 1 (2006) 1-22.

[6] E. Alessio, Bioinorganic Medicinal Chemistry, John Wiley & Sons, (2011) 5-20.

[7] C. Andreini, I. Bertini, G. Cavallaro, G.L. Holliday, J.M. Thornton, JBIC Journal of Biological Inorganic Chemistry, 13 (2008) 1205-1218.

[8] I. Bratsos, T. Gianferrara, E. Alessio, C.G. Hartinger, M.A. Jakupec, B.K. Keppler, Bioinorganic Medicinal Chemistry, (2011) 151-174.

[9] J.P. Parker, Z. Ude, C.J. Marmion, Metallomics, 8 (2016) 43-60.

[10] M. Fanelli, M. Formica, V. Fusi, L. Giorgi, M. Micheloni, P. Paoli, Coordination Chemistry Reviews, 310 (2016) 41-79.

[11] L. Ronconi, P.J. Sadler, Coordination Chemistry Reviews, 251 (2007) 1633-1648.

[12] M.A. Jakupec, M. Galanski, V.B. Arion, C.G. Hartinger, B.K. Keppler, Dalton transactions, (2008) 183-194.

[13] M. Peyrone, European Journal of Organic Chemistry, 51 (1844) 1-29.

[14] R.A. Alderden, M.D. Hall, T.W. Hambley, Journal of Chemical Education, 83 (2006) 721-728.

[15] S. Dasari, P.B. Tchounwou, European Journal of Pharmacology, 740 (2014) 364-378.

[16] A. Werner, Zeitschr. Anorg. Chem, 3 (1893) 267-270.

[17] A. Werner, Zeitschrift für Anorganische und Allgemeine Chemie, 3 (1893) 267-330.

[18] J.J. Wilson, S.J. Lippard, Chemical Reviews, 114 (2013) 4470-4495.

[19] L. Kelland, Nature Reviews Cancer, 7 (2007) 550-573.

[20] J. Reedijk, Proceedings of the National Academy of Sciences, 100 (2003) 3611-3616.

[21] P.S. Sengupta, R. Sinha, G. De, Transition Metal Chemistry, 26 (2001) 638-643.

[22] M. Zaki, F. Arjmand, S. Tabassum, Inorganica Chimica Acta, 444 (2016) 1-22.

[23] E.R. Jamieson, S.J. Lippard, Chemical Reviews, 99 (1999) 2467-2498.

[24] C.J. Jones, J.R. Thornback, Medicinal Applications of Coordination Chemistry, Royal Society of Chemistry, (2007) 94-100.

[25] J.-X. Liang, H.-J. Zhong, G. Yang, K. Vellaisamy, D.-L. Ma, C.-H. Leung, Journal of Inorganic Biochemistry, 177 (2017) 276-286.

[26] S. Medici, M. Peana, V.M. Nurchi, J.I. Lachowicz, G. Crisponi, M.A. Zoroddu, Coordination Chemistry Reviews, 284 (2015) 329-350.

[27] B.J. Reedijk, Platinum Metals Review, 52 (2008) 2-11.

[28] T.G. Appleton, A.J. Bailey, K.J. Barnham, J.R. Hall, Inorganic Chemistry, 31 (1992) 3077-3082.

[29] L. Cubo, A.G. Quiroga, J. Zhang, D.S. Thomas, A. Carnero, C. Navarro-Ranninger, S.J. Berners-Price, Dalton Transactions, (2009) 3457-3466.

[30] T.C. Johnstone, K. Suntharalingam, S.J. Lippard, Chemical Reviews, 116 (2016) 3436-3486.

[31] S.E. Miller, D.A. House, Inorganica Chimica Acta, 187 (1991) 125-132.

[32] M. Gielen, E.R. Tiekink, Metallotherapeutic Drugs and Metal-Based Diagnostic Agents: The Use of Metals in Medicine, John Wiley & Sons, (2005) 5-25.

[33] J.-M. Teuben, J. Reedijk, JBIC Journal of Biological Inorganic Chemistry, 5 (2000) 463-468.

[34] S.E. Crider, R.J. Holbrook, K.J. Franz, Metallomics, 2 (2010) 74-83.

[35] A. Pasini, C. Fiore, Inorganica Chimica Acta, 285 (1999) 249-253.

[36] J. Vinje, E. Sletten, Anti-Cancer Agents in Medicinal Chemistry (Formerly Current Medicinal Chemistry-Anti-Cancer Agents), 7 (2007) 35-54.

[37] X. Wang, Z. Guo, Anti-Cancer Agents in Medicinal Chemistry (Formerly Current Medicinal Chemistry-Anti-Cancer Agents), 7 (2007) 19-34.

[38] S. Manohar, N. Leung, Journal of Nephrology, (2017) 1-11.

[39] S. Sheth, D. Mukherjea, L.P. Rybak, V. Ramkumar, Frontiers in Cellular Neuroscience, 11 (2017) 330-341.

[40] A. Chattopadhyay, A. Dey, P. Karmakar, S. Ray, D. Nandi, A.K. Ghosh, Progress in Reaction Kinetics and Mechanism, 43 (2018) 274-285.

[41] T.W. Hambley, Journal of the Chemical Society, Dalton Transactions, (2001) 2711-2718.

[42] F.-L. Li, J.-P. Liu, R.-X. Bao, G. Yan, X. Feng, Y.-P. Xu, Y.-P. Sun, W. Yan, Z.-Q. Ling, Y. Xiong, Nature Communications, 9 (2018) 501-508.

[43] M. Liu, Z. Han, Q.-X. Zhu, J. Tan, W.-J. Liu, Y.-F. Wang, W. Chen, Y.-L. Zou, Y.-S. Cai, X. Tian, Cancer gene therapy, 25 (2018) 1-12.

[44] F. Peng, H. Zhang, Y. Du, P. Tan, Molecular Medicine Reports, 17 (2018) 4767-4776.

[45] M. Rada, S. Nallanthighal, J. Cha, K. Ryan, J. Sage, C. Eldred, M. Ullo, S. Orsulic, D.-J. Cheon, Oncogene, (2018) 1-20.

[46] C.-Y. Sun, Y. Zhu, X.-F. Li, X.-Q. Wang, L.-P. Tang, Z.-Q. Su, C.-Y. Li, G.-J. Zheng, B. Feng, Frontiers in Pharmacology, 9 (2018) 90-110.

[47] M. Yang, X. Yang, D. Yin, Q. Tang, L. Wang, C. Huang, P. Li, S. Li, Neoplasma, 65 (2018) 42-48.

[48] I.A. Riddell, S.J. Lippard, Metallo-Drugs: Development and Action of Anticancer Agents: Development and Action of Anticancer Agents, 18 (2018) 1-8.

[49] V. Jha, H. Ling, Journal of Molecular Biology, 430 (2018) 1577-1589.

[50] T. Fang, Z. Ye, J. Wu, H. Wang, Chemical Communications, (2018) 5-21.

[51] C.R.R. Rocha, M.M. Silva, A. Quinet, J.B. Cabral-Neto, C.F.M. Menck, Clinics, 73 (2018) 767-785.

[52] L. He, Z. Meng, D. Xu, F. Shao, Scientific Reports, 8 (2018) 767.

[53] A. Saha, A. Pal, R. Goswami, Journal of Chemical and Pharmaceutical Sciences, 11 (2018) 8-19.

[54] F.A. Suliman, D.M. Khodeer, A. Ibrahiem, E.T. Mehanna, M.K. El-Kherbetawy, H.M. Mohammad, S.A. Zaitone, Y.M. Moustafa, International Immunopharmacology, 61 (2018) 8-19.

[55] A. Boot, M.N. Huang, A.W. Ng, S.-C. Ho, J.Q. Lim, Y. Kawakami, K. Chayama, B.T. Teh, H. Nakagawa, S.G. Rozen, Genome Research, (2018) 20-23.

[56] J. Reedijk, European Journal of Inorganic Chemistry, 2009 (2009) 1303-1312.

[57] A.M.J. Fichtinger-Schepman, A.T. van Oosterom, P.H. Lohman, F. Berends, Cancer Research, 47 (1987) 3000-3004.

[58] E. Reed, Y. Ostchega, S.M. Steinberg, S.H. Yuspa, R.C. Young, R.F. Ozols, M.C. Poirier, Cancer Research, 50 (1990) 2256-2260.

[59] E.P. López, Applications in Cancer Chemotherapy Doctoral Thesis. Institute of Chemistry, Faculty of Mathematics & Natural Sciences, Leiden University, (2005) 1-10.

[60] V. Brabec, O. Hrabina, J. Kasparkova, Coordination Chemistry Reviews, (2017) 311-321.

[61] S. Dutta, C. Rivetti, N.R. Gassman, C.G. Young, B.T. Jones, K. Scarpinato, M. Guthold, Journal of Molecular Recognition, (2018) 2718-2731.

[62] L. Saker, S. Ali, C. Masserot, G. Kellermann, J. Poupon, M.-P. Teulade-Fichou, E. Ségal-Bendirdjian, S. Bombard, International Journal of Molecular Sciences, 19 (2018) 1951-1965.

[63] R. Charif, C. Granotier-Beckers, H.C. Bertrand, J. Poupon, E. Ségal-Bendirdjian, M.-P. Teulade-Fichou, F.D. Boussin, S. Bombard, Chemical Research in Toxicology, 30 (2017) 1629-1640.

[64] N. Aztopal, D. Karakas, B. Cevatemre, F. Ari, C. Icsel, M.G. Daidone, E. Ulukaya, Bioorganic & Medicinal Chemistry, 25 (2017) 269-276.

[65] S. Komeda, H. Yoneyama, M. Uemura, A. Muramatsu, N. Okamoto, H. Konishi, H. Takahashi, A. Takagi, W. Fukuda, T. Imanaka, Inorganic Chemistry, 56 (2017) 802-811.

[66] S.T. Pan, Z.L. Li, Z.X. He, J.X. Qiu, S.F. Zhou, Clinical and Experimental Pharmacology and Physiology, 43 (2016) 723-737.

[67] G. Housman, S. Byler, S. Heerboth, K. Lapinska, M. Longacre, N. Snyder, S. Sarkar, Cancers, 6 (2014) 1769-1792.

[68] P. Samuel, R.C. Pink, S.A. Brooks, D.R. Carter, Expert Review of Anticancer Therapy, 16 (2016) 57-70.

[69] K. Luo, X. Gu, J. Liu, G. Zeng, L. Peng, H. Huang, M. Jiang, P. Yang, M. Li, Y. Yang, Experimental Cell Research, 347 (2016) 105-113.

[70] S. Dilruba, G.V. Kalayda, Cancer Chemotherapy and Pharmacology, 77 (2016) 1103-1124.

[71] J. Hrabeta, V. Adam, T. Eckschlager, E. Frei, M. Stiborova, R. Kizek, Anti-Cancer Agents in Medicinal Chemistry (Formerly Current Medicinal Chemistry-Anti-Cancer Agents), 16 (2016) 686-698.

[72] D.L. Wong, M.J. Stillman, Metallomics, 10 (2018) 713-721.

[73] R.P. Perez, T.C. Hamilton, R.F. Ozols, Pharmacology & Therapeutics, 48 (1990) 19-27.

[74] P. Andrews, S. Howell, Cancer cells (Cold Spring Harbor, NY: 1989), 2 (1990) 35-43.

[75] E. Tuzel, K. Yorukoglu, E. Ozkara, Z. Kirkali, Central European Journal of Urology, 68 (2015) 45-68.

[76] T. Kimura, T. Kambe, International Journal of Molecular Sciences, 17 (2016) 335-357.

[77] J.-H. Lee, J.-W. Chae, J.K. Kim, H.J. Kim, J.Y. Chung, Y.-H. Kim, Journal of Controlled Release, 215 (2015) 82-90.

[78] B. Kawahara, S. Ramadoss, G. Chaudhuri, C. Janzen, S. Sen, P.K. Mascharak, Journal of Inorganic Biochemistry, (2018).

[79] A.K. Srivastava, C. Han, R. Zhao, T. Cui, Y. Dai, C. Mao, W. Zhao, X. Zhang, J. Yu, Q.-E. Wang, Proceedings of the National Academy of Sciences, (2015) 201421365.

[80] E. Reed, T.L. Larkins, C.H. Chau, W.D. Figg, DNA Repair: ERCC1, Nucleotide Excision Repair, and Platinum Resistance, in: Handbook of Anticancer Pharmacokinetics and Pharmacodynamics, Springer, 2014, pp. 333-349.

[81] M. Zimmermann, S.-S. Wang, H. Zhang, T.-y. Lin, M. Malfatti, K. Haack, T. Ognibene, H. Yang, S. Airhart, K.W. Turteltaub, Molecular Cancer Therapeutics, 16 (2017) 376-387.

[82] S. Wang, H. Zhang, T.M. Scharadin, M. Zimmermann, B. Hu, A.W. Pan, R. Vinall, T.-y. Lin, G. Cimino, P. Chain, PloS one, 11 (2016) e0146256.

[83] L. Yang, A.-M. Ritchie, D.W. Melton, Oncotarget, 8 (2017) 55241-55260.

[84] A. Sawant, A.M. Floyd, M. Dangeti, W. Lei, R.W. Sobol, S.M. Patrick, DNA repair, 51 (2017) 46-59.

[85] S.G. Awuah, I.A. Riddell, S.J. Lippard, Proceedings of the National Academy of Sciences, 114 (2017) 950-955.

[86] R. Sabarinathan, L. Mularoni, J. Deu-Pons, A. Gonzalez-Perez, N. López-Bigas, Nature, 532 (2016) 264.

[87] P.O. Ongoma, D. Jaganyi, Transition Metal Chemistry, 39 (2014) 407-420.

[88] M.A. Blum Murphy, W. Qiao, N. Mewada, R. Wadhwa, E. Elimova, T. Takashi, L. Ho, A. Phan, J. Baker, J. Ajani, American Journal of Clinical Oncology, 41 (2018) 321-325.

[89] R.-D. Hofheinz, D. Arnold, E. Fokas, M. Kaufmann, T. Hothorn, G. Folprecht, R. Fietkau, W. Hohenberger, M. Ghadimi, T. Liersch, Annals of Oncology, (2018) 111-142.

[90] T. Okuyama, S. Sameshima, E. Takeshita, R. Yoshioka, Y. Yamagata, Y. Ono, N. Tagaya, T. Noie, M. Oya, World Journal of Surgical Oncology, 16 (2018) 101-127.

[91] B. Lippert, Cisplatin: Chemistry and Biochemistry of a Leading Anticancer Drug, John Wiley & Sons, (1999) 5-30.

[92] N. Lamichhane, G.K. Dewkar, G. Sundaresan, L. Wang, P. Jose, M. Otabashi, J.-L. Morelle, N. Farrell, J. Zweit, Journal of Nuclear Medicine, 58 (2017) 1997-2003.

[93] F. Ponte, I. Ritacco, G. Mazzone, N. Russo, E. Sicilia, Inorganica Chimica Acta, 470 (2018) 325-330.

[94] C. Fong, Molecular Mechanisms of Cytotoxic Side Effects of Platinum Anti-Cancer Drugs–a Molecular Orbital Study (2014).

[95] L. Oliveira, J. Caquito Jr, M. Rocha, Biophysical Chemistry, 241 (2018) 8-14.

[96] Y. Mochida, H. Cabral, K. Kataoka, Expert Opinion on Drug Delivery, 14 (2017) 1423-1438.

[97] R.L. Coleman, M.F. Brady, T.J. Herzog, P. Sabbatini, D.K. Armstrong, J.L. Walker, B.-G. Kim, K. Fujiwara, K.S. Tewari, D.M. O'Malley, The Lancet Oncology, 18 (2017) 779-791.

[98] D.M. O'Malley, K.N. Moore, I. Vergote, L.P. Martin, L. Gilbert, A.G. Martin, K. Malek, M.J. Birrer, U.A. Matulonis, Hypertension, 3 (2017) 21-34.

[99] Q. Miow, T. Tan, J. Ye, J. Lau, T. Yokomizo, J. Thiery, S. Mori, Oncogene, 34 (2015) 1899.

[100] J.K. Chan, M.F. Brady, R.T. Penson, H. Huang, M.J. Birrer, J.L. Walker, P.A. DiSilvestro, S.C. Rubin, L.P. Martin, S.A. Davidson, New England Journal of Medicine, 374 (2016) 738-748.

[101] A.E. Teschendorff, S.-H. Lee, A. Jones, H. Fiegl, M. Kalwa, W. Wagner, K. Chindera, I. Evans, L. Dubeau, A. Orjalo, Genome Medicine, 7 (2015) 105-156.

[102] B. Thibault, L. Genre, C. Broca, M. Barbier, C. Zanna, G. Vuagniaux, J.-P. Delord, B. Couderc, in, AACR, (2015).

[103] K. Barkat, M. Ahmad, M.U. Minhas, I. Khalid, Journal of Applied Polymer Science, 134 (2017) 45310-45315.

[104] A. Narmani, M. Kamali, B. Amini, A. Salimi, Y. Panahi, Process Biochemistry, 69 (2018) 178-187.

[105] P. Sundaramoorthy, T. Ramasamy, S.K. Mishra, K.-Y. Jeong, C.S. Yong, J.O. Kim, H.M. Kim, Acta Biomaterialia, 42 (2016) 220-231.

[106] K. Rajpoot, S.K. Jain, Artificial Cells, Nanomedicine, and Biotechnology, 46 (2018) 1236-1247.

[107] A. Sigel, H. Sigel, Metal Ions in Biological Systems: Volume 32: Interactions of Metal Ions with Nucleotides: Nucleic Acids, and Their Constituents, CRC Press, (1996).

[108] N. Farrell, Journal of Medicinal Chemistry, 32 (1989) 2240-2241.

[109] N.H. Farrell, Miles P.; McCormack, John J.; DeAlmeida, Sergio G., in: W.I.P. Organisation (Ed.) The Patent Cooperation Treaty, United States of America, (1988) 1-23.

[110] L.S. Hollis, W.I. Sundquist, J.N. Burstyn, W.J. Heiger-Bernays, S.F. Bellon, K.J. Ahmed, A.R. Amundsen, E.W. Stern, S.J. Lippard, Cancer Research, 51 (1991) 1866-1875.

[111] S.F. Bellon, S.J. Lippard, Biophysical Chemistry, 35 (1990) 179-188.

[112] C. Bauer, T. Peleg-Shulman, D. Gibson, A.H.J. Wang, European Journal of Biochemistry, 256 (1998) 253-260.

[113] P.A. Wangoli, G. Kinunda, New Journal of Chemistry, 42 (2018) 214-227.

[114] D. Yang, S.S. van Boom, J. Reedijk, J.H. van Boom, N. Farrell, A.H.-J. Wang, Nature Structural and Molecular Biology, 2 (1995) 575-591.

[115] Y. Zou, B. Van Houten, N. Farrell, Biochemistry, 33 (1994) 5404-5410.

[116] N. Farrell, Y. Qu, M.P. Hacker, Journal of Medicinal Chemistry, 33 (1990) 2179-2184.

[117] C. Billecke, I. Malik, A. Movsisyan, S. Sulghani, A. Sharif, T. Mikkelsen, N.P. Farrell, O. Bögler, Molecular & Cellular Proteomics, 5 (2006) 35-42.

[118] A.L. Harris, X. Yang, A. Hegmans, L. Povirk, J.J. Ryan, L. Kelland, N.P. Farrell, Inorganic Chemistry, 44 (2005) 9598-9600.

[119] W.B. Dirersa, International Journal of Chemical and Pharmaceutical Analysis, 2 (2014) 40-47.

[120] N.P. Barry, P.J. Sadler, Pure and Applied Chemistry, 86 (2014) 1897-1910.

[121] J. Geng, M. Aioub, M.A. El-Sayed, B.A. Barry, The Journal of Physical Chemistry B, 121 (2017) 8975-8983.

[122] D. Corinti, C. Coletti, N. Re, S. Piccirillo, M. Giampà, M.E. Crestoni, S. Fornarini, RSC Advances, 7 (2017) 15877-15884.

[123] O. Vrana, V. Novohradsky, Z. Medrikova, J. Burdikova, O. Stuchlikova, J. Kasparkova, V. Brabec, Chemistry–A European Journal, 22 (2016) 2728-2735.

[124] D.Y. Lando, C.-L. Chang, A.S. Fridman, I.E. Grigoryan, E.N. Galyuk, Y.-W. Hsueh, C.-K. Hu, Journal of inorganic biochemistry, 137 (2014) 85-93.

[125] V. Brabec, O. Vrana, O. Novakova, J. Kasparkova, Chemical Communications, 52 (2016) 4096-4098.

[126] J.L. Kolanowski, L.J. Dawson, L. Mitchell, Z. Lim, M.E. Graziotto, W.K. Filipek, T.W. Hambley, E.J. New, Sensors and Actuators B: Chemical, 255 (2018) 2721-2724.

[127] E. Wachter, A. Zamora, D.K. Heidary, J. Ruiz, E.C. Glazer, Chemical Communications, 52 (2016) 10121-10124.

[128] U. Kalinowska-Lis, J. Ochocki, K. Matlawska-Wasowska, Coordination Chemistry Reviews, 252 (2008) 1328-1345.

[129] L. Messori, L. Cubo, C. Gabbiani, A. Álvarez-Valdés, E. Michelucci, G. Pieraccini, C. Ríos-Luci, L.G. León, J.M. Padrón, C. Navarro-Ranninger, A. Casini, A.G. Quiroga, Inorganic chemistry, 51 (2012) 1717-1726.

[130] J. Pracharova, T.R. Muchova, E.D. Tomastikova, F.P. Intini, C. Pacifico, G. Natile, J. Kasparkova, V. Brabec, Dalton Transactions, 45 (2016) 13179-13186.

[131] N. Farrell, Qu, Y., Feng, L., Van Houten B., Biochemistry, 29 (1990) 9522-9953.

[132] N. Farrell, Qu, Y., , Inorganic Chemistry, 31 (1992) 930-932.

[133] N. Farrell, Metal *I*ons in Biological Systems, 32 (1996) 603-639.

[134] N. Farrell, L.R. Kelland, J.D. Roberts, M. Van Beusichem, Cancer Research, 52 (1992) 5065-5072.

[135] M. Van Beusichem, N. Farrell, Inorganic Chemistry, 31 (1992) 634-639.

[136] Y. Zou, B. Van Houten, N. Farrell, Biochemistry, 32 (1993) 9632-9638.

[137] E.I. Montero, S. Díaz, A.M. González-Vadillo, J.M. Pérez, C. Alonso, C. Navarro-Ranninger, Journal of Medicinal Chemistry, 42 (1999) 4264-4268.

[138] M.J. Cleare, J.D. Hoeschele, Bioinorganic Chemistry, 2 (1973) 187-210.

[139] M.J. Cleare, P.C. Hydes, D.R. Hepburn, B.W. Malerbi, Antitumor Platinum Complexes: Structure-Activity Relationships, in: Cisplatin, Elsevier, (1980) 149-170.

[140] M. Coluccia, G. Natile, Anti-Cancer Agents in Medicinal Chemistry (Formerly Current Medicinal Chemistry-Anti-Cancer Agents), 7 (2007) 111-123.

[141] L.R. Kelland, F.J. Barnard, I.G. Evans, B.A. Murrer, B.R.C. Thobald, S.B. Wyer, P.M. Goddard, M. Jones, M. Valenti, Journal of Medicinal Chemistry, 38 (1995) 3016-3024.

[142] L.R. Kelland, B.A. Murrer, G. Abel, C.M. Giandomenico, P. Mistry, K.R. Harrap, Cancer Research, 52 (1992) 822-828.

[143] C. Hills, L. Kelland, G. Abel, J. Siracky, A. Wilson, K. Harrap, British Journal of Cancer, 59 (1989) 523-530.

[144] P. Goddard, R. Orr, M. Valenti, C. Barnard, B. Murrer, L. Kelland, K. Harrap, Anticancer Research, 16 (1996) 33-38.

[145] J. Pérez, E. Montero, A. González, A. Alvarez-Valdés, C. Alonso, C. Navarro-Ranninger, Journal of Inorganic Biochemistry, 77 (1999) 37-42.

[146] J.M. Pérez, E.I. Montero, A.G. Quiroga, M.A. Fuertes, C. Alonso, C. Navarro-Ranninger, Metal-Based Drugs, 8 (2001) 29-37.

[147] R. Prokop, J. Kasparkova, O. Novakova, V. Marini, A.M.a. Pizarro, C. Navarro-Ranninger, V. Brabec, Biochemical Pharmacology, 67 (2004) 1097-1109.

[148] E. Khazanov, Y. Barenholz, D. Gibson, Y. Najajreh, Journal of Medicinal Chemistry, 45 (2002) 5196-5204.

[149] F.I. Raynaud, F.E. Boxall, P.M. Goddard, M. Valenti, M. Jones, B.A. Murrer, M. Abrams, L.R. Kelland, Clinical Cancer Research, 3 (1997) 2063-2074.

[150] J. Kasparkova, V. Marini, Y. Najajreh, D. Gibson, V. Brabec, Biochemistry, 42 (2003) 6321-6332.

[151] Y. Najajreh, J.M. Perez, C. Navarro-Ranninger, D. Gibson, Journal of Medicinal chemistry, 45 (2002) 5189-5195.

[152] F.P. Intini, A. Boccarelli, V.C. Francia, C. Pacifico, M.F. Sivo, G. Natile, D. Giordano, P. De Rinaldis, M. Coluccia, JBIC Journal of Biological Inorganic Chemistry, 9 (2004) 768-780.

[153] M. Leng, D. Locker, M.-J. Giraud-Panis, A. Schwartz, F.P. Intini, G. Natile, C. Pisano, A. Boccarelli, D. Giordano, M. Coluccia, Molecular Pharmacology, 58 (2000) 1525-1535.

[154] V. Brabec, O. Vrána, O. Nováková, V. Kleinwächter, F.P. Intini, M. Coluccia, G. Natile, Nucleic Acids Research, 24 (1996) 336-341.

[155] M. Coluccia, A. Nassi, A. Boccarelli, D. Giordano, N. Cardellicchio, D. Locker, M. Leng, M. Sivo, F.P. Intini, G. Natile, Journal of Inorganic Biochemistry, 77 (1999) 31-35.

[156] R. Zaludova, G. Natile, V. Brabec, Anti-Cancer Drug Design, 12 (1997) 295-309.

[157] O. Novakova, J. Kasparkova, J. Malina, G. Natile, V. Brabec, Nucleic Acids Research, 31 (2003) 6450-6460.

[158] M. Coluccia, A. Boccarelli, M.A. Mariggiò, N. Cardellicchio, P. Caputo, F.P. Intini, G. Natile, Chemico-Biological Interactions, 98 (1995) 251-266.

[159] M. Coluccia, A. Nassi, F. Loseto, A. Boccarelli, M.A. Mariggio, D. Giordano, F.P. Intini, P. Caputo, G. Natile, Journal of Medicinal Chemistry, 36 (1993) 510-512.

[160] Y. Liu, M.F. Sivo, G. Natile, E. Sletten, Metal-Based Drugs, 7 (2000) 169-176.

[161] A. Boccarelli, F.P. Intini, R. Sasanelli, M.F. Sivo, M. Coluccia, G. Natile, Journal of Medicinal Chemistry, 49 (2006) 829-837.

[162] C. Ceresa, G. Nicolini, S. Semperboni, M. Bossi, H. Requardt, C. Santini, M. Pellei, A. Bravin, G. Cavaletti, Italian Journal of Anatomy and Embryology, 119 (2014) 1.

[163] C.S. Allardyce, P.J. Dyson, Dalton Transactions, 45 (2016) 3201-3209.

[164] V.H. van Rixel, A. Busemann, A.J. Göttle, S. Bonnet, Journal of Inorganic Biochemistry, 150 (2015) 174-181.

[165] Y. Cheng, Y. Qi, Anti-Cancer Agents in Medicinal Chemistry (Formerly Current Medicinal Chemistry-Anti-Cancer Agents), 17 (2017) 1046-1069.

[166] R.F. Lee, S. Theiner, A. Meibom, G. Koellensperger, B.K. Keppler, P.J. Dyson, Metallomics, 9 (2017) 365-381.

[167] C. Ceresa, G. Nicolini, S. Semperboni, M. Pellei, N. Margiotta, V. Gandin, J. Hoeschele, C. Santini, G. Cavaletti, in: Journal of Alzheimer Disease, IOS Press Nieuwe Hemweg 6B, 1013 BG Amsterdam Netherland, (2016) S55-S56.

[168] N. Muhammad, Z. Guo, Current Opinion in Chemical Biology, 19 (2014) 144-153.

[169] V. Vyas, M. Gupta, D. Malik, Journal of Cancer Research & Therapeutics, 13 (2017).

[170] D. Yang, Z. Hou, Z. Cheng, C. Li, J. Lin, Chemical Society Reviews, 44 (2015) 1416-1448.

[171] L.F. Esteves, H.F. Dos Santos, L.A.S. Costa, Journal of Molecular Graphics and Modelling, 61 (2015) 290-296.

[172] D. Lee, S. Lee, S.H. Shim, H.-J. Lee, Y. Choi, T.S. Jang, K.H. Kim, K.S. Kang, Bioorganic & Medicinal Chemistry Letters, 27 (2017) 2881-2885.

[173] M. Kutwin, E. Sawosz, S. Jaworski, M. Hinzmann, M. Wierzbicki, A. Hotowy, M. Grodzik, A. Winnicka, A. Chwalibog, Archives of Medical Science: AMS, 13 (2017) 1322-1338.

[174] P. Kumar, K. Sulakhiya, C.C. Barua, N. Mundhe, Molecular and Cellular Biochemistry, 431 (2017) 113-122.

[175] R. Sirota, D. Gibson, R. Kohen, Redox Biology, 11 (2017) 170-175.

[176] E.M. Glebov, I.P. Pozdnyakov, D.B. Vasilchenko, A.V. Zadesenets, A.A. Melnikov, I.M. Magin, V.P. Grivin, S.V. Chekalin, V.F. Plyusnin, Journal of Photochemistry and Photobiology A: Chemistry, 354 (2018) 78-85.

[177] F. Li, T. Li, W. Cao, L. Wang, H. Xu, Biomaterials, 133 (2017) 208-218.

[178] E. Armstrong-Gordon, D. Gnjidic, A.J. McLachlan, B. Hosseini, A. Grant, P.J. Beale, N.J. Wheate, Journal of Cancer Research and Clinical Oncology, (2018) 1-8.

[179] F.N. Ekinci Akdemir, M. Albayrak, M. Çalik, Y. Bayir, I. Gülçin, Biomedicines, 5 (2017) 11-18.

[180] B. Lippert, in, Metallo-Drugs: Development and Action of Anticancer Agents, Elsevier Publication, 18 (2018) 546-550.

[181] A. Schmidt, F.E. Kuehn, Chemie in Unserer Zeit, 51 (2017) 86-95.

[182] R.F. Lee, T. Riedel, S. Escrig, C. Maclachlan, G.W. Knott, C.A. Davey, K. Johnsson, A. Meibom, P.J. Dyson, Metallomics, 9 (2017) 1413-1420.

[183] M. Altaf, M. Monim-ul-Mehboob, A.A. Isab, S. ALTUWAIJRI, in, Google Patents, (2018).

[184] T. Lazarević, A. Rilak, Ž.D. Bugarčić, European Journal of Medicinal Chemistry, (2017).

[185] T. Fonseca, M. Morais, T. Rocha, D. Abessa, M. Aureliano, M. Bebianno, Science of the Total Environment, 575 (2017) 162-172.

[186] A.L. Stark, A.G. Madian, S.W. Williams, V. Chen, C. Wing, R.J. Hause Jr, L.A. To, A.L. Gill, J.L. Myers, L.K. Gorsic, Journal of Proteome Research, 16 (2017) 4227-4236.

[187] A. Bergamo, G. Sava, Chemical Society Reviews, 44 (2015) 8818-8835.

[188] E. Van Cutsem, V.M. Moiseyenko, S. Tjulandin, A. Majlis, M. Constenla, C. Boni, A. Rodrigues, M. Fodor, Y. Chao, E. Voznyi, Journal of Clinical Oncology, 24 (2006) 4991-4997.

[189] S. Novokmet, I. Stojic, K. Radonjic, M. Savic, J. Jeremic, Serbian Journal of Experimental and Clinical Research, 18 (2017) 191-194.

[190] M. Taylor, A. Filby, Johnson Matthey Technology Review, 61 (2017) 32-39.

[191] C. Ornelas, J. Caiado, A.C. Melo, M.P. Barbosa, M.C. Castells, M.C.P. dos Santos, International Archives of Allergy and Immunology, 177 (2018) 274-280.

[192] J.L. Bullock, A.A. Holder, Ruthenium Complexes: Photochemical and Biomedical Applications, (2018) 139-160.

[193] J. Lokich, Cancer Investigation, 19 (2001) 756-760.

[194] A. Quiroga, Journal of Inorganic Biochemistry, 114 (2012) 106-112.

[195] M. Navarro, W. Castro, A.R. Higuera-Padilla, A. Sierraalta, M.J. Abad, P. Taylor, R.A. Sánchez-Delgado, Journal of Inorganic Biochemistry, 105 (2011) 1684-1691.

[196] E.I. Montero, S. Díaz, A.M. González-Vadillo, J.M. Pérez, C. Alonso, C. Navarro-Ranninger, Journal of Medicinal Chemistry, 42 (1999) 4264-4268.

[197] Ž.D. Bugarčić, J. Bogojeski, R. van Eldik, Coordination Chemistry Reviews, 292 (2015) 91-106.

[198] S. Jovanović, J. Bogojeski, M. Petković, Ž.D. Bugarčić, Journal of Coordination Chemistry, 68 (2015) 3148-3163.

[199] T. Soldatović, S. Jovanović, Ž.D. Bugarčić, R. van Eldik, Dalton Transactions, 41 (2012) 876-884.

[200] M.A. Sørensen, H. Weihe, M.G. Vinum, J.S. Mortensen, L.H. Doerrer, J. Bendix, Chemical Science, 8 (2017) 3566-3575.

[201] D. Nandi, P. Karmakar, S. Ray, A. Chattopadhyay, R. Sarkar, A.K. Ghosh, Inorganic and Nano-Metal Chemistry, 48 (2018) 16-22.

[202] N.B. Katz, in, Google Patents, (2017).

[203] M.Y. Jomaa, M. Altaf, S. Ahmad, G. Bhatia, J. Singh, S. Altuwaijri, A.A. Isab, BioMetals, 30 (2017) 787-795.

[204] W.M. Abdel-Wahab, F.I. Moussa, N.A. Saad, Drug Design, Development and Therapy, 11 (2017) 901-943.

[205] Y. Ouyang, Y. Peng, J. Li, A. Holmgren, J. Lu, Metallomics, 10 (2018) 218-228.

[206] R. Rezaee, A.A. Momtazi, A. Monemi, A. Sahebkar, Pharmacological Research, 117 (2017) 218-227.

[207] F. Arnesano, M.I. Nardella, G. Natile, Coordination Chemistry Reviews, 374 (2018) 254-260.

[208] M. Frisch, G. Trucks, H. Schlegel, G. Scuseria, M. Robb, J. Cheeseman, G. Scalmani, V. Barone, B. Mennucci, G. Petersson, (2014).

Chapter Two

Kinetics and Mechanisms of Substitution Reactions of d^8 Square-Planar Complexes : Theory and Instrumental Details

2.1 Preamble

Square planar is a molecular geometry in which constituent atoms or group of atoms surrounding a central atom form the corners of a square in the same plane with the central atom [1]. The geometry is mostly adopted by transition metal complexes of a d^8 low spin configuration. Most common examples of metal ions that exhibit such configuration include: Au(III), Ni(II), Pd(II), Pt(II), Ir(I) and Rh(I). Ligand substitution reactions of these metal ions play a fundamental role in most biological and chemical processes. For example, Ni(II) and Pd(II) complexes are employed in homogeneous catalysis while Au(III), Pt(II) etc. are useful in anticancer chemotherapy [2]. In anticancer therapy, drugs such as cisplatin are designed to inhibit tumour growth by substituting the chloride ligand with a guanosine base of DNA [3]. This process has been established to involve the formation of bonds as well as the breaking of bonds.

The breaking and formation of covalent bonds during the interaction of electron-rich and electron-poor centres [4-6], often referred to as nucleophile–electrophile interaction, is one of the basic processes in chemistry. The nucleophile–electrophile interaction is the rationale that underpins the mechanism of reacting species. This process sometimes involves the substitution of an ion, an atom or a group of atoms from the functional site of the electrophile by the incoming nucleophile, a phenomenon known as ligand substitution reactions. Ligand substitution reaction occur when a ligand in a coordination sphere of a functional centre is replaced by another atom, a group of atoms or an ion resulting in a temporary change in the coordination number because of the breaking of bonds (with the leaving group) and the formation of new bonds (with the incoming species) [7]. Substitution reactions can be considered from two important perspectives: the electron rearrangement at the functional centre resulting from bond breaking and making processes; and the kinetics of the bond breaking and formation processes [8].

The kinetics and mechanisms of d^8 low spin metal complexes have been attracting a lot of attention from researchers in recent years [9]. Specifically, among the d^8 metal ions listed

above, substitution reactions of platinum(II) complexes are the most extensively studied and well-established in medicinal inorganic research, essentially because of its redox stability and relatively slow reactivity [9-11]. Consequently, a great number of platinum complexes of specific design have been synthesised and investigated for their kinetic and mechanistic behaviour and preponderance of these studies are reported in literature annually [7, 12-15]. Moreover, the information obtained on platinum(II) complexes can be extrapolated to understand the behaviour of other d^8-metal complexes since the mechanism of substitution behaviour of platinum(II) is similar to other square planar d^8-metal complexes, most especially those of Pd(II) complexes. However, Pd(II) complexes are $ca.10^5$ more reactive than their corresponding platinum(II) complexes [9, 16]. In this chapter, kinetics, mechanisms as well as factoring influencing the substitution reactions of platinum(II) complexes will be examined.

2.2   Mechanisms of Reactions at a d^8 Square-Planar Metal Centre

The mechanism of a reaction can be defined as the pathway by which reactants are transformed into products [17]. It sometimes involves the formation of intermediate species, usually in the first step, which are subsequently consumed in the other steps. In coordination chemistry, nucleophile-electrophile interactions form the basis of reaction mechanisms. The metal site of the complexes is the electrophilic centre while the incoming ligands are the nucleophilic agents [17, 18]. In general, the mechanism of ligand substitution reactions at a d^8 square planar metal centre can be fundamentally classified into three namely: Associative, Dissociative and Interchange.

2.2.1   Associative Mechanism (A)

This mechanism involves the formation of a single intermediate through two transition states in which bond formation takes priority over bond breaking (**Figure 2.1**). In other words, the rate determining step is the one involving the formation of a bond between the metal centre and the incoming nucleophile. The associative mechanism type is the most common mechanism for coordinatively unsaturated metal complexes, such as square-planar complexes, a typical example of these are the platinum(II) complexes [19]. The reaction proceeds mostly via a five-coordinate transition state with an intermediate with a trigonal bipyramidal structure.
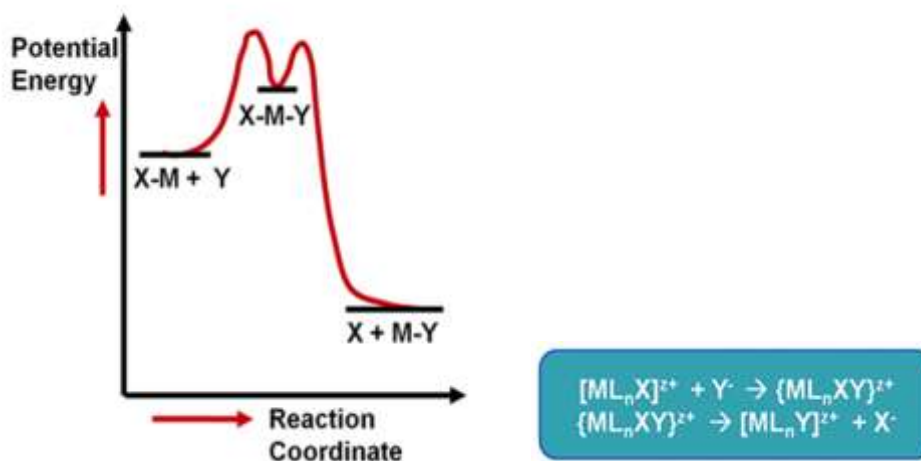
Figure 2.1:   Energy profile and equation of ligand substitution reaction for an associative
mechanism [20].

A case in point is when the entering group, **Y**, and the nucleofuge (leaving group), **X**, are
equivalent in terms of their chemical composition, the energy of the transition states of the bond
formation and breaking processes will be equivalent (**Figure 2.2**). In a non-coordinating solvent
and when the concentration of **Y** is in excess, the rate of substitution will largely be determined
by the character of the incoming nucleophile. The incoming group, **Y** is involved in both the
initial and the final stages of the transition state but the spatial arrangement of the complex is
maintained [12, 21].
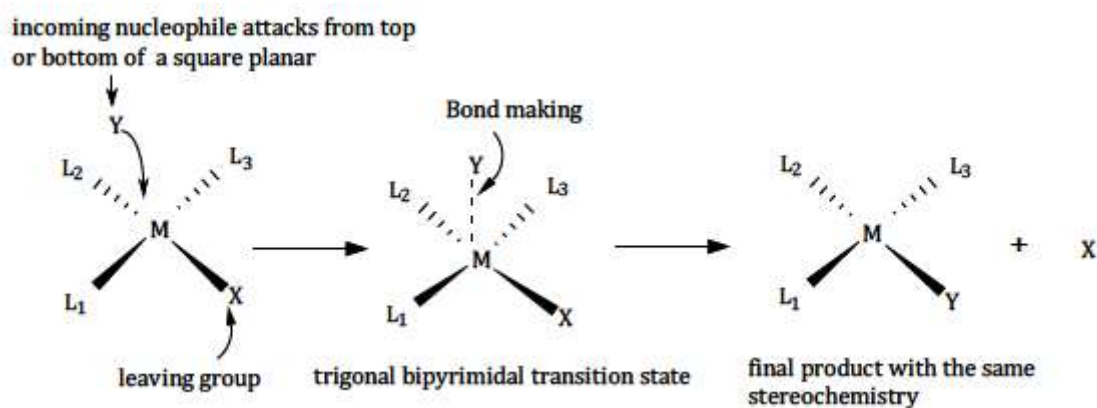
Figure 2.2:   A typical associative mode of ligand substitution at a square planar metal centre [22].

In a typical associative mechanism, all the participating ligand species, such as the chelate ligand, the leaving group and the incoming nucleophile can influence the activation energy and the stability of the reaction. This will, subsequently, impact the rate of the substitution reaction of the complex. Consequently, most ligand substitution reactions are carried out by varying the nature of the ligands [23].

During substitution, the electrophilic d^8 square-planar platinum(II) metal centre usually undergoes an associative mechanism involving a five-coordinate, trigonal bipyramidal transition state which has eighteen electrons in the valence shell [24]. This is made possible because of the empty $6p_z$ orbitals in the platinum(II) centre that can readily accommodate the extra electrons from the incoming nucleophiles [12, 15, 17]. Moreover, square-planar complexes are normally less crowded, hence, the incoming ligand can access the metal site both from above and below the plane, and still retain its geometry as shown in **Figure 2.2**.

2.2.2 Dissociative Mechanism (D)

This mechanism is normally displayed in metal complexes with an octahedral geometry. Most of the first-row transition metal series in the periodic table exhibit this mechanism during a substitution process because they have attained their saturated coordination number of six. Typically, the nucleofuge (the leaving group ligand) is lost in the first step, producing an intermediate with a reduced coordination number. The bond between the leaving group and the metal breaks completely before the nucleophile (incoming group) can attach itself to the metal centre. The intermediate formed during the bond breaking process usually have a lower coordination number. This allows the intermediate to selectively choose the potential ligands in the surrounding medium before it reacts with the incoming group [15]. The reaction rate of the electrophile with the incoming group is dependent on the character of the nucleofuge (leaving group) and is independent of the concentration and the nature of the incoming group. The nucleofuge moves from the coordination shell, which favours the solvent attack as the solvent is present in large access, hence, the product is formed while the leaving group is still in proximity. A typical energy profile and equation of dissociative mode of substitution at a square planar metal centre is shown below in **Figure 2.3**. For square planar platinum(II) complexes, non-stereo specific products are formed through dissociative mechanism. During dissociative mechanism, the complex forms a T-shaped three coordinate intermediate, which undergoes intermolecular transformation of '*cis*-like' configuration to form a '*trans*-like'

configuration. The mechanism is rare for square-planar platinum(II) complexes because an increase of electron density at the platinum(II) centre generally prevents the approach of the nucleophiles and stabilisation of the coordinatively unsaturated 14-electron intermediate. However, a dissociative mechanism will be dominant for substitution at a square-planar metal centre under the following three conditions, viz. in the presence of very bulky ligands, good leaving groups and strongly coordinating solvent [15, 25, 26]. With regards to bulky ligands, it essentially forestalls the nucleophile from approaching the metal centre.
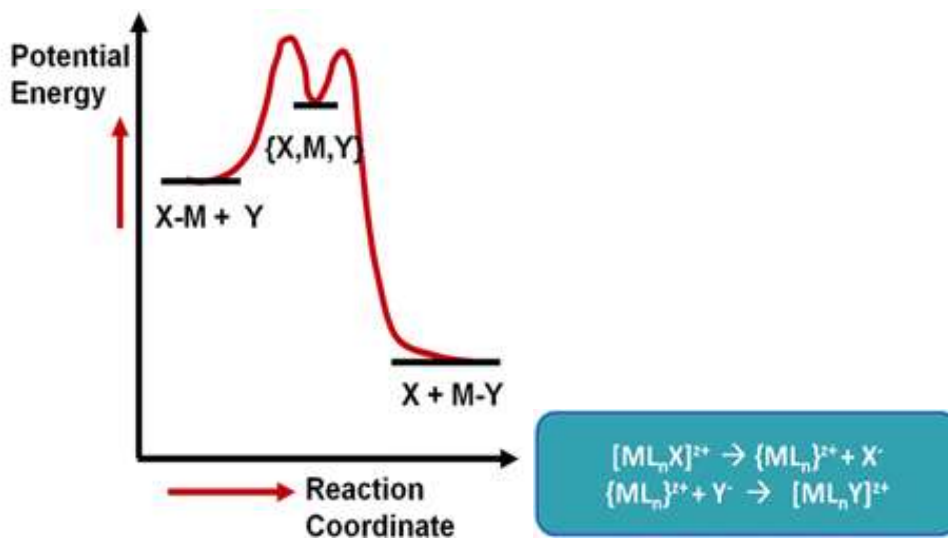
Figure 2.3:   Energy profile and equation of a typical ligand substitution reaction for a dissociative mechanism type [20].

Similarly, if the bond breaking between the metal centre and the leaving group dominates upon the approach of the nucleophile, a dissociative mechanism will be favoured. This is usually the case in the presence of strongly coordinating solvent because the solvent is in excess, it can easily facilitate the knock-off of the nucleofuge which results in the formation of the intermediate with a reduced coordination number. Unlike octahedral complexes, square-planar complexes essentially favour an associative mode of substitution, especially platinum(II) complexes. However, dissociative mechanisms have been reported in some square-planar complexes [25, 26].

2.2.3   Interchange Mechanism

One major feature of the interchange mechanism is the absence of an intermediate (**Figure 2.4**); both the nucleofuge and the nucleophile are involved in the formation of a specie known as the

activated complex [20]. In this mechanism, for the single activated complex to be formed, formation between the metal centre and the incoming nucleophile, and bond breaking between the metal and the leaving group occur in concert. There is an interplay of two possible scenarios in an interchange mechanism.
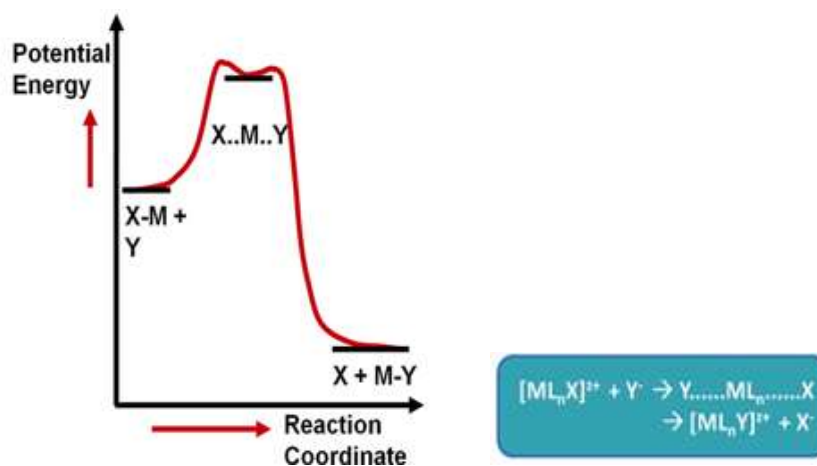
Figure 2.4:   Energy profile and equation of a typical ligand substitution reaction for an interchange mechanism type [20].

Firstly, if the rate of reaction depends on the nature of the incoming nucleophile, since the rate limiting step involves bond formation between the incoming nucleophile and the metal centre in the transition state, then the phenomenon is known as an associatively activated interchange mechanism (I_a). In this case, the bond-breaking process is less important even though the two steps exist in concert leading to the formation of the single activated complex. Secondly, if on the other hand, the breaking away of the nucleofuge from the inner coordination sphere is initiated as the nucleophile begins to approach the inner coordination sphere (the reactive centre) from the outer coordination sphere, in which case, bond-breaking dominates over bond-formation in the transition state, this is called a dissociatively activated interchange mechanism (I_d). This mechanism, in most cases, is initiated by the surrounding solvent molecules since they are present in the reaction medium in excess relative to the concentration of the nucleofuge, even before the nucleophile is introduced into the reaction medium. Thus, the possibility of solvent molecules attaching itself to the reactive metal centre is very high, hence, there is no discrimination between the nucleophile and the solvent molecules.

2.3   Kinetic Measurements

2.3.1   Determination of Rate Constants for Ligand Substitution Reactions

It has been well-established in kinetic experiments that the rate of any reaction is dependent on the concentration of the reactants, operating temperature, pressure etc. The reaction rate and its corresponding rate constant can be determined by monitoring the concentration of one of the reactant or product species as a function of time. This is evaluated by following the time dependence of a variable which correlate with concentration and/or absorbance. For diluted solutions, the absorbance and concentration are directly proportional according to the Beer-Lambert law [27]. Kinetic measurements of ligand substitution reactions of platinum(II) complexes are often performed by monitoring the change in absorbance at suitable wavelengths as a function of time [15]. Ideally, since all chemical reactions are reversible, these substitution reactions essentially do not go to completion but rather towards equilibrium and can be written as

$$A + B \quad \underset{k_{-2}}{\overset{k_2}{\rightleftharpoons}} \quad C$$

or

$$ML_3X + Y \quad \underset{k_{-2}}{\overset{k_2}{\rightleftharpoons}} \quad ML_3Y + X$$

(2.1)
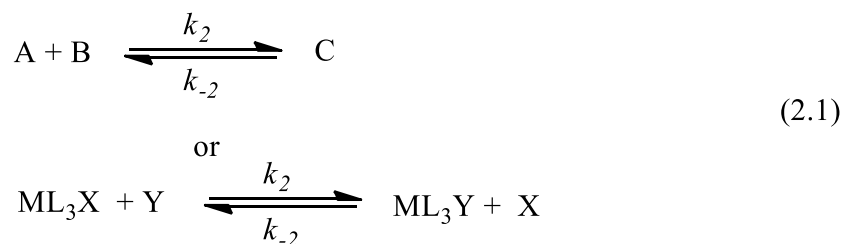
where   A = metal complex (ML$_3$X),   B = Incoming nucleophile Y,
X = nucleofuge (leaving group),
k$_2$ = second-order rate constant for the attack of the incoming nucleophile
k$_{-2}$= second-order rate constant of the reverse reaction

From the foregoing, the forward reaction is second-order while that of the reverse reaction is first-order [27]. The overall reaction, for both forward and backward processes, will display a mixed-order behaviour which often complicates the study. However, ligand substitution reactions for the forward reaction can be simplified by performing the study under *pseudo* first-order conditions [27] in which the concentration of the incoming nucleophile is at least in a ten-fold excess of that of the metal complex ([B]$_0$ >>>[A]$_0$) and the rate of formation of product C or the rate of disappearance of reactant A or B can be written as:

$$-\frac{d[A]}{dt} = -\frac{d[B]}{dt} = \frac{d[C]}{dt} = k_2[A]_t[B]_t - k_{-2}[C]_t$$

(2.2)

the mass balances at any time, *t,* can be expressed as:

$$[A]_t = [A]_0 - [C]_t \quad and \quad [B]_t = [B]_0 - [C]_t \tag{2.3}$$

At equilibrium, it can be written as:

$$[A]_e = [A]_0 - [C]_e \quad and \quad [B]_e = [B]_0 - [C]_e \tag{2.4}$$

Also, at equilibrium, the rates of the forward and the reverse reactions are equal, hence,

$$-\frac{d[A]}{dt} = k_2[A]_e[B]_e - k_{-2}[C]_e = 0 \tag{2.6}$$

Therefore, $\qquad\qquad k_2[A]_e[B]_e = k_{-2}[C]_e \tag{2.7}$

Rearranging *equation* 2.4 and substituting it into *equation* 2.7, we have:

$$k_2[A]_e[B]_e = k_{-2}([A]_0 - [A]_e) \tag{2.8}$$

Expanding the *equation,* we get: $\quad k_{-2}[A]_0 = k_2[A]_e[B]_e + k_{-2}[A]_e \tag{2.9}$

Rearranging *equation* 2.3 and substituting it into equation 2.2 gives:

$$-\frac{d[A]}{dt} = k_2[A]_t[B]_t - k_{-2}([A]_0 - [A]_t) \tag{2.10}$$

Thus, $\qquad\qquad k_2[A]_t[B]_t - k_{-2}[A]_0 = k_{-2}[A]_t \tag{2.11}$

Combining *equations* 2.9 and 2.11, we obtain:

$$-\frac{d[A]}{dt} = k_2[A]_t[B]_t - k_2[A]_e[B]_e - k_{-2}[A]_e + k_{-2}[A]_t \tag{2.12}$$

Under *pseudo* first-order conditions when $[B]_0 >>> [A]_0,$ *equation* 2.12 becomes

$$-\frac{d[A]}{dt} = k_2[A]_t[B]_0 - k_2[A]_e[B]_0 - k_{-2}[A]_e + k_{-2}[A]_t \tag{2.13}$$

Re-writing *equation* 2.13 gives

$$-\frac{d[A]}{dt} = (k_2[B]_0 + k_{-2})([A]_t - [A]_e) \tag{2.14}$$

Rearranging 2.14 and finding the integral of the resulting equation give:

$$\int_{[A]_0}^{[A]_t} \frac{d[A]}{([A]_t - [A]_e)} = -(k_2[B]_0 + k_{-2}) \int_0^t dt \tag{2.15}$$

$$\ln\left(\frac{[A]_t - [A]_e}{[A]_0 - [A]_e}\right) = -(k_2[B]_0 + k_{-2})t \tag{2.16}$$

When $k_{obs} = k_2[B]_0 + k_{-2}$, *equation* 2.16 will become:

$$\ln \left(\frac{[A]_t - [A]_e}{[A]_0 - [A]_e} \right) = -k_{obs}\, t \qquad (2.17)$$

Where k_{obs} = observed first-order or observed pseudo first-order rate constant

$[B]_0$ = is the initial concentration of the nucleophile = [NU].

Hence, a linear graph is obtained from the plot of k_{obs} against [NU] with a slope of k_2 and an intercept of k_{-2}. The equilibrium constant, K is evaluated from k_2/k_{-2}. K depicts the thermodynamic equilibrium position of the reaction [28, 29]. **Figure 2.5** shows a typical plot obtained for the substitution reaction of **tPt** with neutral thiourea-based nucleophiles (where **tPt** is diaqua transplatin).
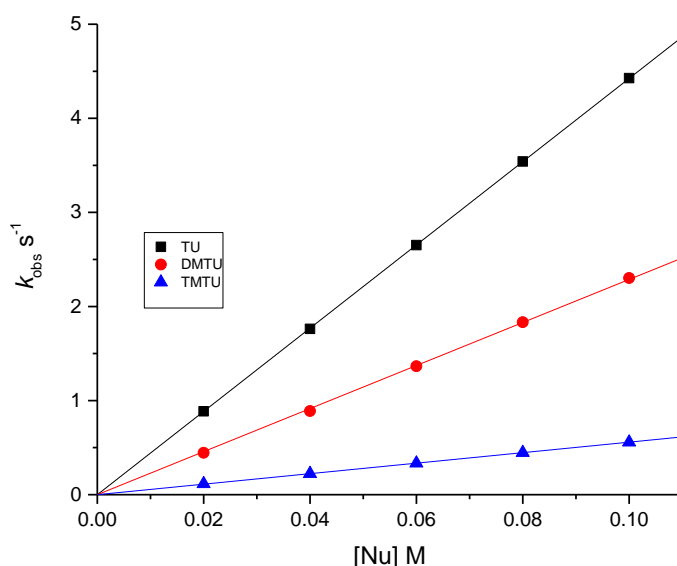
Figure 2.5: *Pseudo* first-order rate constants plotted as a function of the concentration of the entering nucleophiles for the substitution reaction of the diaqua **tPt** complex by thiourea (TU), dimethythiourea (DMTU), and tetramethylthiourea (TMTU) in water at 298 K.

The k_2 is dependent upon the character and concentration of the incoming nucleophile (**Figure 2.5**) [13, 15]. A plot which passes through zero implies that the forward reaction is irreversible and goes to completion. However, if there is a significantly positive intercept, this may be attributed to the reverse reaction or a parallel solvolysis reaction [13, 15, 24]. Some kinetic studies are performed in coordinating solvents [7], such as water, methanol etc., which are normally present in excess. In a situation where the contribution from the reverse reaction is negligible, then the k_{-2} term can be ascribed as a measure of the solvolysis pathway [12, 13, 17].

In such cases, the k_{-2} pathway involves two sequential associative steps, *viz.* the rate-determining step in which a solvent-metal complex bond is formed followed by the rapid substitution of the coordinated solvent molecule by the incoming nucleophile (**Figure 2.6**). This solvent associated pathway has been reported for the substitution kinetics of several square planar complexes [12, 18, 30-33]. This solvolysis pathway follows first-order kinetics and is hence independent of the concentration of the incoming nucleophile. The second pathway involves the direct nucleophilic attack by the incoming ligand, Y and so the k_2 is sensitive to the nature of the incoming nucleophile.

$$k_{obs} = k_2[\text{NU}] \qquad\qquad (2.18)$$

Notably, all the kinetics of substitution reactions reported in chapter three to chapter six have the k_{-2} term to be negligible, hence, under *pseudo* first-order conditions the values of k_2 can be calculated directly from Equation 2.18.
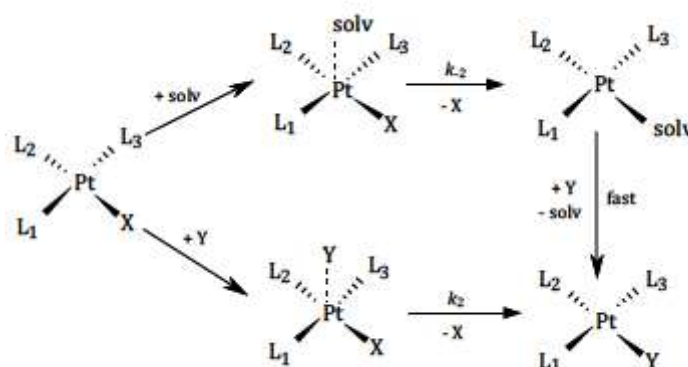
Figure 2.6:   A proposed dual reaction pathway for an associative substitution mechanism at the platinum(II) centre, where solv = solvent [22].

2.3.2   Activation Parameters

The evaluation of rate constants as a function of temperature are ordinarily employed to determine the reactions' activation parameters [12, 18, 33]. These parameters are pivotal in order to identify the mechanism of the reaction. Through the Transition State Theory, the enthalpy of activation ($\Delta H^{\#}$) and the entropy of activation ($\Delta S^{\#}$) are derived. In practice, to measure $\Delta H^{\#}$ and $\Delta S^{\#}$, the observed second-order rate constant is measured at different temperatures. The third activation parameter, volume of activation, $\Delta V^{\#}$ is measured by varying

the pressure of the reaction medium. The activation parameters together with the second-order rate constants obtained can thus be used to postulate the mechanism of any reaction.

2.3.2.1   Determination of Enthalpy of Activation, ($\Delta H^\#$) and Entropy of Activation, ($\Delta S^\#$)

Both $\Delta H^\#$ and $\Delta S^\#$ of the reactions are normally obtained from the temperature dependence studies of their rate constants based on the transition state theory [24, 34]. According to this theory, it is assumed that many reactions between A (metal centre) and B (incoming nucleophile) proceed via a pre-equilibrium mechanism between the reactants and the transition-state species (activated complex, $AB^\#$) before it is converted to the product C [26]. The mechanism is presented in *equation* 2.19.

$$A + B \underset{k_{-1}}{\overset{k_1}{\rightleftharpoons}} [AB]^\# \longrightarrow C$$

(2.19)
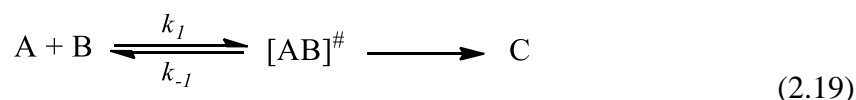
The rate law for the reaction above can be expressed as:

$$-\frac{d[A]}{dt} = k_1[AB]^\#$$

(2.20)

At equilibrium,

$$K^\# = \frac{k_1}{k_{-1}} = \frac{[AB\}_e^\#}{[A]_e[B]_e}$$

(2.21)

By rearranging, you get:

$$[AB\}_e^\# = K^\#[A]_e[B]_e$$

(2.22)

Substituting *equation* 2.22 into *equation* 2.20

$$-\frac{d[A]}{dt} = \frac{K_bT}{h}K^\#[A]_e[B]_e$$

(2.23)

However,
$$-\frac{d[A]}{dt} = k_2[A]_t[B]_t$$

(2.24)

Comparing *equations* 2.23 and 2.24

$$\therefore \quad k_2 = \frac{K_bT}{h}K^\#$$

(2.25)

Where k_b *= Boltzmann's constant (1.38 x 10^{-23} J/K)*

h *= Planck's constant (6.626 x 10^{-34} J s) [27]*

Expressing the pre-equilibrium constant, we have:

$$\Delta G^{\#} = -RT \, In \, K^{\#} \qquad (2.26)$$

$$\Delta G^{\#} = Activation \; Gibb's \; free \; energy$$

But $\quad \Delta G^{\#} = \Delta H^{\#} - T\Delta S^{\#} \qquad (2.27)$

By combining *equations* 2.25 and 2.26 gives:

$$In \, K^{\#} = -\frac{\Delta H^{\#}}{RT} + \frac{\Delta S^{\#}}{R} \qquad (2.28)$$

Substituting *equations* 2.28 into 2.25 gives the Eyring equation:

$$k_2 = \frac{K_b T}{h} e^{-\frac{\Delta H^{\#}}{RT}}. e^{\frac{\Delta S^{\#}}{R}} \qquad (2.29)$$

Rearranging and taking the natural logarithm of both sides gives:

$$\ln\left(\frac{k_2}{T}\right) = -\frac{\Delta H^{\#}}{R}.\frac{1}{T} + \left(\ln\frac{k_b}{h} + \frac{\Delta S^{\#}}{R}\right) \qquad (2.30)$$

$$\ln\left(\frac{k_2}{T}\right) = -\frac{\Delta H^{\#}}{R}.\frac{1}{T} + \left(23.8 + \frac{\Delta S^{\#}}{R}\right) \qquad (2.31)$$

The activation enthalpy, $\Delta H^{\#}$ and entropy, $\Delta S^{\#}$ values can be derived from a plot of $\ln(k_2/T)$ versus 1/T which gives a linear graph with a negative slope (**Figure 2.7**). The activation enthalpy value can be calculated from this slope while the entropy of activation can be determined from the intercept on the vertical axis.
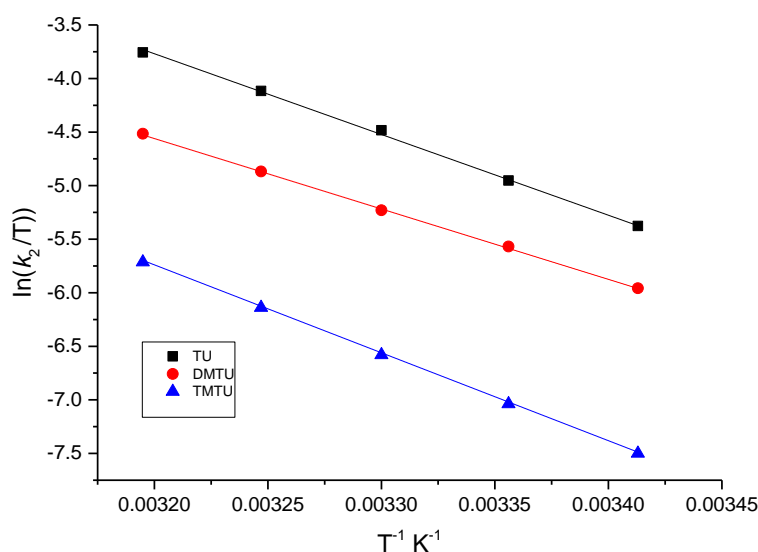
Figure 2.7: Plot of $\ln(k_2/T)$ against $1/T$ for the reaction of diaqua **tPt** with the thiourea nucleophiles in water at various temperatures ranging from 293 to 313 K.

The graph is literally referred to as the Eyring plot [35]. The magnitude of the two activation parameters can be employed to describe the mechanism of any substitution reaction. For an associative activated mechanism, the value of $\Delta H^{\#}$ tend to be relatively small whereas that of $\Delta S^{\#}$ tends to be significantly negative. However, in a dissociative activated mechanism, the $\Delta H^{\#}$ value is normally large while that of $\Delta S^{\#}$ will be positive [15, 36]. Oftentimes, when these activation parameters are used to predict the mechanism of a reaction, such inference are ordinarily made from the kinetic data derived from the substitution reaction of the metal complex with different nucleophiles. The drawback in using this method is that the activation entropy, $\Delta S^{\#}$ is normally obtained from the intercept on the vertical axis of the graph by extrapolating the graph to indeterminable temperatures. Consequently, the attendant errors that accompany the determined $\Delta S^{\#}$ values are customarily three times higher than that of $\Delta H^{\#}$ [36]. Accordingly, it is more reliable to use the volume of activation, ($\Delta V^{\#}$) in assigning a reaction mechanism. This is because $\Delta V^{\#}$ is often calculated by measuring the bimolecular rate constants, k_2 as the pressures of the reaction media are being varied. However, in order to make a meaningful description on the mode of activation, the sign and the magnitude of both the activation enthalpy and entropy are imperative.

61

2.3.2.2   Volume of Activation ($\Delta V^{\#}$)

The activation volume, $\Delta V^{\#}$ is a more reliable parameter for describing the underlying mechanism of any reaction as compared to the use of enthalpy and entropy of activation alone. The volume of activation denotes the change in partial volume as the reaction proceeds from reactants to the transition state, in such a way that the volume profile of the reaction mixture can be analysed in terms of the changes in the overall volume of the reactants [37-39]. $\Delta V^{\#}$ is derived from different observed rate constants, k_{obs}, and determined at different applied pressures. Pressure dependence studies of the rate constants result in the volume of activation as outlined in the thermodynamic equation below.

$$\Delta V = \left(\frac{\delta \Delta G}{\delta P}\right)_T \tag{2.32}$$

But $\Delta G^{\#} = -RT \ln K^{\#}$ and by combining this with *equation* 2.32, it can be rewritten as

$$\left(\frac{\delta \ln K^{\#}}{\delta P}\right)_T = -\frac{\Delta V^{\#}}{RT} \tag{2.33}$$

Where $\Delta V^{\#}$ = the volume of activation and is equal to the difference between the partial molar volumes.

Combining *equations* 2.25 and 2.33 gives:

$$\delta \left(\frac{\ln k_2}{\delta P}\right)_T = -\frac{\Delta V^{\#}}{RT} \tag{2.34}$$

From *equation* 2.34, it can be deduced that if rate constant, k_2 increases with increasing pressure, $\Delta V^{\#}$ is negative. If on the other hand, $\Delta V^{\#}$ has a positive value, this implies that there is a decrease in the second-order rate constant k_2 as the pressure of the reacting mixtures increasing.

Rearranging *equation* 2.34 and integrating both sides within the limits gives:

$$\int_{(k_2)_0}^{k_2} \ln k_2 = -\frac{\Delta V^{\#}}{RT} \int_0^P \delta P \tag{2.35}$$

$$\ln k_2 = \ln(k_2)_0 - \frac{\Delta V^{\#}}{RT} P \tag{2.36}$$

$$\ln(k_2)_0 = \textit{the rate constant at zero pressure}$$

A linear graph with a negative slope of $\frac{\Delta V^{\#}}{RT}$ is derived from the plot of ln k_2 verses P. The volume of activation, $(\Delta V^{\#})$ is a combination of both an intrinsic contribution $(\Delta V^{\#}_{int})$ due to changes in internuclear distances within the reactants to form the transition state and an electrostrictive contribution $(\Delta V^{\#}_{elec})$. For ligand substitution reactions involving charged species, the experimentally obtained $\Delta V^{\#}$ is dominated by $\Delta V^{\#}_{elec}$ due to changes in charge that occur during the reaction. However, this is not case for solvent exchange reactions due to the absence of electrostrictive changes $\Delta V^{\#} \approx \Delta V^{\#}_{int}$, the activation step for bond formation [27, 37, 40]. Moreover, a positive value of $\Delta V^{\#}$ implies a dissociative mechanism while a negative value indicates an associative mechanism. The errors associated with the volume of activation are relatively small compared to the entropy of activation because the activation volumes are determined from the slope of the graph. Therefore, a high pressure between 100 - 200 MPa is required to have a significant effect on the reaction rates.

2.4   Instruments Employed in Kinetics Studies

The performance of kinetic measurements often involve monitoring the dependence of a certain physical quantity, such as concentration, pressure, pH, conductivity, absorbance, density etc., as a function of time [27]. The concentration of the products or the reactants in the reaction are commonly a function of the physical parameter being measured. The values obtained from the kinetic measurement is then fitted into a suitable equation to determine the rate constant [12]. Different techniques, such as nuclear magnetic resonance (NMR), UV/Visible spectrophotometry and pulsed methods are used to investigate the rate of reactions [27, 28, 41]. The choice of instrument employed to monitor the reaction kinetics depends on the nature and rapidity of the reaction [42]. Irrespective of the technique employed, the measured physical property must be proportional to the concentration as a function of time after mixing. The reactants must be mixed within the shortest time possible depending on the reaction time scale. Physical conditions, such as temperature, pressure etc., must be accurately controlled. A chemical reaction is broadly considered as fast if it can attain half of the initial concentration of the reactant that is being monitored within 10 seconds [43]. Experimental determination of the rate constant of very fast reactions, such as proton transfer, enzymes and non-covalent complex formation [15] which are outside the limit of the classical laboratory time-scale are studied using specialised instruments. The time-scale for fast reactions varies between 1 minute to 10^{-14} seconds [36]. Sometimes, fast reactions are investigated by bringing their rates into the

classical laboratory time-range by tuning the reaction conditions, such as temperature, concentration or the solvent. This method is only reliable if the half-life of the reaction is greater than 1 hour. Basically, the two main methods often used to study fast reactions include flow methods and pulse methods [44, 45].

However, significantly slow reactions are usually studied using classical methods, such as UV/Visible spectrophotometry, which involves first mixing of the reagents first and then determining the decrease in the concentration of the reactant(s) or the increase in the concentration of the product(s) as a function of time. The mixing time for the starting reacting species and taken measurement should be negligible so that it does not impact on the actual rate of the reaction. Although there are several methods available for kinetic studies [15, 27, 42, 44, 45], the UV/Visible spectrophotometry and the stopped-flow techniques are employed in this research project.

2.4.1 UV/Visible Spectrophotometry

Oftentimes, a slow substitution reaction, that is a reaction that lasts beyond 16 minutes, is followed using a UV/Visible spectrophotometer. UV/Visible spectrophotometry is a technique [17] which is sensitive enough to detect sample concentrations in the range 10^{-4} to 10^{-6} M [35]. The instrument consists of two light sources, one in the visible (tungsten lamp, for detection ranging from 800 to 350 nm) and the other in ultraviolet (deuterium lamp, for detection ranging from 350-200 nm), a monochromator, reference and sample compartments, temperature control unit, detector, the data processer and the output-readout system [46]. The detector that is commonly employed is a photomultiplier tube. In a UV/Visible spectrophotometer, radiation from the light source passes through a monochromator, then the light is dispersed by the grating prisms and the monochromator allows light of a single wavelength to pass through. The light with a single wavelength with intensity, I_0, passes through the sample cell called a cuvette with length, l where the sample absorbs some light. Contemporary spectrophotometers are based on a double-beam design where it manages the light alternatively to pass through the sample cell and the reference cell using a chopper which is a motor that rotates a mirror into and out of the light path [46, 47]. The basic set-up of the UV/Visible spectrophotometer is presented in **Figure 2.8**.
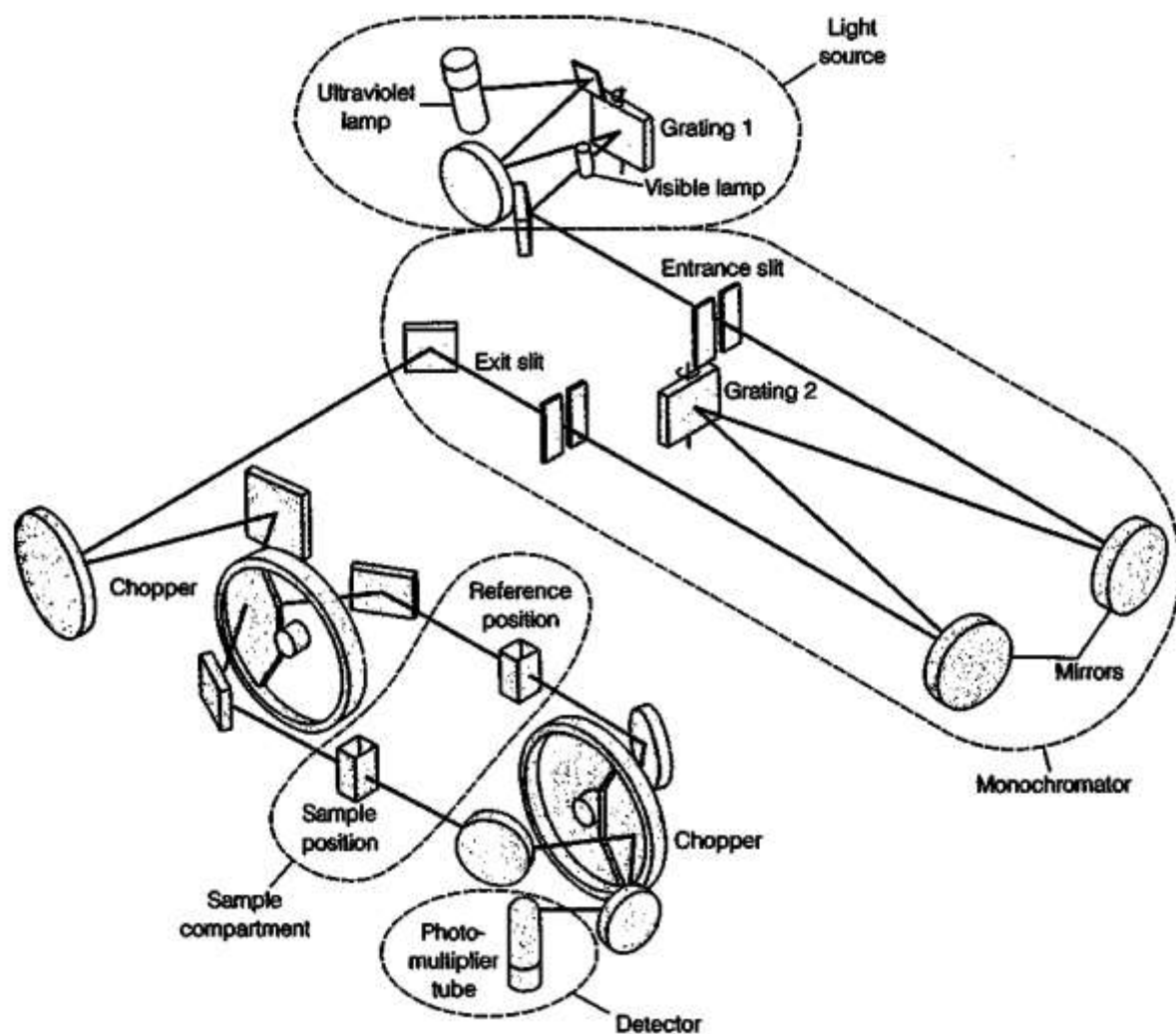
Figure 2.8:   Schematic diagram of a double beam UV/Visible Spectrophotometer [7].

The extent of interaction of the sample with transmittance or absorbance is determined by measuring both the intensity of the incident transmittance or absorbance, I_0 (without the sample) and the transmitted intensity, I (with the sample). The light transmitted from the sample is expressed as follows:

$$T = \frac{I_0}{I} \qquad\qquad (2.37)$$

where I_0 = the intensity of the incident light obtained from the solvent reference cell,
I = the intensity of the transmitted light from the power source after passing through the sample cell

Absorbance can be expressed as

$$A = -\log T \tag{2.38}$$

In ligand substitution kinetics, absorbance values are used instead of transmittance because there is a linear relationship between absorbance and two important parameters, the concentration of the reacting species and the path length of the cuvette, as stated by Beer-Lambert's law (*equation* 2.38).

$$A = \varepsilon C l \tag{2.39}$$

$$\varepsilon = molar\ absorptivity\ \left(\frac{M}{cm}\right), \quad C = concentration\ (M)$$

$$l = path\ length\ (cm)$$

For any simple first-order process,

$$X \xrightarrow{\ k_1\ } Y \tag{2.40}$$

The absorption at any time t, (A_t) is given as:

$$A_t = \varepsilon_X[X] + \varepsilon_Y[Y] \tag{2.41}$$

where, A_t = the absorbance at any time, t, ε_X and ε_Y = molar absorptivity of X and Y species respectively.

If the reaction proceeds to completion, the absorption is given by:

$$A_\infty = \varepsilon_X[X]_0 + \varepsilon_Y[Y]_0 \tag{2.42}$$

where A_∞ = absorbance upon completion of reaction, $[X]_0\ and\ [Y]_0$ = initial concentration of X and Y species respectively

The kinetic analysis relating the optical absorbance to the first-order rate constant (*equation* 2.38) can be obtained from the integrated rate-law given in *equation* 2.43. The absorbance-time resolved data in kinetic reactions are used directly to calculate the observed rate constants using *equation* 2.43.

$$\ln\frac{[X]_0}{[X]_t} = \ln\left(\frac{A_0 - A_\infty}{A_t - A_\infty}\right) = k_{obs}t \qquad (2.43)$$

In this study, relatively slow substitution reactions were performed on a Cary 100 Bio UV/Visible spectrophotometer with a cell compartment thermostated by a Varian Peltier temperature controller having an accuracy of $\pm$ 0.05 °C. UV/Visible scans were recorded at predetermined time intervals over the wavelength range of 200 to 800 nm immediately after mixing the reacting species. The obtained kinetic data were graphically analysed using the Origin 9.1® software suite [48] to give the kinetic trace with the time taken for the reaction to go to completion. The time obtained from the kinetic trace gave the observed first-order rate constant, k_{obs}. It is pertinent to mention that the UV/Visible absorption spectroscopy is also used to carry out spectrophotometric titrations, especially in pK_a determination experiments. The pK_a values of the coordinated aqua ligand is an important thermodynamic set of data used to estimate the electrophilicity of the metal centre [49-55].

2.4.2   Flow Techniques

Flow techniques are normally employed to investigate reactions that take place in milliseconds time scale. The mixing time in flow methods varies roughly from 1 millisecond to 10 seconds. These methods are used to monitor quite fast reactions with half-lives of about 10^{-2} seconds [42, 47]. Generally, flow techniques allow two reactant solutions to be rapidly mixed under pressure in a reaction mixing chamber. The changes in the concentrations of the reactants or products are then measured at various time intervals at different positions of the tube. The flow methods can be either **continuous-flow** or **stopped-flow** techniques. The design of the flow instrument is often associated with monitoring of reaction progress by UV/Visible spectrophotometry techniques in which *equation* 2.43 is used to calculate the observed rate constants.

2.4.3   Continuous Flow Method

A simple continuous-flow method, shown schematically in **Figure 2.9.** Continuous flow is applied when studying rapidly fast reactions, reactions within one second [36, 56]. In the continuous-flow method, two reacting solutions (A and B, **Figure 2.9**) are driven into the

mixing chamber by the pistons and the resulting solution then flows into the observation tube. This solution is then spectroscopically detected at a specific distance (*d*) from the mixer where a steady state is attained. One of the limitations of this technique is that it requires a large amount of reacting solutions. The use of the stopped-flow technique provides an alternative to overcome this limitation [27, 40].
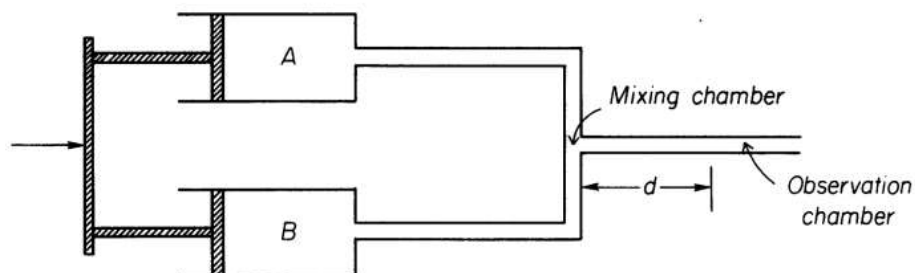
Figure 2.9: Schematic diagram of a continuous flow kinetic system [22].

2.4.4 Stopped-Flow Method

The stopped-flow method (**Figure 2.10**) is commonly used as a tool in the investigation of mechanisms of molecular kinetic processes in the time range from milliseconds to hundreds of seconds. Throughout this research project, an Applied Photophysics SX.20 stopped-flow reaction analyser coupled to an online data acquisition system was employed to study the moderately fast reactions. The temperature of the instrument was controlled to within ± 0.1 °C. For experiments requiring the stopped flow technique, small volumes of solutions are rapidly driven from syringes by a compressed gas-driven piston (800 kPa) into a high efficiency mixer to initiate a fast reaction at a set temperature. The new reaction mixture is rapidly moved into an observation cell while the previous contents of the cell are flushed out. The volume of the respective reactants that is fed into the mixing chamber is limited by the stop syringe which provides the "stopped-flow". The composition of the reaction mixture is then spectrophotometrically followed at a pre-set wavelength whereby the amount of light transmitted through the mixed solution undergo changes as the reaction proceeds in the stationary mixed solution. A photomultiplier unit converts the transmitted light into an electric current and a signal is fed to the computer over a suitable time range. The kinetic traces acquired under *pseudo* first-order conditions are then fitted to exponential functions to evaluate the observed *pseudo* first-order rate constant. Some examples of the stopped flow kinetic traces are shown in **Figures 3.3**, **4.3, 5.3** and **6.3** in *Chapters Three, Four, Five* and *Six* respectively. In

68

general, the stopped-flow technique is the most widely accepted technique for studying very fast reactions which have a half-life range of ca. 100 to 10^3 seconds [27, 40].
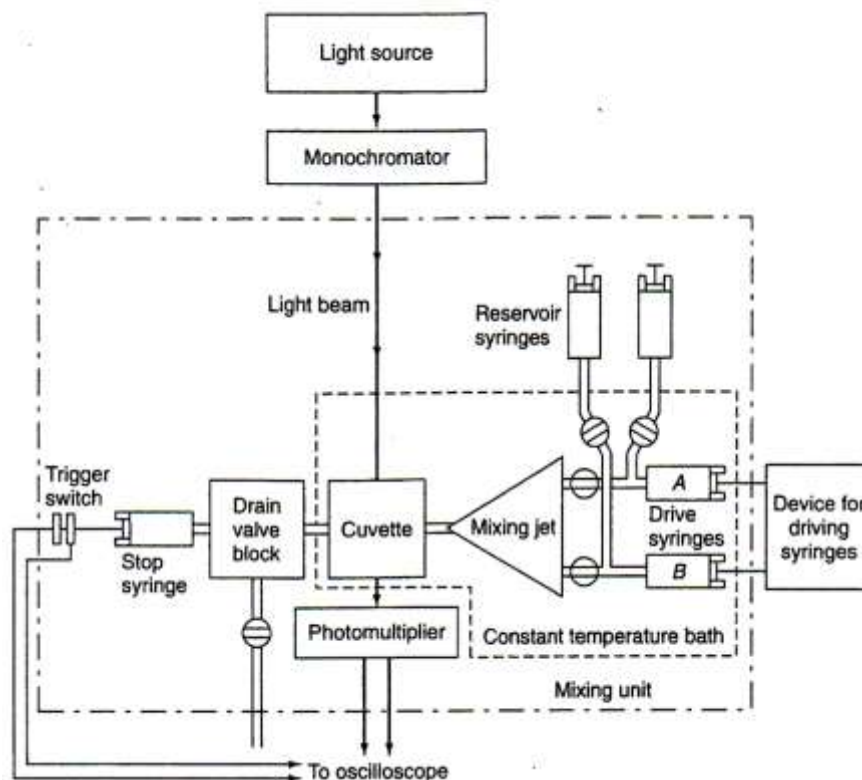
Figure 2.10   Diagrammatic representation of the stopped-flow [35].

2.5   Factors Influencing the Reactivity at a d^8 Square-Planar Platinum(II) Centre

2.5.1   The Influence of Incoming Nucleophiles

Several kinetic investigations have established that the associative mechanism of ligand substitution reactions in platinum(II) complexes depends on the nucleophilicity of the different incoming groups [12, 13, 15, 33, 35, 46]. The idea of nucleophilicity gives a quantitative measure of the ability of a Lewis base to act as an incoming group and to influence a reaction rate in a nucleophilic substitution process. The extent of nucleophilicity is established by determining the relative rate of the reaction of different nucleophilic groups with a standard substrate. In inorganic reaction mechanisms, the substitution reactions of *trans*-[Pt(py)$_2$Cl$_2$] in methanol solution is normally employed as the standard and the nucleophilicity factor is often expressed for Pt(II) complexes in terms of n_{Pt} index given by *equation* 2.44 [57].

$$n_{Pt} = \log \frac{k_2}{k_{-2}} \tag{2.44}$$

69

where k_2 = the rate constant for the reaction of the incoming nucleophile, k_{-2} = the rate constant for solvent attack (methanol)

Several studies on the platinum(II) complexes have reported the order of nucleophilic reactivity as follows [58, 59]:

$$R_3P > TU > SCN^- > N_3^- > NO_2^- > Br^- > Py > Aniline \sim NH_3 \sim Cl^- > H_2O > OH^-$$
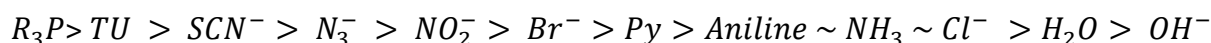
The nucleophilicity index, n_{Pt} obtained is applicable to other Pt(II) systems according to the expression given in *equation* 2.45 [60, 61].

$$\log k_2 = S(n_{Pt}) + \log k_{-2} \qquad\qquad (2.45)$$

The equation above indicates that for a specific substrate except for complexes with π acceptor ligands, there is linear free energy relationship between log k_2 for a certain nucleophile and nucleophilicity index, n_{Pt} value (**Figure 2.11**). The substrates with π-acceptor ligands are exceptions because they can form metal-ligand π-bonding at the transition state thereby lowering the energy of the transition state. This also depends on the π-donor ability of the metal complex which makes some nucleophilic species to be more reactive towards some better π-donor metal complexes or less reactive to certain complexes. The slope *S* of the plots in **Figure 2.11**, is the nucleophilic discrimination factor and the intercept log k_{-2} , is the intrinsic factor. The former is dependent on the nature of the complex and is a relative measure of its ability to discriminate between the various incoming nucleophiles.
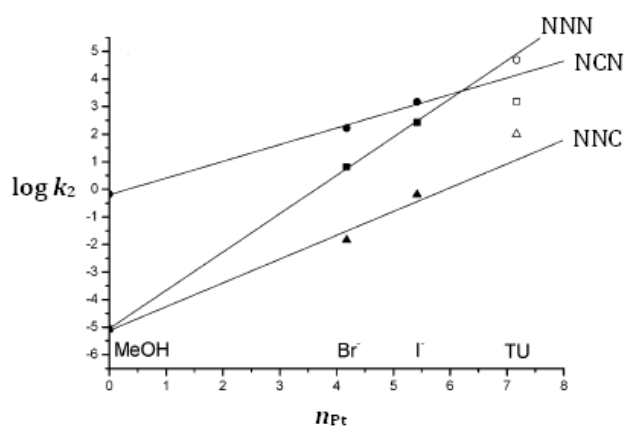
Figure 2.11: Plots of log k_2 against n_{Pt} for the determination of the nucleophilic discrimination factor, *S* of Pt(II) complexes [30] where: **NNC** = [Pt(N−N−C)Cl] (N−N−CH = 6-phenyl-2,2'-bipyridine), **NCN** = [Pt(N−C−N)Cl] (N−CH−N = 1,3-di(2-pyridyl)benzene), and **NNN** = [Pt(N−N−N)Cl]Cl (N−N−N = 2,2':6',2'-terpyridine).

70

A large value of *S* implies that the complex is very sensitive to changes in the nature of the nucleophilic reagent. The magnitude of k_{-2} is a function of the "intrinsic" reactivity of the platinum complex with the poorest nucleophilic reagent whose effect can be measured in any solution [61]. With such a poor nucleophile, the complex is expected to drive the reaction to the activated complex of the reaction. If on the other hand, the value of k_{-2} is small, the tendency of the complex to react is minor and will rely more on the nucleophile. It is pertinent to recall that nucleophilicity is a kinetic term which, in most cases, correlated with the polarizability of the incoming ligand, basicity and the nature of the substituent on the ligand.

2.5.1.1 Polarizability of the Nucleophile

It is widely accepted that polarizable molecules and ions, such as thiourea, iodide ion and unsaturated systems are more nucleophilic than their basicities can afford [62]. For neutral nucleophiles, size dictates the nucleophilicity and this is because larger elements have a bigger, more diffuse and more polarizable electron density. This electron density enhances the formation of a more effective orbital overlap in the transition state of bimolecular nucleophilic substitution reactions, which results in a transition state that is of lower energy and a nucleophilic substitution that take place at a faster rate. This is also corroborated by the hard and soft acid-base theory. "Hard" nucleophiles preferentially favours "hard" metal centres whereas "soft" nucleophiles prefer "soft" substrates or metal centres [15]. The term soft nucleophiles refer to the relatively polarizable nucleophiles while hard nucleophiles allude to relatively non-polarizable. Like soft bases, soft nucleophiles have high HOMO energy thereby making them to be effective as nucleophiles [5, 63, 64]. In solution, polarizable nucleophiles are superior to non-polarizable nucleophiles because they can respond easily to the demand for charge reorganisation. For ionic nucleophiles, the polarizability of the nucleophilicity follows the order $I^- > Br^- > Cl^- > F^-$. This polarizability order explains the trend in reactivities of the ionic nucleophiles as reported in a number of kinetics studies [65, 66].

2.5.1.2 Basicity of the Nucleophile

Basicity has a vital role in determining the nucleophilic reactivity toward Pt(II) complexes [62, 65, 67]. As already observed in the cases of Pd(II) complexes [68], the reactivity of platinum(II) complexes is linearly related to the basicity of the incoming nucleophiles [69, 70]. Pitteri *et al.*

[70] observed that for a reversible substitution reaction, there is a relatively large dependence of reactivity upon the basicity of the nucleophile in the reverse process as compared to the forward reaction. The observation indicates that the formation of the transition state involves a structure containing a well-formed Pt–X and a weak Pt–Nu, where X and Nu are leaving group and the incoming nucleophile respectively. In general, the relationship between basicity of the nucleophiles and the rate constant of a given substitution reaction can be described by *equation 2.46*.

$$\log k_2 = \alpha(pK_a) + constant \tag{2.46}$$

A straight line graph is obtained from the plot of log k_2 versus pK_a with the slope of α, which denotes the ability of the Pt(II) centre to screen the incoming ligands of different basicity [60, 61]. The positive slopes imply an increase in the electron density around the reactive metal centre which is typical of an associative mode of substitution behaviour. The negative slope is an indication of the solvolytic reverse reaction [71, 72].

2.5.2 The Character of Non-participating Groups in the Complex

2.5.2.1 *Trans* Effect

The idea of the *trans* effect was introduced by Chernyaev in 1926 to elucidate on the empirical observation that the rate of substitution of a ligand in a square planar or octahedral metal complex depends on the group *trans* to it much more so than groups in *cis* positions [18]. Following this discovery, the kinetics of many other systems have been rationalised using the *trans* effect [51, 73]. The *trans* effect can be best described as the effect of a coordinated ligand upon the rate of substitution of ligands opposite to it. The ligand *trans* to the leaving group can influence the reaction rate by several orders of magnitude between10^5-10^6 [74].

Generally, the substitution rate of the leaving group by the incoming group is faster if the *trans* ligand is a strong σ donor or a good π-acceptor [75]. However, relatively hard pure σ- donors, such as NH_3, H_2O and OH^- have a weak *trans*-directing effect. This clear contradiction appears to imply that there is another factor responsible to *trans* directing of substitution and this is the *trans* influence. *Trans* influence is the degree to which a ligand weakens the bond that is *trans* to itself. This is completely a thermodynamic effect and manifests itself as changes in bond lengths, force constants and vibrational frequencies [76]. For instance, for a series of *trans*-metal complexes if a *trans* ligand T is changed, the M- X bond length is very sensitive to the

electronegativity of T (where T, M and X stands for *trans* ligand, metal centre and leaving group respectively). If the electronegativity of the ligand that is *trans* to the leaving group, X decreases, the distance M- X increases. This increase in length results from a weakened bond in the ground state and leads to the increase in the reactivity of the association process. Basically, the structural *trans* influence follows the order:

$$H^- > R_3P > SCN^- > I^- > CH_3 \sim Olefins \sim CO \sim CN^- > Br^- > Cl^- > NH_3 > OH^-$$
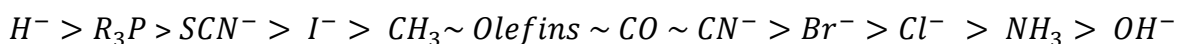
2.5.2.2 σ -Donation *Trans* Effect

Based on the polarization theory, the *trans* effect is considered to be predominantly electrostatic in origin and transmitted through σ-bonds, also known as σ-*trans* effect [76]. In the ground state and in square planar complexes, such as Pt(II), strong σ-donor ligands donate electrons very efficiently to the metal via σ-bonds. The efficient sigma donor capability can be attributed to their good overlap with the metal orbital which results in an interaction thereby lowering the overall energy (**Figure 2.12**). In other words, if the *trans* ligand is a strong σ-donor, the metal's *p*-orbital bonds more preferentially with it than the ligand *trans* to it. This results into elongation and weakening of the M-X bond while strengthening the M-T bond (**Figure 2.13**). In substitution reactions, the weak bond will break easily thereby leading to the increase in the substitution rate.
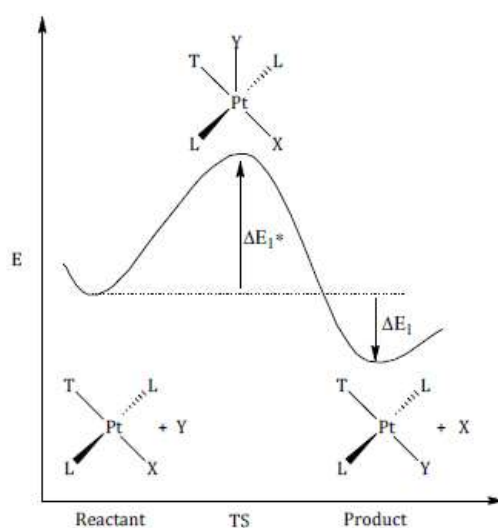
Figure 2.12: Sketch showing the effect of a σ-donor *trans* ligands on energies of ground state and transition state of a square-planar platinum(II) complex. TS = transition state [77-79].

The σ-trans effect order which is approximately the order of decreasing polarizability of the ligands is [12, 15]:

$$H^- > R_3P > SCN^- > I^- > CH_3 > CO > CN^- > Br^- > Cl^- > NH_3 > OH^-$$
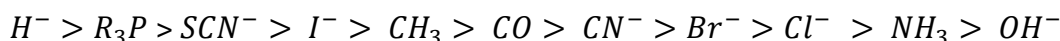
Since the polarizability of the metal ion is important, this theory readily accounts for the observation that the *trans* effect is greatest in the most polarizable or softest platinum(II) complexes than those of Pd(II).
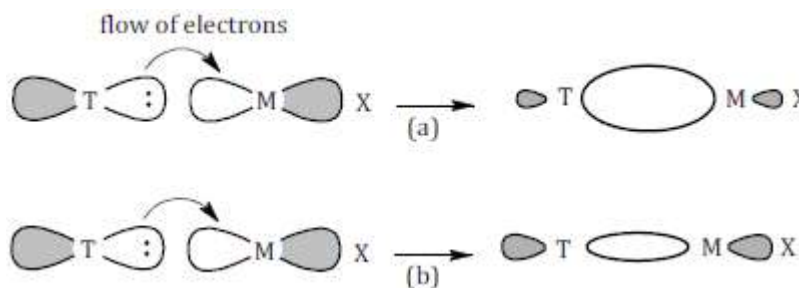
Figure 2.13: Sigma-bonding effect [60]. (a) Strong sigma-donor ligand T , the sigma-bond strength of M-T is much greater than that of M-X , (b) weak sigma-donor *trans* ligand gets poorer overlap with the metal orbital

Particularly, as electrons are donated from the filled ligand orbital to the vacant metal orbital, this kind of interaction will diminish the total (positive) natural bonding order (NBO charge) of the platinum(II) centre due to an increase in electron density in the *xy* plane. An increase in the rate of substitution reaction in platinum(II) complexes as a result of the *trans* σ-donation effect was reported in previous studies [80, 81].

2.5.2.3 π -Back-Donation *Trans* Effect

In the π-*trans* effect theory for d^8 square-planar complexes, such as platinum(II) [75] the trigonal bipyramidal intermediate can be stabilised by removing the electron density from π-orbitals of the incoming group Y (via metal d orbitals) to π-acceptor orbitals of the *trans* ligand T (**Figure 2.14**) [82]. This electronic communication through π-bonding is only possible if the three ligands and the metal centre all lie in the same plane in the transition state thereby enhancing effective delocalization of the extra charge from the metal. Pi-back bonding also favours low energy of the transition state resulting in a low activation energy for the substitution reaction (**Figure 2.15**) [83]. Calculation of the overlap of the valence orbitals of several ligands with the platinum *6pπ* orbital presupposes a pi-*trans* effect order of increasing nucleophilicity [12, 15, 18, 36, 83]:

$$C_2H_2 \approx CO > CN^- > NO_2^- > SCN^- > I^- > Br^- > Cl^- > NH_3 > OH^-$$
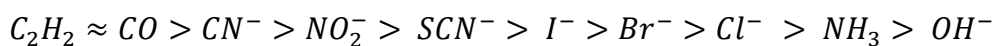
The overall *trans* effect trend combines both σ- and π-*trans* effects as follows [ibid.]:

$$C_2H_2 \approx CO > CN^- > R_3P > H^- > CH_3 \approx SCN_2H_4 > I^- > Br^- > Cl^- > Py, NH_3 > OH^- > H_2O$$
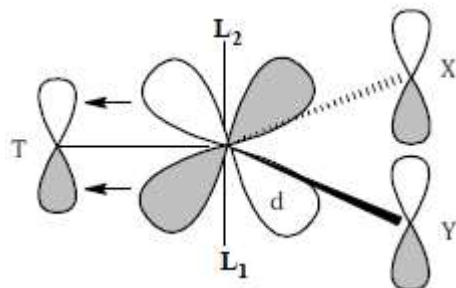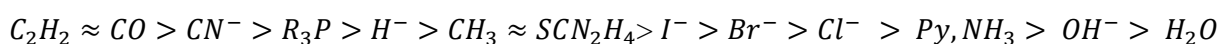
Figure 2.14:   Schematic diagram of the π-bonding mechanism for the t*rans*-effect [18].
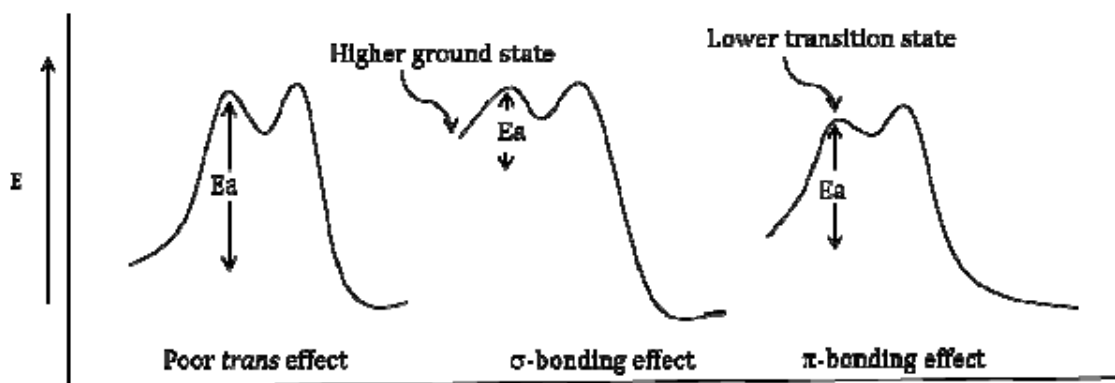
Figure 2.15:   *Trans* effect on activation energy [19].

π-Acceptor groups, unlike σ-donor groups, increase the total NBO charge of the platinum(II) atom by decreasing the electron density in the *xz* plane through π-back-donation. It also enhances a nucleophilic attack in the *xz* plane thereby stabilising the corresponding penta-coordinated transition state [84]. Systematic adjustment of the position of π-acceptor groups (*cis/trans*) affects the electronic communication in the system, thus, has an effect on the reactivity of the platinum(II) centre with *cis* π-back bonding found to be stronger than *trans* π-back bonding [85]. Until recently, it was widely acknowledged that an increase in π-surface and hence π-acceptor properties in a system enhances the nucleophilic substitution process of platinum(II) complexes [66, 86-88]. However, in a recent study [66], it was observed that an increased π-surface of isoquinoline does not accelerate the rate of substitution reactions but

rather it decelerates the reactivity by a magnitude of three mainly because the isoquinoline is a net σ-donor.

2.5.2.4 *Cis* Effect

The ligand that is *cis* to the nucleofuge exerts a veritably small electronic effect. This effect becomes prominent only when the nucleophile is poor in terms of its donor capacity. This effect, however, becomes significant when the *cis* ligands are big which preclude the incoming nucleophile from accessing the axial position of the metal centre [89, 90] and sometimes, bring about a mechanistic change from an associative to a dissociative mechanism. This is made possible because, in associative ligand substitution reactions, a trigonal-bipyramidal transition state is greatly strained by *cis* blocking but not nearly so crowded by *trans* blocking. Reports in literature reveals that *cis* blocking causes the relative drop in the rate of reaction by a factor of thousands compared to *trans* blocking [91]. Besides the *cis* steric hindrance, the *cis* σ- donor effect also increases the electron density at the metal centre and slows down the reactivity of the platinum(II) complex [92]. Unlike the *cis* σ- donor effect, the *cis* π-effect reduces electron density at the platinum(II) centre thereby accelerating its reactivity.

2.5.3 Role of the Leaving Group

The role of the leaving group on the rate of the substitution reaction is dependent on the following: nature of the reaction centre, nature of incoming nucleophiles and the nature of the *trans* ligand [38]. Hence, it will be inappropriate to make a clear-cut general trend. For complexes in which leaving group effects occur, it is presumed that bond breakage of the five-coordinate intermediate produced during an associative mode of substitution may considerably contribute towards the observed kinetic variables and may even be the rate-determining step under rigorous conditions, such as strongly bonded leaving groups [76]. A set of reactions which have been employed to investigate the role of the leaving group effect on the substitution kinetics of square planar complexes is given in *equation* 2.47 below [7].

$$\left[\text{Pt(dien)X}\right]^{(2-n)+} + \text{NU}^{x-1} \longrightarrow \left[\text{Pt(dien)(NU)}\right]^{(2-x)+} + \text{X}^{n-1} \qquad (2.47)$$
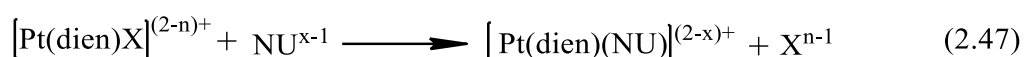
In the study above, the strongly complexing dien ligand has rendered the three other coordination positions and the incoming ligand (NU) that most often used is pyridine (py). The

reaction rates obtained in aqueous solution are given in **Table 2.1** and the rate constant for the displacement of X decreases in the order [76]:

$$NO_3^- > H_2O > Cl^- > Br^- > I^- > N_3^- > SCN^- > NO_2 > CN^-$$
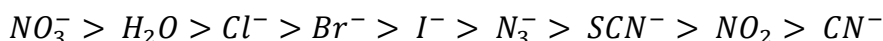
Table 2.1: The role of the leaving group on reaction rate of platinum(II) complexes in water at 298 K [ibid.].

Leaving group, X	k_{obs}, s^{-1}
NO_3^-	very fast
H_2O	1900
Cl^-	35
Br^-	23
I^-	10
N_3^-	0.83
SCN^-	0.3
NO_2^-	0.05
CN^-	0.017

A considerable difference in the relative rates of different leaving groups observed reveals that a substantial perturbation of the Pt-X bond in the transition state does not lead to a dissociation process but only requires the Pt-X bond breaking a significant contribution comparable to that of Pt-py bond forming. Needless to say, the leaving groups high in the *trans*-effect series are substituted at a slower rate. This is in good agreement with the combined σ- and π-*trans*-effect theory which presupposes that good *trans*-effect groups will be strongly bonded to the metal. An opposite case scenario, that a poor *trans* labiliser is readily replaced need not be true. The hydroxyl ion, for instance, is a very poor *trans* labiliser, it is, however, very difficult to substitute. The same is true for the ammine ligand [12, 18, 93]. Basically, groups which best stabilise a negative charge are the best leaving groups, example of such are the weakest bases they are very stable anions and are, thus, the best leaving groups.

2.5.4 Effect of Solvent

Serving as the reaction medium in which the reaction occurs, the solvent may, in some cases, compete with the incoming nucleophile and rapidly substitute the nucleofuge thereby rendering

the reaction rate to be independent of the concentration of incoming nucleophile. This has been reported for substitution reactions of platinum(II) complexes proceeding through the solvent pathway [32, 67]. The effect of the solvent used in substitution kinetics of square-planar complexes in the overall reaction rate depends on the coordination capability of the solvent [7, 12]. This effect has been experimentally studied for the chloride exchange reaction for *trans*-Pt(py)$_2$Cl$_2$ as shown in *equation* 2.48, **Table 2.2**.

$$\textit{trans-}\text{Pt(Py)}_2\text{Cl}_2 \; + \; {}^{36}\text{Cl}^- \longrightarrow \textit{trans-}\text{Pt(Py)}_2\text{Cl} \, ({}^{36}\text{Cl}^-) \; + \; \text{Cl}^- \qquad (2.48)$$
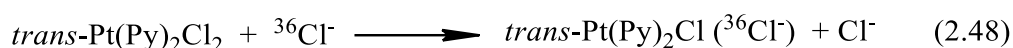
Table 2.2:   Chloride Exchange Reaction: The Effect of Solvent at 298 K [94].

Coordinating	$k_{-2}/(10^{-5} \text{ s}^{-1})$	Weakly coordinating	$k_2/\text{M}^{-1}\text{s}^{-1}$
DMSO	380	CCl$_4$	10^4
H$_2$O	3.5	C$_6$H$_6$	10^2
EtOH	1.4	i-BuOH	10^{-1}
PrOH	0.4	Me$_2$C(O)	10^{-2}
		DMF	10^{-3}

The results obtained indicate that the reactions in strongly coordinating solvents often proceed through a solvolysis pathway. The concentration of the chloride ligand influences the solvolysis pathway. However, for the weakly or non-coordinating solvents, the opposite is true. The rates of the reaction in coordinating solvents, such as DMSO etc., showed a direct dependence on the nucleophilicity of the solvent, $(k_s \gg k_{cl}[Cl^-])$. This is also because the soft platinum(II) site preferentially coordinate to the large sulfur atom in DMSO. For poorly coordinating (or non-coordinating) solvents, such as CCl$_4$, larger reaction rates have been reported by Romeo *et al.,* when the chloride ion acts as the nucleophile $(k_{cl}[Cl^-] > k_s)$ [18, 26, 95]. The Lewis acidity of the solvent and reactivity often predicted via linear free energy relationships between different parameters is believed to be a function of the solvation of the incoming nucleophile.

2.5.5 Effect of Steric Hindrance

In an associative mechanism, the transition state of ligand substitution reactions is more crowded than the ground state because there is a total of five groups around the reactive centre. Consequently, the steric bulk and the size of the incoming nucleophile can play a dominant role to determine the rate of the substitution process. Moreover, the effect of steric hindrance on the reaction rate can be either because of the steric demand in the inert ligand or in the incoming nucleophile. Likewise, an increase in the steric demand of the inert ligands often retard the rate of substitution. Steric hindrance not only slows down the associative attack of a bulky nucleophile but also sometimes have a remarkable effect on the nature of the substitution mechanism. This presupposes that steric effects are more dominant than electronic effects [14]. Studies have shown that steric barriers due to methyl and ethyl substituents on the tridentate (Rndien) ligands retard the substitution rate of $[Pd(R_ndien)Cl]^+$ complexes by a factor of 5 on increasing the size of the substituent, R, as compared to the complex that is less sterically hindered (**Table 2.3**).

Table 2.3: Rate constants and activation parameters for the substitution of chloride ions by iodine ions in $[Pd(R_ndien)Cl]^+$ in water at 298 K (n = 0. 3-5) [94].

$R_n$dien	$k_1\,s^{-1}$	$\Delta H^{\neq}\,kJ\,mol^{-1}$	$\Delta S^{\neq}\,J\,K^{-1}\,mol^{-1}$	$\Delta V^{\neq}\,cm^3\,mol^{-1}$
dien	44	43	-69	-10.0
1,4,7-Et₃dien	10	41	-86	-10.8
1,1,7,7-Et₄dien	2.2×10^{-3}	66	-74	-14.9
1,1,4,7,7-Me₅dien	0.28	50	-88	-10.9
1,1,4,7,7-Et₅dien	7.2×10^{-4}	59	-106	-12.8

A similar trend is expected to be followed by the complexes with a platinum(II) centre, even though, this has not yet been studied extensively. The successive experimental chapters of this thesis clearly demonstrate that increasing the steric bulk of the spectator ligands and of the incoming nucleophiles, such as neutral thiourea-based nucleophiles, respectively decreases the substitution rate in all the investigated *trans*-platinum(II) complexes. However, no alteration in mechanism due to steric hindrance is reported in this study.

References

[1] V. Bhatt, Essentials of Coordination Chemistry: A Simplified Approach with 3D Visuals, Academic Press (2015) 161-250.

[2] T. Lazarević, A. Rilak, Ž.D. Bugarčić, European Journal of Medicinal Chemistry, (2017) 8-31.

[3] V. Brabec, O. Hrabina, J. Kasparkova, Coordination Chemistry Reviews, (2017) 2-31.

[4] F. Carey, R. Sundberg. Advanced Organic Chemistry, New York (2001) 981-1003.

[5] F.A. Carey, R.J. Sundberg, Advanced Organic Chemistry: Part A: Structure and Mechanisms, Springer Science & Business Media, (2007) 389.

[6] I.M. Wekesa, D. Jaganyi, Dalton Transactions, 43 (2014) 2549-2558.

[7] M.L. Tobe, J. Burgess, Inorganic Reaction Mechanisms, Longman, (1999) 31-38.

[8] L.G. Arnaut, S.J. Formosinho, H. Burrows, Chemical Kinetics: From Molecular Structure to Chemical Reactivity, Elsevier, (2006) 2-13.

[9] Ž.D. Bugarčić, J. Bogojeski, R. van Eldik, Coordination Chemistry Reviews, 292 (2015) 91-106.

[10] A. Mambanda, D. Jaganyi, Advances in Inorganic Chemistry, Elsevier, (2017) 243-276.

[11] J.E. Park, Y.K. Kang, Bulletin of the Korean Chemical Society, 37 (2016) 1057-1063.

[12] J.D. Atwood, Inorganic and Organometallic Reaction Mechanisms, VCH Publishers, (1997) 32-64.

[13] R.A. Henderson, The Mechanism of Reactions at Transition Metal Sites, Oxford University Press, (2003) 1-30.

[14] R.B. Jordan, Reaction Mechanisms of Inorganic and Organometallic Systems, Oxford University Press, (2007) 8-10.

[15] S. Asperger, Chemical Kinetics and Inorganic Reaction Mechanisms, Springer Science & Business Media, (2011) 20-35.

[16] M. Fanelli, M. Formica, V. Fusi, L. Giorgi, M. Micheloni, P. Paoli, Coordination Chemistry Reviews, 310 (2016) 41-79.

[17] R.G. Wilkins, Kinetics and Mechanisms of Reactions of Transition Metal Complexes, VCH Publishers, (1991) 1-5.

[18] F. Basolo, R.G. Pearson, Mechanisms of Inorganic Reactions; 2nd ed.; Wiley:

New York, (1958) 193-195, 369-400.

[19] G. Miessler, D. Tarr, Inorganic Chemistry, Pearson Prentice Hall, New Jersey, NJ, USA, (2004) 400-426.

[20] G. Chauhan, K. Pant, K. Nigam, Environmental Science: Processes & Impacts, 17 (2015) 12-40.

[21] M. Rashidi, S.M. Nabavizadeh, A. Zare, S. Jamali, R.J. Puddephatt, Inorganic Chemistry, 49 (2010) 8435-8443.

[22] G. Kinunda, PhD Thesis: A Kinetic and Mechanistic Study on the Substitution

Behaviour of Mononuclear and Dinuclear Platinum(II) Complex, University of KwaZulu-Natal (2013) 1-15.

[23] J. Burgess, C.D. Hubbard, Advanced Inorganic Chemistry, 54 (2003) 71-155.

[24] L. Helm, A.E. Merbach, Chemical Reviews, 105 (2005) 1923-1960.

[25] M.R. Plutino, L. Monsù Scolaro, R. Romeo, A. Grassi, Inorganic Chemistry, 39 (2000) 2712-2720.

[26] R. Romeo, L.M. Scolaro, M.R. Plutino, F.F. de Biani, G. Bottari, A. Romeo, Inorganica Chimica Acta, 350 (2003) 143-151.

[27] P. Atkins, J. De Paula, J. Keeler, Atkins' Physical Chemistry, Oxford University Press, (2018) 30-100.

[28] P. Atkins, J. De Paula, Physical Chemistry For the Life sciences, Oxford University Press, USA, (2011) 25-50.

[29] R. Chang, Physical Chemistry For the Biosciences, University Science Books, (2005) 1-35.

[30] A. Hofmann, L. Dahlenburg, R. van Eldik, Inorganic Chemistry, 42 (2003) 6528-6538.

[31] P.O. Ongoma, D. Jaganyi, Dalton Transactions, 42 (2013) 2724-2734.

[32] A. Shaira, D. Reddy, D. Jaganyi, Dalton Transactions, 42 (2013) 8426-8436.

[33] D. Benson, Mechanisms of Inorganic Reactions in Solution, McGraw-Hill: London (1968) 20-60.

[34] D.T. Richens, Chemical Reviews, 105 (2005) 1961-2002.

[35] K. Laidler, J. Meiser, B.C. Sanctuary, Physical Chemistry, 4th ed., Houghton

Mifflin Company: New York (2003) 372-395.

[36] J.H. Espenson, Chemical Kinetics and Reaction Mechanisms, Citeseer, (1995) 150-165.

[37] A. Drljaca, C. Hubbard, R. Van Eldik, T. Asano, M. Basilevsky, W. Le Noble, Chemical Reviews, 98 (1998) 2167-2290.

[38] M. Kotowski, R. Van Eldik, Coordination Chemistry Reviews, 93 (1989) 19-57.

[39] D. Stranks, Pure and Applied Chemistry, 38 (1974) 303-323.

[40] K.A. Connors, Chemical Kinetics: The Study of Reaction Rates in Solution, John Wiley & Sons, (1990) 1-25.

[41] H. Kuhn, H.-D. Försterling, D.H. Waldeck, Principles of Physical Chemistry, John Wiley & Sons, (2009) 1-16.

[42] A. Adamson, A Textbook of Physical Chemistry, Elsevier (2012) 2-8.

[43] D.A. Skoog, D.M. West, F.J. Holler, S. Crouch, Fundamentals of Analytical Chemistry, Nelson Education, (2013) 720-776.

[44] H. Bisswanger, Enzyme Kinetics: Principles and Methods, John Wiley & Sons, (2017) 295-304.

[45] D.L. Sparks, Kinetics and Mechanisms of Chemical Reactions at the Soil Mineral/Water Interface, in: Soil Physical Chemistry, Second Edition, CRC Press, (2018) 135-192.

[46] L. Que, University Science, Sausilito Google Scholar, (2000) 187.

[47] R.A. Scott, C.M. Lukehart, Applications of Physical Methods to Inorganic and Bioinorganic Chemistry, John Wiley & Sons, (2013) 1-12.

[48] E. Seifert, OriginPro 9.1: Scientific Data Analysis and Graphing Software® Software Review, ACS Publications, (2014) 1.

[49] W.P. Asman, D. Jaganyi, International Journal of Chemical Kinetics, 49 (2017) 545-561.

[50] S. Hochreuther, S.T. Nandibewoor, R. Puchta, R. van Eldik, Dalton Transactions, 41 (2012) 512-522.

[51] S. Hochreuther, R. Puchta, R. van Eldik, Inorganic chemistry, 50 (2011) 8984-8996.

[52] S. Jovanović, J. Bogojeski, M. Petković, Ž.D. Bugarčić, Journal of Coordination Chemistry, 68 (2015) 3148-3163.

[53] G. Kinunda, D. Jaganyi, Transition Metal Chemistry, 39 (2014) 939-949.

[54] P.O. Ongoma, D. Jaganyi, Transition Metal Chemistry, 39 (2014) 407-420.

[55] P.A. Wangoli, G. Kinunda, New Journal of Chemistry, 42 (2018) 214-227.

[56] F. Wilkinson, Chemical Kinetics and Reaction Mechanism, Van Nostrand Reinhold Company, (1980) 1-11, 65-100.

[57] R.G. Pearson, H.R. Sobel, J. Songstad, Journal of the American Chemical Society, 90 (1968) 319-326.

[58] D. Banerjea, F. Basolo, R.G. Pearson, Journal of the American Chemical Society, 79 (1957) 4055-4062.

[59] H.B. Gray, Journal of the American Chemical Society, 84 (1962) 1548-1552.

[60] U. Belluco, Organometallic and Coordination Chemistry of Platinum, Academic Press, (1974) 138-220.

[61] F.R. Hartley, Chemistry of the Platinum Group Metals: Recent Developments, Elsevier, (2013) 9-50.

[62] J.O. Edwards, R.G. Pearson, Journal of the American Chemical Society, 84 (1962) 16-24.

[63] V. Polo, J. Andres, S. Berski, L.R. Domingo, B. Silvi, The Journal of Physical Chemistry A, 112 (2008) 7128-7136.

[64] M.B. Smith, J. March, March's Advanced Organic Chemistry: Reactions, Mechanisms, and Structure, John Wiley & Sons, (2007) 1-5.

[65] D. Jaganyi, F. Tiba, O.Q. Munro, B. Petrović, Ž.D. Bugarčić, Dalton Transactions, (2006) 2943-2949.

[66] P. Ongoma, D. Jaganyi, Dalton Transactions, 41 (2012) 10724-10730.

[67] D. Reddy, K.J. Akerman, M.P. Akerman, D. Jaganyi, Transition Metal Chemistry, 36 (2011) 593-602.

[68] Ž.D. Bugarčić, B. Petrović, E. Zangrando, Inorganica chimica acta, 357 (2004) 2650-2656.

[69] Ž.D. Bugarčić, S.T. Nandibewoor, M.S. Hamza, F. Heinemann, R. van Eldik, Dalton Transactions, (2006) 2984-2990.

[70] M. Bellicini, L. Cattalini, G. Marangoni, B. Pitteri, Journal of the Chemical Society, Dalton Transactions, (1994) 1805-1811.

[71] R. Cross, Advances in Inorganic Chemistry, Elsevier, (1989) 219-292.

[72] R.J. Cross, Chemical Society Reviews, 14 (1985) 197-223.

[73] A. Mambanda, D. Jaganyi, Dalton Transactions, 40 (2011) 79-91.

[74] J.R. Gispert, Coordination Chemistry, Wiley-VCH Weinheim, (2008) 1-55.

[75] L. Orgel, Journal of Inorganic and Nuclear Chemistry, 2 (1956) 137-140.

[76] P.N. Kapoor, R. Kakkar, Journal of Molecular Structure: Theochem, 679 (2004) 149-156.

[77] D.V. Khoroshun, D.G. Musaev, K. Morokuma, Journal of Computational Chemistry, 28 (2007) 423-441.

[78] P. Sajith, C.H. Suresh, Dalton Transactions, 39 (2010) 815-822.

[79] P. Sajith, C.H. Suresh, Journal of Organometallic Chemistry, 696 (2011) 2086-2092.

[80] A.C. Albéniz, P. Espinet, B. Martín-Ruiz, Dalton Transactions, (2007) 3710-3714.

[81] A.S. Fleischhacker, R.G. Matthews, Biochemistry, 46 (2007) 12382-12392.

[82] N. Kuznik, O.F. Wendt, Journal of the Chemical Society, Dalton Transactions, (2002) 3074-3078.

[83] L. Vanquickenborne, J. Vranckx, C. Goeller-Walrand, Journal of the American Chemical Society, 96 (1974) 4121-4125.

[84] Z. Chval, M. Sip, J.V. Burda, Journal of Computational Chemistry, 29 (2008) 2370-2381.

[85] A. Hofmann, D. Jaganyi, O.Q. Munro, G. Liehr, R. van Eldik, Inorganic Chemistry, 42 (2003) 1688-1700.

[86] D. Reddy, D. Jaganyi, International Journal of Chemical Kinetics, 43 (2011) 161-174.

[87] T. Soldatović, S. Jovanović, Ž.D. Bugarčić, R. van Eldik, Dalton Transactions, 41 (2012) 876-884.

[88] A. Mambanda, D. Jaganyi, S. Hochreuther, R. van Eldik, Dalton Transactions, 39 (2010) 3595-3608.

[89] J. Bogojeski, R. Jelić, D. Petrović, E. Herdtweck, P.G. Jones, M. Tamm, Ž.D. Bugarčić, Dalton Transactions, 40 (2011) 6515-6523.

[90] M. Đurović, J. Bogojeski, B. Petrović, D. Petrović, F.W. Heinemann, Ž.D. Bugarčić, Polyhedron, 41 (2012) 70-76.

[91] D.O. Cooke, Inorganic reaction mechanisms, Chemical Society, 1979.

[92] D. Jaganyi, D. Reddy, J. Gertenbach, A. Hofmann, R. van Eldik, Dalton Transactions, (2004) 299-304.

[93] J.D. Atwood, Inorganic and Organometallic Reaction Mechanisms, John Wiley & Sons, Canada, 1985.

[94] C.F. Weber, R. van Eldik, European Journal of Inorganic Chemistry, 2005 (2005) 4755-4761.

[95] A. Shaira, PhD Thesis, Heterometallic Ruthenium(II)-Platinum(II) Complexes- A New Paradigm: A Kinetic, Mechanistic and Computational Investigation into Substitution Behaviour, University of KwaZulu-Natal, Pietermaritzburg (2014) 1-35.

Chapter Three

A Kinetic and Mechanistic Study of Analogous Bifunctional Dialkylamine Platinum(II) Complexes

Abstract

This study was aimed at investigating the comparative substitution behaviour of analogous *cis/trans*-Pt(II) complexes with dialkylamine inert ligands. The rate of substitution of aqua ligands by three nucleophiles: thiourea (TU), 1,3-dimethylthiourea (DMTU) and 1,1,3,3-tetramethylthiourea (TMTU), for the complexes: $[cis\text{-}Pt(OH_2)_2(NH_3)_2](ClO_4)_2$ (**cPt**), $[cis\text{-}Pt(OH_2)_2(NH_2CH_3)_2](ClO_4)_2$ (**cPtM**), $[cis\text{-}Pt(OH_2)_2\{NH_2CH(CH_3)_2\}_2](ClO_4)_2$ (**cPtR**), $[trans\text{-}Pt(OH_2)_2(NH_3)_2](ClO_4)_2$ (**tPt**), $[trans\text{-}Pt(OH_2)_2(NH_2CH_3)_2](ClO_4)_2$ (**tPtM**) and $[trans\text{-}Pt(OH_2)_2\{NH_2CH(CH_3)_2\}_2](ClO_4)_2$ (**tPtR**) was investigated under *pseudo* first-order conditions as a function of concentration and temperature by stopped-flow and UV/Visible spectrophotometry. The reactions of the *cis*-complexes proceeded in two concerted steps whereas those of the *trans*-complexes followed a single step. The *cis*-complexes followed second-order kinetics with respect to each complex and nucleophile whilst the *trans*-analogues proceeded by first-order kinetics. The *pseudo* first-order rate constants, k_{obs} obeyed the rate law: $k_{obs} = k_2[\text{nucleophile}]$. The *trans*-complexes were observed to be approximately 10^3 more reactive than their corresponding *cis*-analogues. The electronic and the steric hindrance due to the geometries of the complexes control the overall reaction pattern. The order of reactivity of the complexes is **tPt** > **tPtM** > **tPtR** > **cPt** > **cPtM** > **cPtR**. The reactivity of the nucleophiles with the complexes decreases with an increase in steric demand in the order: TU > DMTU > TMTU. The *trans*-dialkylamine complexes formed distinctly different kinetic products relative to their *cis*-analogues. ^{195}Pt NMR spectroscopic results confirmed the final kinetic products of each of the *cis*- and *trans*-complexes. The negative entropy of activation ($\Delta S^{\neq}$) values in all the complexes investigated assert an associative substitution mechanism, with the mechanism being more pronounced in the *cis*-complexes than in their *trans*-analogues.

3.1 Introduction

The fortuitous revelation of *cis*-diamminedichloroplatinum(II), cisplatin, as an anticancer agent has galvanised interest in medicinal inorganic chemistry research in the last five decades with many more platinum-based chemotherapeutics being developed [1, 2]. The finding *ab initio*, that the *trans*-isomer of cisplatin lacked any biological activity influenced the early structure–activity relationships that a *cis* geometry of the two leaving groups is crucial for the biological activity of platinum-based anticancer agents [2-7]. Consequently, all *trans*-platinum complexes were presumably thought to be impotent as antitumour drugs.

However, it has been suggested that the cytotoxic potential of *trans*-platinum complexes could be greatly enhanced by bulky spectator monodentate amine ligands. Farrell *et al.* have reported that some *trans* complexes with general formula [PtCl$_2$L$_2$] showed significant cytotoxities when *L* is a planar heterocyclic ligand such as pyridine or thiazole [3]. Similarly, Navarro-Ranninger *et al.* have reported a new class of biologically active *trans*-platinum(II) complexes with asymmetric aliphatic amines, *trans*-[PtCl$_2$(*L*)(*L'*)] [8]. These discoveries have revolutionized the development of new platinum-based anticancer agents because these *trans*-platinum compounds exhibited significantly high cytotoxicities, both *in vitro* and *in vivo,* against cisplatin resistant tumour cell lines. Hence, their pharmacodynamics may, however, be much more complex and completely different relative to that already established for *cis* configured platinum(II) complexes [7]. Efforts to further understand the mechanism of action of *cis*-configured platinum(II) complexes have been ubiquitous.

Moreover, the kinetic and mechanistic study of substitution of platinum(II) complexes with *cis* configurations has been well established. Both Jaganyi *et al*. [9-12] and van Eldik *et al*. [13] have reported that the substitution behaviours of platinum(II) complexes of *cis* configuration with thiol-based nucleophiles undergo dechelation to give two or more thiourea-substituted platinum(II) complexes in a two or more step process. Nonetheless, the substitution kinetics and mechanism of platinum(II) complexes in which the chloride leaving groups are *trans* to each other on the platinum centre is still relatively unknown.

Song *et al.* [14] recently reported that there is a possibility of transformation in transplatin to cisplatin under UVA irradiation. Their findings are based on the fact that transplatin, which was observed to be veritably non-toxic in the dark to all cell lines, was found to be of comparable toxicity with cisplatin under UVA irradiation. The authors attribute this observation, among other things, to the transformation of transplatin to cisplatin under UVA light. However, Brabec and co-workers [15]

have demonstrated through NMR spectroscopy that the loss of chloride ligands of transplatin upon irradiation resulted in the formation of bifunctional adducts and subsequently led to the remarkable increase of its toxicity level in cancer cells. They debunked the claim that transplatin is transformed to cisplatin under UVA irradiation by using three independent methods after which they concluded that transplatin upon UVA irradiation does not rearrange to its *cis* isomer.

In order to further the understanding of the mechanistic behaviours of these platinum(II) complexes, analogous *cis* and *trans*-dialkylamine dichloroplatinum(II) complexes of the general form, [PtX$_2$L$_2$], were investigated (see **Figure 3.1**). Our central aim is to ascertain how bifunctional *trans*-platinum(II) complexes will substitute kinetically relative to their *cis* isomers by using bio-relevant thiourea-based nucleophiles such as, thiourea (TU), 1,3-dimethyl-2-thiourea (DMTU) and 1,1,3,3-tetramethyl-2-thiourea (TMTU).
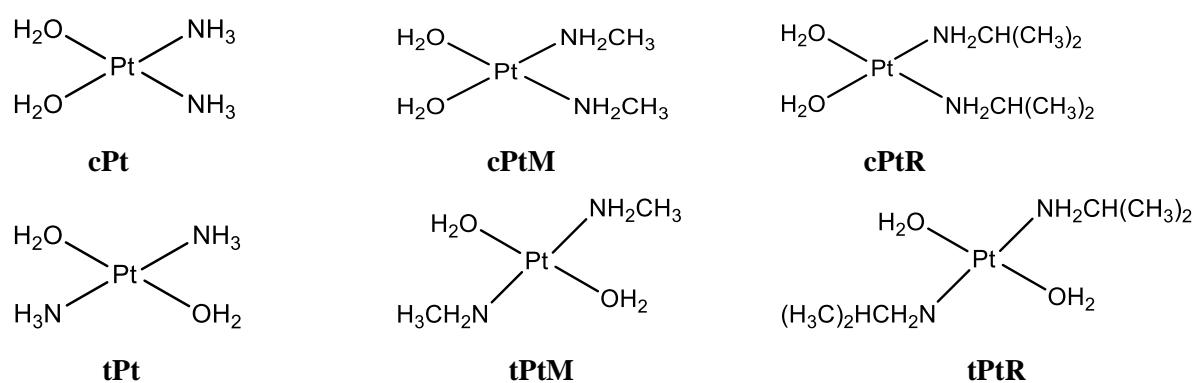
Figure 3.1: Structures of the studied *cis*-platinum(II) complexes and their *trans*-analogues. The charges and counterions on the complexes have been omitted for the sake of clarity.

3.2   Experimental

3.2.1   Chemicals and Reagents

Methylamine hydrochloride (ma), isopropylamine (ipram) (99.5%), K$_2$PtCl$_4$ (98%), *cis*-[Pt(NH$_3$)$_2$Cl$_2$] (99.9%), *trans*-[Pt(NH$_3$)$_2$Cl$_2$], KOH, AgClO$_4$ (97%), NaClO$_4$·H$_2$O (98%), HCl (32%) and HClO$_4$ (70%) were purchased from Sigma-Aldrich and were used without further purification. The nucleophiles: thiourea (TU, 99%)), 1,3-dimethyl-2-thiourea (DMTU, 99%) and 1,1,3,3-tetramethyl-2-thiourea (TMTU, 98%) used for the kinetic determinations were also obtained from Sigma-Aldrich. All preparations of aqueous solutions were done using ultrapure water.

3.2.2 Synthesis of Complexes

3.2.2.1 General Procedure for the Synthesis of *cis*-Pt(amine)$_2$Cl$_2$

The chlorido complexes *cis*-[Pt(ma)$_2$Cl$_2$](**cPtM**) and *cis*-[Pt(ipram)$_2$Cl$_2$] (**cPtR**) were synthesised according to literature procedures reported by Messori *et al.* [2] and Pantoja *et al.* [16] with slight modifications. K$_2$PtCl$_4$ (500 mg, 1.2 mmol) was dissolved in water (5 mL) and treated with KI (1 g, 6 mmol) at room temperature to produce a dark brown solution of K$_2$PtI$_4$ after 15 minutes of stirring.

The iodo derivative of *cis*-[Pt(ma)$_2$Cl$_2$] (**cPtM**) was first prepared by slowly adding four equivalents of methylamine hydrochloride (4.8 mmol) to the dark brown solution of K$_2$PtI$_4$. The mixture was subsequently treated with four equivalents of KOH (269 mg, 4.8 mmol) in the dark at room temperature. After the addition was completed, the reaction mixture was stirred in the dark at room temperature for five hours to give a yellow precipitate, *cis*-[Pt(ma)$_2$I$_2$]. The precipitate was obtained by filtration, washed thoroughly with warm water, diethyl ether and air dried.

To prepare the iodo derivative of *cis*-[Pt(ipram)$_2$Cl$_2$] (**cPtR**), four equivalents of isopropyl amine (4.80 mmol) was added slowly to the dark brown solution of K$_2$PtI$_4$. The resulting mixture was stirred five hours at room temperature to produce a yellow precipitate, *cis*-[Pt(ipram)$_2$I$_2$], which was filtered, washed intensively with warm water, diethyl ether and allowed to dry by air.

The iodo complexes were converted to their chlorido analogues by suspending the iodo complexes, viz. *cis*-[Pt(ma)$_2$I$_2$] (441 mg, 0.864 mmol) /*cis*-[Pt(ipram)$_2$I$_2$] (585 mg, 1.03 mmol), in 10 mL of water and treated with 1.9 equivalent AgClO$_4$. The mixture was stirred overnight in the dark. A yellow precipitate of AgI was removed by filtration through a 0.45µm nylon membrane and to the filtrate, four equivalents of KCl was added and stirred at 40 °C for six hours. The resulting precipitate was left overnight at 4 °C. The yellow solids, *cis*-[Pt(ma)$_2$Cl$_2$] and *cis*-[Pt(ipram)$_2$Cl$_2$ respectively, were filtered, washed with water and air dried.

***cis*-[Pt(ma)$_2$Cl$_2$] (cPtM)** Yield: 85 mg (30%). ^{1}H NMR (500 MHz, DMSO-d$_6$), δ(ppm): 2.26 (t, 6H); 4.88 (s, 4H). ^{195}Pt NMR (107 MHz, DMSO-d$_6$), δ(ppm): -2214.4. TOF MS/ES$^+$ (Accurate mass), *m/z:* (M + Na)$^+$: 350.97 (C$_2$H$_{10}$N$_2$NaPtCl$_2$, species). Anal. Calc. for C$_2$H$_{10}$N$_2$PtCl$_2$: N, 8.54; C, 7.32; H, 3.07. Found: N, 8.60; C, 6.99; H, 2.76.

***cis*-[Pt(ipram)$_2$Cl$_2$] (cPtR)** Yield: 296 mg (75%). ^{1}H NMR (500 MHz, DMSO-d$_6$), δ(ppm): 1.22 (d, 12H); 3.11 (sept., 2H); 4.75 (s, 4H). ^{195}Pt NMR (107 MHz, DMSO-d$_6$), δ(ppm): -2218.5. TOF MS/ES$^+$ (Accurate mass), *m/z:* (M + Na)$^+$: 407.03 (C$_6$H$_{18}$N$_2$NaPtCl$_2$, species). Anal. Calc. for C$_6$H$_{18}$N$_2$PtCl$_2$: N, 7.29; C, 18.76; H, 4.72. Found: N, 7.50; C, 18.54; H, 4.45.

3.2.2.2   Synthesis of *trans*-[Pt(ma)$_2$Cl$_2$]

trans-[Pt(ma)$_2$Cl$_2$] was obtained following the synthetic procedure outlined by Messori *et al.*[2] with a few modifications. A suspension of *cis*-[Pt(ma)$_2$I$_2$] (220 mg, 0.432 mmol) in water was treated with 5 equivalents of methylamine hydrochloride (2.16 mmol). The resulting mixture was stirred at room temperature for 12 hours to give a colourless solution. The resulting solution was concentrated at 70 °C until a bright orange precipitate was detected and then left to stand overnight at 4 °C. The orange solid, *trans*-[Pt(ma)$_2$I$_2$] was filtered, washed with warm water and air dried.

trans-[Pt(ma)$_2$I$_2$] (177 mg, 0.346 mmol) was suspended in 10 mL of water and treated with 1.9 equivalents AgClO$_4$. The mixture was stirred overnight in the dark. AgI was removed by filtration through a 0.45 µm nylon membrane and to the filtrate, a four equivalent of KCl was added and stirred at 40 °C for six hours to give a yellow precipitate of *trans*-[Pt(ma)$_2$Cl$_2$]. The solution was left to stand overnight at 4 °C. The product was filtered, washed thoroughly with warm water and air dried.

***trans*-[Pt(ma)$_2$Cl$_2$] (tPtM)** Yield: 12.8 mg (9%). ^{1}H NMR (500 MHz, DMSO-d$_6$), δ(ppm): 2.33 (t, 6H); 4.24 (s, 4H). ^{195}Pt NMR (107 MHz, DMSO-d$_6$), δ(ppm): -2195. TOF MS/ES$^+$, *m/z:* (M + Na)$^+$: 350.96 (C$_2$H$_{10}$N$_2$NaPtCl$_2$, species). Anal. Calc. for C$_2$H$_{10}$N$_2$PtCl$_2$: N, 8.54; C, 7.32; H, 3.07. Found: N, 8.61; C, 6.97; H, 2.60.

3.2.2.3   Synthesis of *trans*-[Pt(ipram)$_2$Cl$_2$]

The *trans*-[Pt(ipram)$_2$Cl$_2$] was synthesised following the method reported by Navarro-Ranninger *et al.* [17]. To a suspension of *cis*-[Pt(ipram)$_2$Cl$_2$ (200 mg, 0.521 mmol), 4 equivalents of isopropylamine was added. The resulting mixture was heated at 70 °C and stirred until a colourless solution was obtained which was then heated at reflux for 30 minutes. The solution was left to cool to room temperature and concentrated HCl (0.364 mL) was added and subsequently heated at reflux for 8 hours. The yellow solution obtained was cooled in an ice bath and left to stand at 4 °C overnight. The product was obtained by filtration and thoroughly washed with water and dried in air.

***trans*-[Pt(ipram)₂Cl₂] (tPtR)** Yield: 80 mg (40%). ^{1}H NMR (500 MHz, DMSO-d₆), δ(ppm): 1.19 (d, 12H); 3.03 (sept., 2H); 4.20 (s, 4H). ^{195}Pt NMR (107 MHz, DMSO-d₆), δ(ppm): -2205. TOF MS/ES⁺, *m/z:* (M + Na)⁺: 407 (C₆H₁₈N₂PtCl₂, species). Anal. Calc. for C₆H₁₈N₂PtCl₂: N, 7.29; C, 18.76; H, 4.72. Found: N, 7.53; C, 18.51; H, 4.36.

3.3 Instrumentation and Physical Measurements

^{1}H, ^{13}C and ^{195}Pt NMR spectroscopic analyses were carried out on a Bruker Avance III 500 MHz. All ^{1}H and ^{13}C NMR chemical shifts were referenced to Si(CH₃)₄ while ^{195}Pt NMR chemical shifts were externally referenced to K₂[PtCl₆]. ^{195}Pt NMR has been established as an effective method for the determination of the coordination details at the metal centre since its chemical shifts are largely influenced, among other things, by the nature of the coordinated donor atoms [18]. A Waters Micromass LCT Premier spectrometer was employed for mass determination of the complexes. Elemental analyses of synthesised complexes were recorded on Thermo Scientific Flash 2000. The pH of the aqueous solutions of the complexes was recorded using a Jenway 4330 Conductivity/pH meter fitted with a Micro 4.5 diameter glass electrode which was calibrated at 25 °C using buffer solutions of pH 4.0, 7.0 and 10.0 purchased from Merck. A Varian Cary 100 Bio UV/Visible spectrophotometer thermostatted by a Varian Peltier temperature controller was used to obtain the UV/Visible absorption spectra for the determination of pK_a values and kinetic studies of slow reactions. Kinetic measurements of moderately fast reactions were monitored on an Applied Photophysics SX20 stopped-flow analyser coupled to an online data acquisition system. The temperature of the instrument was kept within ±0.05 °C for all the measurements. Analyses of the pH and time-dependent kinetic spectral data were performed using the Origin 9.1® software suite.

3.4 Preparation of Platinum(II) Aqua Complexes and Determination of their pK_a Values

The aqueous solutions of the complexes **cPt**, **tPt**, **cPtM**, **tPtM**, **cPtR** and **tPtR** were prepared according to literature [9,11]. A suitable amount of AgClO₄ was added to each of the corresponding chloro complexes at a molar ratio of 1: 1.98. Both the chloro complex and the AgClO₄ were dissolved in 0.01M HClO₄ and the mixture was vigorously stirred in the dark at 45 °C for 24 hours. The AgCl precipitate obtained was filtered off through a 0.45 µm nylon membrane. The filtrate was diluted to 300 mL with 0.01 M HClO₄.

Spectrophotometric pH titrations were performed using NaOH as a base in the pH range of 2-10 at 25 °C. To avoid absorbance corrections resulting from dilution, a large amount (300 mL) of the

complexes were used for the titrations. Adjustments in pH were made by a stepwise addition of crushed NaOH pellets in the pH range 1–3, while a pasteur pipette was used for dropwise additions of NaOH solutions of different concentrations (1.0, 0.5, 0.1 and 0.01 M) or same concentrations of $HClO_4$ acid (for reversibility of the pH) were added to the solution in the pH range of 4–10 until the desired pH was attained prior to withdrawal of a 1.0 mL aliquot from the solution for pH measurement and 2.0 mL aliquots for spectrophotometric monitoring. The 1.0 mL aliquot after each pH measurement was discarded to avoid in situ contamination of the complex solution by chloride ions leaching from the pH electrode.

3.5 Computational Estimations

Density functional Theoretical (DFT) estimations of the complexes **cPt**, **tPt**, **cPtM**, **tPtM**, **cPtR** and **tPtR** were performed at the DFT level B3LYP [19] with the LANL2DZ basis set [20] using the Gaussian ′09 programme suite. B3LYP relates to the hybrid functional Becke's three-parameter formulation, which has been proven to be superior to conventional functionals. The LANL2DZ is double-zeta basis set containing effective core potential (ECP) representations of electrons near the nuclei for transition metal complexes [21]. The theoretical calculations of the complexes were executed in water taking into account the effects of the solvent by employing conductor polarisable continuum model (CPCM) formalism [22, 23]. The complexes were optimized in their aqua form as cations of +2 charge, and the singlet states were used because of low electronic spin of platinum(II) complexes.

3.6 Results and Discussion

3.6.1 pK_a Determination of the Diaqua Complexes

To obtain information on the acidity of the coordinated water moeities and the reactivity of all the aqua complexes, their pK_a values were determined. To this end, a spectrophotometric pH titration with NaOH as a base in the pH range 2–10 was carried out. The pH dependence of the aqua complex was observed by UV/Visible spectrophotometry. The pK_a values of the coordinated aqua ligands were obtained by plotting the absorbance at a specific wavelength as a function of pH. The typical spectral changes recorded during the pH titration with NaOH are presented in **Figure 3.2** for the *trans*-aqua complexes **tPtR**. The overall process can be presented by **Scheme 3.1**.
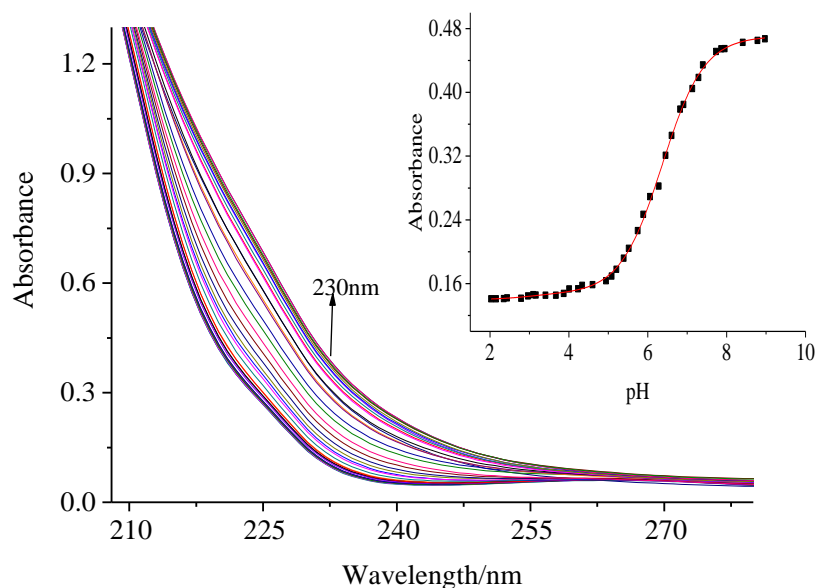
Figure 3.2: UV/Visible spectra of the diaqua tPtR complex recorded as a function of pH in the range 2-10 at 298 K. Inset: Titration curve at 230 nm.
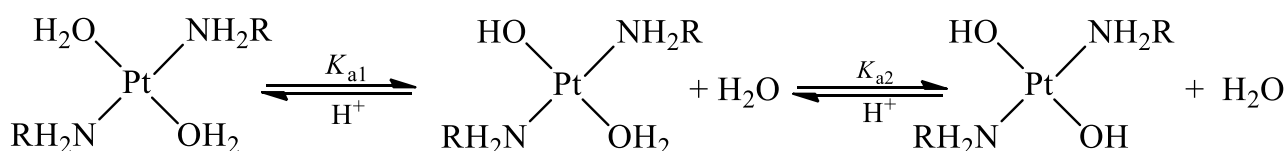
Scheme 3.1: Proposed stepwise deprotonation for the pH dependence of the *trans*-platinum(II) complexes. The charge on the complexes were omitted for clarity

The spectral data was analysed using Origin 9.1$^{®}$ [24] to obtain the resulting pK_a values for the aqua moieties by fitting the data to a double sigmoidal function which gave the best statistical fit and afforded two pK_a values which are indicative of the fact that there are three coloured species for each of the aqua complexes present in solution as a function of pH. The data obtained for the deprotonation of the aqua moieties from the complexes are summarised in **Table 3.1**.

Table 3.1: Summary of pK_a values for the deprotonation steps of aqua moieties from the analogous *cis*- and *trans*-platinum(II) complexes.

	cPt	tPt	cPtM	tPtM	cPtR	tPtR
pK_{a1}	4.99 ± 0.01	4.24 ± 0.05	5.40 ± 0.29	4.56 ± 0.06	6.61 ± 0.62	5.92 ± 0.07
pK_{a2}	7.26 ± 0.01	6.91 ± 0.04	7.52 ± 0.12	7.05 ± 0.03	7.62 ± 0.12	7.28 ± 0.16

A closer inspection of the data in **Table 3.1** shows that the pK_{a1} and pK_{a2} values for the deprotonation of the first and second coordinated water molecules for all the *trans*-complexes are significantly lower

than those of their corresponding *cis*-analogues. The *trans*-aqua complexes are clearly more acidic than their corresponding *cis*-counterparts. The deprotonation of the first coordinated water ligand increase in the order **tPt** (pK_{a1} 4.24) < **tPtM** (pK_{a1} 4.56) < **cPt** (pK_{a1} 4.99) < **cPtM** (pK_{a1} 5.40) < **tPtR** (pK_{a1} 5.92) < **cPtR** (pK_{a1} 6.61). A similar trend is observed for the deprotonation of the second aqua molecule, albeit at higher pH values relative to the first. The higher acidity of the *trans* complexes as compared to the analogous *cis* complexes has been previously reported in a related study involving analogous *cis*- and *trans*-complexes using NMR spectroscopy [25, 26]. Since pK_a values are associated with the electrophilicity of the metal centre [27], it can be inferred, therefore, that the geometry of the complexes bears significant influence on the electrophilicity of the metal centre in the investigated complexes. The DFT-calculated NBO charges for the corresponding *cis/trans*-analogues in **Table 3.2** underpin the observed experimental data.

Table 3.2: A summary of the DFT calculated data for the investigated analogous *cis*- and *trans*-platinum(II) complexes at B3LYP/LANL2DZ level of theory.

Parameters	cPt	tPt	cPtM	tPtM	cPtR	tPtR
Bond Length/Distance (Å)						
cis/trans-**Pt–OH$_2$**	2.106	2.058	2.116	2.063	2.120	2.066
a	2.482	2.575	2.535	2.984	2.455	3.116
b	3.458	3.460	3.415	3.446	3.435	3.465
NBO Charge						
Pt^{2+}	0.774	0.808	0.754	0.791	0.736	0.758
Dipole Moment	0.425	0.002	2.420	0.002	6.404	0.002

All the *trans*-configured platinum(II) complexes have a slightly lower charge on the platinum centre as compared to each of their corresponding *cis*-isomers. The difference in NBO charge on the platinum centre between analogous *cis/trans*-platinum(II) complexes can be attributed to the remarkable difference in charge distribution as expressed as the dipole moment between the two configurations [28, 29]. The *cis*-configuration enhances charge separation within a molecule compared to the *trans*-configuration. Hence, whereas the charge separation in the *trans*-platinum(II)

complexes are negligible, those of their analogues *cis*-platinum(II) complexes are quite significant. Furthermore, the dipole moment is expectedly the same, and veritably zero, for all the *trans*-complexes. There is, however, a significant increase in the dipole moments in all the *cis*-complexes as the steric bulk of the amine spectator ligands increases from ammine to isopropylamine. This can be ascribed to the increase in the inductive negative charge in the *cis*-complexes resulting from the increase in the sigma donor abilities of the amine moieties [30, 31].

Additionally, contrary to what was previously reported by Cubo *et al*. [26], the nature of the aliphatic amine moieties has a significant effect on the pK_a values of all the studied complexes. For instance, in the *trans*-complexes, the pK_a value of transplatin, **tPt**, is 0.32 and 1.68 pH units lower than that of **tPtM** and **tPtR** respectively. This is corroborated by the remarkable difference in the DFT-calculated NBO charges on the platinum centres with **tPt** being more electrophilic than the other two *trans*-complexes having bulkier amine ligands. Similarly, this trend is also observed in the *cis*-complexes. Cisplatin, **cPt** is 0.41 and 1.62 pH units lower than the bulkier *cis*-complexes, **cPtM** and **cPtR** respectively. This phenomenon is quite consistent with the electrophilicity of the platinum centres based on their NBO charges.

The pK_a values of the second aqua ligands are higher than the first one i.e. pK_{a1} < pK_{a2}. This has been previously observed [1, 9, 25-27, 32, 33] and has been attributed to the general reduction in the overall charge from +2 to +1 on the platinum centre resulting from the formation of the first hydroxo species. Another reason posited for this observation is the possibility of hydrogen bonding between the aqua/hydroxo groups resulting from the first deprotonation step. However, this possibility is much more prominent in the *cis*-configured complexes compared to their *trans*-counterparts because of the proximity of the aqua/hydroxo groups in the *cis*-complexes due to their geometry.

3.6.2   Kinetic Analysis

The kinetics of the substitution of the coordinated water ligands in the analogous *cis*- and *trans*-dialkylamine platinum(II) complexes were investigated spectrophotometrically by monitoring the changes in absorbance at suitable wavelengths as a function of time at 298 K. The proposed reaction pathways for the reaction of the analogous *cis*- and *trans*-platinum(II) complexes with the neutral nucleophiles are presented in **Schemes 3.2** and **3.3**. The reactions with the diaqua complexes were performed at pH 2 in order to ensure that all the complexes **cPt**, **cPtM**, **cPtR**, **tPt**, **tPtM** and **tPtR** are present in their diaqua form based on the reported pK_a values in **Table 3.1**.
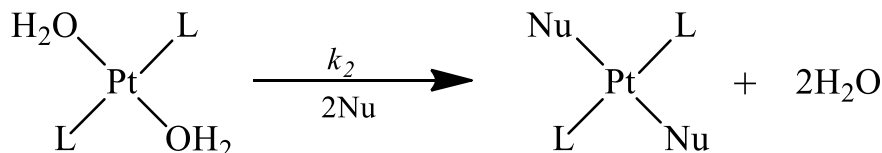
Scheme 3.2: Proposed pathway for the reaction of the *trans*-platinum(II) complexes with the thiourea-based nucleophiles.
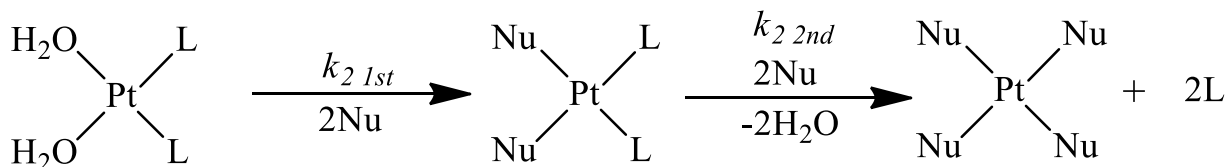
Scheme 3.3: Proposed pathway for the reaction of the *cis*-platinum(II) complexes with the thiourea-based nucleophiles.

The substitution reactions of all the studied *cis*-platinum(II) complexes proceeded in two concerted reaction steps whereas those of the *trans*-platinum(II) followed a single reaction step. All the reaction steps in both the *cis*- and the *trans*-platinum(II) complexes showed a clear dependence on the concentration of the nucleophile. Kinetic traces for the *cis*-platinum(II) complexes all gave an excellent fit to a double exponential function which is indicative of a two-step process whereas those of the *trans*-platinum(II) complexes fitted perfectly to a single exponential, typical for one-step reaction.

The so-obtained *pseudo*-first-order rate constants, k_{obs1} and k_{obs2} for the *cis*-complexes and k_{obs} for the *trans*-complexes, computed from the kinetic traces were plotted against the concentration of the entering nucleophiles (**Figure 3.3**). A linear dependence, without any intercept, on the nucleophile concentration was observed for all the studied reactions. The linear fits pass through the origin which is indicative of the fact that the possibility of parallel or reverse reactions are negligible or absent. The dependence of the observed *pseudo*-first-order rate constants on the concentration of the entering nucleophile obeyed the rate law presented in *equation* 3.1, where k_2 represent the second-order rate constants for the substitution reactions of the analogous *cis*- and *trans*-dialkylamine platinum(II) complexes.

$$k_{obs} = k_2[Nu] \qquad (3.1)$$
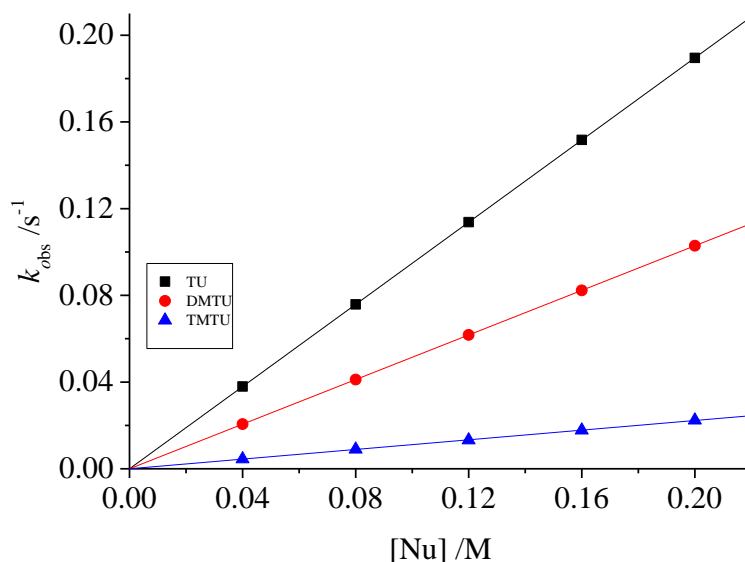
Figure 3.3: *Pseudo* first-order rate constants plotted as a function of the concentration of the entering nucleophiles for the substitution reaction of the diaqua **tPtR** complex by TU, DMTU, and TMTU at pH = 2.0 (0.09 M NaClO$_4$ + 0.01 M HClO$_4$) and 298 K

The comparative second-order rate constants for the substitution processes of the corresponding analogous *cis-* and *trans-*dialkylamine platinum(II) complexes are summarised in **Table 3.3**. In the case of the *cis-*platinum(II) complexes, the substitutions turned out to be rather slow in which the first and the second steps occurred in concert. The reactions with the bulkiest nucleophile, TMTU, was too slow to be followed to completion for all the *cis-*configured platinum(II) complexes. The second-order rate constant, $k_{2\ 1st}$, for the first step of the reactions of the *cis-*platinum(II) complexes with the thiourea-based nucleophiles was assigned to the substitution of both labile aqua ligands, whereas the second step was ascribed to the displacement of the monodentate amine moieties consequent upon the strong *trans* effect of the coordinated thioureas. However, in the *trans-*platinum(II) complexes, the single step observed was assigned to the simultaneous removal of the two aqua ligands.

3.6.3   NMR Studies

Substitution of the chloride ligands in all the studied complexes with on an excess thiourea (TU) was investigated by ^{195}Pt NMR spectroscopy. A typical ^{195}Pt NMR spectra for the substitution of **cPtR** and **tPtR** with TU respectively are presented in **Figures 3.4** and 3.**5**. In both cases, at t = 0, a signal due to the starting complexes [*cis-*Pt{NH$_2$CH(CH$_3$)$_2$}Cl$_2$] and [*trans-*Pt{NH$_2$CH(CH$_3$)$_2$}Cl$_2$] were observed at –2218.5 ppm and –2206 ppm respectively. In the case of the *cis-*configured complex, there is the formation of an intermediate species at –3382 ppm which is assigned to the substitution of the two chloro ligands [*cis-*Pt{NH$_2$CH(CH$_3$)$_2$}(TU)$_2$]$^{2+}$, followed by the eventual substitution of the two amine moieties via a strong *trans* effect of the TU to

give the final product after 24 hours at –4092 ppm assigned to $[Pt(TU)_4]^{2+}$. Notably, the final products of all the *cis*-configured complexes were obtained at –4092 ppm. However, in the case of the [*trans*-Pt{NH$_2$CH(CH$_3$)$_2$}Cl$_2$], the signal of the final product was found at -3209 ppm within 20 minutes and remained the same after 24 hours. The signal of the final product of the **tPtR** was ascribed to [*trans*-Pt{NH$_2$CH(CH$_3$)$_2$}(TU)$_2$]. The final products of all the *trans*-platinum(II) complexes, however, appear between -3170 ppm and -3210 ppm.
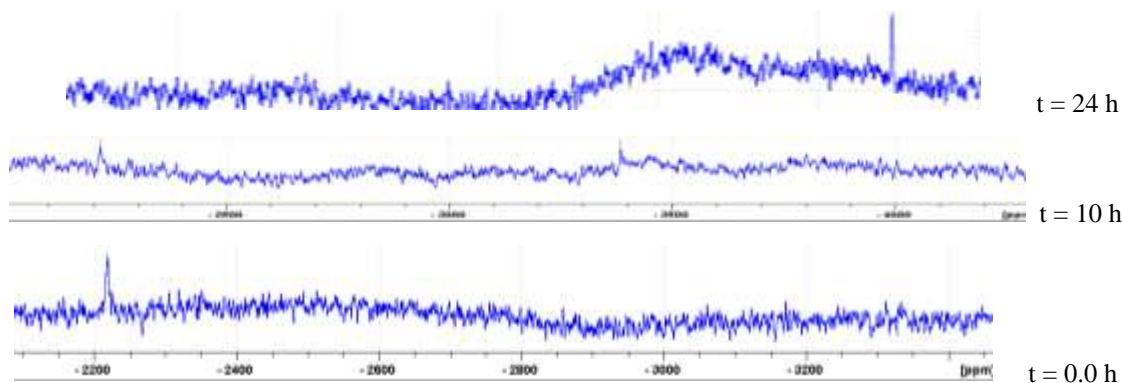
Figure 3.4: ^{195}Pt NMR spectra of the reaction mixture of **cPtR-Cl** with six mole equivalents of TU, showing pure **cPtR-Cl** ($\delta = –2218.5$ ppm) before the reaction, the intermediate species ($\delta = –3382$ ppm) formed during course of the reaction, [*cis*-Pt{NH$_2$CH(CH$_3$)$_2$}$_2$(TU)$_2$]$^{2+}$ and the final degradation product ($\delta = –4092$ ppm) corresponding to $[Pt(TU)_4]^{2+}$.
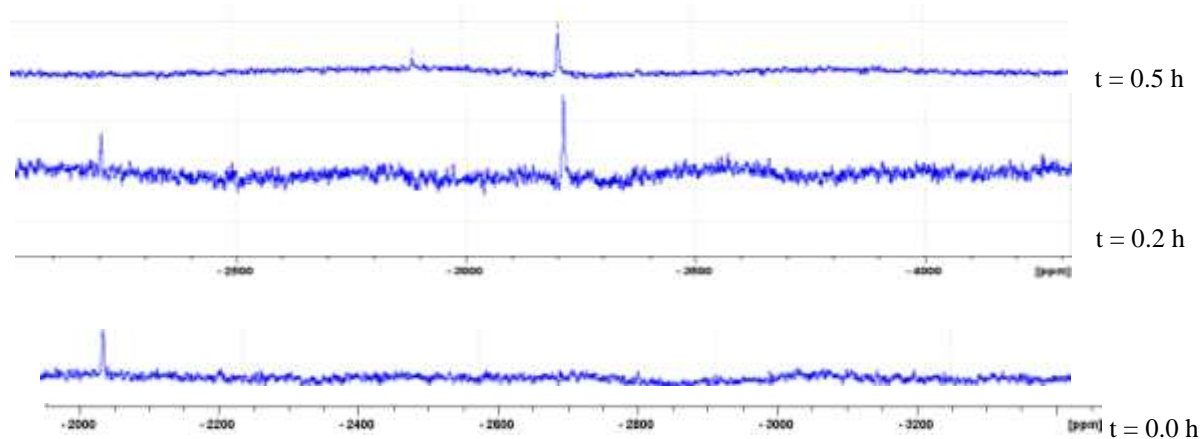
Figure 3.5: ^{195}Pt NMR spectra of the reaction mixture of **tPtR-Cl** with six mole equivalents of TU, showing pure **tPtR-Cl** ($\delta = –2206$ ppm) before the reaction, and the final stable biadduct product ($\delta = –3209$ ppm) ascribed to [*trans*-Pt{NH$_2$CH(CH$_3$)$_2$}$_2$(TU)$_2$]$^{2+}$.

Based on the NMR results, it is reasonably concluded, therefore, that the *cis*- and the *trans*-platinum(II) complexes do not form the same kinetic product with TU. The presence of the strong labilising thiourea nucleophiles at the platinum(II) centre forces the substitution of the amine ligands attached to the metal centre in all the *cis*-configured platinum(II) complexes. This result is consistent with what have been previously reported by other researchers in related studies [9, 13, 31-33]. The

substitution of the amine groups was not observed in any of the *trans*-configured platinum(II) complexes. Unlike the notion posited by Song *et al*. [14], our current findings are congruous with the earlier findings of Brabec *et al.* [15].

It has been well-established that the pK_a values of the coordinated aqua ligand is an experimental indicator of the electron density around the metal centre [27, 34]. Hence, the lower the pK_a value the more electrophilic and in most cases, the more reactive a metal complex is. In this study, both the experimental and the theoretical findings perfectly aligned. All the *trans*-complexes are more electrophilic than their corresponding *cis*-counterparts based on their respective pK_a values and this phenomenon is underpinned by the DFT-calculated charges on the platinum centres for both the *cis*- and the *trans*-dialkylamine platinum(II) complexes respectively. The general trend of the second order rate constants for the substitution of aqua ligands by the entering nucleophiles is as follows: tPt > tPtM > tPtR > cPt > cPtM > cPtR. Each of the *trans*-platinum(II) complexes is ca. 10^3 times more reactive than its corresponding *cis*-platinum(II) analogues. This trend agrees very well with the electrophilicity of their respective platinum centre based on the experimentally determined pK_a values and the DFT-calculated NBO charges.

Moreover, a thorough look at the DFT-calculated data in **Table 3.2** shows that the average bond length between the platinum centre and the aqua ligands is higher in all the *cis*-configured platinum(II) complexes compared to their corresponding *trans*-complexes. This implies that the substitution of the aqua moieties by the entering nucleophiles are ordinarily expected to occur faster in the *cis*-complexes than those of their corresponding *trans*-counterparts because their aqua ligands should have been more labile in the ground state. Hence, the second order rate constants of the *cis*-complexes in the first step should have been greater than those of their corresponding *trans*-analogues. This is not unexpected because of the *trans* effect between H_2O and NH_3 with the ammine ligand having a greater *trans* effect than the aqua ligand. This, however, was not the case based on the second-order rate constants obtained, which is summarised in **Table 3.3**.

Table 3.3: Second-order rate constants for the reaction of the investigated analogous diaqua *cis*- and *trans*-platinum(II) complexes with thiourea nucleophiles at pH = 2.0 (0.9 M $NaClO_4$ + 0.01 M $HClO_4$) and 298 K

Complex	Nucleophiles	$k_{2(1st)}$ x10^{-3}/$M^{-1}s^{-1}$	$k_{2(2nd)}$ x 10^{-3}/$M^{-1}s^{-1}$
cPt	TU	97.6 ± 0.4	21.4 ± 0.06
	DMTU	44.2 ± 0.2	8.6 ± 0.03
	TMTU	Too slow	Too slow
cPtM	TU	58.3 ± 0.2	8.2 ± 0.02
	DMTU	36.3 ± 0.1	3.8 ± 0.01
	TMTU	Too slow	Too slow
cPtR	TU	2.8 ± 0.02	
	DMTU	1.9 ± 0.02	Too slow
	TMTU	Too slow	
tPt	TU	44.2 ± 0.03	
	DMTU	22.9 ± 0.11	
	TMTU	5.6 ± 0.01	-
tPtM		35.4 ± 0.11	
	DMTU	18.2 ± 0.02	
	TMTU	3.8 ± 0.03	-
tPtR	TU	19.0 ± 0.0016	
	DMTU	10.3 ± 0.0001	-
	TMTU	2.2 ± 0.0065	

Besides, the electronic factors such as the electrophilicity of the metal centre favouring a greater reactivity of the *trans*-complexes over their corresponding *cis*-isomers, steric hindrances also play a prominent role. Steric hindrance is greater in the *cis*-complexes as compared to their *trans*-analogues [16]. The *trans*-configuration greatly minimises steric hindrance which enhances the axial approach of the entering nucleophile. The *cis*-geometry, on the other hand, amplifies steric hindrances which is anticipated to hinder the axial approach of the incoming nucleophile to the metal centre. This became more pronounced with the increasing bulkiness of the amine moieties. In the same vein, the steric effect, in the *trans*-complexes, increase as the amine ligands become bulkier.

Furthermore, the increased steric hindrance in the *cis*-configured complexes is also enhanced through intramolecular hydrogen bonding. This is underpinned by the average interatomic distance between the hydrogen atoms on the nitrogen of the amine moiety and the oxygen atom of the aqua ligand as

well as the average interatomic distance between the hydrogen of the aqua ligand and the nitrogen atom of the amine ligands. These distances are shorter in the *cis*-complexes compared to their corresponding *trans*-counterparts. The increased possibility of intramolecular hydrogen bonding interactions in the *cis*-platinum(II) complexes forestalls the entering nucleophiles from reaching the platinum centre, thereby retarding the reactivity of the *cis*-complexes relative to those of their *trans*-isomers. This observation has been previously reported [12, 35]. Intramolecular hydrogen bonding increases steric hindrances around the metal centre thereby retarding the activation of the substitution process in the *cis*-configured complexes. This possibility of steric hindrance due to intramolecular hydrogen bonding is remarkably minimised in the *trans*-configured complexes, hence, their increased reactivity.

Another factor that contributed to the increased steric hindrance in the *cis*-complexes as compared to their corresponding *trans*-analogues, is the solvation of the hydrogen atoms on the nitrogen atom of the amine moieties. The solvated hydrogen atom increases steric crowdedness around the metal centre, thus, slowed down the attack of the nucleophile on the reaction site. This effect is also present in the *trans*-complexes. However, the remote distance between the -NH$_2$R moiety and the leaving aqua ligand minimises the steric crowdedness around the metal centre, hence, the unhindered approach of the nucleophile. The proximity of aqua and amine moieties in the *cis*-complexes enhances crowdedness around the substitution sites. Generally, substitution of the aqua moieties from the studied *cis* and *trans*-platinum(II) complexes exhibits an apparent dependence on the steric hindrance of the entering nucleophiles. Hence, the reactivity of the thiourea nucleophiles with the complexes decreases with increase in steric demand in the following order: TU > DMTU > TMTU.

Table 3.4: Summary of the activation parameters for substitution of coordinated aqua moieties from the investigated analogous *cis-* and *trans-*platinum(II) complexes with thiourea nucleophiles in the temperature range 293–313 K.

Complex	Nu	$\Delta H^\ddagger_1$ (kJ/mol)	$\Delta H^\ddagger_2$ (kJ/mol)	$\Delta S^\ddagger_1$ (J mol^{-1} K^{-1})	$\Delta S^\ddagger_2$ (J mol^{-1} K^{-1})
cPt	TU	17 ± 0.03	58 ± 0.08	-189 ± 0.1	-84 ± 0.3
	DMTU	48 ± 0.08	57 ± 0.09	-111 ± 0.3	-95 ± 0.3
cPtM	TU	63 ± 7	75 ± 6	-57 ± 3	-34 ± 2
	DMTU	57 ± 1	65 ± 1	-79 ± 6	-74 ± 4
cPtR	TU	54 ± 5		-112 ± 16	
	DMTU	57 ± 5	-	-108 ± 2	-
tPt	TU	63 ± 2		-29 ± 6	
	DMTU	55 ± 1	-	-61 ± 4	-
	TMTU	68 ± 2		-27 ± 6	
tPtM	TU	58 ± 3		-34 ± 10	
	DMTU	62 ± 1	-	-43 ± 3	-
	TMTU	60 ± 2		-64 ± 7	
tPtR	TU	58 ± 2		-51 ± 7	
	DMTU	54 ± 2	-	-69 ± 5	-
	TMTU	57 ± 1		-72 ± 3	
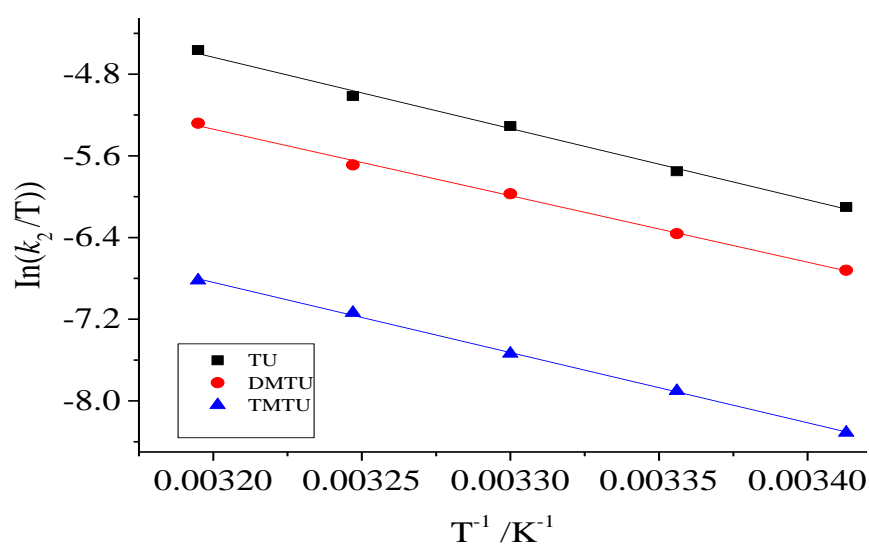
Figure 3.6: Plot of ln(k_2/T) against 1/T for the reaction of **tPtR** with the thiourea-based nucleophiles at various temperatures ranging from 293 to 313 K.

$$ln\left(\frac{k_2}{T}\right) = -\frac{\Delta H^{\#}}{RT} + \left(23.8 + \frac{\Delta S^{\#}}{R}\right) \qquad (3.2)$$

The activation parameters $\Delta H^{\#}$ and $\Delta S^{\#}$ were calculated using the Eyring equation (*equation* 3.2) by measuring the rate constants for each of the substitution reactions of the investigated platinum(II) complexes with the thiourea-based nucleophiles as a function of temperature (**Figure 3.6**) and are summarized in **Table 3.4**. In general, ligand substitution for all the investigated complexes, regardless of their configurations, followed an associative mechanism and are characterized by negative intrinsic activation entropy values resulting from bond formation in the transition state [35-42]. The activation entropies for both the *cis*- and *trans*-configured complexes confirm the associative character for the substitution process with this character being generally more prominent in the *cis*-complexes compared to their *trans*-counterparts. This implies that bond-making in the transition state is more favoured in the *cis*-complexes than in the *trans*-complexes.

3.7   Conclusion

A series of analogues bifunctional dialkylamine *cis*- and *trans*-platinum(II) complexes were synthesised, characterised and investigated for comparative substitution reactions with thiourea-based nucleophiles. Substitution of the *cis*-complexes followed a concerted two-step process while those of the *trans*-complexes proceeded by a single step. The *trans*-complexes are *ca.* 10^3 more reactive than their *cis*-analogues. Electronic as well as steric effects controlled the overall reaction pattern. The negative entropy of activation values obtained for all the studied complexes affirmed an associative mode of substitution. The *cis*-complexes formed a different kinetic product as completely substituted and were confirmed by ^{195}Pt NMR spectroscopy. The *trans*-complexes are thermodynamically more stable to complete substitution by the thiol-nucleophiles and hence, their use as alternative platinum-based anticancer agents can be further explored.

References

[1] S. Jovanović, J. Bogojeski, M. Petković, Ž.D. Bugarčić, Journal of Coordination Chemistry, 68 (2015) 3148-3163.

[2] L. Messori, L. Cubo, C. Gabbiani, A. Álvarez-Valdés, E. Michelucci, G. Pieraccini, C. Ríos-Luci, L.G. León, J.M. Padrón, C. Navarro-Ranninger, Inorganic Chemistry, 51 (2012) 1717-1726.

[3] J.J. Wilson, S.J. Lippard, Chemical Reviews, 114 (2013) 4470-4495.

[4] A. Quiroga, F. Ramos-Lima, A. Alvarez-Valdés, M. Font-Bardía, A. Bergamo, G. Sava, C. Navarro-Ranninger, Polyhedron, 30 (2011) 1646-1650.

[5] A. Quiroga, Journal of Inorganic Biochemistry, 114 (2012) 106-112.

[6] K. Ossipov, Y.Y. Scaffidi-Domianello, I.F. Seregina, M. Galanski, B.K. Keppler, A.R. Timerbaev, M.A. Bolshov, Journal of Inorganic Biochemistry, 137 (2014) 40-45.

[7] W.B. Dirersa, International Journal of Chemical and Pharmaceutical Analysis, 2 (2014) 40-47.

[8] E.I. Montero, S. Díaz, A.M. González-Vadillo, J.M. Pérez, C. Alonso, C. Navarro-Ranninger, Journal of Medicinal Chemistry, 42 (1999) 4264-4268.

[9] W.P. Asman, D. Jaganyi, International Journal of Chemical Kinetics, (2017) 1-20.

[10] P.O. Ongoma, D. Jaganyi, Transition Metal Chemistry, 38 (2013) 587-601.

[11] P.O. Ongoma, D. Jaganyi, Dalton Transactions, 42 (2013) 2724-2734.

[12] P.O. Ongoma, D. Jaganyi, Transition Metal Chemistry, 39 (2014) 407-420.

[13] S. Hochreuther, S.T. Nandibewoor, R. Puchta, R. van Eldik, Dalton Transactions, 41 (2012) 512-522.

[14] H. Song, W. Li, R. Qi, L. Yan, X. Jing, M. Zheng, H. Xiao, Chemical Communications, 51 (2015) 11493-11495.

[15] V. Brabec, O. Vrana, O. Novakova, J. Kasparkova, Chemical Communications, 52 (2016) 4096-4098.

[16] E. Pantoja, A. Gallipoli, S. van Zutphen, S. Komeda, D. Reddy, D. Jaganyi, M. Lutz, D.M. Tooke, A.L. Spek, C. Navarro-Ranninger, Journal of Inorganic Biochemistry, 100 (2006) 1955-1964.

[17] E.I. Montero, S. Díaz, A.M. González-Vadillo, J.M. Pérez, C. Alonso, C. Navarro-Ranninger, Journal of Medicinal Chemistry, 42 (1999) 4264-4268.

[18] A.K. Connors, Chemical Kinetics of the Reaction Rates in Solution, Wiley-VCH, New York, (1990) 2-20.

[19] A.D. Becke, The Journal of Chemical Physics, 96 (1992) 2155-2160.

[20] P.J. Hay, W.R. Wadt, The Journal of Chemical Physics, 82 (1985) 299-310.

[21] T.A. Hilder, J.M. Hill, Nanotechnology, 18 (2007) 275704-275710.

[22] V. Barone, M. Cossi, The Journal of Physical Chemistry A, 102 (1998) 1995-2001.

[23] M. Cossi, N. Rega, G. Scalmani, V. Barone, Journal of Computational Chemistry, 24 (2003) 669-681.

[24] E. Seifert. OriginPro 9.1: Scientific Data Analysis and Graphing Software®- Software Review. Journal of Chemical Information and Modeling, 54, (2014) 1552-1566.

[25] T.G. Appleton, A.J. Bailey, K.J. Barnham, J.R. Hall, Inorganic Chemistry, 31 (1992) 3077-3082.

[26] L. Cubo, A.G. Quiroga, J. Zhang, D.S. Thomas, A. Carnero, C. Navarro-Ranninger, S.J. Berners-Price, Dalton Transactions, (2009) 3457-3466.

[27] A. Hofmann, D. Jaganyi, O.Q. Munro, G. Liehr, R. van Eldik, Inorganic Chemistry, 42 (2003) 1688-1700.

[28] P. Atkins, J. de Paula, Elements of Physical Chemistry, 5th ed., Oxford University Press, Great Britain, (2009) 1-30.

[29] K. Tiwari, P. Arora, N. Pandey, P. Pandey, H.C. Joshi, S. Pant, Journal of Molecular Liquids, 200 (2014) 460-464.

[30] D. Reddy, D. Jaganyi, International Journal of Chemical Kinetics, 43 (2011) 161-174.

[31] S. Hochreuther, R. Puchta, R. van Eldik, Inorganic Chemistry, 50 (2011) 8984-8996.

[32] P.W. Asman, Journal of Coordination Chemistry, (2017) 1-20.

[33] P.W. Asman, Inorganica Chimica Acta, 469 (2018) 341-352.

[34] B. Petrović, Z.i.D. Bugarčić, A. Dees, I. Ivanović-Burmazović, F.W. Heinemann, R. Puchta, S.N. Steinmann, C. Corminboeuf, R. Van Eldik, Inorganic Chemistry, 51 (2012) 1516-1529.

[35] H. Ertürk, R. Puchta, R. van Eldik, European Journal of Inorganic Chemistry, 2009 (2009) 1331-1338.

[36] B.B. Khusi, A. Mambanda, D. Jaganyi, Transition Metal Chemistry, 41 (2016) 191-203.

[37] G. Kinunda, D. Jaganyi, Transition Metal Chemistry, 39 (2014) 939-949.

[38] T.R. Papo, D. Jaganyi, Journal of Coordination Chemistry, 68 (2015) 794-807.

[39] D. Reddy, D. Jaganyi, Dalton Transactions, (2008) 6724-6731.

[40] A. Shaira, D. Jaganyi, Journal of Coordination Chemistry, 68 (2015) 3013-3031.

[41] T. Soldatović, S. Jovanović, Ž.D. Bugarčić, R. van Eldik, Dalton Transactions, 41 (2012) 876-884.

[42] P.A. Wangoli, G.B. Kinunda, New Journal of Chemistry, (2017) 214-227.

Chapter Four

A Kinetic Investigation of Mononuclear *trans*-Platinum(II) Complexes with Mixed Amine Ligands

Abstract

This study was aimed at investigating the substitution behaviour of mononuclear *trans*-platinum(II) complexes with mixed amine ligands. The rate of substitution of the chloride moeities from the complexes *trans*-Pt(NH$_3$)(NH$_2$C$_2$H$_5$)Cl$_2$ (**tPt2**), *trans*-Pt(NH$_3$)(NH$_2$C$_3$H$_7$)Cl$_2$ (**tPt3**), *trans*-Pt(NH$_3$)(NH$_2$C$_4$H$_9$)Cl$_2$ (**tPt4**) and *trans*-Pt(NH$_3$)(NH$_2$C$_5$H$_{11}$)Cl$_2$ (**tPt5**), by three nucleophiles, viz. thiourea (TU), 1-methyl-2-thiourea (MTU) and 1,3-dimethyl-2-thiourea (DMTU), was studied under *pseudo* first-order conditions as a function of concentration and temperature by stopped-flow spectrophotometry. Substitution at each of the *trans*-platinum(II) complexes proceeds via a single-step and obeys first-order kinetics. The *pseudo* first-order rate constants, k_{obs} obeyed the rate law: $k_{obs} = k_2$[nucleophile]. The reactivity of the complexes was largely dependent on the length of the alkyl chain of the alkylamine moiety of the complexes. Computational modelling using density functional theory (DFT) calculations showed that an increase in chain length by a methylene unit has no direct electronic consequence on the metal centre but did however, pose significant steric hindrance on the substitution sites due to the flexibility of the alkyl chains and thus governed the overall reaction pattern. The order of reactivity of the complexes is **tPt2** > **tPt3** > **tPt4** > **tPt5**. The reactivity of the nucleophiles with the complexes decreases with increasing steric demand in the following order: TU > MTU > DMTU. [195]Pt NMR kinetic studies established that the mixed amine ligands remain coordinated to the metal centre in the final kinetic product. This implies that mononuclear *trans*-platinum(II) complexes are resistant to complete substitution of ligands by the incoming thiourea nucleophiles at the reaction sites. The low positive values of activation enthalpy and large negative values of activation entropy indicate an associative mechanism of substitution.

4.1   Introduction

The flaws that are associated with cisplatin anticancer treatment such as severe side effects, lack of selectivity, inherent and acquired resistance, and transient retention in the bloodstream, have stimulated a great deal of research activity among synthetic inorganic chemists to the end that some more potent and veritably less toxic anticancer agents can be developed [1-6]. Platinum compounds with distinctively different DNA binding modes from cisplatin are some of the prospective anticancer agents that are currently under consideration [7, 8]. Top among those compounds are complexes in which the inert or spectator amine ligands are of *trans* stereochemistry [7, 9-14]. It has been well established that *trans*-diamminedichloroplatinum(II), i.e. transplatin, a *trans* isomer of cisplatin is biologically inert against cancer cell lines. Its dearth of activity has been suggested to have originated in part from kinetic instability thereby making it susceptible to deactivation.

This was the genesis of the initial thinking amongst researchers in the field that platinum complexes with only the *cis* configuration are therapeutically useful as cytotoxic drugs. When one or both ammine ligands in transplatin are substituted by bulky ligands, the resulting compounds have been found to be active with an increased toxicity [7]. It is believed that the bulky ligands might have restricted ligand substitution of the chloride ions, thus minimizing the formation of by-products between platinum and cellular components thereby enhancing platinum interaction with DNA.

These ideas have inspired the design and synthesis of novel platinum complexes with *trans*-stereochemistry. Farrell *et al.* [7] and Navarro-Ranninger *et al.* [15, 16], have reported classes of biologically active *trans*-platinum compounds that have led to some researchers jettisoning the previously held structure-activity relationship that only *cis*-platinum complexes are equipped with antitumor potential. In fact, Navarro-Ranninger and co-workers disclosed some novel *trans*-platinum(II) complexes with asymmetric aliphatic amines which showed cytotoxic properties against some cisplatin resistant cell lines. These compounds exhibited radically different pharmacodynamics from those already established for cisplatin. Consequently, the exigent need to further explore these alternative potential platinum-based anticancer agents cannot be over-emphasized. Despite the burgeoning interest among medicinal inorganic chemists to develop more

effective *trans*-platinum complexes, the detailed mechanistic study of these compounds is still relatively non-existent when compared to the level of information available on their cis-derivatives. Moreover, the dearth of understanding of the substitution behaviours and stability of these compounds have impeded the design possibilities and synthesis of new and more active platinum-based chemotherapeutic agents with low toxicities. A recent controversy on the interaction of transplatin with DNA has galvanised our interest to investigate ligand substitution kinetics of these complexes.

Song *et al*. [17] have posited that transplatin is most probably transformed to the *cis*-isomer under UVA irradiation. Their speculations were hinged on the fact that transplatin, which is generally known to be non-toxic in the dark to all tumour cell lines, was found to be relatively of the same toxicity level with cisplatin under UVA irradiation. However, Brabec *et al*. [18] quashed that notion by employing three independent methods to show that transplatin does not isomerize to cisplatin in the presence of UVA light.

Subsequently, in our previous study (*Chapter 3*), we had compared the substitution behaviour of the symmetrical *trans*-platinum(II) complexes with their corresponding *cis*-analogues. Our findings, among other things, showed that the *trans* complexes do not form the same kinetic product as the corresponding *cis* complexes. To our knowledge, we also provided for the first time detailed comparative mechanistic data between transplatin and cisplatin and their derivatives using spectrophotometric techniques. This present study is aimed at further extending the understanding of ligand substitution kinetics of *trans*-platinum(II) complexes. To this end, *trans*-platinum(II) complexes of mixed amine spectator ligands, as presented in **Figure 4.1** below, were investigated.

H_3N — Pt — Cl
Cl — Pt — NH_2R
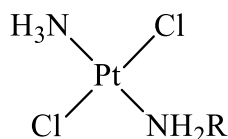
tPt2 R = C_2H_5
tPt3 R = C_3H_7
tPt4 R = C_4H_9
tPt5 R = C_5H_{11}

Figure 4.1: Structures of the mononuclear *trans*-platinum(II) complexes with mixed amine ligands selected for the current study.

4.2 Experimental

4.2.1 Chemicals

The ligands, ethylamine (70%), propylamine (99%), butylamine (99.5%), amylamine (99%), HCl (37%), cisplatin (99.9%), lithium trifluoromethanesulfonate, methanol, lithium chloride (99.0%), the nucleophiles: thiourea (99%), 1-methyl-2-thiourea (99%) and 1,3-dimethyl-2-thiourea (99%), were all purchased from Sigma Aldrich and were used without further purifications. All other chemicals used are of the highest purity available commercially. Ultrapure water was used in the preparations of all aqueous solutions.

4.2.2 General Synthetic Procedure for the Preparation of the Mixed *trans*-Platinum(II) Complexes

The general synthetic procedure for the mixed *trans*-platinum(II) complexes has been reported by Wilson and Lippard [7]. Cisplatin (100 mg, 0.333 mmol) was suspended in water (2 mL) and 8 equivalents of the appropriate alkylamine ligand was added. The resulting mixture was heated at

90 °C until the solution became colourless. After the solution was cooled to room temperature, it was then treated with 32% (v/v) concentrated HCl (2.5 mL) followed by stirring and heating at 90 °C for 48 hours. The resulting yellow solution was placed in an iced bath to induce precipitation of the appropriate *trans*-platinum(II) complex which was recovered by filtration, washed intensively with water and diethyl ether, and air dried at room temperature.

tPt2 yield: 49 mg (45%). ^{1}H NMR (500 MHz, DMF-d$_7$), δ(ppm): 1.26 (t, 3H); 2.73 (sextet 2H); 3.72 (s, 3H), 4.38 (s, 2H). ^{195}Pt NMR (107 MHz, DMF-d$_7$), δ(ppm): -2165.7. TOF MS/ES$^+$, *m/z:* (M + Na)$^+$: 350.9 (C$_2$H$_8$NaN$_2$PtCl$_2$, species). Anal. Cal for C$_2$H$_{10}$N$_2$PtCl$_2$: N, 8.54; C, 7.32; H, 3.07. Found: N, 8.50; C, 7.00; H, 2.86.

tPt3 yield: 91 mg (80%). ^{1}H NMR (500 MHz, DMF-d$_7$), δ(ppm): 0.93 (t, 3H); 1.77 (sextet, 2H); 2.65 (quintet, 2H), 3.74 (s, 3H), 4.36 (s, 2H). ^{195}Pt NMR (107 MHz, DMF-d$_7$), δ(ppm): -2163. TOF MS/ES$^+$, *m/z:* (M$^+$): 340 (C$_3$H$_{10}$N$_2$PtCl$_2$, species). Anal. Cal for C$_3$H$_{12}$N$_2$PtCl$_2$: N, 8.19; C, 10.53; H, 3.54. Found: N, 8.12; C, 10.50; H, 3.27.

tPt4 yield: 89 mg (75%). ^{1}H NMR (500 MHz, DMF-d$_7$), δ(ppm): 0.92 (t, 3H); 1.37 (sextet, 2H); 1.74 (quintet, 1.74); 2.69 (quintet, 2H), 3.74 (s, 3H), 4.34 (s, 2H). ^{195}Pt NMR (107 MHz, DMF-d$_7$), δ(ppm): -2163. TOF MS/ES$^+$, *m/z:* (M + Na. CH$_3$OH)$^+$: 413 (C$_5$H$_{18}$N$_2$NaOPtCl$_2$, species). Anal. Cal for C$_4$H$_{14}$N$_2$PtCl$_2$: N, 7.87; C, 13.49; H, 3.96. Found: N, 7.84; C, 13.59; H, 3.91.

tPt5 yield: 68 mg (55%). ^{1}H NMR (500 MHz, DMF-d$_7$), δ(ppm): 0.90 (t, 3H); 1.32 (sextet, 2H); 1.76 (quintets, 2H); 2.68 (quintet, 2H), 3.73 (s, 3H), 4.34 (s, 2H). ^{195}Pt NMR (107 MHz, DMF-d$_7$), δ(ppm): -2162. TOF MS/ES$^+$, *m/z:* (M + Na. CH$_3$OH)$^+$: 422 (C$_6$H$_{20}$N$_2$NaOPtCl$_2$, species). Anal. Cal for C$_5$H$_{16}$N$_2$PtCl$_2$: N, 7.57; C, 16.22; H, 4.36. Found: N, 7.50; C, 16.35; H, 4.57.

4.3   Instrumentation and Physical Measurements

A Waters Micro-mass LCT Premier spectrometer was used for mass determination of the *trans*-platinum(II) complexes. Elemental analyses of the synthesised complexes were performed on a ThermoScientific Flash 2000. ^{1}H and ^{195}Pt NMR spectroscopic analyses were carried out on a Bruker Avance III 500MHz. This was also employed to monitor ^{195}Pt-NMR of the substitution reactions of the *trans*-platinum(II) complex **tPt3** with thiourea (TU). All ^{1}H chemical shifts were referenced to Si(CH$_3$)$_4$ and ^{195}Pt NMR chemical shifts were externally referenced to K$_2$[PtCl$_6$][19]. For the determination of the coordination features at the platinum centre, ^{195}Pt NMR is usually employed and this has been established as an effective technique because its chemical shifts are largely affected, among other things, by the nature of the coordinated donor atoms [20]. All kinetic measurements were carried out on an Applied Photophysics SX.20 stopped-flow analyser coupled to an online data acquisition system and kinetic traces were evaluated using the Origin 9.1$^®$ software [21]. The temperature of the instrument was kept within ± 0.05 ^{o}C for all the measurements.

4.4   Computational Modelling

Prefatory density functional theoretical (DFT) optimization modelling of the *trans*-platinum(II) complexes **tPt2-tPt4** was performed at the DFT level B3LYP [22] with the LANL2DZ basis set

[23] using the Gaussian 09 programme suite (**Table 4.1**). B3LYP relates to the hybrid functional Becke's three-parameter formulation, which has been proven to be superior to classical functionals. LANL2DZ is double-zeta basis set which comprises effective core potential (ECP) representations of electrons near the nuclei for transition metal complexes especially for platinum complexes [3, 24-28]. The theoretical calculations of the complexes were performed in methanol taking into account the effects of the solvent by employing conductor polarisable continuum model (CPCM) formalism [29, 30]. The complexes were optimized in their neutral form, and at singlet states because of the low electronic spin of platinum(II) complexes.

Table 4.1: A summary of the DFT calculated data for the investigated *trans*-platinum(II) complexes at B3LYP/LANL2DZ level of theory.

Parameters	tPt2	tPt3	tPt4	tPt5
Bond Length (Å)				
Pt—Cl	2.446	2.447	2.445	2.445
NBO Charge				
Pt	0.099	0.090	0.092	0.090
-NH_2R	–0.673	–0.685	–0.688	–0.698
MO Energies (eV)				
HOMO	–1.86	–1.86	–1.86	–1.85
LUMO	–6.22	–6.23	–6.23	–6.22
ΔE	4.36	4.37	4.37	4.36
Dipole Moment (D)	0.837	0.883	1.002	1.086

R = alkyl group

4.5   Kinetic Measurements

Substitution of the chloride moieties from each of the four *trans*-platinum(II) complexes (**Figure 4.1**) by three different thiourea nucleophiles: thiourea (TU), 1-methyl-2-thiourea (MTU) and 1,3-dimethyl-2-thiourea (DMTU) was investigated under *pseudo* first-order-conditions with at least a 20-fold excess of the nucleophile. Spectral changes resulting from the mixing of the complex and the nucleophile solutions were observed over the wavelength range 200-800 nm to establish an appropriate wavelength at which the kinetic measurements could be performed on the stopped-

flow spectrophotometer. The reactions were initiated by the mixing of equal volumes of a solution of the metal complex with a solution of the nucleophile directly in the stopped-flow machine. All reported rate constants represent an average value of at least seven independent kinetic runs for each experimental measurement. The temperature dependence of the rate constants was observed over a range of 20–40 °C at an interval of 5 °C.
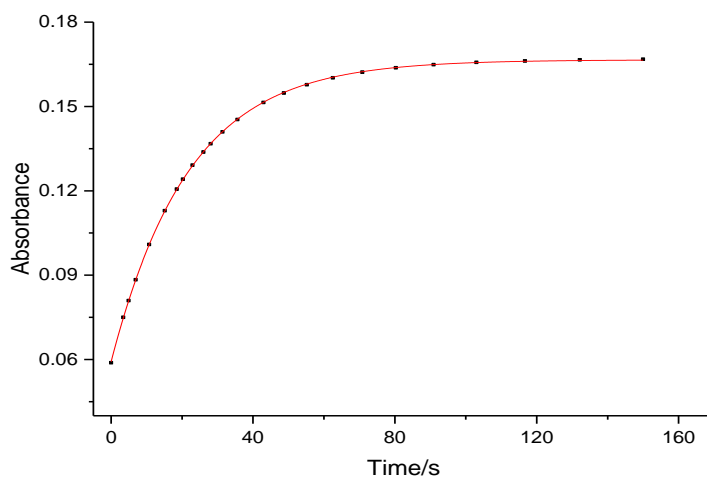
Figure 4.2:   Kinetic trace obtained on the stopped-flow spectrophotometer for the reaction of **tPt2** and TU monitored at 335 nm in methanol, $I = 0.09$ M $LiCF_3SO_3$ and 10 mM LiCl at 298 K.
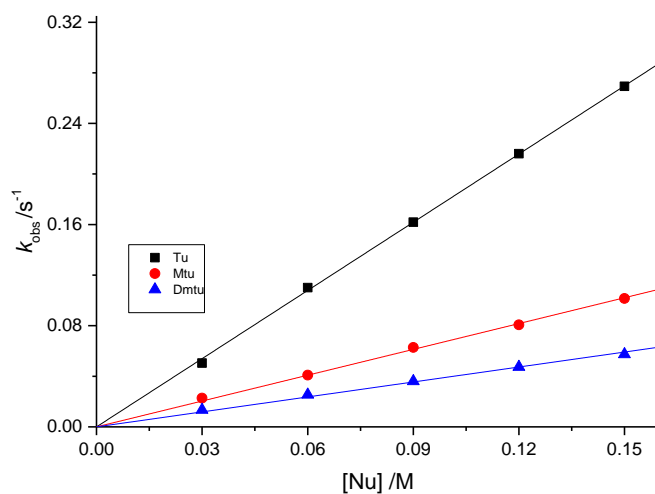
Figure 4.3:   Dependence of k_{obs} on the concentration of entering nucleophiles for the chloride substitution of **tPt2** in methanol, $I = 0.09$ M $LiCF_3SO_3$ and 10 mM LiCl at 298 K.

111

Table 4.2: Second-order rate constants and activation parameters for the reactions of mononuclear *trans*-platinum(II) complexes with thiourea-based nucleophiles in 0.09 M $LiCF_3SO_3$ and 10 mM LiCl methanolic solution.

Complex	Nucleophile	$k_2 \times 10^{-2}$ /$M^{-1}s^{-1}$	$\Delta H^{\#}$ /kJ mol^{-1}	$\Delta S^{\#}$ /J K^{-1} mol^{-1}
tPt2	TU	109.8 ± 0.9	58 ± 2	-73 ± 8
	MTU	68.1 ± 0.6	56 ± 1	-65 ± 4
	DMTU	39.4 ± 1	58 ± 2	-118 ± 4
tPt3	TU	83.4 ± 0.4	55 ± 3	-64 ± 9
	MTU	71.4 ± 0.3	57 ± 0.6	-58 ± 2
	DMTU	34.9 ± 0.6	43 ± 2	-108 ± 8
tPt4	TU	80.8 ± 1	53 ± 0.8	-128 ± 3
	MTU	60.3 ± 0.3	55 ± 4	-126 ± 13
	DMTU	33.3 ± 0.1	62 ± 0.7	-105 ± 2
tPt5	TU	64.1 ± 1	65 ± 2	-91 ± 6
	MTU	50.7 ± 0.3	68 ± 0.8	-82 ± 3
	DMTU	29.4 ± 0.2	63 ± 2	-104 ± 6

4.6 Results and Discussion

The substitution of the labile chloride ligands from each of the platinum(II) complexes (**Figure 4.1**) by neutral thiourea-based nucleophiles viz: thiourea (TU), 1-methyl-2-thiourea (MTU) and 1,3-dimethyl-2-thiourea (DMTU) was studied under *pseudo* first-order conditions and monitored on a stopped-flow spectrophotometer. The ionic strength of the reacting solution was maintained using lithium triflate because the triflate ion ($CF_3SO_3^-$) does not coordinate to platinum(II). Spectra changes resulting from mixing the complexes and the nucleophiles were recorded at an appropriate wavelength and a typical representative kinetic trace obtained on the stopped-flow spectrophotometer is shown in **Figure 4.2**. All kinetic traces for the substitution reactions gave an excellent fit to first-order exponential decay to generate the observed *pseudo* first-order rate constants, k_{obs}. This indicates a single step process. These first-order rate constants were plotted

against the entering nucleophile concentration to elicit the second-order rate constants, k_2, from the slopes (**Figure 4.3**) and it obeyed the rate expression described in *equation* 4.1 below. The plots gave straight line fits with zero intercepts for each of the entering nucleophiles indicating that the solvent cannot effectively displace the coordinated nucleophile [19, 31, 32]. All reactions for the displacement of the chloride ligands from the *trans*-platinum(II) complexes were investigated in the presence of a slight excess of chloride ions (10 mM) in order to suppress spontaneous solvolysis reactions. The proposed mechanism for the reaction of the mononuclear *trans*-platinum(II) complexes with thiourea nucleophiles is given in **Scheme 4.1**.

$$k_{obs} = k_2[\text{Nu}] \qquad (4.1)$$
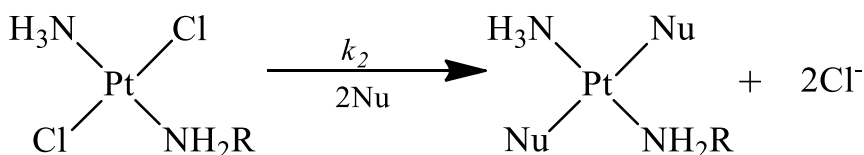
Scheme 4.1: Proposed pathway for the reaction of the *trans*-platinum(II) complexes with thiourea nucleophiles.

The activation parameters, enthalpy of activation, $\Delta H^{\#}$ and entropy of activation, $\Delta S^{\#}$ were determined using the Eyring equation (*equation* 4.2) by measuring the rate constants for each of the substitution reactions of the investigated platinum(II) complexes with thiourea nucleophiles as a function of temperature is shown in **Figure 4.4**. The activation data from the plots are summarised in **Table 4.2**.

$$ln\left(\frac{k_2}{T}\right) = -\left(\frac{\Delta H^{\#}}{RT}\right) + \left(23.8 + \frac{\Delta S^{\#}}{R}\right) \quad (4.2)$$
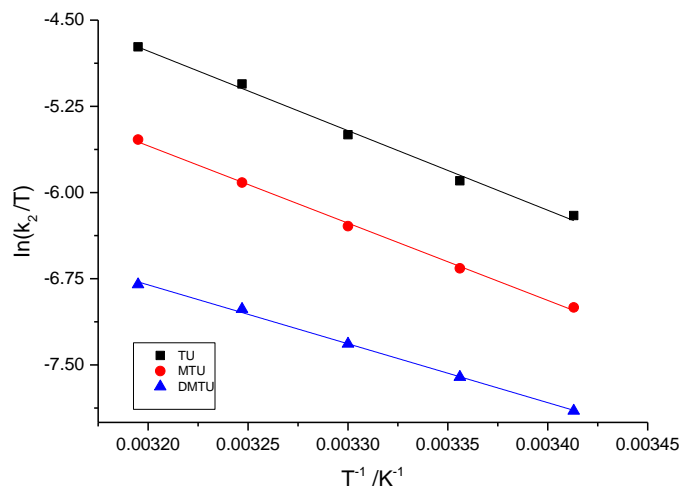
Figure 4.4: Eyring plots for the determination of activation enthalpies and entropies for the reaction of **tPt2** with TU, MTU and DMTU

Comparing the second-order rate constants for the substitution of the chloride moieties from the *trans*-platinum(II) complexes, **tPt2-tPt5** by the nucleophile TU, the reactivity trends follows: **tPt2** > **tPt3** > **tPt4** > **tPt5** with **tPt2** and **tPt5** being the most and the least reactive respectively. A similar reactivity trend is observed for the remaining nucleophiles *viz*. MTU and DMTU as shown in **Table 4.2**. The observed reactivity of these *trans*-platinum(II) complexes can be rationalised in terms of electronic and steric effects. The notable difference in the second-order rate constant for the substitution of the chloride ligands from these complexes was largely controlled by the steric effect due to the chain length of the flexible alkyl amine ligands. The proposed mechanism of the substitution reactions of the *trans*-platinum(II) complexes with thiourea nucleophiles is described in **Scheme 4.1**. The simultaneous substitution of the chloride ligands from the *trans*-platinum(II) complexes were characterised by a single step and this was verified by [195]Pt NMR, which has been known to be profoundly sensitive to the nature of the binding atoms or ligands on the platinum centre [33, 34]. The [195]Pt NMR spectra for the chloride substitution of **tPt3** by TU is presented in **Figure 4.5**.

t = 20 mins

t = 0 mins
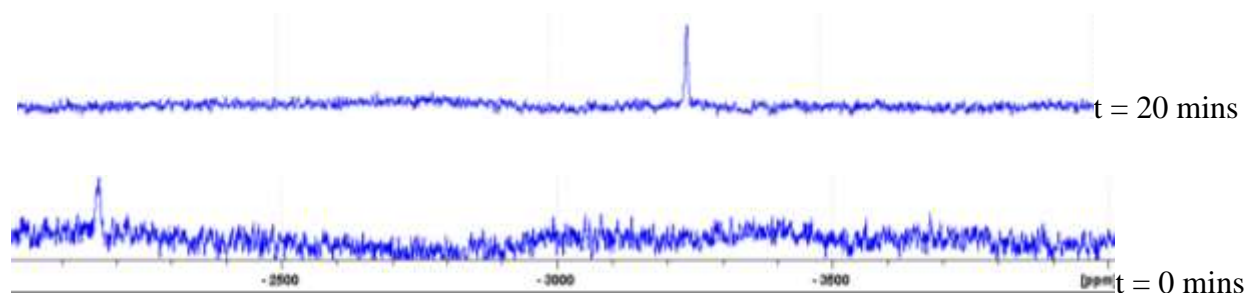
Figure 4.5: ^{195}Pt NMR spectra of the reaction mixture of **tPt3** with six mole equivalents of TU, showing pure **tPt3** (δ = -2169 ppm) before the reaction, and the final stable biadduct product (δ = -3256 ppm) ascribed to [*trans*-Pt (NH$_3$){NH$_2$(CH$_2$)$_2$CH$_3$}(TU)$_2$]$^{2+}$.

The initial peak of the pure **tPt3** was at -2169 ppm and the final peak of the biadduct *trans*-Pt(II) product formed from the simultaneous substitution of the two chloride ligands by thiourea (TU) was obtained at -3256 ppm within twenty minutes of the reaction and remain at the same point after 24 hours. This is consistent with our previous studies (*Chapter 3*). The final peak observed for the biadduct product at around -3200 ppm agrees very well with previous reports in literature for the formation of [Pt(TU)$_2$]$^{2+}$ [25, 35-38].

Juxtaposing the summarised second-order rate constant values presented in **Table 4.2** with the DFT-calculated parameters that is shown in **Table 4.1**, it can be seen that the electronic effect favours a higher reactivity of **tPt2** compared to the rest of the *trans*-platinumt(II) complexes (**tPt3-tPt5**). From **Table 4.1**, it is obvious that the increase in the chain length by the addition of the methylene group results in veritably a negligible change in the HOMO-LUMO energy gap in all the complexes. The only parameter which increases moderately as the chain length of the alkyl group increases by the addition of the methylene unit is the dipole moment. The dipole moment is a measure of the charge separation within a molecule [39] and hence, an increase in the dipole moment is expected with the addition of the methylene unit in the alkyl chain length because the parameter correlates to the inductive negative charge in the complexes.

There is increase in the inductive negative charge resulting from the increasing chain length of the alkyl group. This fact is underpinned by the successive increase in the DFT-calculated NBO charge on the nitrogen atom of the alkylamine ligand in the complexes. However, the inductive negative charge of the alkylamine ligand has very little or no influence on the platinum centre particularly

115

as the chain length increases from three to five carbon atoms. With the exception of **tPt2**, the DFT-calculated NBO charge of the platinum centres for the remaining complexes is relatively the same. Complex **tPt2** is more electrophilic than the other *trans*-platinum(II) complexes and this is reflected by its greater reactivity compared to the other complexes.

However, the difference in reactivity of the complexes **tPt3**-**tPt5** cannot be ascribed to the electronic effects because there are very small differences in the electronic properties of these complexes. Based on the electronic data from the DFT-calculations the second-order rate constant values for these complexes should have been relatively the same. It is reasonable to conclude that the electronic effect due to the increase in the chain length of the flexible alkylamine ligand bears small influence on the reactivity of the *trans*-platinum(II) complexes with mixed amine ligands [37, 40, 41]. However, the increasing chain length of the flexible alkylamine ligand creates steric interruption at the reaction sites resulting in the observed difference in the reactivity between the three other complexes **tPt3**, **tPt4** and **tPt5**. The tendency for steric interference at the platinum centre increases as the chain length increases from three to five carbon atoms thereby causing a notable decrease in the substitution of the chloride ligands by the thiourea nucleophiles. The chain length in the complexes only blocks the approach of the entering nucleophiles to the substitution site, i.e. the platinum centre [25, 40, 41].

The reactivity of the nucleophiles follows the trend: TU > MTU > DMTU for all the *trans*-platinum(II) complexes and this is consistent with the order of increasing steric hindrance due to the sizes of these nucleophiles. All available activation parameters, $\Delta H^{\#}$ and $\Delta S^{\#}$ presented in **Table 4.2** support the operation of an associative mechanism [3, 4, 42, 43]. In general, the substitution of reactions of square-planar platinum(II) complexes regardless of their stereochemistry proceed according to an associative mechanism [28, 44-50]. The remarkably negative values of entropy of activation and moderately positive values of enthalpy of activation presuppose that the activation process in the investigated *trans*-platinum(II) complexes are profoundly dominated by bond making [31, 32, 44, 51,].

116

4.7   Conclusion

This study has demonstrated the kinetic behaviour and mechanistic data for the substitution reactions of mononuclear *trans*-platinum(II) complexes with asymmetric(mixed) amine ligands. The reaction of these complexes proceeds via a single step. The overall reaction pattern was largely dominated by steric effects. An increase in chain length of the alkylamine group by the addition of the methylene unit has veritably no significant influence on the electronic properties of these complexes. Besides **tPt2** whose substitution reaction was driven by the electronic factor, the rest of the *trans*-platinum(II) complexes, **tPt3**, **tPt4** and **tPt5** were nearly the same electronically and hence, the notable difference in their reactivity was largely due to the tendency of the increasing carbon chain length of the alkylamine group in the complexes that interferes with the reaction site thereby shielding the entering nucleophiles from directly attacking the platinum centre for the substitution of the chloride ligands. All the studied complexes followed an associative mode of activation as indicated by the large negative intrinsic entropy values.

References

[1] S. Komeda, H. Yoneyama, M. Uemura, A. Muramatsu, N. Okamoto, H. Konishi, H. Takahashi, A. Takagi, W. Fukuda, T. Imanaka, Inorganic Chemistry, 56 (2017) 802-811.

[2] N. Aztopal, D. Karakas, B. Cevatemre, F. Ari, C. Icsel, M.G. Daidone, E. Ulukaya, Bioorganic & Medicinal Chemistry, 25 (2017) 269-276.

[3] S.V. Nkabinde, G. Kinunda, D. Jaganyi, Inorganica Chimica Acta, 466 (2017) 298-307.

[4] W.P. Asman, D. Jaganyi, International Journal of Chemical Kinetics, (2017).

[5] M.M. Milutinović, S.K. Elmroth, G. Davidović, A. Rilak, O.R. Klisurić, I. Bratsos, Ž.D. Bugarčić, Dalton Transactions, 46 (2017) 2360-2369.

[6] T.C. Johnstone, K. Suntharalingam, S.J. Lippard, Chemical Reviews, 116 (2016) 3436-3486.

[7] J.J. Wilson, S.J. Lippard, Chemical Reviews, 114 (2013) 4470-4495.

[8] E.Y. Chua, G.E. Davey, C.F. Chin, P. Dröge, W.H. Ang, C.A. Davey, Nucleic Acids Research, 43 (2015) 5284-5296.

[9] Z. Du, Q. Luo, L. Yang, T. Bing, X. Li, W. Guo, K. Wu, Y. Zhao, S. Xiong, D. Shangguan, Journal of the American Chemical Society, 136 (2014) 2948-2951.

[10] J.M. Herrera, F. Mendes, S. Gama, I. Santos, C. Navarro Ranninger, S. Cabrera, A.N.G. Quiroga, Inorganic Chemistry, 53 (2014) 12627-12634.

[11] F. Navas, F. Mendes, I. Santos, C. Navarro-Ranninger, S. Cabrera, A.n.G. Quiroga, Inorganic Chemistry, (2017).

[12] K. Ossipov, Y.Y. Scaffidi-Domianello, I.F. Seregina, M. Galanski, B.K. Keppler, A.R. Timerbaev, M.A. Bolshov, Journal of Inorganic Biochemistry, 137 (2014) 40-45.

[13] N. Muhammad, Z. Guo, Current Opinion in Chemical Biology, 19 (2014) 144-153.

[14] A. Quiroga, Journal of Inorganic Biochemistry, 114 (2012) 106-112.

[15] E.I. Montero, S. Díaz, A.M. González-Vadillo, J.M. Pérez, C. Alonso, C. Navarro-Ranninger, Journal of Medicinal Chemistry, 42 (1999) 4264-4268.

[16] J.M. Pérez, M.A. Fuertes, C. Alonso, C. Navarro-Ranninger, Critical Reviews in Oncology/Hematology, 35 (2000) 109-120.

[17] H. Song, W. Li, R. Qi, L. Yan, X. Jing, M. Zheng, H. Xiao, Chemical Communications, 51 (2015) 11493-11495.

[18] V. Brabec, O. Vrana, O. Novakova, J. Kasparkova, Chemical Communications, 52 (2016) 4096-4098.

[19] A. Hofmann, L. Dahlenburg, R. van Eldik, Inorganic Chemistry, 42 (2003) 6528-6538.

[20] A.K. Connors, Chemical Kinetics of the Reaction Rates in Solution, Wiley-VCH, New York, (1990) 2-20.

[21] E. Seifert. OriginPro 9.1: Scientific Data Analysis and Graphing Software®- Software Review. Journal of Chemical Information and Modeling, 54(5) (2014) 1552.

[22] A.D. Becke, The Journal of Chemical Physics, 96 (1992) 2155-2160.

[23] P.J. Hay, W.R. Wadt, The Journal of Chemical Physics, 82 (1985) 299-310.

[24] T.A. Hilder, J.M. Hill, Nanotechnology, 18 (2007) 275704.

[25] G. Kinunda, D. Jaganyi, Transition Metal Chemistry, 41 (2016) 235-248.

[26] T.R. Papo, D. Jaganyi, Transition Metal Chemistry, 40 (2015) 53-60.

[27] A. Shaira, D. Jaganyi, Journal of Coordination Chemistry, 68 (2015) 3013-3031.

[28] I.M. Wekesa, D. Jaganyi, Journal of Coordination Chemistry, 69 (2016) 389-403.

[29] V. Barone, M. Cossi, The Journal of Physical Chemistry A, 102 (1998) 1995-2001.

[30] M. Cossi, N. Rega, G. Scalmani, V. Barone, Journal of Computational Chemistry, 24 (2003) 669-681.

[31] Ž.D. Bugarčić, S.T. Nandibewoor, M.S. Hamza, F. Heinemann, R. van Eldik, Dalton Transactions, (2006) 2984-2990.

[32] H. Ertürk, R. Puchta, R. van Eldik, European Journal of Inorganic Chemistry, 29 (2009) 1331-1338.

[33] A. Fazlur-Rahman, J. Verkade, Inorganic Chemistry, 31 (1992) 2064-2069.

[34] J.R. Priqueler, I.S. Butler, F.D. Rochon, Applied Spectroscopy Reviews, 41 (2006) 185-226.

[35] T.G. Appleton, J.W. Connor, J.R. Hall, P.D. Prenzler, Inorganic Chemistry, 28 (1989) 2030-2037.

[36] R.E. Norman, J.D. Ranford, P.J. Sadler, Inorganic Chemistry, 31 (1992) 877-888.

[37] P.O. Ongoma, D. Jaganyi, Transition Metal Chemistry, 39 (2014) 407-420.

[38] J.A. Todd, D. Caiazza, E.R. Tiekink, L.M. Rendina, Inorganica Chimica Acta, 352 (2003) 208-212.

[39] P. Atkins, J. de Paula, Elements of Physical Chemistry, 5th ed., Oxford University Press, Great Britain, (2009) 1-30.

[40] A. Mambanda, D. Jaganyi, Dalton Transactions, 40 (2011) 79-91.

[41] A. Mambanda, D. Jaganyi, S. Hochreuther, R. van Eldik, Dalton Transactions, 39 (2010) 3595-3608.

[42] P.W. Asman, Journal of Coordination Chemistry, (2017) 1-20.

[43] P.W. Asman, Inorganica Chimica Acta, 469 (2018) 341-352.

[44] D. Jaganyi, A. Hofmann, R. van Eldik, Angewandte Chemie International Edition, 40 (2001) 1680-1683.

[45] D. Jaganyi, D. Reddy, J. Gertenbach, A. Hofmann, R. van Eldik, Dalton Transactions, (2004) 299-304.

[46] D. Jaganyi, F. Tiba, O.Q. Munro, B. Petrović, Ž.D. Bugarčić, Dalton Transactions, (2006) 2943-2949.

[47] P. Ongoma, D. Jaganyi, Dalton Transactions, 41 (2012) 10724-10730.

[48] D. Reddy, D. Jaganyi, Dalton Transactions, (2008) 6724-6731.

[49] P.A. Wangoli, G.B. Kinunda, New Journal of Chemistry, (2017).

[50] I.M. Wekesa, Dalton Transactions, (2014) 2549-2558 .

[51] S. Hochreuther, S.T. Nandibewoor, R. Puchta, R. van Eldik, Dalton Transactions, 41 (2012) 512-522.

[52] A. Hofmann, D. Jaganyi, O.Q. Munro, G. Liehr, R. van Eldik, Inorganic Chemistry, 42 (2003) 1688-1700.

Chapter Five

An Investigation of Comparative Substitution Behaviour of Bifunctional *trans*-Platinum(II) Complexes with Symmetric and Asymmetric Alkylamine Ligands

Abstract

This study was undertaken to investigate the comparative substitution behaviour of mononuclear *trans*-platinum(II) complexes with symmetric and asymmetric amine ligands. The rate of substitution of the aqua moeities from the complexes *trans*-[Pt(NH$_3$)$_2$(H$_2$O)$_2$](ClO$_4$)$_2$ (**tPt**), *trans*-[Pt(NH$_3$)(NH$_2$C$_2$H$_5$)(H$_2$O)$_2$](ClO$_4$)$_2$, (**tPt2H$_2$O**), *trans*-[Pt(NH$_3$)(NH$_2$C$_3$H$_7$)(H$_2$O)$_2$](ClO$_4$)$_2$, (**tPt3H$_2$O**), [*trans*-Pt(OH$_2$)$_2$(NH$_2$CH$_3$)$_2$](ClO$_4$)$_2$ (**tPtM**) and [*trans*-Pt(OH$_2$)$_2${NH$_2$CH(CH$_3$)$_2$}$_2$](ClO$_4$)$_2$ (**tPtR**), by three nucleophiles, viz. thiourea (TU), 1,3-dimethylthiourea (DMTU) and 1,1,3,3-tetramethylthiourea (TMTU) was studied under *pseudo* first-order conditions as a function of concentration and temperature by stopped-flow spectrophotometry. All the substitution reactions of each of the *trans*-platinum(II) complexes proceeds by first-order kinetics in a single step. The *pseudo* first-order rate constants, k_{obs} obeyed the rate law: $k_{obss} = k_2$[nucleophile]. The reactivity of the complexes was essentially governed by both steric and electronic factors. Comparing the second-order rate constants for the substitution reactions of the mononuclear diaqua *trans*-platinum(II) complexes with the thiourea-based nucleophiles, the observed trend follows: **tPt** > **tPt2H$_2$O** > **tPtM** > **tPt3H$_2$O** > **tPtR.** This reactivity trend is consistent with the pK_a values obtained for the first deprotonation step. The reactivity of the nucleophiles with the complexes decreases with an increase in steric demand in the following order: TU > DMTU > TMTU. The low positive values of enthalpy of activation and large negative values of entropy of activation indicate an associative mechanism of substitution in all the complexes. The computational modelling using density functional theory (DFT) calculations was employed to provide theoretical interpretation of kinetic data.

5.1 Introduction

The development of new platinum-based anticancer agents that can circumvent some of the drawbacks, such as high toxicity in cancer patients [1-8], and can show improved activity towards cisplatin resistant cell lines, has been exhaustively focused on compounds with *cis* geometry [9]. This is largely because transplatin, the *trans*-isomer of cisplatin, is inactive. Research efforts to understand the dearth of the activity of transplatin reported two major findings [10-13]. Firstly, kinetic instability which bring about prompt deactivation of the complex and secondly, the formation of DNA adducts characterised by a regioselectivity and a stereochemistry that are radically different from those of cisplatin. These findings initially led to the general assumption among researchers that the presence of two leaving groups in *cis* positions is prerequisite for antitumour activity of platinum complexes and hence, most compounds reported were based on that structure-activity relationship [12-14]. Despite a large number of these *cis*-configured compounds reported every year, only a handful of them has made it to clinical trials [15, 16]. Moreover, even the clinical application of the successful ones has been compromised by flaws that are associated with cisplatin [17]. The urgent need to develop platinum-based complexes that can form DNA adducts that are qualitatively and quantitatively different from those already established for cisplatin and its analogues strongly supports the hypothesis that an active *trans*-platinum complex may have a different spectrum of activity. An attempt to develop *trans*-platinum with cytotoxic activity led Farrell *et al.* [13, 18] to incorporate bulky amine ligands, such as aromatic N-donor and other heterocycles, into the structure of transplatin. The resulting series of *trans*-platinum(II) complexes not only showed phenomenal cytotoxicity better than cisplatin against certain cancer cell lines but also exhibited superior activity against cisplatin-resistant cell lines [9].

Following the success of Farrell and his group, several other *trans*-platinum complexes with different aromatic, alicyclic and aliphatic bulky ligands have been synthesised [9], many of which have shown profound cytotoxicity even against cisplatin resistant cell lines. Navarro-Ranninger *et al.* [19] reported some *trans*-platinum(II) complexes with bulky asymmetrical aliphatic amine ligands. These complexes were found to have comparable activity in cisplatin sensitive cells to that of cisplatin and significantly higher than that of cisplatin in several cisplatin resistant cancer cell lines. In a related study, Quiroga *et al.* [20] reported the reactivity and biological properties of a series of isomeric *cis*- and *trans*-platinum(II) complexes with symmetrical aliphatic amine and iodide ligands as the leaving groups. Although both sets of complexes were found to be cytotoxic, however, the *trans* isomers were observed to be

generally more effective than their *cis* counterparts when tested against a panel of human tumour cell lines.

In general, the improved cytotoxic activity of the *trans*-platinum(II) complexes with sterically demanding ligands has been attributed to the reduction in the rate of displacement of leaving groups which, in most cases, are chloride ligands [9, 13, 21]. In *chapter three*, we reported the kinetic data and mechanisms of substitution of a series of isomeric *cis*- and *trans*-platinum(II) complexes with symmetrical dialkylamine and aqua leaving groups. These complexes are akin to those reported by Quiroga *et al.* [20]. Our findings, among other things, revealed that while all the investigated *trans*-platinum(II) complexes displayed similarity in their ligand substitution pattern and in their mechanisms, their rate of ligand substitution, however, decreases with an increase in a sterically demanding dialkylamine group (see *Chapter Three*).

Furthermore, in *chapter four*, we reported the substitution behaviour of some mononuclear *trans*-platinum(II) complexes with mixed or asymmetrical amine ligands. In an effort to gain an in-depth understanding of the substitution behaviour of these mononuclear *trans*-platinum(II) complexes, it is imperative to explore a comparative study of the substitution behaviour of some bifunctional mononuclear *trans*-platinum(II) complexes with symmetrical and asymmetrical alkylamine ligands. To this end, we will be investigating the substitution of diaqua moieties from some *trans*-platinum(II) complexes with alkylamine and dialkylamine ligands respectively in reference to aquated transplatin (**Figure 5.1**).
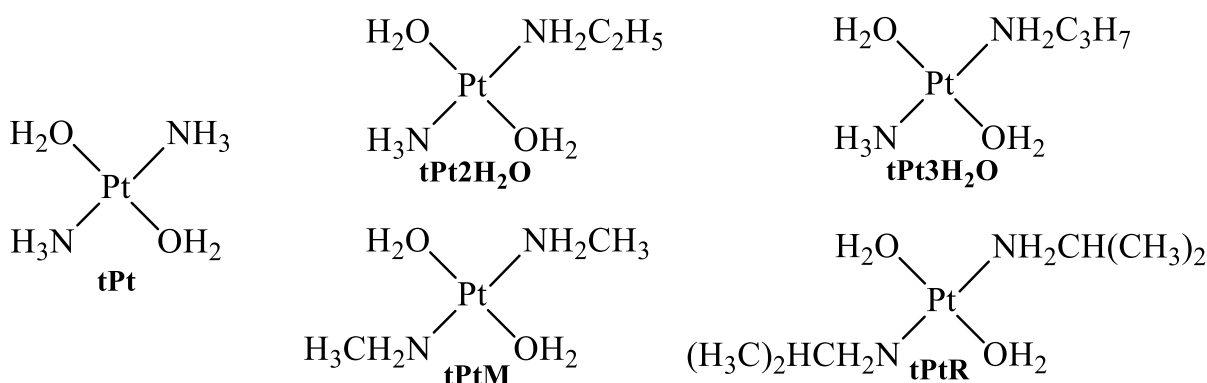
Figure 5.1: Structures and abbreviations of the investigated complexes. The charges and counterions of the complexes have been omitted for clarity.

123

5.2 Experimental

5.2.1 Chemicals and Reagents

Methylamine hydrochloride, isopropylamine (99.5%), ethylamine solution (70%), propylamine (99%), K_2PtCl_4 (98%), cis-[Pt(NH_3)_2Cl_2] (99.9%), trans-[Pt(NH_3)_2Cl_2] , KOH, AgClO_4 (97%), NaClO_4.H_2O (98%), HCl (32%) and HClO_4 (70%) were purchased from Sigma Aldrich and were used without further purification. The nucleophiles: thiourea (TU, 99%)), 1,3-dimethyl-2-thiourea (DMTU, 99%) and 1,1,3,3-tetramethyl-2-thiourea (TMTU, 98%) used for the kinetic determinations were obtained from Aldrich. All preparations of aqueous solutions were done using ultra-pure water.

5.2.2 General Synthetic Procedure of the Mixed *trans*-Platinum(II) Complexes

The general synthetic procedure of the mixed *trans*-platinum(II) complexes has been reported by Wilson and Lippard [13]. Cisplatin (100 mg, 0.333 mmol) was suspended in water (2 mL) and 8 equivalents of appropriate alkylamine ligand was added. The resulting mixture was heated at 90 °C until the solution became colourless. After the solution was cooled to room temperature, it was treated with 32% (v/v) concentrated HCl (2.5 mL) followed by stirring and heating at 90 °C for 48 hours. The resulting yellow solution was placed in an iced bath to induce precipitation of the appropriate *trans*-platinum(II) complex which was recovered by filtration, washed intensively with water, diethyl ether and air dried at room temperature.

tPt2H₂O yield: 49 mg (45%). ^{1}H NMR (500 MHz, DMF-d$_7$), δ(ppm): 1.26 (t, 3H); 2.73 (sextet 2H); 3.72 (s, 3H), 4.38 (s, 2H). ^{195}Pt NMR (107 MHz, DMF-d$_7$), δ(ppm): -2164. TOF MS/ES$^+$, *m/z:* (M − Cl + Na.)$^+$: 315 ($C_2H_{12}N_2PtCl$, species). Anal. Cal for $C_2H_{10}N_2PtCl_2$: N, 8.54; C, 7.32; H, 3.07. Found: N, 8.50; C, 7.00; H, 2.86.

tPt3H₂O yield: 91 mg (80%). ^{1}H NMR (500 MHz, DMF-d$_7$), δ(ppm): 0.93 (t, 3H); 1.77 (sextet, 2H); 2.65 (quintet, 2H), 3.74 (s, 3H), 4.36 (s, 2H). ^{195}Pt NMR (107 MHz, DMF-d$_7$), δ(ppm): -2163. TOF MS/ES$^+$, *m/z:* (M$^+$): 340 ($C_3H_{10}N_2PtCl_2$, species). Anal. Cal for $C_3H_{12}N_2PtCl_2$: N, 8.19; C, 10.53; H, 3.54. Found: N, 8.12; C, 10.50; H, 3.27.

5.2.2.1 Synthesis of *trans*-[Pt(ma)₂Cl₂] (tPtM)

trans-[Pt(ma)_2Cl_2] was obtained following the synthetic procedure outlined by Messori *et al.* [20] with a few modifications. The iodo derivative of *cis*-[Pt(ma)_2Cl_2] was first

prepared by slowly adding four equivalents of methylamine hydrochloride (4.8 mmol) to the dark brown solution of K_2PtI_4. The mixture was subsequently treated with four equivalents of KOH (269 mg, 4.8 mmol) in the dark at room temperature. After the addition was completed, the reaction mixture was stirred in the dark at room temperature for five hours to yield a yellow precipitate, *cis*-[Pt(ma)$_2$I$_2$]. The precipitate was obtained by filtration, washed thoroughly with warm water and diethyl ether, and air dried.

Subsequently, a suspension of *cis*-[Pt(ma)$_2$I$_2$] (220 mg, 0.432 mmol) in water was treated with 5 equivalents of methylamine hydrochloride (2.16 mmol). The resulting mixture was stirred at room temperature for 12 hours to give a colourless solution. The resulting solution was concentrated at 70 °C until a bright orange precipitate was detected and then left to stand overnight at 4 °C. The orange solid, *trans*-[Pt(ma)$_2$I$_2$] was filtered, washed with warm water and air dried.

trans-[Pt(ma)$_2$I$_2$] (177 mg, 0.346 mmol) was suspended in 10 mL of water and treated with 1.9 equivalents AgClO$_4$. The mixture was stirred overnight in the dark. AgI was removed by filtration through a 0.45 µm nylon membrane and to the filtrate, four equivalents of KCl was added and stirred at 40 °C for six hours to give a yellow solution of *trans*-[Pt(ma)$_2$Cl$_2$]. The solution was left to stand overnight at 4 °C. The product was filtered, washed thoroughly with warm water and air dried.

***trans*-[Pt(ma)$_2$Cl$_2$] (tPtM)** yield: 12.8 mg (9%). ^{1}H NMR (500 MHz, DMSO-d$_6$), δ(ppm): 2.14 (t, 6H); 4.25 (s, 4H). ^{195}Pt NMR (107 MHz, DMSO-d$_6$), δ(ppm): -2195. TOF MS/ES$^+$, *m/z:* (M + Na)$^+$: 350.96 (C$_2$H$_{10}$N$_2$NaPtCl$_2$, species). Anal. Calc. for C$_2$H$_{10}$N$_2$PtCl$_2$: N, 8.54; C, 7.32; H, 3.07. Found: N, 8.61; C, 6.97; H, 2.60.

5.2.2.2   Synthesis of *trans*-[Pt(ipram)$_2$Cl$_2$] (tPtR)

trans-[Pt(ipram)$_2$Cl$_2$] was synthesised following the method reported by Navarro-Ranninger *et al.* [19]. To a suspension of *cis*-[Pt(ipram)$_2$Cl$_2$ (200 mg, 0.521 mmol), 4 equivalents of isopropylamine was added. The resulting mixture was heated at 70 °C and stirred until a colourless solution was obtained which was then heated at reflux for 30 minutes. The solution was left to cool to room temperature and concentrated HCl (0.364 mL) acid was added and subsequently heated at reflux for 8 hours. The yellow solution obtained was cooled in an ice bath and left to stand at 4 °C overnight. The product was obtained by filtration and was thoroughly washed with water and dried in air.

trans-[Pt(ipram)₂Cl₂] (tPtR) yield: 80 mg (40%). ^1H NMR (500 MHz, DMSO-d₆), δ(ppm): 1.18 (d, 12H); 3.02 (sept., 2H); 4.20 (s, 4H). ^{195}Pt NMR (107 MHz, DMSO-d₆), δ(ppm): -2205. TOF MS/ES⁺, *m/z:* (M + Na)⁺: 407 ($C_6H_{18}N_2PtCl_2$, species). Anal. Calc. for $C_6H_{18}N_2PtCl_2$: N, 7.29; C, 18.76; H, 4.72. Found: N, 7.53; C, 18.51; H, 4.36.

5.3 Instrumentation and Physical Measurements

^1H, ^{13}C and ^{195}Pt NMR spectroscopic analyses were carried out on a Bruker Avance III 500MHz. All ^1H and ^{13}C NMR chemical shifts were referenced to $Si(CH_3)_4$ while ^{195}Pt NMR chemical shifts were externally referenced to $K_2[PtCl_6]$. A Waters Micro-mass LCT Premier spectrometer was employed for mass determination of the complexes. Elemental analyses of synthesised complexes were recorded on a Thermo Scientific Flash 2000. The pH of aqueous solutions of the complexes was recorded using a Jenway 4330 Conductivity/pH meter fitted with a Micro 4.5 diameter glass electrode which was calibrated at 25 °C using buffer solutions of pH 4.0, 7.0 and 10.0 purchased from Merck. A Varian Cary 100 Bio UV/Visible spectrophotometer thermostated by a Varian Peltier temperature controller was used to obtain the UV/Visible absorption spectra for the determination of pK_a values and kinetic studies of slow reactions. Kinetic measurements of all reactions were monitored on an Applied Photophysics SX.20 stopped-flow analyser coupled to an online data acquisition system. The temperature of the instrument was kept within ±0.05 °C for all the measurements. Analyses of the pH and time-dependent kinetic spectral data were performed using Origin 9.1 [22].

5.4 Preparation of Platinum(II) Aqua Complexes and Determination of their pK_a Values

The aqueous solutions of the complexes **tPt**, **tPt2H₂O**, **tPt3H₂O**, **tPtM**, and **tPtR** were prepared following the literature procedure by adding a suitable amount of $AgClO_4$ to each of the corresponding chloride complexes at a molar ratio of 1: 1.98 [23, 24]. Both the chloride complex and the $AgClO_4$ were dissolved in 0.01M $HClO_4$ and the mixture was vigorously stirred in the dark at 45 °C for 24 hours. The AgCl precipitate obtained was filtered off through a 0.45µm nylon membrane. The filtrate was diluted to 300 mL with 0.01 M $HClO_4$. Spectrophotometric pH titrations were performed using NaOH as a base in the pH range of 1-10 at 25 °C. To avoid absorbance corrections resulting from dilution, a large amount (300 mL)

of the complexes were used for the titrations. Adjustments in pH were made by stepwise additions of crushed NaOH pellets in the pH range 1-3, while a pasteur pipette was used for dropwise additions of NaOH solutions of different concentrations (1.0, 0.5, 0.1 and 0.01 M) or the same concentrations of $HClO_4$ acid (for reversibility of the pH) were added to the solution in the pH range of 4-10 until the desired pH was attained prior to the withdrawal of a 1.0 mL aliquot from the solution for pH measurements and 2 mL aliquots for spectrophotometric monitoring. The 1 mL aliquot after each pH measurement was discarded to avoid in situ contamination of the complex solution by chloride ions leaching from the pH electrode.

5.5   Kinetic Measurements

Substitution of the aqua moieties from each of the five *trans*-platinum(II) complexes with symmetrical and asymmetrical amine ligands respectively (**Figure 5.1**) by three different thiourea nucleophiles: thiourea (TU),   1,3-dimethyl-2-thiourea (DMTU) and 1,1,3,3-tetramethyl-2-thiourea (TMTU) was investigated under *pseudo*-first-order conditions with at least a 20-fold excess of the nucleophile. Spectra changes resulting from the mixing of the complex and the nucleophile solutions were observed over the wavelength range 200-800 nm to establish an appropriate wavelength at which kinetic measurements could be performed on the stopped-flow spectrophotometer. The reactions were initiated by the mixing of equal volumes of a solution of the *trans*-platinum(II) complexes with a solution of the nucleophile directly in the stopped-flow machine. All reported rate constants represent an average value of at least seven independent kinetic runs for each experimental measurement. The temperature dependence of the rate constants was observed over a range of 20-40 °C at an interval of 5 °C.

5.6   Results and Discussion

5.6.1   Theoretical Aspects

Density functional Theoretical (DFT) calculations of the complexes **tPt**, **tPt2H₂O**, **tPt3H₂O, tPtM** and **tPtR** were carried out at the DFT level B3LYP [25] with the LANL2DZ basis set [26] using the Gaussian 09 programme suite. B3LYP relates to the hybrid functional Becke's three-parameter formulation, which has been proven to be superior to conventional functionals. LANL2DZ is a double-zeta basis set containing effective core potential (ECP) representations

of electrons near the nuclei for transition metal complexes [27]. The theoretical calculations of the complexes were executed in water taking into account the effects of the solvent by employing conductor polarisable continuum model (CPCM) formalism [28, 29]. The complexes were optimized in their aqua form as cations of +2 charge, and the singlet states were used because of low electronic spin of platinum(II) complexes. **Table 5.1** shows the extracted data obtained from the DFT calculations.

Table 5.1: An extract from the DFT calculated data for the investigated mononuclear *trans*-platinum(II) complexes at B3LYP/LANL2DZ level of theory.

Parameters	tPt	tPt2H$_2$O	tPt3H$_2$O	tPtM	tPtR
NBO Charge on Pt	0.808	0.783	0.785	0.791	0.758
Gap Energy (eV)					
LUMO	-2.46	-2.42	-2.42	-2.40	-2.39
HOMO	-7.17	-7.12	-7.11	-7.08	-7.04
ΔE	4.71	4.70	4.69	4.68	4.68
μ	4.82	4.77	4.77	4.74	4.72
ω	4.92	4.84	4.84	4.80	4.76
η	2.36	2.35	2.35	2.34	2.34

where μ = electronic chemical potential, ω = electrophilicity index and η = chemical hardness

A closer look at **Table 5.1** reveals a corresponding decrease in the NBO charges on the platinum(II) ions as the amine moieties become bulkier in all the *trans*-platinum(II) complexes with symmetric amine ligands (**tPt**, **tPtM** and **tPtR**). For complexes **tPt2H$_2$O** and **tPt3H$_2$O** with asymmetric amine ligands, the NBO remains relatively the same. However, the gap energies in all the complexes are veritably constant. Although, there is a corresponding increase in the HOMO energy, through inductive electron donation, as the number of carbon atoms on

the amine moieties increases. However, the electron donation from the alkylamine has no significant contribution to the LUMO energy.

Furthermore, on the basis of other DFT descriptors, such as chemical potential (μ), electrophilicity index (ω) and chemical hardness (η), which are sometimes used to predict the reactivity of inorganic and organic compounds [30, 31], one can observe an interesting trend. The electronic chemical potential, which is often described as the negative of electronegativity of a chemical species [32, 33], is obtained using *equation* 5.1. Essentially, it measures the escaping tendency of electrons from an equilibrium system [34-36]. The higher the electronic chemical potential, the more reactive the chemical species. Chemical hardness is defined by *equation* 5.2 and it relates to the stability and reactivity of a chemical compound. Generally, it determines the resistance to change in the electron distribution in a collection of nuclei and electrons [37, 38]. The chemical hardness for all the investigated *trans*-platinum(II) complexes are relatively the same. The electrophilicity index, which is a measure of the electrophilicity (tendency to accept electrons) of the chemical species [39-42], is obtained from *equation* 5.3.

$$\mu = \frac{E_{Homo} + E_{Lumo}}{2} \qquad (5.1)$$

$$\eta = \frac{E_{Homo} - E_{Lumo}}{2} \qquad (5.2)$$

$$\omega = \frac{\mu^2}{2\eta} \qquad (5.3)$$

Expectedly, the chemical potential and electrophilicity index of **tPt** is significantly higher than those of the other complexes, with **tPtR** having the lowest values. For *trans*-platinum(II) complexes with symmetric amine ligands, **tPtM** and **tPtR**, the trend of the theoretical data obtained is supported by the experimental data. However, for the complexes with asymmetric amine ligands, **tPt2H₂O** and **tPt3H₂O**, which have essentially the same electronic descriptor values, the experimental data obtained do not correlate with the theoretical data. Further details are provided in the Kinetic Analysis (vide infra).

5.6.2 *pKₐ* Determination of the Diaqua Complexes

To obtain information on the acidity of the bonded water ligands and the reactivity of all the aqua complexes, their pK_a values were determined. To this end, a spectrophotometric pH

titration with NaOH as a base in the pH range 2–10 was carried out. The pH dependence of the aqua complex was observed by UV/Visible spectrophotometry. The pK_a values of the coordinated aqua ligands were obtained by plotting absorbance at a specific wavelength as a function of pH. The typical spectral changes recorded during the pH titration with NaOH are presented in **Figure 5.2** for the *trans*-aqua complexes **tPt**. The overall process can be presented by **Schemes 5.1 and 5.2**.

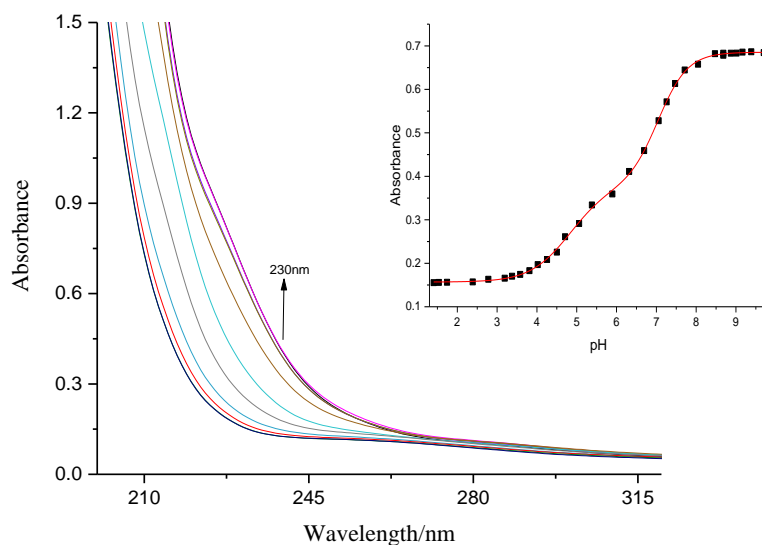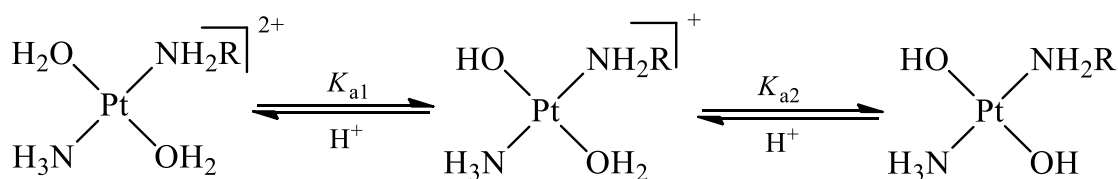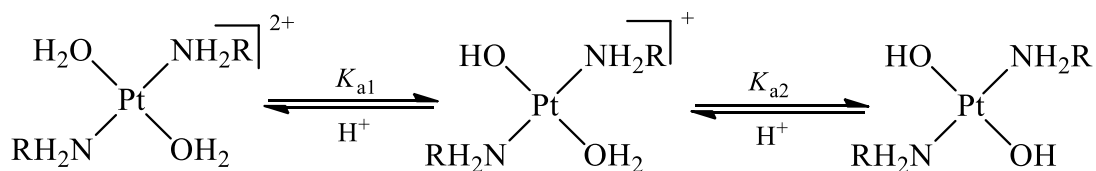**Figure 5.2**:   UV/Visible spectra of the diaqua **tPt** complex recorded as a function of pH in the range 2-10 at 25 °C. Inset: Titration curve at 230 nm.

Scheme 5.1:   Proposed stepwise deprotonation for the pH dependence of the asymmetric *trans*-platinum(II) complexes.

Scheme 5.2:   Proposed stepwise deprotonation for the pH dependence of the symmetric *trans*-platinum(II) complexes.

The spectra data was analysed using the Origin 9.1® [22] to obtain the resulting pK_a values for the diaqua moieties by fitting the data to a double sigmoidal function which gave the best statistical fit and afforded two pK_a values which indicates that there are three coloured species for each of the aqua complexes present in solution as a function of pH. **Table 5.2** is a summary of the data obtained for the deprotonation of the diaaqua moieties from the complexes.

Table 5.2: Summary of pK_a values from the diaqua *trans*-platinum(II) complexes.

	tPt	tPt2H$_2$O	tPt3H$_2$O	tPtM	tPtR
pK_{a1}	4.24 ± 0.05	4.28 ± 0.35	4.80 ± 0.24	4.56 ± 0.06	5.92 ± 0.07
pK_{a2}	6.91 ± 0.04	6.79 ± 0.1	7.74 ± 0.31	7.05 ± 0.03	7.28 ± 0.16

The pK_a values obtained for the deprotonation of the first aqua ligand show that the acidity of the mononuclear *trans*-Pt(II) complexes followed the trend **tPt** (4.24) > **tPt2H$_2$O** (4.28) > **tPtM** (4.56) > **tPt3H$_2$O** (4.80) > **tPtR** (5.92). The acidity of the complexes decreases with increasing number of carbon atoms on the alkylamine and the dialkylamine moieties for the asymmetric and the symmetric *trans*-platinum(II) complexes respectively. Although, one would have expected **tPt2H$_2$O** with an asymmetric amine ligand and **tPtM** with a symmetrical amine ligand, which have the same number of carbon atoms, to display the same level of acidity. However, **tPt2H$_2$O** (pK_a 4.28) is more acidic than **tPtM** (pK_a 4.56). This experimental data contradicts the theoretical DFT calculation data in which the platinum(II) centre in **tPt2H$_2$O** has an NBO charge that is about 0.08 unit less than that of **tPtM.** However, the electrophilicity index (ω) of both complexes agrees with their respective pK_a value. Essentially, the electrophilicity index is superior to the NBO charge in predicting electrophilicity and reactivity of a complex because the NBO charge indicates only the individual atomic charge, whereas the electrophilicity index describes the resulting charge of the entire complex [33, 43]. In general, pK_a values are usually associated with the electrophilicity of the metal centre [44]. Moreover, on the basis of the DFT descriptors, such as NBO charges, electronic chemical potential, chemical hardness and electrophilicity index, one would expect the *trans*-platinum(II) complexes with asymmetric amines, **tPt2H$_2$O** and **tPt3H$_2$O**, to exhibit the same pK_a values. However, the pK_a value of **tPt3H$_2$O** is 0.52 unit higher than that of **tPt3H$_2$O**. This may be due to the steric factor resulting from the flexible alkylamine ligand.

The second deprotonation step for the symmetric *trans*-platinum(II) complexes follows the expected trend as the first with the pK_{a2} value of **tPt** (6.91) being less than those of **tPtM** (7.05)

and **tPtR** (7.28). However, the second pK_a values in the asymmetric *trans*-platinum(II) complexes is quite unexpected on the basis of their DFT obtained electronic descriptors with **tPt2H$_2$O** (pK_{a2} 6.79) being about a unity less than that of **tPt3H$_2$O** (pK_{a2} 7.74). Besides, the usual reduction in the overall charge from +2 to +1 at the platinum site following the first deprotonation step which makes the metal centre to be less electrophilic, this observation can also be attributed to the steric factor resulting from the increase in chain length of the flexible alkylamine. The overall trend for the second deprotonation step follows: **tPt2H$_2$O** (6.79) > **tPt** (6.91) > **tPtM** (7.05) > **tPtR** (7.28) > **tPt3H$_2$O** (7.74). In general, for the first deprotonation step, the acidity of the mononuclear *trans*-platinum(II) complexes decreases with the increasing number of carbon atoms on the amine moieties. Nevertheless, the second deprotonation step did not show any consistent trend.

5.6.3   Kinetic Analysis

The substitution reactions of all the studied mononuclear *trans*-platinum(II) complexes followed a single reaction step. The reaction step in all the *trans*-platinum(II) complexes is dependent on the concentration of the nucleophiles. Kinetic traces for the *trans*-platinum(II) complexes fitted perfectly to a single exponential, typical for one-step reaction. The so-obtained *pseudo*-first-order rate constant, k_{obs} for the *trans*-complexes, computed from the kinetic traces were plotted against the concentration of the entering nucleophiles (**Figure 5.3**). A linear dependence on the nucleophile concentration was observed for all the studied reactions without any intercept. The linear fits pass through the origin which indicates that there is no parallel or reverse reaction. The dependence of the observed *pseudo*-first-order rate constants on the concentration of the entering nucleophile obeyed the rate law presented in *equation* 5.4, where k_2 represent the second-order rate constants for the substitution reactions of the mononuclear *trans*-platinum(II) complexes. **Table 5.3** provides the summary of the second-order rate constants and the activation parameters for all the investigated mononuclear *trans*-platinum(II) complexes.

$$k_{obs} = k_2[\text{nucleophile}] \hspace{3cm} (5.4)$$

Table 5.3:   Second-order rate constants and activation parameters for the reaction of the studied diaqua *trans*-platinum(II) complexes with thiourea nucleophiles at pH = 2.0 (0.9 M NaClO4 + 0.01 M HClO4) and 293-313 K.

Complex	Nucleophiles	k_2 /M^{-1}s^{-1}	$\Delta H^{\#}$ kJ/mol	$\Delta S^{\#}$ J/mol/K
tPt	TU	44.2 ± 0.03	63 ± 2	-29 ± 6
	DMTU	22.9 ± 0.11	55 ± 1	-61 ± 4
	TMTU	5.6 ± 0.01	68 ± 2	-27 ± 6
tPt2H₂O	TU	38.5 ± 0.034	56 ± 1	-26 ± 3
	DMTU	19.6 ± 0.025	50 ± 0.9	-52 ± 3
	TMTU	4.1 ± 0.002	54 ± 2	-51 ± 6
tPt3H₂O	TU	28.4 ± 0.02	57 ± 1	-26 ± 3
	DMTU	15.7 ± 0.04	49 ± 1	-55 ± 3
	TMTU	3.0 ± 0.02	57 ± 0.8	-46 ± 3
tPtM	TU	35.4 ± 0.11	58 ± 3	-34 ± 10
	DMTU	18.2 ± 0.02	62 ± 1	-43 ± 3
	TMTU	3.8 ± 0.03	60 ± 2	-64 ± 7
tPtR	TU	19.0 ± 0.0016	58 ± 2	-51 ± 7
	DMTU	10.3 ± 0.0001	54 ± 2	-69 ± 5
	TMTU	2.2 ± 0.0065	57 ± 1	-72 ±3

Comparing the second-order rate constants for the substitution reactions of the mononuclear diaqua *trans*-platinum(II) complexes with the thiourea-based nucleophiles, the observed trend follows: **tPt** > **tPt2H₂O** > **tPtM** > **tPt3H₂O** > **tPtR.** This reactivity trend is consistent with the pK_a values obtained for the first deprotonation step. The high reactivity of **tPt** in relation to the rest of the complexes can be rationalised in terms of both electronic and steric effects. **tPt** is less sterically hindered, a feature which has been attributed not only to its geometry (see *Chapter Three*) but also because of the significantly less sterically demanding ammine ligands around it. Hence, the incoming nucleophiles, most especially the less sterically hindered thiourea (TU), can approach the complex easily for the substitution process.

A closer inspection of the second-order rate constants summarised in **Table 5.3**, reveals that **tPt2H₂O** with the asymmetric amine ligands is slightly more reactive than the **tPtM** with symmetric amine ligands, although they have the same number of carbon atoms in the alkylamine ligand(s). This is in good agreement with the chemical potential and electrophilicity index obtained from the DFT calculations. However, this observed reactivity is not in line with the NBO charges on the platinum(II) centre with **tPtM** having a higher NBO charge than **tPt2H₂O**. In relation to the reactivity of metal complexes, the electrophilicity index is a better electronic descriptor than NBO charge since it measures the overall charge of the complex rather than the charge on a single atom [45, 46]. One factor that can be responsible for the difference in their electrophilicity indices, and subsequently their pK_a values and hence, their reactivity, is the charge separation in both complexes. The charges in **tPtM** are evenly distributed around the metal centre unlike in **tPt2H₂O**. The asymmetric nature of the inert amine ligands around the platinum site in **tPt2H₂O** results in a more electrophilic metal centre as supported by its electrophilicity index and its pK_a value.

In addition, when comparing the reactivity of **tPt3H₂O** and **tPtR,** one would have expected the second-order rate constant of **tPt3H₂O** to be significantly higher than that of **tPtR**, since its pK_{a1} value is about 1.12 units higher than that of **tPtR.** From an electronic factor viewpoint, one would expect the positive inductive donor effect of the diisopropylamine in **tPtR** as well as the electronic chemical potential and the electrophilicity index which are much higher in **tPt3H₂O**, to make the reactivity of **tPtR** to be far less than that of **tPt3H₂O**. It appears there is more steric hindrance in **tPt3H₂O** as compared to **tPtR**. Even though **tPtR** has six carbon atoms which are evenly distributed around the platinum centre, the flexible nature of the alkylamine ligand in **tPt3H₂O** tends to pose more steric hindrance on the substitution site than the relatively rigid dialkylamine ligands in **tPtR** resulting from its branched nature. The flexible nature of the amine ligand in **tPt3H₂O** can interfere with the approach of the incoming nucleophiles from attacking the metal centre and thereby lowering its reactivity, otherwise, the second-rate constant of **tPt3H₂O** should have been in the same range with those of **tPt2H₂O** and **tPtM**.

A similar trend is observed in the reactivity of **tPt2H₂O** and **tPt3H₂O**. Based on their electronic properties, both complexes with asymmetric alkylamine ligands should have shown the same substitution rate towards the thiourea-based nucleophiles. However, the longer chain length of the flexible alkylamine ligand in **tPt3H₂O** creates a steric hindrance by preventing the approaching nucleophiles for easy substitution. In general, the second-order rate constants in all the mononuclear diaqua *trans*-platinum(II) complexes show a noticeable dependence on the

steric bulk of the thiourea-based nucleophiles. It is noted that thiourea, TU, in all the investigated complexes, is more reactive by nearly a factor of 2 than the more sterically hindered dimethylthiourea, DMTU. The most sterically hindered nucleophile, 1,1,3,3-tetramethylthiourea, TMTU reacts significantly slower than the less hindered TU and DMTU in all the studied complexes (**Figure 5.3**).

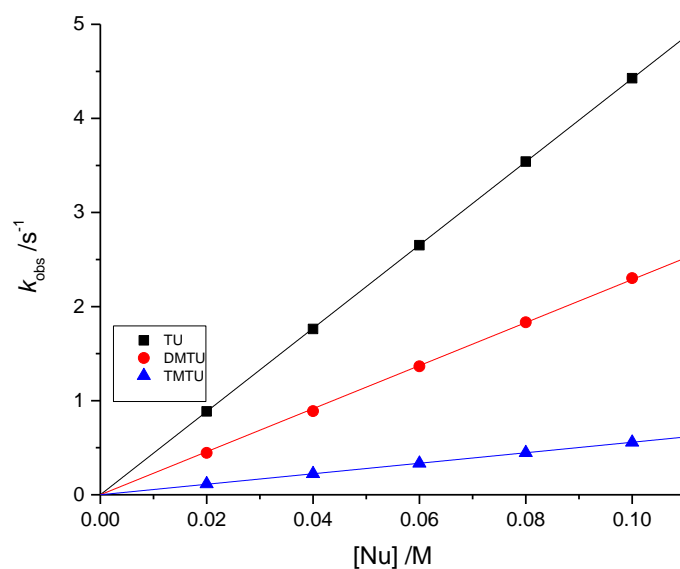**Figure 5.3:**   *Pseudo* first-order rate constants plotted as a function of the concentration of the entering nucleophiles for the substitution reaction of the diaqua **tPt** complex by TU. DMTU, and TMTU at pH = 2.0 (0.09 M NaClO$_4$ + 0.01 M HClO$_4$) and 298 K.
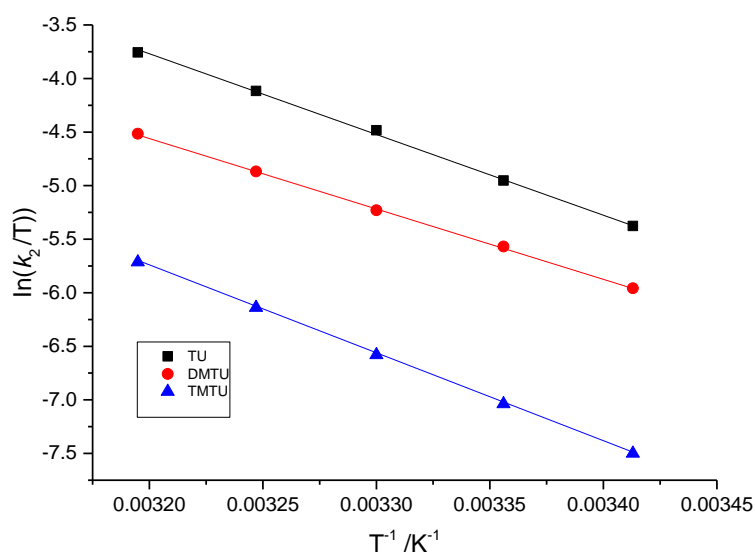
$$ln\left(\frac{k_2}{T}\right) = -\left(\frac{\Delta H^{\#}}{RT}\right) + \left(23.8 + \frac{\Delta S^{\#}}{R}\right) \qquad (5.5)$$

135

Figure 5.4: Plot of $ln(k_2/T)$ against 1/T for the reaction of diaqua **tPt** with the thiourea nucleophiles at various temperatures ranging from 293 to 313 K

Temperature dependence studies were carried out to gain more insight into the nature of the substitution mechanism from the activation parameters. The activation enthalpies, $\Delta H^{\#}$ and entropies, $\Delta S^{\#}$ were determined by measuring the rate constants of substitution at a fixed concentration of the nucleophiles as a function of temperature. The activation parameters were computed using the Eyring plots in *equation* 5.5. **Figure 5.4** shows the Eyring plots for all the three nucleophiles and the results are summarised in **Table 5.3**. A moderately positive activation enthalpy in all the investigated complexes and a negative activation entropy favour an association mechanism which is ubiquitous in most d^8 square planar complexes [47-52].

5.7   Conclusion

In conclusion, this study has explored the comparative substitution behaviour of some mononuclear bifunctional diaqua *trans*-platinum(II) complexes with symmetric and asymmetric alkylamine ligands. The acidity of the complexes was found to decrease with increasing chain length in both the symmetric and asymmetric alkylamine ligand complexes. Diaqua transplatin, **tPt** is observed to be the most acidic and subsequently the most electrophilic, hence, the most reactive. The reactivity of the **tPt** is generally favoured by not only the electronic factors but also by the sterically less hindered inert ammine ligands. Even

136

though, the *trans*-platinum(II) complexes with asymmetric alkylamine ligands, **tPt2H₂O** and **tPt3H₂O**, exhibit similar electronic properties based on data obtained from the theoretical calculations, however, the experimental data contradicts this observation. The observed difference in their pK_a values and in their substitution rates, is attributed to the steric factor. Although, **tPt2H₂O** with asymmetric amine ligands and **tPtM** with symmetric dialkylamine ligands, have the same number of carbon atoms, the difference in their symmetry did not only influence their electronic properties but also their reactivity, with **tPt2H₂O** being slightly more reactive than **tPtM**. The nature of the alkylamine ligands is also observed to influence the reaction rates, with the long flexible chain of the propylamine ligand in **tPt3H₂O** posing more steric hindrance at the reaction site than the branched diisopropylamine in **tPtR**. All the *trans*-platinum(II) complexes show similar substitution patterns and the overall reaction rates are driven by both electronic and steric factors. The proposed reaction scheme is the same for all the three thiourea-based nucleophiles employed in this study. However, the rate constants obtained are different as anticipated. The rate constants decrease in the order TU > DMTU > TMTU, which can be accounted for by the increase in steric hindrance. An associative mode of activation of substitution was observed for the reactions of all the *trans*-platinum(II) complexes with all the nucleophiles owing to the intrinsic negative entropies obtained.

References

[1] A. Ahmad, A. Mitrofanova, S. Ansari, J. Shi, Y. Yang, S. Merscher, A. Fornoni, Y. Zeidan, B. Marples, American Association Cancer Research, (2018) 1-50.

[2] K.H. Bae, S. Tan, A. Yamashita, W.X. Ang, S.J. Gao, S. Wang, J.E. Chung, M. Kurisawa, Biomaterials, 148 (2017) 41-53.

[3] M. Chovanec, M. Abu Zaid, N. Hanna, N. El-Kouri, L. Einhorn, C. Albany, Annals of Oncology, 28 (2017) 2670-2679.

[4] P.P. Dakup, K.I. Porter, A.A. Little, R.P. Gajula, H. Zhang, E. Skornyakov, M.G. Kemp, H.P. Van Dongen, S. Gaddameedhi, Oncotarget, 9 (2018) 14524.

[5] C. Fung, P. Dinh, S. Ardeshir-Rouhani-Fard, K. Schaffer, S.D. Fossa, L.B. Travis, Advances in Urology, (2018) 867-892.

[6] B. Oronsky, T.R. Reid, C. Larson, C.A. Carter, C.E. Brzezniak, A. Oronsky, P. Cabrales, Journal of Cancer Research and Clinical Oncology, 143 (2017) 1671-1677.

[7] S. Spreckelmeyer, N. Estrada-Ortiz, G.G. Prins, M. Van Der Zee, B. Gammelgaard, S. Stürup, I.A. De Graaf, G.M. Groothuis, A. Casini, Metallomics, 9 (2017) 1786-1795.

[8] F.-Y. Wang, X.-M. Tang, X. Wang, K.-B. Huang, H.-W. Feng, Z.-F. Chen, Y.-N. Liu, H. Liang, European Journal of Medicinal Chemistry, (2018) 1.

[9] M. Coluccia, G. Natile, Anti-Cancer Agents in Medicinal Chemistry (Formerly Current Medicinal Chemistry-Anti-Cancer Agents), 7 (2007) 111-123.

[10] V. Brabec, O. Vrana, O. Novakova, J. Kasparkova, Chemical Communications, 52 (2016) 4096-4098.

[11] W.B. Dirersa, International Journal of Chemical and Pharmaceutical Analysis, 2 (2014) 40-47.

[12] A. Quiroga, Journal of Inorganic Biochemistry, 114 (2012) 106-112.

[13] J.J. Wilson, S.J. Lippard, Chemical Reviews, 114 (2013) 4470-4495.

[14] K. Ossipov, Y.Y. Scaffidi-Domianello, I.F. Seregina, M. Galanski, B.K. Keppler, A.R. Timerbaev, M.A. Bolshov, Journal of Inorganic Biochemistry, 137 (2014) 40-45.

[15] N. Aztopal, D. Karakas, B. Cevatemre, F. Ari, C. Icsel, M.G. Daidone, E. Ulukaya, Bioorganic & Medicinal Chemistry, 25 (2017) 269-276.

[16] P.O. Ongoma, D. Jaganyi, Transition Metal Chemistry, 39 (2014) 407-420.

[17] J.P. Parker, Z. Ude, C.J. Marmion, Metallomics, 8 (2016) 43-60.

[18] N. Farrell, Journal of Medicinal Chemistry, 32 (1989) 2240-2241.

[19] E.I. Montero, S. Díaz, A.M. González-Vadillo, J.M. Pérez, C. Alonso, C. Navarro-Ranninger, Journal of Medicinal Chemistry, 42 (1999) 4264-4268.

[20] L. Messori, L. Cubo, C. Gabbiani, A. Álvarez-Valdés, E. Michelucci, G. Pieraccini, C. Ríos-Luci, L.G. León, J.M. Padrón, C. Navarro-Ranninger, A. Casini, A.G. Quiroga, Inorganic Chemistry, 51 (2012) 1717-1726.

[21] T.C. Johnstone, K. Suntharalingam, S.J. Lippard, Chemical Reviews, 116 (2016) 3436-3486.

[22] E. Seifert. OriginPro 9.1: Scientific Data Analysis and Graphing Software®- Software Review. Journal of Chemical Information and Modeling, 54(5) (2014) 1552.

[23] W.P. Asman, D. Jaganyi, International Journal of Chemical Kinetics, (2017).

[24] P.O. Ongoma, D. Jaganyi, Dalton Transactions, 42 (2013) 2724-2734.

[25] A.D. Becke, The Journal of Chemical Physics, 96 (1992) 2155-2160.

[26] P.J. Hay, W.R. Wadt, The Journal of Chemical Physics, 82 (1985) 299-310.

[27] T.A. Hilder, J.M. Hill, Nanotechnology, 18 (2007) 275704-275761.

[28] V. Barone, M. Cossi, The Journal of Physical Chemistry A, 102 (1998) 1995-2001.

[29] M. Cossi, N. Rega, G. Scalmani, V. Barone, Journal of Computational Chemistry, 24 (2003) 669-681.

[30] L.J. Bartolotti, P.W. Ayers, The Journal of Physical Chemistry A, 109 (2005) 1146-1151.

[31] P. Geerlings, F. De Proft, W. Langenaeker, Chemical Reviews, 103 (2003) 1793-1874.

[32] R. Shankar, K. Senthilkumar, P. Kolandaivel, International Journal of Quantum Chemistry, 109 (2009) 764-771.

[33] N. Sheela, S. Muthu, S. Sampathkrishnan, Spectrochimica Acta Part A: Molecular and Biomolecular Spectroscopy, 120 (2014) 237-251.

[34] M. Franco-Pérez, P.W. Ayers, J.L. Gázquez, A. Vela, Physical Chemistry Chemical Physics, 19 (2017) 13687-13695.

[35] C.A. Gonzalez, E. Squitieri, H.J. Franco, L.C. Rincon, The Journal of Physical Chemistry A, 121 (2017) 648-660.

[36] J. Lee, K. Haule, Physical Review B, 95 (2017) 155104-155134.

[37] R.D. Vargas-Sánchez, A.M. Mendoza-Wilson, R.R. Balandrán-Quintana, G.R. Torrescano-Urrutia, A. Sánchez-Escalante, Computational and Theoretical Chemistry, 1058 (2015) 21-27.

[38] F. Mendizabal, D. Donoso, R. Salazar, J. Chil. Chem. Soc., 58 (2013) 1562-1570.

[39] A.R. Jupp, T.C. Johnstone, D.W. Stephan, Dalton Transactions, 47 (2018) 7029-7035.

[40] I.B. Obot, S. Kaya, C. Kaya, Conceptual Density Functional Theory and Its Application to Corrosion Inhibition Studies, in: Conceptual Density Functional Theory and Its Application in the Chemical Domain, Apple Academic Press, (2018) 213-234.

[41] D. Paul, J. Deb, B. Bhattacharya, U. Sarkar, International Journal of Nanoscience, 17 (2018) 1760026-1760087.

[42] N. Santschi, T. Nauser, ChemPhysChem, 18 (2017) 2973-2976.

[43] I.M. Wekesa, D. Jaganyi, Dalton Transactions, 43 (2014) 2549-2558.

[44] A. Hofmann, D. Jaganyi, O.Q. Munro, G. Liehr, R. van Eldik, Inorganic Chemistry, 42 (2003) 1688-1700.

[45] R.A. Costa, P.O. Pitt, M.L.B. Pinheiro, K.M. Oliveira, K.S. Salomé, A. Barison, E.V. Costa, Spectrochimica Acta Part A: Molecular and Biomolecular Spectroscopy, 174 (2017) 94-104.

[46] J.O. Juárez-Sánchez, D.H. Galván, A. Posada-Amarillas, Computational and Theoretical Chemistry, 1103 (2017) 71-82.

[47] W.P. Asman, D. Jaganyi, International Journal of Chemical Kinetics, 49 (2017) 545-561.

[48] P. Atkins, J. De Paula, J. Keeler, Atkins' physical Chemistry, Oxford University Press, (2018) 1-26.

[49] S. Hochreuther, R. Puchta, R. van Eldik, Inorganic Chemistry, 50 (2011) 8984-8996.

[50] A. Mambanda, D. Jaganyi, Advances in Inorganic Chemistry, Elsevier, (2017) 243-276.

[51] T. Soldatović, S. Jovanović, Ž.D. Bugarčić, R. van Eldik, Dalton Transactions, 41 (2012) 876-884.

[52] P.A. Wangoli, G. Kinunda, New Journal of Chemistry, 42 (2018) 214-227.

Chapter Six

Understanding the Role of Flexible Alkyl-α,ω-diamine Linkers on the Substitution Behaviour of Dinuclear *trans*-Platinum(II) Complexes: A Kinetic and Mechanistic Study

Abstract

In this study, we investigated the role of flexible alkyl-α,ω-diamine linkers on the substitution behaviour of dinuclear *trans*-platinum(II) complexes. The substitution reactions of four dinuclear *trans*-platinum(II) complexes viz. $[PtNH_3Cl_2]_2$-μ-$NH_2(CH_2)_2NH_2]$ (**P12**), $[PtNH_3Cl_2]_2$-μ-$NH_2(CH_2)_3NH_2]$ (**P13**), $[PtNH_3Cl_2]_2$-μ-$NH_2(CH_2)_4NH_2]$ (**P14**) and $[PtNH_3Cl_2]_2$-μ-$NH_2(CH_2)_5NH_2]$ (**P15**) with three neutral thiourea-based nucleophiles specifically: thiourea (TU), 1-methyl-2-thiourea (MTU) and 1,3-dimethyl-2-thiourea (DMTU) were studied quantitatively under *pseudo* first-order conditions as a function of concentration and temperature by conventional UV/Visible and stopped-flow spectrophotometers. Ligand substitutions for the complexes proceeded in three consecutive steps. Each step follows first-order kinetics with the respective complex and nucleophile. The *pseudo* first-order rate constants, $k_{obs(1/2/3)}$, for sequential substitution of the chloride ligands and subsequent displacement of the linker obeyed the rate law: $k_{obs(1/2/3)} = k_{(1/2/3)}$[nucleophile]. The $k_{obs(3)}$ could not be monitored to completion because it was too slow. Both electronic and steric effects drive the overall substitution pattern. However, our findings reveal that upon the substitution of the chloride moieties by the thiourea-based nucleophiles at the platinum centres, the σ-donor capacity via the inductive effect of these electron-rich nucleophiles overcompensate the steric strain imposed by the nucleophiles as well as by the alkanediamine linker on the substitution sites. Consequently, electronic factors governed the overall reaction pattern of these complexes. ^{195}Pt NMR results confirmed the simultaneous substitution of all the chloride leaving groups by thiourea-based nucleophiles, followed by the subsequent but successive displacement of the ammine groups and the flexible alkanediamine linker from the metal centres. The reactivity order of the complexes: **P12** > **P13** > **P14** > **P15.** The order of reactivity of the nucleophiles with the complexes decreases with the increase in steric bulk in the nucleophiles: TU > MTU > DMTU. The small positive enthalpy values and the large but negative entropy values confirm the associative mode of activation for all the studied complexes. The computational modelling using density functional theory (DFT) calculations was employed to rationalise the kinetic trend.

6.1   Introduction

Platinum complexes have been extensively proficient not only for optoelectronic applications [1-4] but also in bioinorganic medicine most especially as anticancer drugs subsequent to the accidental discovery of the cytostatic activity of cisplatin by Barnett Rosenberg in 1969 [5-8]. Nearly five decades later, research efforts by medicinal inorganic chemists have led to the production of thousands of platinum-based compounds, some of which have been evaluated for anticancer activities but only a handful has made it to the clinical phase. Among the platinum complexes that have reached the clinical phase, carboplatin and oxaliplatin, which are derivatives of cisplatin, are the most successful, especially against testicular, cervical, colorectal, bladder and ovarian cancers [9, 10]. The success of these drugs has, however, been hampered by their severe side effects; lack of selectivity; short retention in the bloodstream; and inherent and acquired resistance [9-13]. Consequently, researchers have continued to seek the development of more effective anticancer agents with a radically different binding mode to the DNA and that can accommodate a wider spectrum of applications.

Farrell and co-workers [14, 15] were the first to extend the frontier of development of novel anticancer agents which incorporated non-classical platinum complexes such as *trans*-platinum and polynuclear platinum complexes that have showed remarkable cytostatic potentials even against cisplatin resistant cell lines [16, 17]. Studies have shown that these polynuclear platinum(II) complexes display riveting biological activities, *in vitro* against lung, pancreatic and melanoma cancers [10, 16] as compared to cisplatin and its analogues. Unlike mononuclear platinum(II) compounds, polynuclear complexes interact with the DNA via their structure-activity relationships (SARs). Their SARs have been reported to correlate with the length of the linker and the average distance between the platinum(II) centres [18-21].

Moreover, several studies have revealed that the cytotoxicity and reactivity of these multinuclear platinum(II) complexes have been linked to the distance between the platinum centres and their reactivity are also influenced by the nature of the linker between the platinum centres [5, 10, 21-24]. Multinuclear complexes with flexible and hydrophilic linker have been reported to form interstrand and intrastrand DNA adducts that are very tough to repair by the cellular proteins. As a result, improve the overall cytotoxicity of these compounds [10, 18, 21].

Furthermore, reports have shown that the reactivity of the first metal centre in some of dinuclear platinum(II) complexes, is independent of the other [24-26]. Nevertheless, in most cases, the

interaction between the two platinum(II) centres has been reported [5, 18, 24, 27-30]. Jaganyi *et al*. [18, 24, 27, 29, 31, 32], Van Eldik *et al*. [22, 30, 33] and Farrell *et al.* [16, 17] have all reported that the reactivity of dinuclear platinum(II) complexes with flexible alkyl-α,ω-diamine linkers is hinged on the average distance between the platinum centres and it diminishes as the length of the aliphatic chain increases. The geometry as well as the molecular symmetry assumed by these complexes, is also one of the prerequisites that determine the reactivity of the dinuclear platinum(II) centres [21, 29, 34].

Recently, studies have shown that BBR3464, a triplatin tetranitrate complex ((*trans*-PtCl(NH$_3$)$_2$)$_2$(*trans*-Pt(NH$_3$)$_2$(NH$_2$(CH$_2$)$_6$NH$_2$)$_2$))(NO$_3$)$_4$ and its analogues with monodentate amine ligands and with leaving groups which are *trans* to the alkyl-α,ω-diamine flexible linker on the two platinum centres were found to dechelate *in vitro* via the release of the flexible linker under the strong *trans* effect of coordinated thiols and nitrito nucleophiles [35]. Still in the same vein, Jaganyi *et al.* [31] reported that the dinuclear platinum(II) with alkyl-α,ω-diamine linker in which the leaving groups on each of the platinum centres are *trans* to the flexible linker is stable to dechelation upon coordination to thiourea-based nucleophiles. Dechelation, which normally leads to the deactivation of the platinum centre before the cytotoxic drug could reach its target molecule, has been reported to be mostly responsible for toxic behaviour in several *cis*-configured platinum complexes [36-40].

However, our previous studies, *Chapters 3* and *4*, have shown that classical mononuclear *trans*-configured platinum(II) complexes are stable to complete dechelation unlike their *cis*-configured counterparts. The stability of the mononuclear *trans*-configured platinum(II) complexes has increased the potential to serve as a prospective anticancer drug with the possibility of low toxicity. Moreover, Ongoma and Jaganyi [18] have reported the stability of 1,1/*c,c* dinuclear platinum(II) complexes to strong thiourea-based nucleophiles. Consequently, one of the important aspects to the extensive study of these phenomena will be to explore the substitution kinetics of the dinuclear *trans*-platinum(II) complexes with alkyl-α,ω-diamine flexible linkers in which the leaving groups are *trans* to each other on each of the platinum centres. In other words, the platinum centres in the dinuclear complexes are similar to the traditional mononuclear *trans*-platinum(II) complexes. To this extent, the objective of this study is to understand the role of flexible alkyl-α,ω-diamine linkers on the substitution behaviour and stability of these dinuclear *trans*-platinum(II) complexes. The structures of the complexes to be studied are presented below in **Figure 6.1**:
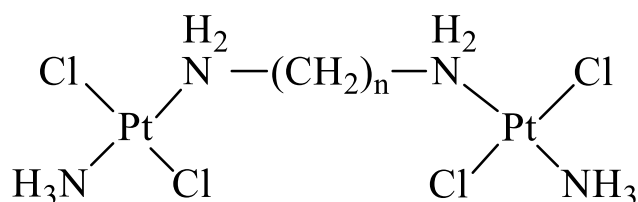
n = 2 (**P12**), 3 (**P13**), 4 (**P14**), 5 (**P15**)

Figure 6.1: Structures and abbreviations of the investigated dinuclear *trans*-platinum(II) complexes.

6.2 Experimental

6.2.1 Chemicals

HCl (37%), dimethylformamide, cisplatin (99.9%), lithium trifluoromethanesulphonate, methanol (AR), lithium chloride (99%), the nucleophiles: thiourea (TU), 1-methyl-2-thiourea (MTU), 1,3-dimethyl-2-thiourea (DMTU) and the ligands: 1,2-diaminoethane (99%), 1,3-diaminopropane (99%), 1,4-diaminobutane (99%) and 1,5-diaminopentane(95%) were all purchased from Sigma Aldrich. All the reagents were used without further purification. All other chemicals used are of the highest purity available commercially. Ultrapure water was used in the preparations of all aqueous solutions.

6.2.2 General Synthetic Procedure of the Mixed *trans*-Platinum(II) Complexes

6.2.2.1 Preparation of the Metal Precursor, NH$_4$[Pt(NH$_3$)Cl$_3$]

NH$_4$[Pt(NH$_3$)Cl$_3$] was prepared according to synthetic procedure outlined by Oksanen and Leskela [41]. To a suspension of 1.00 g (3.33 mmol) of cisplatin in 20 mL of water, 10 mL of 37% (v/v) conc. HCl was added and the resulting mixture was refluxed for 12 hours. The unreacted cisplatin was quickly removed by filtration and the filtrate was then carefully evaporated to dryness at temperature of 45 °C in the fume hood. Orange crystals of NH$_4$[PtNH$_3$Cl$_3$] was obtained with 90% yield. The product was dried in air after it was washed with ethanol.

144

6.2.2.2 Synthesis of the Dinuclear *trans*-platinum(II) complexes

The dinuclear *trans*-platinum(II) complexes were synthesised following a literature procedure by Farrell [15] with a slight modification. 200 mg (0.6 mmol) of $NH_4[PtNH_3Cl_3]$ was dissolved by stirring in 5 mL methanol at room temperature. A methanolic solution of the appropriate diaminoalkane bridging ligand (0.3 mmol in 5 mL methanol) was added dropwise to the dissolved solution of the metal. The resulting solution was vigorously stirred at room temperature for 24 hours. A yellow solid of the appropriate dinuclear *trans*-platinum(II) complex was obtained. The solid was washed with 5 mL of water, 10 mL of ethanol and subsequently left to dry in air.

P12 yield: 103 mg (55%). ^1H NMR (500 MHz, DMF-d$_7$), δ(ppm): 3.45 (s, 4H). ^{195}Pt NMR (500 MHz MHz, DMF-d$_7$), δ(ppm): -2259.8. TOF MS/ES$^+$, *m/z:* (M + Na)$^+$: 368 ($C_2H_{11}Cl_2N_3NaPt$, species). Anal. Calc. for $C_2H_{10}N_2PtCl_2$: N, 8.54; C, 7.32; H, 3.07. Found: N, 8.50; C, 7.00; H, 2.86

P13 yield: 92 mg (48%). ^1H NMR (500 MHz, DMF-d$_7$), δ(ppm): 1.90 (quintet, 4H); 2.94 (t, 4H). ^{195}Pt NMR (500 MHz, DMF-d$_7$), δ(ppm): -2260.2. TOF MS/ES$^+$, *m/z:* (M + Na)$^+$: 383 ($C_3H_{13}N_3NaPtCl_2$, species). Anal. Calc. for $C_3H_{12}N_2PtCl_2$: N, 8.19; C, 10.53; H, 3.54. Found: N, 8.12; C, 10.50; H, 3.27.

P14 yield: 69 mg (35%). ^1H NMR (500 MHz, DMF-d$_7$), δ(ppm): 2.10 (m, 4H); 3.34 (t, 4H) ^{195}Pt NMR (500 MHz MHz, DMF-d$_7$), δ(ppm): -2262.8. TOF MS/ES$^+$, *m/z:* (M + Na)$^+$: 397 ($C_4H_{15}N_3NaPtCl_2$, species). Anal. Calc. for $C_4H_{14}N_2PtCl_2$: N, 7.87; C, 13.49; H, 3.96. Found: N, 7.84; C, 13.59; H, 3.91.

P15 yield: 80 mg (40%). ^1H NMR (500 MHz, DMF-d$_7$), δ(ppm): 1.78 (quintet, 2H); 2.02 (quintet, 4H), 3.25 (t, 4H). ^{195}Pt NMR (500 MHz MHz, DMF-d$_7$), δ(ppm): -2265.3. TOF MS/ES$^+$, *m/z:* (M + Na)$^+$: 411 ($C_5H_{17}N_3NaPtCl_2$, species). Anal. Calc. for $C_5H_{16}N_2PtCl_2$: N, 7.57; C, 16.22; H, 4.36. Found: N, 7.50; C, 16.35; H, 4.57.

6.2.3   Preparation of Complex and Nucleophile Solutions for Kinetic Measurement

The chloride dinuclear *trans*-platinum(II) complexes of known concentration were prepared by dissolving a specified amount in 5 % DMF to enhance the solubility and topped up with 95 % of a methanolic solvent system which included 0.09 M lithium triflate (LiCF$_3$SO$_3$) for ionic strength adjusted by addition of 10 mM lithium chloride (LiCl) to prevent any solvolysis of the complexes. The nucleophile solutions were prepared shortly before use by dissolving 0.1 M

LiCF$_3$SO$_3$ solution in methanol. The ionic strength of the solution was maintained using lithium triflate because the triflate ion (CF$_3$SO$_3^-$) does not coordinate to platinum(II) [22, 27-29].

6.3   Instrumentation and Physical Measurements

^{1}H and ^{195}Pt NMR spectroscopic analyses were carried out on a Bruker Avance III 500MHz NMR. All ^{1}H chemical shifts were referenced to Si(CH$_3$)$_4$ and ^{195}Pt NMR chemical shifts were externally referenced to K$_2$[PtCl$_6$] [42]. The Bruker Avance III 500MHz NMR was also used to monitor ^{195}Pt-NMR of the substitution reactions of the dinuclear *trans*-platinum(II) complex, **P13**   with thiourea (TU). ^{195}Pt NMR is usually employed for the determination of the coordination features at the platinum centre because its chemical shifts are largely affected, among other things, by the nature of the coordinated donor atoms [43]. A Waters Micro-mass LCT Premier spectrometer was used for the mass determination of the *trans*-platinum(II) complexes. Elemental analyses of the synthesised complexes were performed on a Thermo Scientific Flash 2000. All the kinetic measurements were carried out on an Applied Photophysics SX.20 stopped-flow analyser coupled to an online data acquisition system and kinetic traces were evaluated using the Origin 9.1$^®$ software [44]. The temperature of the instrument was kept within $\pm$ 0.05 °C for all the measurements.

6.4   Computational Modelling

Density functional theoretical (DFT) optimization modelling of the *trans*-platinum(II) complexes **P12-P15** was carried out at the DFT level B3LYP [45] with the LANL2DZ basis set [46] using the Gaussian 09 programme suite in the gas phase (**Table 6.1**). B3LYP relates to the hybrid functional Becke's three-parameter formulation, which has been proven to be very efficient relative to the classical functionals. LANL2DZ is a double-zeta basis set which comprises effective core potential (ECP) representations of electrons near the nuclei for transition metal complexes especially for platinum complexes [24, 32, 47-50]. The complexes were optimised in their neutral form, and at singlet states because of the low electronic spin of platinum(II) complexes.

6.5   Kinetic Measurements

The kinetics of substitution of the coordinated chloride ligands from the dinuclear *trans*-platinum(II) complexes by three thiourea nucleophiles viz. thiourea (TU), N-methylthiourea (MTU) and N,N-dimethyl-2-thiourea (DMTU) were studied under *pseudo* first-order conditions on the stopped-flow and/or UV/Visible spectrophotometers. The nucleophile concentration was at least in a 40-fold excess compared to that of the dinuclear *trans*-platinum(II) complexes in all reactions. This ensured at least a 10-fold of nucleophile concentration at the respective platinum centre and hence drive the reaction to completion. The reactions were advanced by mixing equal volumes of the solutions of the dinuclear platinum(II) complexes with the solutions of the respective thiourea nucleophile at suitable wavelengths. The kinetic data obtained were graphically analysed using Origin® 9.1 [44]. The temperature was controlled throughout all kinetic experiments within an accuracy of ±0.05 °C. The dependence of the rate constants on temperature was studied over a range of 20-40 °C at a 5 °C interval. The rate constants reported represent an average value of at least three to five independent kinetic runs for reactions performed on the stopped-flow spectrophotometer and of at least a duplicate run for those followed on the UV/Visible spectrophotometer. The k_{obs} values were determined from nonlinear least-square fits by fitting the exponential function in *equation 6.1* to the time dependent absorbance [51, 52].

$$A_t = A_\infty + (A_0 - A_\infty)exp^{(-k_{obs}.t)}$$ (6.1)

where A_0, A_t and A_∞ represent the absorbance of the reaction mixture at the start of the reaction, at time t, and at the end of the reaction, respectively. Activation parameters (enthalpies and entropies) were determined from a linear least-squares analysis of $\ln(k_2/T)$ versus $1/T$ using the Eyring plots as shown in *equation 6.2*.

$$ln\left(\frac{k_2}{T}\right) = -\left(\frac{\Delta H^{\#}}{RT}\right) + \left(23.8 + \frac{\Delta S^{\#}}{R}\right)$$ (6.2)

6.6   Results and Discussion

6.6.2   Computational Analysis

In order to gain an in-depth insight into how the bridging flexible alkyl-α,ω-diamine linkers influence the reactivity and stability of the dinuclear *trans*-platinum(II) centres, it was

imperative to evaluate the molecular structures and electronic properties of the complexes under investigated. Minimum energy structures were calculated for each of the chloride-coordinated dinuclear *trans*-platinum(II) complexes (**P12-P15**) at the B3LYP/LANL2DZ level of theory in the gas phase. All the chloride complexes were optimised in their neutral form. An extract of the DFT-calculated data is presented in **Table 6.1**.

Table 6.1: An extract of the DFT calculated data for the investigated dinuclear *trans*-platinum(II) complexes at B3LYP/LANL2DZ level of theory

Parameter	P12	P13	P14	P15
NBO Charges Pt$_1$/ Pt$_2$	0.035 -	0.031 -	0.028 -	0.023 -
-N$_{amine}$	0.689	0.692	0.694	0.698
MO energy HOMO/eV	1.895	- 1.87	- 1.88	- 1.76
LUMO/eV	6.20	-6.10	-6.14	-6.04
ΔE/eV	4.03	4.23	4.26	4.27
Bond length (Å) Pt-Pt	7.039	7.820	8.813	9.879
Pt-N$_{amine}$	2.070	2.069	2.066	2.066
Pt-N$_{ammine}$	2.073	2.074	2.077	2.077

A closer inspection of the extracted data in **Table 6.1** reveals that there is a general increase in the energy gap, ΔE$_{(HOMO-LUMO)}$, of the frontier orbitals as the chain length of the flexible alkyl linker is increased. A similar trend has been reported by Jaganyi *et al.* [18, 31] in related studies. This observation is, however, contrary to what was obtained for their mononuclear counterparts in which the gradual increase in the alkyl chain length did not have any significant electronic contribution to the HOMO-LUMO energy gap (see *Chapter 4*). It is also observed that the platinum centres in all the chloride-coordinated dinuclear *trans*-platinum(II) complexes carry symmetrical natural bond order (NBO) charges which indicate that the metal centres have the same electronic environment [18, 22, 28, 31]. The NBO charges on the platinum centres decrease as the chain length of the flexible alkyl linker increases.

6.6.3 Ligand Substitutions

The kinetics of the substitution of the coordinated chloride ligands in the dinuclear *trans*-platinum(II) complexes with flexible alkyl linker were investigated spectrophotometrically by monitoring the changes in absorbance at suitable wavelengths as function of time on stopped-flow and UV/Visible spectrophotometers. A typical kinetic trace obtained on the stopped-flow

is shown in **Figure 6.2** whereas **Figure 6.3** is a representation of the kinetic traces obtained on the conventional UV/Visible spectrophotometer. The proposed reaction pathways for the substitution process of the *trans*-platinum(II) complexes with neutral thiourea-based nucleophiles namely: TU, MTU and DMTU are presented in **Schemes 6.1**.

where
n = 2, 3, 4, 5
Nu = TU, MTU, DMTU
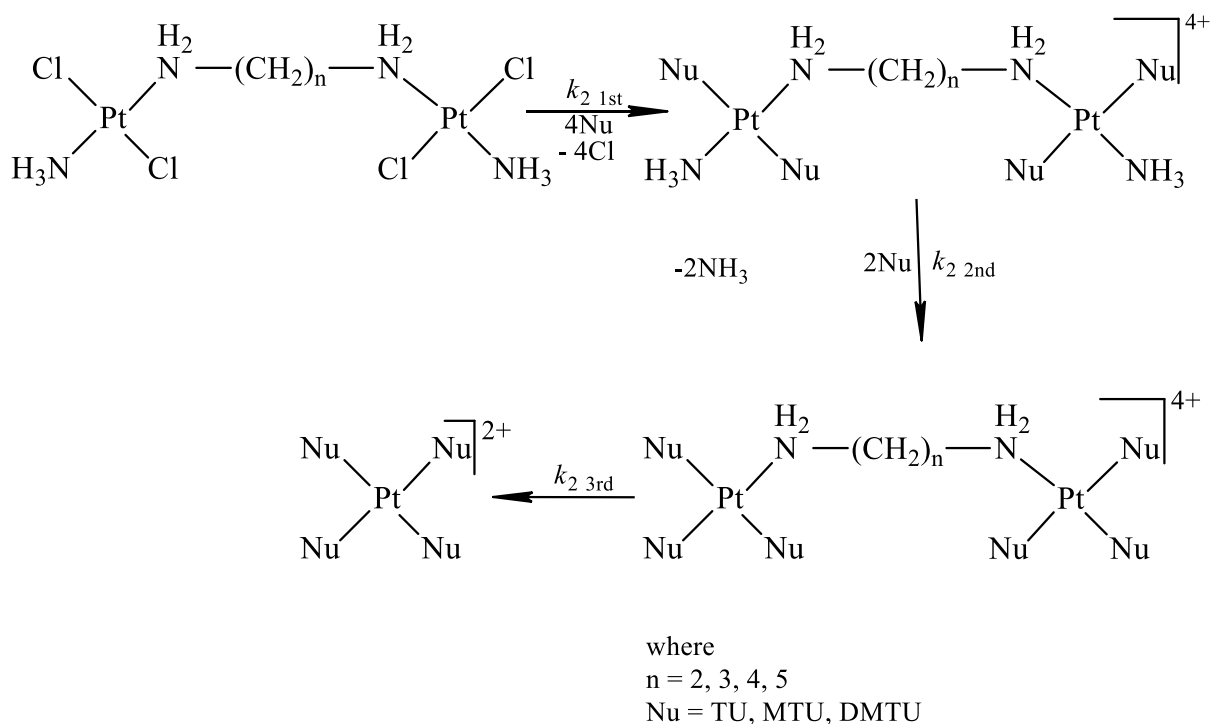
Scheme 6.1: Proposed mechanism of the chloride substitution from the studied complexes by a series of thiourea nucleophiles (Nu).

All the kinetic traces fitted perfectly into single exponential functions. The *pseudo* first-order rate constants, k_{obs} obtained were observed to have a linear dependence on the concentration of the thiourea-based nucleophiles. The second-order rate constant, k_2 for the reaction of each complex with the nucleophiles were determined from the slopes of the plots of the *pseudo* first-order rate constants, k_{obs} against the concentration of the nucleophiles using the Origin 9.1$^{®}$ [44].
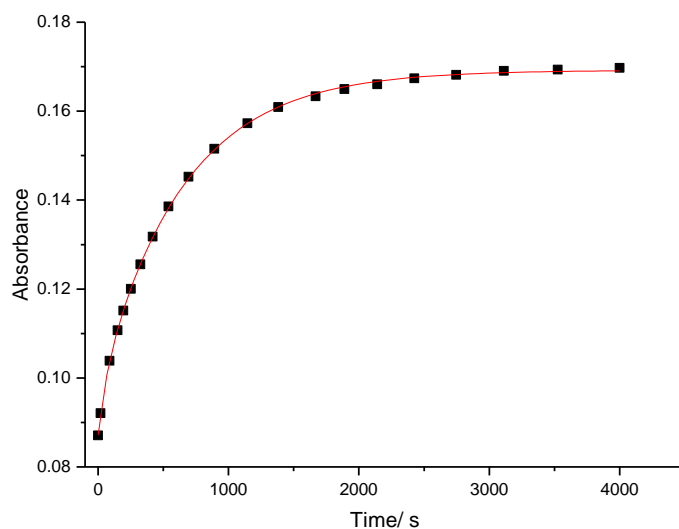
Figure 6.2: A typical trace of the reaction of **P13** and DMTU for the simultaneous substitution of the four chloride ligands from the stopped-flow measurement recorded at 351 nm, T = 298 K, I = 0.1 M (0.09 M LiCF$_3$SO$_3$/10 mM LiCl).
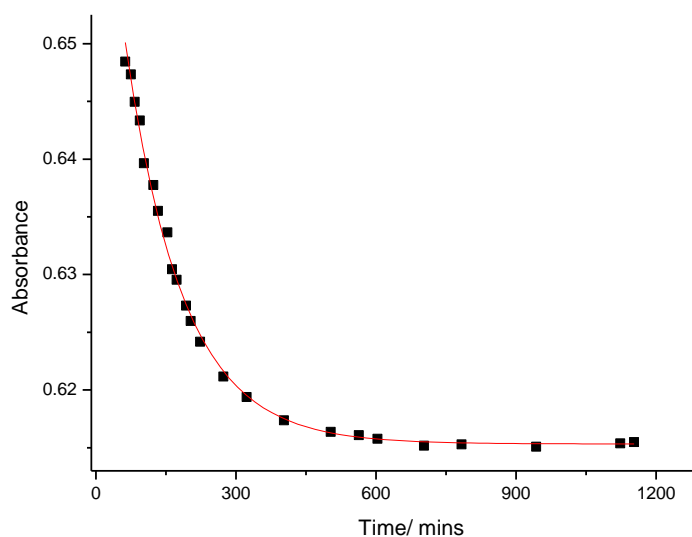
Figure 6.3: A typical trace of the reaction of **P13** and DMTU for the simultaneous substitution of the two ammine ligands from the UV/Visible measurement recorded at 351 nm, T = 298 K, *I* = 0.1 M (0.09 M LiCF$_3$SO$_3$/10 mM LiCl).

The summary of the second-order rate constants is shown in **Table 6.2**. Based on this observation, *equation* 6.3 represents the corresponding rate laws for the consecutive reaction steps

$$k_{obs(1,2)} = k_{-2} + k_2[\text{Nu}] \approx k_2[\text{Nu}] \qquad (6.3)$$

where k_{-2} = rate constant for the solvent path; k_2 = rate constant for the direct path, [Nu] = nucleophile concentration.

150

The contribution of the solvent through the solvolytic path (k_{-2}) is negligible or veritably absent. The values of the second-order rate constants, k_2 obtained from the linear regression analysis from *equation 6.2* are summarized in **Table 6.2**.

The substitution reactions of all the investigated dinuclear *trans*-platinum(II) complexes with thiourea-based nucleophiles proceeded by three separate steps. The first step, a moderately fast step followed on the stopped-flow, was assigned to the simultaneous substitution of the four chloro ligands from the two platinum centres. The second step, a slower step monitored on the UV/Visible spectrophotometer, was attributed to the simultaneous removal of the ammine (NH_3) ligand, which is at *cis*-position to the incoming nucleophiles, from the two metal centres. The third step was ascribed to the release of the flexible bridging alkyl linker owing to the total displacement of all the ligands by the incoming nucleophiles at the platinum centres. This step, however, was extremely slow to be followed to completion on the UV/Visible spectrophotometer.

Table 6.2: Summary of second-order rate constants and activation parameters for the reaction of the dinuclear *trans*-platinum(II) complexes with thiourea-based nucleophiles in the temperature range of 293-33 K.

Complex	NU	$k_{2,1st}$ ×10⁻³ M⁻¹s⁻¹	$\Delta H^{\#}_{1st}$ kJmol⁻¹	$\Delta S^{\#}_{1st}$ Jmol⁻¹K⁻¹	$k_{2,\,2nd}$ ×10⁻⁶ M⁻¹s⁻¹	$\Delta H^{\#}_{2nd}$ kJmol⁻¹	$\Delta S^{\#}_{2nd}$ Jmol⁻¹K⁻¹
P12	TU	26.1 ± 0.047	50.3 ± 2	-113.2 ± 2	155.4 ± 0.01	51.0 ± 0.6	-152.7 ± 3
	MTU	16.8 ± 0.001	53.8 ± 3	-103.7 ± 9	96.4 ± 0.06	63.2 ± 2	-115.7 ± 5
	DMTU	5.8 ± 0.017	46.6 ± 2	-137.3 ± 7	55.5 ± 0.06	69.7 ± 0.8	-98.9 ± 3
P13	TU	16.1 ± 0.028	45.7 ± 0.3	-132.8 ± 0.9	106.3 ±	71.8 ± 0.3	-86.0 ± 1
	MTU	10.2 ± 0.024	49.0 ± 2	-124.9 ± 6	0.001	59.6 ± 1	-129.6 ± 3
	DMTU	4.2 ± 0.003	61.6 ± 2	-89.6 ± 5	77.0 ± 0.004	59.9 ± 0.7	-132.9 ± 2
					46.0 ± 0.027		
P14	TU	11.5 ± 0.004	48.8 ± 3	-124.6 ± 8	78.0 ± 0.37	43.7 ± 0.4	-182.8 ± 1
	MTU	8.4 ± 0.018	43.5 ± 1	-143.4 ± 4	54.4 ± 0.23	34.4 ± 1	-178.7 ± 4
	DMTU	2.8 ± 0.003	57.5 ± 1	-106.7 ± 4	40.1 ± 0.55	53.4 ± 0.1	-156.7 ± 0.3
P15	TU	6.2 ± 0.004	47.1 ± 0.8	-135.2 ± 3	73.2 ± 0.27	43.1 ± 0.7	-185.8 ± 2
	MTU	5.0 ± 0.009	49.8 ± 0.7	-127.9 ± 2	45.6 ± 0.08	41.9 ± 11	-151.8 ± 2
	DMTU	2.1 ± 0.012	62.7 ± 1	-92.5 ± 4	34.8 ± 0.55	41.8 ± 0.7	-196.0 ± 2

6.6.4 NMR Studies

To establish the stepwise mechanism proposed in **Scheme 6.2**, the reaction between **P13** with twenty mole equivalents of TU in DMF was monitored by [195]Pt NMR spectroscopy. The [195]Pt NMR has been established to be an effective technique to determine coordination details at the platinum centre owing to the fact that its chemical shift is largely influenced by the number of coordinated donor atoms on the platinum(II) centre [53].
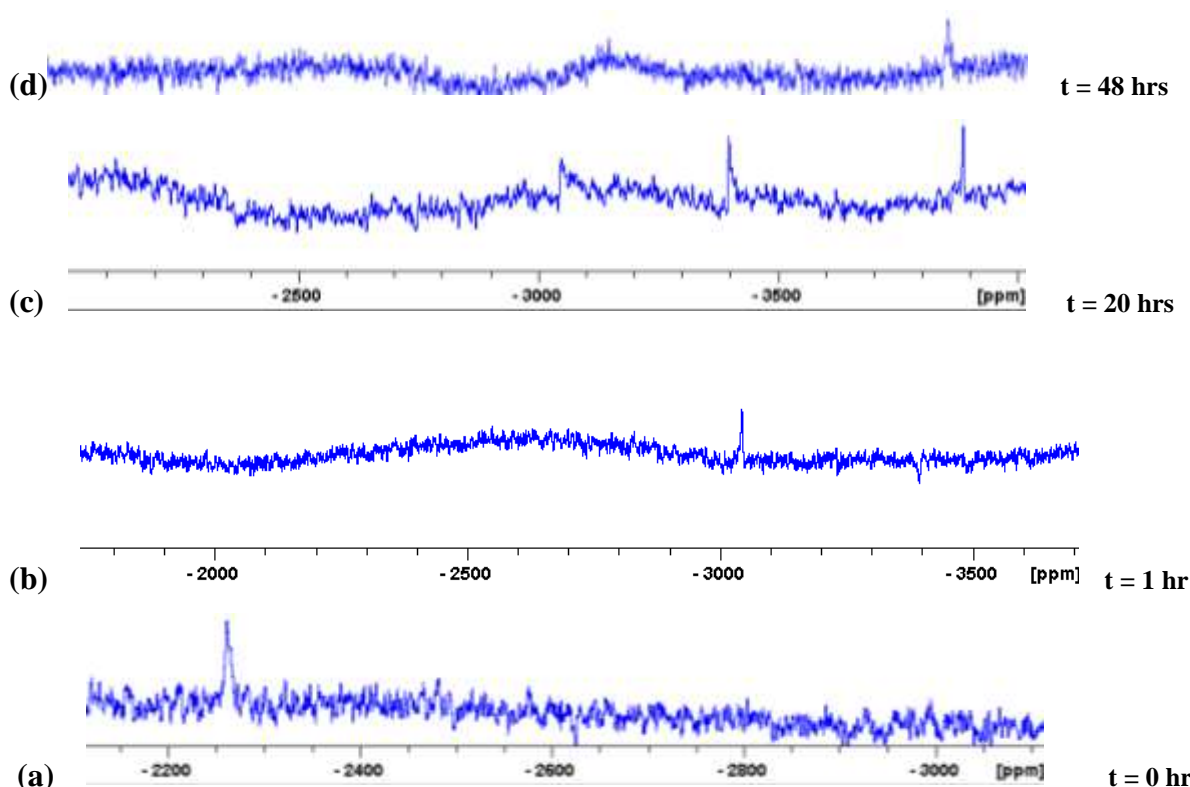

Figure 6.4: (a) [195]Pt NMR spectra of the reaction mixture of **P13** with twenty mole equivalents of TU, showing pure **P13** (δ = -2261.2 ppm) before the reaction, **(b)** the first transient species obtained after one hour at -3044.7 ppm corresponding to $[PtNH_3TU_2]_2$-μ-$NH_2(CH_2)_3NH_2]^{4+}$, **(c)** appearance of two additional peaks obtained after 20 hours at -3396.3 ppm and -3886.6 ppm corresponding to $[trans$-$\{Pt(TU)_3\}_2$-μ-$NH_2(CH_2)_3NH_2]^{4+}$ and $[Pt(TU)_4]^{2+}$ respectively and **(d)** the peak (δ = -3886.6 ppm) ascribed to the final degradation product $[Pt(TU)_4]^{2+}$, persisted after 48 hours.

The peak in **(a)** at -2261.2 ppm in **Figure 6.4** corresponds to the unreacted starting complex **P13**. This peak disappeared after one hour and was replaced by a new peak in **(b)** obtained at -3044.7 ppm indicating the formation of a new species in the solution. This peak persisted until after twenty hours when two new additional peaks emerged at -3396.3 ppm and -3886.6 ppm respectively in **(c)**. The peak at -3044.7 ppm is assigned to the species $[trans$-$\{PtNH_3(TU)_2\}_2$-

153

μ-NH$_2$(CH$_2$)$_3$NH$_2$]$^{4+}$ in which the two chloride moieties on the respective platinum centre have been substituted by thiourea. The peak at -3396.3 ppm is ascribed to the displacements of the ammine ligands by a third thiourea on both metal centres, [*trans*-{Pt(TU)$_3$}$_2$-μ-NH$_2$(CH$_2$)$_3$NH$_2$]$^{4+}$ and the final peak in (**d**), which remained persistent after 48 hours, at -3886.6 ppm is assigned to the final product in which the flexible alkanediamine linker has been released for the coordination of the fourth thiourea nucleophile on the platinum sites, [Pt(TU)$_4$]$^{4+}$. The NMR results are consistent with what have been previously reported in literature [18, 62-65].

Hence, it is reasonable to conclude that the presence of strong labilising thiourea nucleophiles at the platinum centres facilitate the displacement of the ammine ligands and the cleavage of the flexible alkanediamine bridging ligand. This conclusion corroborates the earlier work reported by Ongoma and Jaganyi [18] in which the alkanediamine bridging ligand and the ammine group remained bonded to the metal centres in the presence of the strong labilising thiourea-based nucleophiles. However, the study did not rule the fact that a longer reaction time may be required to cause the cleavage of the ammine groups and of the flexible alkanediamine bridging ligand from the platinum centres. This present study further extends the earlier report and clearly establish that the presence of two strong labilising thiourea nucleophiles at the respective platinum centres in the dinuclear platinum(II) complexes with alkanediamine bridging ligands and a longer reaction time will cause the displacement of the ammine group and the cleavage of the linker from the metal centres. Therefore, based on our reports in *Chapters 3* and *4*, it is logical to assert that dinuclear *trans*-platinum(II) complexes with alkanediamine bridging ligands are not as stable as their mononuclear *trans*-platinum(II) counterparts in the presence of strong S-donor nucleophiles.

Furthermore, comparing the substitution process of the dinuclear *trans*-platinum(II) complexes with that of their corresponding mononuclear analogue reveals that the dinuclear *trans*-platinum(II) complexes have similar substitution patterns with their corresponding mononuclear isomers. In other words, there is a simultaneous substitution of chloride leaving groups by the thiourea nucleophiles in both sets of complexes. However, the substitution process is faster in the mononuclear *trans*-platinum(II) complexes as compared to their corresponding dinuclear counterparts. The mononuclear *trans*-platinum(II) complexes were found to be at least forty times more reactive than their corresponding dinuclear complexes.

Although, one would expect that the coordination of the other end of the alkanediamine linker to the second metal centre would have minimised the steric hinderance posed by the flexible

154

alkylamine group on the substitution sites in the mononuclear *trans*-platinum(II) complexes. Nevertheless, the dinuclear *trans*-platinum(II) complexes appear to have experienced more steric restrictions than their corresponding mononuclear analogues because of the presence of the alkanediamine bridging linker as well as the incoming thiourea nucleophiles at the platinum sites. Moreover, in the case of the mononuclear *trans*-platinum(II) complexes, the flexible alkylamine group had little or no electronic communication with the platinum centre based on the DFT data obtained (see *Chapter 4*) as well as the experimental data obtained from the pK_a values (see *Chapter 5*).

However, the coordination of the other end of the flexible alkanediamine linker to the second metal centre not only enhances electronic communication between the linker and the platinum centre but also poses steric strain on the substitution process. A similar trend has been observed before by other researchers [21, 29]. Evidence of increased electronic communication between the platinum(II) centres and the alkanediamine bridging ligand can be seen from the significant reduction in the NBO charges when those of the dinuclear *trans*-platinum(II) complexes are compared to those of their corresponding mononuclear analogues (see **Table 4.1** in *Chapter 4*). The electronic communication through the σ-donor ability (σ-inductive effect) of the alkanediamine linker to the platinum centre increases the electron density on the metal site and thus reduces its electrophilicity. Subsequently, there is a significant decrease in the reactivity of the dinuclear *trans*-platinum(II) complexes compared to their corresponding mononuclear analogues.

Besides the electronic factor, steric effects resulting from the symmetry adopted by the dinuclear complexes due to the chain length, depending on the (even or odd) number of carbon atoms in the chain, has been reported by several researchers to be also responsible for the lowering in reactivity of the dinuclear complexes relative to their mononuclear counterparts [21, 29]. In the previous study in *Chapter 3*, we reported that the *trans*-configured platinum centre, in which the leaving groups are *trans* to each on the same metal centre, minimises steric hindrance as compared to the *cis*-configured complexes. However, the steric restraints resulting from the coordination of the bridging ligand to the two metal centres override the advantage due to the *trans*-configuration of the metal centre. Therefore, it is reasonable to conclude that the overall reaction pattern of the dinuclear *trans*-platinum(II) complexes is governed by both electronic and steric effects.

After a closer inspection of the second-order rate constants for the first kinetic step as presented in **Table 6.2**, it is quite evident that there is a gradual decrease in reactivity as the chain length increases. Comparing the second-order rate constants for the substitution reaction of the dinuclear *trans*-platinum(II) complexes with the thiourea (TU) nucleophile, the reactivity pattern is **P12** > **P13** > **P14** > **P15**. The first step is assigned to the simultaneous substitution of the four chloride moieties by the incoming thiourea-based nucleophiles.

While one would have expected the symmetry adopted by the dinuclear complexes resulting from the number of carbon atoms (even or odd) in the chain length of the alkanediamine bridging ligand to have a remarkable effect on the reactivity pattern as previously reported from other studies [21, 29], the overall reaction rates were governed by the σ-inductive effect of the alkanediamine linker on the platinum centre as supported by the NBO charges. The NBO charges on the metal decreases gradually with each addition of the methylene (*-CH₂*) unit. This observation contrasts with reports in previous studies in which the alkanediamine bridging ligand was believed to have no significant electronic contribution to the metal centre [21, 27, 29]. Based on the kinetic results in the present study, the gradual increase in the σ-donor ability of the bridging ligand to the substitution sites resulting from the increase in chain length overrides its steric influence on the reactivity of the dinuclear complexes.

A similar trend was observed for the second kinetic step which followed the reactivity order: **P12** > **P13** > **P14** > **P15**. This second step has been attributed to the slow displacement of the ammine ligand because of the strong labilising effect of the S-donor nucleophiles. However, in this study, we are reporting for the first time a third kinetic step which was too slow to be followed to completion on the UV/Visible spectrophotometer. The step is ascribed to the bonding of the fourth thiourea-based nucleophiles to, and the cleavage of the bridging ligand from, the metal centres. Until now, researchers have assumed that dinuclear *trans*-platinum(II) or structurally related complexes are stable to dechelation when compared to those in which the leaving groups adopt *cis*-configuration to each other or in *trans* position to the bridging alkanediamine linker [18, 31]. The cleavage of the bridging ligand was made possible because of the stronger labilising effect of the three thiourea-based nucleophiles on each of the platinum(II) centres.

The DFT optimisation of the product of the first kinetic step in which all the chloride leaving groups have been replaced by thiourea evidently showed a considerable increase in the bond lengths between the ammine group and the platinum(II) ion on one hand, and between the

platinum(II) ion and the bridging alkanediamine linker on the other (**Scheme 6.2**). The elongation of these bond lengths is consequent upon the remarkable increase in the electron density at the metal centre because of the strong inductive effect of the S-donor nucleophiles. Despite the increase in the overall charge at the platinum centre, the inductive effect of the S-donor nucleophiles coupled with that of the bridging alkanediamine linker counteract the impact of the surge in positive charge at the reaction sites resulting from the departure of the four chloro leaving groups. Based on the results from previous studies [18, 31], one would have expected that the steric strain imposed by the alkanediamine bridging ligand as well as the presence of the two thiourea nucleophiles already bonded to the platinum centres will prevent the coordination of the third and the fourth thiourea-based nucleophiles to the respective platinum centres due to the subsequent and successive removal of the ammine group and the bridging ligand from the platinum sites.

(a)

(b)
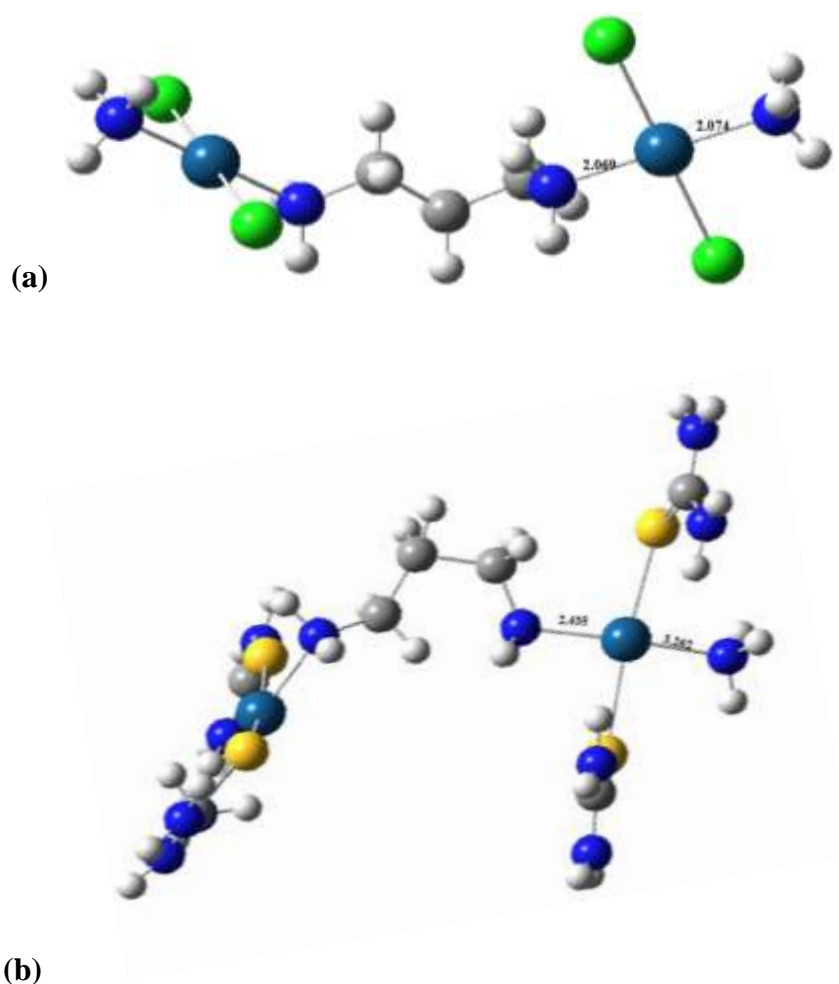
Scheme 6.2: (a) An optimised structure for the chloro complex P13 showing the bond lengths of the ammine ligand and the bridging alkanediamine ligand respectively from the platinum centre (b) An optimised structure for the complex P13 in which the chloro moieties have been replaced by TU indicating the bond lengths of the ammine ligand and the bridging alkanediamine ligand respectively from the platinum centre.

However, the electron donor capacity of the electron rich thiourea-based nucleophiles via sigma bonds to the platinum centre overrule the imposed steric effect by the entering nucleophiles as well as the flexible linker. In other words, the electronic effect clearly took precedence over the steric factor. The order of reactivity of the thiourea-based nucleophiles with dinuclear *trans*-platinum(II) complexes decreases with increase in steric demand in the following order: TU > MTU > DMTU. The *pseudo* first-order rate constants, $k_{obs\ 1st}$ and $k_{obs\ 2nd}$, obtained for the first and second steps in all the dinuclear *trans*-platinum(II) complexes from the kinetic traces were plotted against the concentration of the entering nucleophiles (**Figures 6.5 and 6.6**).
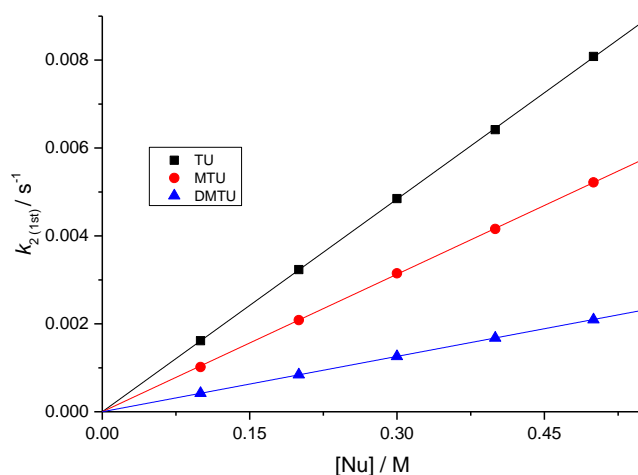

Figure 6.5:   *Pseudo* first-order rate constants plotted as a function of the concentration of the entering nucleophiles for the substitution of the four chloride ligands in **P13** complex by TU. MTU, and DMTU at 298 K, I = 0.1 M (0.09 M LiCF$_3$SO$_3$ + 0.01 M LiCl).
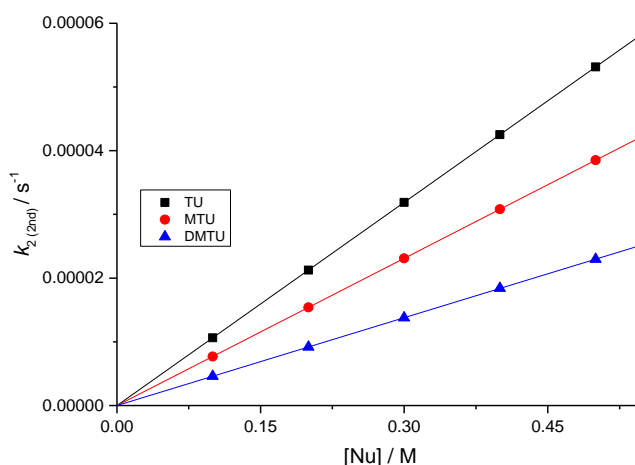

Figure 6.6:   *Pseudo* first-order rate constants plotted as a function of the concentration of the entering nucleophiles for the substitution of the both ammine ligands in **P13** by TU. MTU, and DMTU at 298 K, I = 0.1 M (0.09 M LiCF$_3$SO$_3$ + 0.01 M LiCl).

6.6.5 Activation Parameters

The temperature dependence of the rate constant, k_2, was investigated over the range 293-313 K in increments of 5 degrees. The Eyring plots for the reaction of **P13** with the thiourea-based nucleophiles for the first and second step respectively are outlined in **Figures 6.7** and **6.8.**
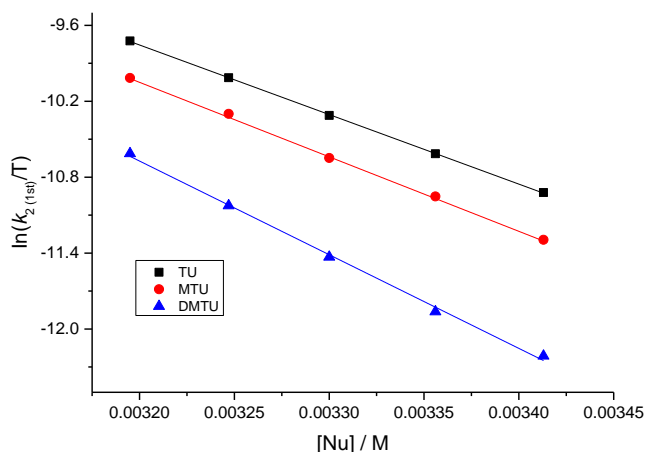

Figure 6.7: Plots of $ln(k_{2\ (1st)}/T)$ against 1/T for the reaction of **P13** with the thiourea nucleophiles at various temperatures ranging from 293 to 313 K.
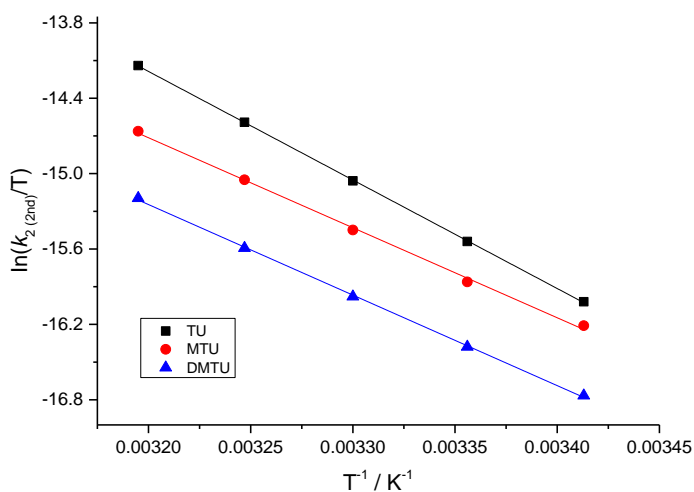

Figure 6.8: Plots of $\ln(k_{2\ (2nd)}/T)$ against 1/T for the reaction of **P13** with the thiourea nucleophiles at various temperatures ranging from 293 to 313 K.

The corresponding values for the activation parameters of enthalpy, $\Delta H^{\#}$, and entropy, $\Delta S^{\#}$, are summarized in **Table 6.2**. These results are temperature dependent and are consistent with an associative substitution mechanism for d^8 square planar platinum(II) complexes owing to the negative activation entropy values as reported in the literature [9,10,55].

6.7   Conclusion

This study explores the effect of a progressive increase in the chain length of alkanediamine bridging ligands on the substitution kinetics of some dinuclear *trans*-platinum(II) complexes. Our findings revealed that upon the substitution of the chloride moieties by the thiourea-based nucleophiles at the platinum centres, the σ-donor capacity via inductive effect of these electron-rich nucleophiles over compensate the steric strain imposed by the nucleophiles as well as by the alkanediamine linker on the substitution sites. Consequently, electronic factors governed the overall reaction pattern of these complexes. [195]Pt NMR results confirmed the simultaneous substitution of all the chloro leaving group by thiourea-based nucleophiles within one hour of the start of the reaction followed by the subsequent but successive displacement of the ammine groups and the flexible alkanediamine linker from the metal centres after 20 hours. Contrary to reports from previous related studies [18, 31], our findings clearly proves that dinuclear *trans*-platinum(II) complexes, in which the leaving groups are *trans* to each on the same metal centre, are just as unstable to the strong labilising effect of the S-donor nucleophile as their *cis*-configured counterparts. Thus, these complexes are not as promising as their corresponding mononuclear *trans*-platinum(II) analogues in anticancer chemotherapy. The mononuclear *trans*-platinum(II) complexes have been well-established to show a high stability to strong S-donor nucleophiles (see *chapters three* and *four*) [8, 66-68] which are known to play an important role in bioinorganic processes. However, the dinuclear *trans*-platinum(II) complexes showed a similar pattern as their corresponding mononuclear *trans*-platinum(II) isomers, for the substitution of the chloride moieties in the first step. The small positive enthalpy and the large but negative entropy confirm the associative mode of activation for all the studied complexes. This is an indication that the mechanistic reactions of these complexes are characterised by bond formation in the transition state as expected for all d^8 square planar complexes [51, 54-61].

References

[1] D. Cui, H. Chen, X. Bai, in: International Conference on Optoelectronics and Microelectronics Technology and Application, International Society for Optics and Photonics, (2017) 102441E.

[2] L. Dobrzański, M. Szindler, M.P. vel Prokopowicz, A. Drygała, K. Lukaszkowicz, T. Jung, M. Szindler, Journal of Achievements in Materials and Manufacturing Engineering, 68 (2015) 5-10.

[3] S. Radu, M. Ionică, R.A. Macovei, G. Caragea, M. Forje, I. Grecu, M. Vlădescu, O. Viscol, in: Advanced Topics in Optoelectronics, Microelectronics, and Nanotechnologies VIII, International Society for Optics and Photonics, (2016) 100103J.

[4] S. Stanca, F. Hänschke, G. Zieger, J. Dellith, A. Ihring, A. Undisz, H.-G. Meyer, Scientific reports, 7 (2017) 14955.

[5] S. Jovanović, J. Bogojeski, M. Petković, Ž.D. Bugarčić, Journal of Coordination Chemistry, 68 (2015) 3148-3163.

[6] B. Lippert, Cisplatin: Chemistry and Biochemistry of a Leading Anticancer Drug, Wiley-VCH, New York, (1999) 1-23.

[7] L. Messori, L. Cubo, C. Gabbiani, A. Álvarez-Valdés, E. Michelucci, G. Pieraccini, C. Ríos-Luci, L.G. León, J.M. Padrón, C. Navarro-Ranninger, Inorganic Chemistry, 51 (2012) 1717-1726.

[8] J.J. Wilson, S.J. Lippard, Chemical Reviews, 114 (2013) 4470-4495.

[9] S. Dilruba, G.V. Kalayda, Cancer Chemotherapy and Pharmacology, 77 (2016) 1103-1124.

[10] T.C. Johnstone, K. Suntharalingam, S.J. Lippard, Chemical Reviews, 116 (2016) 3436-3486.

[11] N. Aztopal, D. Karakas, B. Cevatemre, F. Ari, C. Icsel, M.G. Daidone, E. Ulukaya, Bioorganic & Medicinal Chemistry, 25 (2017) 269-276.

[12] S. Komeda, H. Yoneyama, M. Uemura, A. Muramatsu, N. Okamoto, H. Konishi, H. Takahashi, A. Takagi, W. Fukuda, T. Imanaka, Inorganic Chemistry, 56 (2017) 802-811.

[13] M.M. Milutinović, S.K. Elmroth, G. Davidović, A. Rilak, O.R. Klisurić, I. Bratsos, Ž.D. Bugarčić, Dalton Transactions, 46 (2017) 2360-2369.

[14] N. Farrell, Journal of Medicinal Chemistry, 32 (1989) 2240-2241.

[15] N.H. Farrell, Miles P.; McCormack, John J.; DeAlmeida, Sergio G., in: W.I.P. Organisation (Ed.) The Patent Cooperation Treaty, United States of America, (1988) 1-23.

[16] N. Farrell, Qu, Y., Feng, L., Van Houten B., Biochemistry, 29 (1990) 9522-9953 I.

[17] N. Farrell, Qu, Y., , Inorganic Chemistry, 31 (1992) 930-932.

[18] P.O. Ongoma, D. Jaganyi, Transition Metal Chemistry, 39 (2014) 407-420.

[19] V. Brabec, J. Kasparkova, V. Menon, N.P. Farrell, Metallo-Drugs: Development and Action of Anticancer Agents: Development and Action of Anticancer Agents, 18 (2018) 43.

[20] O. Hrabina, J. Kasparkova, T. Suchankova, V. Novohradsky, Z. Guo, V. Brabec, Metallomics, 9 (2017) 494-500.

[21] P.A. Wangoli, G. Kinunda, New Journal of Chemistry, 42 (2018) 214-227.

[22] S. Hochreuther, R. Puchta, R. van Eldik, Inorganic Chemistry, 50 (2011) 8984-8996.

[23] P.O. Ongoma, D. Jaganyi, Dalton Transactions, 42 (2013) 2724-2734.

[24] A. Shaira, D. Jaganyi, Journal of Coordination Chemistry, 68 (2015) 3013-3031.

[25] M.S. Davies, J.W. Cox, S.J. Berners-Price, W. Barklage, Y. Qu, N. Farrell, Inorganic Chemistry, 39 (2000) 1710-1715.

[26] M.S. Davies, D.S. Thomas, A. Hegmans, S.J. Berners-Price, N. Farrell, Inorganic Chemistry, 41 (2002) 1101-1109.

[27] A. Mambanda, D. Jaganyi, Dalton Transactions, 40 (2011) 79-91.

[28] A. Mambanda, D. Jaganyi, Dalton Transactions, 41 (2012) 908-920.

[29] A. Mambanda, D. Jaganyi, S. Hochreuther, R. van Eldik, Dalton Transactions, 39 (2010) 3595-3608.

[30] T. Soldatović, S. Jovanović, Ž.D. Bugarčić, R. van Eldik, Dalton Transactions, 41 (2012) 876-884.

[31] D. Jaganyi, V. Munisamy, D. Reddy, International Journal of Chemical Kinetics, 38 (2006) 202-210.

[32] G. Kinunda, D. Jaganyi, Transition Metal Chemistry, 41 (2016) 235-248.

[33] A. Hofmann, R. van Eldik, Dalton Transactions, (2003) 2979-2985.

[34] P.W. Asman, Inorganica Chimica Acta, 469 (2018) 341-352.

[35] M.E. Oehlsen, A. Hegmans, Y. Qu, N. Farrell, Journal of Biological Inorganic Chemistry, 10 (2005) 433-442.

[36] S. Dasari, P.B. Tchounwou, European Journal of Pharmacology, 740 (2014) 364-378.

[37] S.R. Dasari, V. Velma, C.G. Yedjou, P.B. Tchounwou, International Journal of Cancer Research and Molecular Mechanisms, (2015) 1-12.

[38] J. Hrabeta, V. Adam, T. Eckschlager, E. Frei, M. Stiborova, R. Kizek, Anti-Cancer Agents in Medicinal Chemistry (Formerly Current Medicinal Chemistry-Anti-Cancer Agents), 16 (2016) 686-698.

[39] I. Lambert, B. Sørensen, International Journal of Molecular Sciences, 19 (2018) 2249.

[40] I.A. Riddell, S.J. Lippard, Metallo-Drugs: Development and Action of Anticancer Agents: Development and Action of Anticancer Agents, 18 (2018) 1-58.

[41] A.L. Oskanen, Markku, Acta Chemica Scandinavica, 48 (1994) 483-489.

[42] A. Hofmann, L. Dahlenburg, R. van Eldik, Inorganic Chemistry, 42 (2003) 6528-6538.

[43] A.K. Connors, Chemical Kinetics of the Reaction Rates in Solution, Wiley-VCH, New York, (1990) 1-100.

[44] E. Seifert. OriginPro 9.1: Scientific Data Analysis and Graphing Software®- Software Review. Journal of Chemical Information and Modelling, 54(5), (2014) 1552-1568.

[45] A.D. Becke, The Journal of Chemical Physics, 96 (1992) 2155-2160.

[46] P.J. Hay, W.R. Wadt, The Journal of Chemical Physics, 82 (1985) 299-310.

[47] T.A. Hilder, J.M. Hill, Nanotechnology, 18 (2007) 275704-275726.

[48] S.V. Nkabinde, G. Kinunda, D. Jaganyi, Inorganica Chimica Acta, 466 (2017) 298-307.

[49] T.R. Papo, D. Jaganyi, Transition Metal Chemistry, 40 (2015) 53-60.

[50] I.M. Wekesa, D. Jaganyi, Journal of Coordination Chemistry, 69 (2016) 389-403.

[51] P. Atkins, J. De Paula, J. Keeler, Atkins' Physical Chemistry, Oxford University Press, (2018) 1-60.

[52] J.D. Atwood, Inorganic and Organometallic Reaction Mechanisms, John Wiley & Sons, Canada, (1985) 1-35.

[53] P.W. Asman, Journal of Coordination Chemistry, (2017) 1-20.

[54] W.P. Asman, D. Jaganyi, International Journal of Chemical Kinetics, 49 (2017) 545-561.

[55] R. Bellam, J. Deogratius, A. Mambanda, R.S. Robinson, New Journal of Chemistry, (2018).

[56] D. Ćoćić, S. Jovanović, M. Nišavić, D. Baskić, D. Todorović, S. Popović, Ž.D. Bugarčić, B. Petrović, Journal of Inorganic Biochemistry, 175 (2017) 67-79.

[57] A. Mambanda, D. Jaganyi, Advances in Inorganic Chemistry, Elsevier, (2017) 243-276.

[58] W.M. Mthiyane, A. Mambanda, D. Jaganyi, Transition Metal Chemistry, 42 (2017) 739-751.

[59] W.M. Mthiyane, A. Mambanda, D. Jaganyi, International Journal of Chemical Kinetics, (2018).

[60] R.O. Omondi, D. Jaganyi, S.O. Ojwach, A.A. Fatokun, Inorganica Chimica Acta, (2018).

[61] H. Ertürk, A. Hofmann, R. Puchta, R. van Eldik, Dalton Transactions, (2007) 2295-2301.

[62] Y. Kasherman, S. Sturup, D. Gibson, JBIC Journal of Biological Inorganic Chemistry, 14 (2009) 387-399.

[63] G. Ma, Y. Min, F. Huang, T. Jiang, Y. Liu, Chemical Communications, 46 (2010) 6938-6940.

[64] M.E. Oehlsen, Y. Qu, N. Farrell, Inorganic Chemistry, 42 (2003) 5498-5506.

[65] V. Brabec, O. Vrana, O. Novakova, J. Kasparkova, Chemical Communications, 52 (2016) 4096-4098.

[66] A. Quiroga, Journal of Inorganic Biochemistry, 114 (2012) 106-112.

[67] A. Quiroga, F. Ramos-Lima, A. Alvarez-Valdés, M. Font-Bardía, A. Bergamo, G. Sava, C. Navarro-Ranninger, Polyhedron, 30 (2011) 1646-1650.

Chapter Seven

Summary and Future Research

7.1   Summary

This research project was undertaken to investigate the kinetic and mechanistic behaviour of some mononuclear and dinuclear *trans*-platinum complexes which are relevant in anticancer chemotherapy. This project is crucial because it will not only help to shed more light into the substitution behaviour, and hence the pharmacodynamics, of this promising class of platinum-based compounds in anticancer research, but also provide useful information which can serve as the basis for the design and development of versatile and more efficient anticancer drugs with comparably low toxicity, improved cellular uptake and good retention time in the blood. The *trans*-platinum(II) complexes studied for their kinetic and mechanistic behaviour in this thesis are mainly those with aliphatic amine ligands. The ligand substitution reactions of these complexes, in their diaqua or dichloro form respectively, were carried out with a series of biologically relevant neutral thiourea-based nucleophiles, such as thiourea (TU), methyl-2-thiourea (MTU), 1,3-dimethyl-2-thiourea (DMTU) and 1,1,3,3-tetramethyl-2-thiourea (TMTU). The results obtained are discussed and reported in *Chapter Three* to *Chapter Six* of this Thesis. Each of the preceding chapters are summarised below.

Chapter One provides an insight into the involvement of metal complexes in the anticancer research through the accidental discovery of the biological activity of cisplatin by Barnet Rosenberg in the 1960's. A detailed review of the successes of cisplatin: its mode of action and its interaction with its target molecule, the DNA of the cancer cell, and its failures: its mechanism of deactivation, were discussed in this chapter. Other platinum-based complexes, such as *cis*-configured platinum(II) and (IV) complexes, multinuclear platinum complexes, designed and synthesised with the hope to overcome the flaws that are associated with the continued clinical application of cisplatin, were also highlighted. The final aspect of chapter one considers the deliberate modification of the structure of transplatin with bulky groups to elicit a new class of platinum-based compounds which are quite promising in anticancer chemotherapy judging by the reported biological activity of these complexes, most especially against cisplatin-resistant cancer cell lines.

Chapter Two provides a highlight of the kinetic and mechanistic properties of the substitution reactions of d^8 square planar complexes using platinum(II) complexes as a case study. Important theories usually employed to analyse kinetic data and contemporary methods which are engaged to collect kinetic data were also discussed in this chapter. The concluding aspect of the chapter gave a synopsis of the factors influencing the reactivity of d^8 square planar complexes.

Chapter Three reports a comparative study of the kinetic and mechanistic behaviour of bifunctional analogous *cis* and *trans*-dialkylamine diaquaplatinum(II) complexes of the general form, $[PtX_2L_2]$. The structures of the studied complexes are provided in **Figure 7.1**.
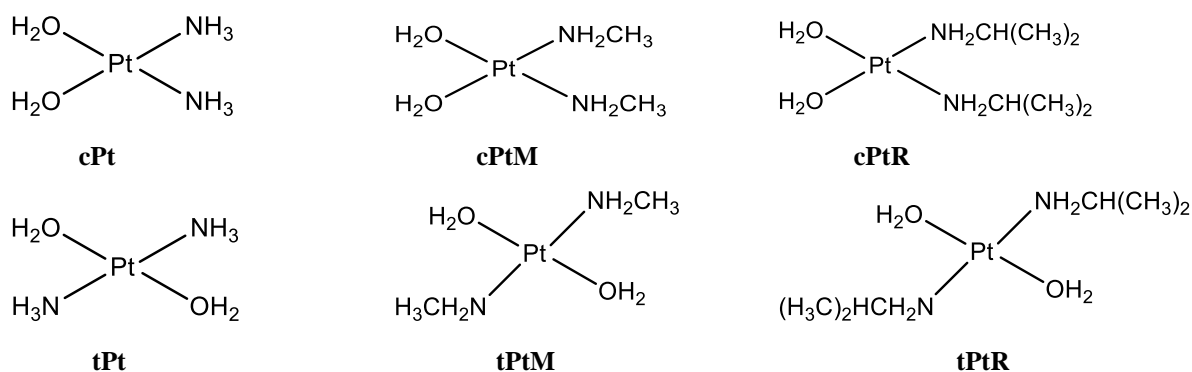

Figure 7.1:   Structures of the studied *cis*-platinum(II) complexes and their *trans*-analogues. The charges and counter ions on the complexes have been omitted for the sake of clarity.

In this study, it was observed that the reaction of the *cis*-complexes proceeded in two concerted steps whereas those of the *trans*-complexes followed a single step. The *trans*-complexes were observed to be approximately 10^3 more reactive than their corresponding *cis*-analogues. The decrease in the rate of ligand substitution in the *cis*-platinum(II) complexes were found be largely influenced by the steric hindrance due to their structural pattern. The geometry of the *cis*-complexes enhance the intramolecular hydrogen bonding within their molecules and thus retard the approach of the incoming nucleophile for substitution purposes. The *cis*-geometry also facilitates steric crowdedness of the substitution sites due to the solvation of the nitrogen atoms of the alkylamine ligands. Whereas these steric effects were also manifested in their corresponding *trans*-isomers, the *trans*-geometry, however, helps to minimise these effects. The *trans*-complexes were found to be more acidic, and hence more electrophilic, than their corresponding *cis*-counterparts based on the pK_a data obtained from the spectrophotometric titration and NBO charges on the platinum centre derived from the DFT calculations.

In a likely manner, the *cis-* and the *trans-*complexes were found to form different kinetic products. The *cis-*complexes were found to undergo complete substitution (dechelation) due to the presence of the strong labilising effects of the thiourea-based nucleophiles, unlike the *trans-*complexes which were partially substituted by these nucleophiles. The complete substitution process in cisplatin and its *cis-*configured analogues has been reported to be responsible for their severe toxicities, whereas the comparably low toxicity in the *trans-*platinum(II) complexes has been attributed to their partial substitution with thiol molecules. [195]Pt NMR spectroscopy was employed to demonstrate the stepwise substitution of the respective series of complexes with thiourea and to confirm their final kinetic products.

In **Chapter Four**, a kinetic investigation of mononuclear *trans-*platinum(II) complexes with mixed amine ligands was reported. The study was carried out to further the understanding of the substitution behaviour of bifunctional mononuclear *trans-*platinum(II) complexes. The structures of the investigated complexes are summarized in **Figure 7.2** below.
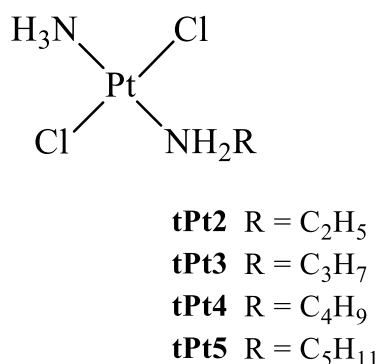
$$H_3N \diagdown \quad \diagup Cl$$
$$Pt$$
$$Cl \diagup \quad \diagdown NH_2R$$

tPt2 R = C_2H_5
tPt3 R = C_3H_7
tPt4 R = C_4H_9
tPt5 R = C_5H_{11}

Figure 7.2:   Structures of the mononuclear *trans-*platinum(II) complexes with mixed amine ligands.

The substitution reactions of each of the *trans-*platinum(II) complexes followed first-order kinetics in a single step. Expectedly, no dechelation step was observed in these complexes, this is consistent with the pattern found in the *trans-*complexes studied in **Chapter Three**. [195]Pt NMR spectroscopy was employed to confirm their final kinetic products. The reactivity of these complexes was observed to be largely dependent on the length of the alkyl chain of the alkylamine moiety of the complexes. The computational modelling using density functional theory (DFT) calculations showed that an increase in chain length by a methylene unit has no direct electronic communication with the metal centre. However, the progressive increase in chain length posed a significant steric hindrance on the substitution sites due to the flexibility of the alkyl chains and thus governed the overall reaction pattern.

In *Chapter Five*, a comparative study of the substitution behaviour and mechanism of some bifunctional *trans*-platinum(II) complexes with symmetric and asymmetric alkylamine ligands was reported. The structures of the investigated complexes are presented below in **Figure 7.3**:
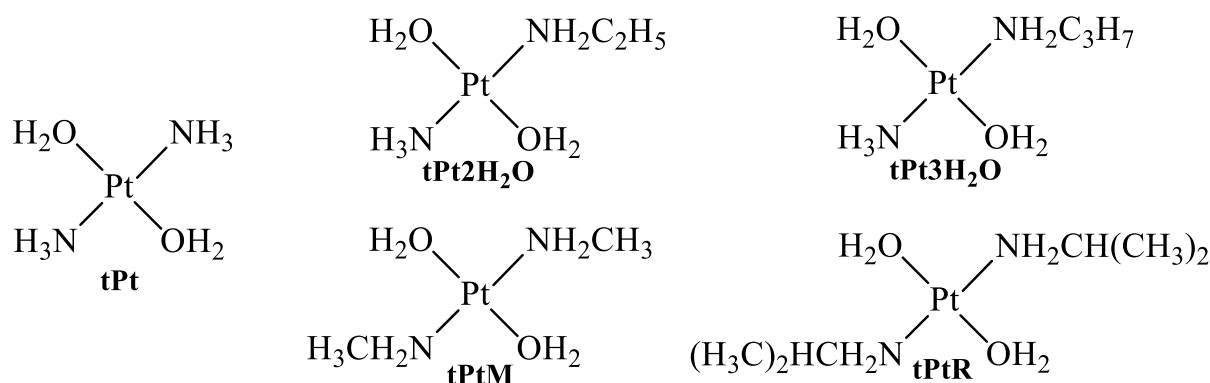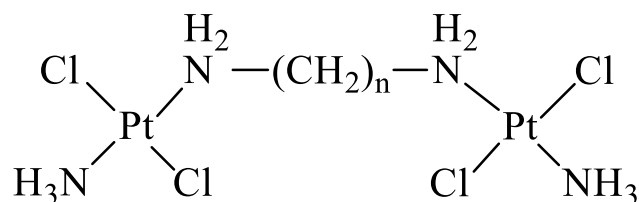

Figure 7.3:   Structures and abbreviations of the investigated complexes. The charges and counter ions th ofe complexes have been omitted for clarity.

The classical diaqua transplatin complex, **tPt** was found to be more reactive than the other *trans*-platinum(II) complexes. The number of carbon atoms in the alkylamine chain length, for the asymmetric complexes, and in the dialkylamine chain length for symmetric complexes, generally influenced the electrophilicity as well as the reactivity of the complexes. From the theoretical data obtained using DFT, **tPt2H₂O** and **tPt3H₂O** exhibit similar electronic properties but the extra methylene group in **tPt3H₂O** caused a considerable difference in the acidity and hence their reactivity. Although, **tPt2H₂O** with asymmetric amine ligands and **tPtM** with symmetric dialkylamine ligands, have the same number of carbon atoms, the difference in their symmetry did not only influence their electronic properties but also their reactivity, with **tPt2H₂O** being slightly more reactive than **tPtM**. The nature of the alkylamine ligands is also observed to influence the reaction rates, with the long flexible chain of the propylamine ligand in **tPt3H₂O** posing more steric hindrance at the reaction site than the branched diisopropylamine in **tPtR**. All the *trans*-platinum(II) complexes showed similar substitution patterns and the overall reaction rates are driven by both electronic and steric factors.

In *Chapter Six*, the kinetic and mechanistic investigation of dinuclear *trans*-platinum(II) complexes with flexible alkyl-α,ω-diamine linkers were presented. The chloride leaving group were trans to each other on each of the platinum centres. The central aim of the study was to

167

gain insight into the role that the flexible alkyl-α,ω-diamine linkers will play in the substitution kinetics and hence the stability to dechelation, of these dinuclear *trans*-platinum(II) complexes. The structures of the studied complexes are presented in **Figure 7.4**.

$$n = 2 \ (\textbf{P12}), \ 3 \ (\textbf{P13}), \ 4 \ (\textbf{P14}), \ 5 \ (\textbf{P15})$$

Figure 7.4:   Structures and abbreviations of the investigated dinuclear *trans*-platinum(II) complexes

Based on the DFT calculated NBO charges on the platinum centres, the electrophilicity of the dinuclear complexes decreases with progressive increase in the flexible linker chain length and thus controlled the overall reaction pattern. The dinuclear *trans*-platinum(II) complexes were observed to have a similar substitution pattern in the first step with their corresponding mononuclear analogues. However, unlike the mononuclear analogues, they are unstable to the strong labilising effect of the thiourea-based nucleophiles because they were found to undergo complete substitution. ^{195}Pt NMR spectroscopy was employed to demonstrate the stepwise substitution of these complexes with thiourea and to confirm their final kinetic products which is tetrathiourea-substituted platinum centres, $Pt(TU)_4$. This observation makes these dinuclear *trans*-platinum(II) complexes to be less promising than their corresponding mononuclear counterparts in anticancer chemotherapy

In all the work presented in **Chapters Three** to **Chapter six**, the negative entropy of activation and the positive enthalpy of activation clearly affirmed an associative mode of activation for all the studied platinum complexes. In all the reported work, the reactivity of the complexes is generally sensitive to the steric bulk of the incoming nucleophiles. Essentially, the reactivity of the complexes decreases with attendant increase in the size of the nucleophiles.

7.2   Ongoing work but not included in this Thesis

In order to gain further understanding into the kinetic and mechanistic behaviour of the substitution reactions of the mono- and dinuclear *trans*-platinum complexes, as an extension of the work reported in this thesis, the following studies are currently being undertaken:

1. Tuning the substitution behaviour of the mononuclear *trans*-platinum(II) complexes through the influence of the planar π-acceptor ligands, such as pyridine. The effect of the systematic replacement of the ammine ligands around the transplatin structure with planar pyridine ligands will provide further insight into mechanism of these mononuclear *trans*-platinum(II) complexes. The structures of the complexes being investigated are presented in **Figure 7.5**.
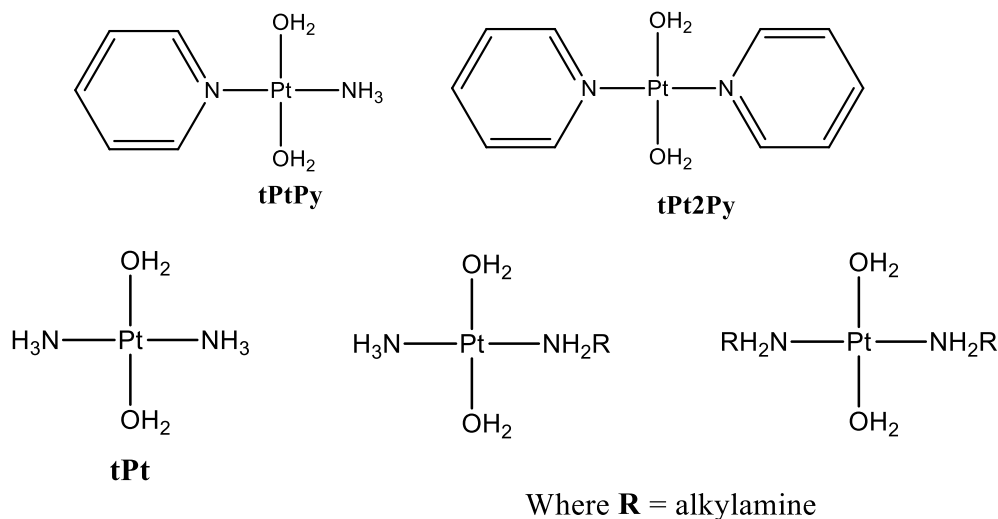

Figure 7.5: Structures of the diaqua mononuclear *trans*-platinum(II) complexes. The charges and counter ion have been omitted for clarity.

tPtPy and **tPt2Py** are currently being synthesised. After full characterisation of the complexes, a spectrophotometric titration will be carried out to ascertain their pK_a values to establish a suitable pH for their kinetic investigation.

2. A kinetic investigation of the mononuclear *trans*-platinum(II) complexes and the effect of the substituents on the planar amine ligands on the mechanism. The structures of the complexes being investigated is shown in **Figure 7.6**.
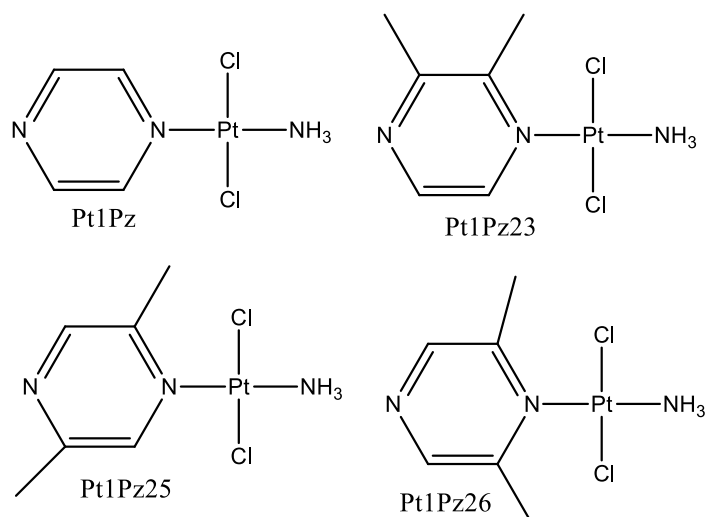
Figure 7.6: Structures of *trans*-platinum(II) complexes with planar pyrazine derivatives.

All the complexes have been synthesised and fully characterised and currently being investigated for their substitution behaviour.

3. The role of substituted diazine linkers on the kinetics and mechanism of the dinuclear *trans*-platinum(II) complexes. This is being undertaken to ascertain the effect of the substituted diazine linker on the stability of these dinuclear *trans*-platinum(II) complexes. **Figure 7.7** presents the structures of the complexes.
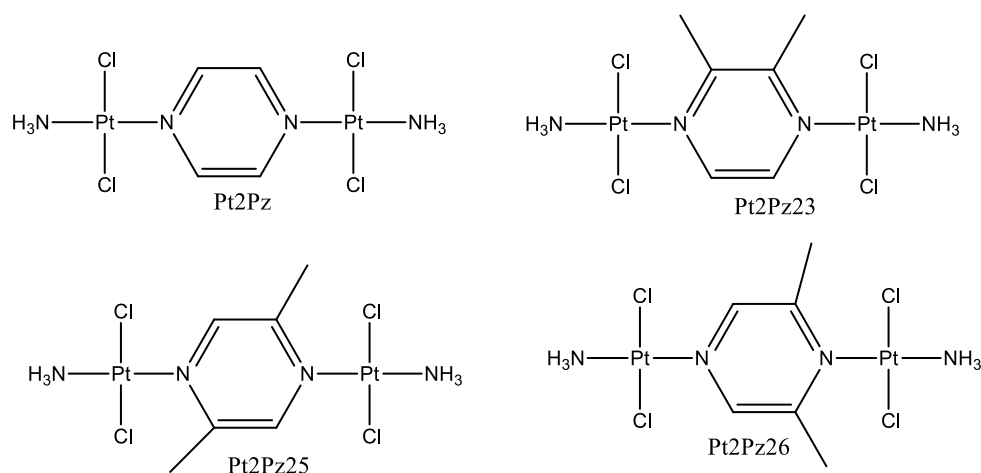

Figure 7.7: Dinuclear *trans*-platinum(II) complexes with substituted diazine bridging ligands

All the complexes involved in this study have been synthesised and are in the process of being investigated for their substitution behaviour.

4. The work on the dinuclear *trans*-platinum(II) complexes above can be further expanded by investigating the role of extended conjugation of the rigid bridging diazine ligand on the substitution kinetics and stability of the following dinuclear *trans*-platinum(II) complexes which are presented in **Figure 7.8**.
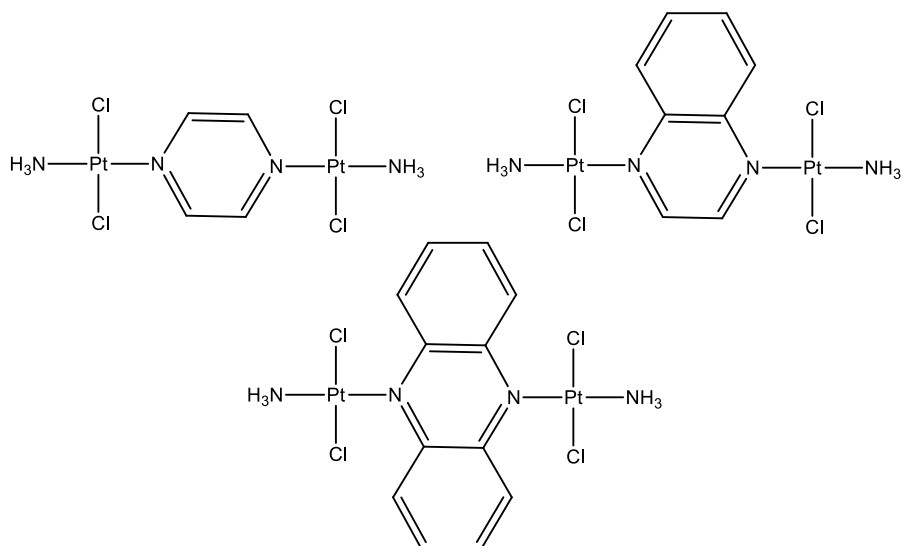

Figure 7.8: Dinuclear *trans*-platinum(II) complexes with diazine bridging ligands with extended conjugation.

The complexes are currently being synthesised, thereafter they will be fully characterised and subjected to DNA binding studies and their substitution kinetics will be investigated.

5. The work mentioned above can be extended further to investigate the role of the internuclear distance between the platinum centres on the kinetics and mechanism of the dinuclear *trans*-platinum(II) complexes with the following complexes being considered (**Figure 7.9**).
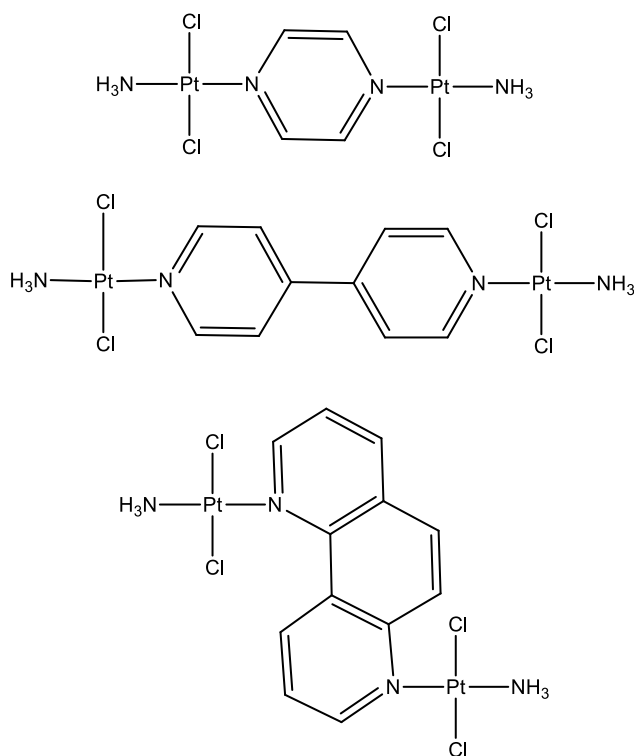
Figure 7.9:   Dinuclear *trans*-platinum(II) complexes with different internuclear distances between the platinum centres.

These complexes have been synthesised and presently being characterised for DNA binding studies and kinetic investigate ions.

The anticancer usefulness of the dinuclear *trans*-platinum(II) complexes presented in **Figures 7.7** to **7.9** will largely depend not only on their interaction with DNA but also their stability towards the strong labilising effect of the thiol-based nucleophiles, such as thiourea (TU), glutathione (GSH), guanosine 5'monophospahte (GMP) etc.

7.3 Future Work

In the proximate future, the stability of the dinuclear *trans*-platinum(II) complexes to degradation can be further tested by replacing the ammine (NH_3) ligands in these complexes with sulfur containing molecules, such as dimethylsulfoxide, DMSO etc. other than any N-donor ligands. Also, planar bridging ligands with other homo- or hetero-atoms, such as carbon, sulfur, oxygen etc. can be considered as well.